# A Systems Biology Approach to Signalling Pathway and Gene Network Regulation Modelling in Mastitis

---

A thesis
submitted in partial fulfilment
of the requirements for the Degree of
Doctor of Philosophy
in Computational Systems Biology

at
Lincoln University
by
Nicoline van Loenen-den Breems

---

Lincoln University
2011

Abstract of a thesis submitted in partial fulfilment of the requirements for the Degree Doctor of Philosophy.

# A Systems Biology Approach to Signalling Pathway and Gene Network Regulation Modelling in Mastitis

by

Nicoline van Loenen-den Breems

Mastitis, an inflammation in the mammary gland, is one of three major diseases in the dairy industry. One in three cows will encounter the disease which is also a problem in humans and other species. While *E. coli* bacterial infections lead to acute mastitis, *S. aureus* lead to chronic mastitis. Dynamics of the regulation and identification of differentially expressed genes between two bacterial infections are important factors for understanding mastitis and assist in the development of pharmaceutical and breeding targets.

Previous studies have identified differentially expressed genes. However, they have not compared expression between two bacterial infections over time. Neither have the dynamics of the signalling and gene network regulation that leads to the differential expressions been investigated. This thesis aims to provide new insight into immune defence in mastitis by analysing dynamics of the signalling and gene regulation in mammary epithelial cells.

The main focus is to develop a mathematical model of the signalling and gene network regulation in mastitis. First, the genes differentially regulated between the two clinical presentations of the disease are identified. Time series microarray experiments of *E. coli* and *S. aureus* challenged mammary epithelial cells are analysed, and confirm that each type of mastitis has a significantly different gene expression time profile from healthy cells. The differentially expressed gene time profiles are then compared between the bacterial challenges. RANTES is identified as the key cytokine which is responsible for two distinctly different time profiles between the bacterial challenges.

In this second part the mathematical model is developed and a systems biology approach applied to investigate the complex dynamics of signalling proteins and gene network regulation of three different cytokines (RANTES, IL8 and TNFα) in mastitis. A modification

to a conversion method allows us to use relative microarray expression data in the model. The method opens up a large amount of datasets for use in future modelling. The model explains signalling and gene network regulation of three cytokines in acute mastitis. No fit could be found for the *S. aureus* experimental data indicating that there is a difference in the regulatory mechanisms between the two types of mastitis.

In the third part sensitivity analysis is used to investigate the role of parameters on the model output. The analysis reveals that each cytokine is sensitive to specific parameter changes. This indicates different dynamics in the regulatory mechanism. As a result, pharmaceutical and breeding targets need to be evaluated in the context of all cytokines to prevent undesirable side effects. The importance of modelling prior to experimental design is also revealed; each cytokine has a specific time frame for the most informative experimental measurement.

In the fourth part robustness analysis is used to investigate the role of the bacterial load on the model output. Robustness analyses indicate that robustness does not originate in the nuclear NFκB time profile and is specific for each cytokine. Finally, future directions of the model and biological experiments are discussed.

**Keywords**: systems biology, mathematical modelling, gene network regulation, cell signalling, microarray, clustering, mastitis, ODE, *E. coli*, *S. aureus*, RANTES, TNFα, IκB, NFκB

# Acknowledgements

This thesis has benefited greatly from my interaction with a large number of people to whom I am very grateful.

I would like to express my gratitude to Prof. Don Kulasiri, my supervisor, for his guidance and encouragement during my PhD study. I would also like to thank Dr. Wynand Verwoerd for his suggestions and discussions about my research.

Lincoln University is full of wonderful people with a wide variety of research interests. I am forever grateful to Associate Prof. Jon Hickford, who encouraged me to start this journey. I would particularly like to thank Dr. Lan Nguyen Khuyen and Dr Jagannath Aryal for the sharing of ideas and discussions as well as their continuing friendship. I would also like to thank Dr. Sami Aikio and Dr. Leo van Iersel, who were always there to point me into the right direction for some matlab commands and provided great friendship and encouragement.

The data used in this thesis part of the EADGENE network and I would like to thank Professor Hans-Martin Seyfert for hosting me in his institute and granting access to the raw data.

I would like to express my great appreciation for the Patrick Shannon Scholarship from Livestock Improvement Corporation, LIC and the William Machin Scholarship. I would not have been able to do this work without their financial support.

Finally, I would never been able to do this work without the years of encouragement and support from my husband and daughter. My daughter has been a great inspiration and this thesis is dedicated to her.

Nicoline van Loenen-den Breems

Lincoln, New Zealand

2011

# Table of Contents

# List of Tables

# List of Figures

# Abbreviations

| | |
|---|---|
| DNA | Deoxyribo Nucleic acid |
| GB | GeneBank |
| GO | Gene Ontology |
| IKK | IκB kinase |
| IκB | Inhibitor kappa B |
| IL8 | Interleukin 8 |
| KEGG | Kyoto Encyclopedia of Genes and Genomes |
| LPS | LippoPolySaccharide |
| LTA | LipoTeichoic Acid |
| MM | MisMatch |
| mRNA | messenger Ribo Nucleic Acid |
| NFκB | Nuclear Factor-kappa-B |
| ODE | Ordinary Differential Equations |
| PAMP | Pathogen-Associated-Molecular-Pattern |
| pbMEC | primary bovine Mammary Epithelial Cells |
| PM | Perfect Match |
| RANTES | Chemokine CC5 (also known as CCL5) |
| STEM | Short Time Expression Miner |
| TLR | Toll Like Receptor |
| TNFα | Tumor Necrosis Factor alpha |
| UG | UniGene |
| WT | Wild Type |

# Chapter 1
# Modelling and mastitis: History, challenges and motivations

*This chapter introduces the research objective of this study. The reason for applying a systems approach to signalling and gene regulation modelling is motivated. The structure of the thesis is outlined and the main contributions are stated. At the end of the chapter a roadmap of the thesis with an overview of the chapters is given.*

## 1.1 Systems Biology, mastitis and mathematics an unusual combination or not?

Mastitis is an inflammation in the mammary gland and one of the three major diseases in the dairy industry world wide (de Ketelaere *et al.*, 2006). Mastitis is the most frequent and costly disease in dairy cows (Seegers *et al.*, 2003) but is also a problem in humans (Wang *et al.*, 2007). One in three dairy cows will encounter the disease at least once in a lifetime. Research has focused on management strategies, identification of molecular differences between pathogens and the identification of the wide variety of proteins (cytokines, signalling molecules, chemokines, and receptors) involved in the immune reaction to the pathogen of the mammary gland. A range of proteins in parallel signal transduction pathways and their ways of communication: phosphorylation, degradation, recruitment, inhibition, translocation and binding, have been identified in the immune systems reaction (Rainard & Riollet, 2006). A wide variety of pathogens, gram positive and negative bacteria, viruses and fungi, each invoking a different reaction in the immune system have also been identified (Wellenberg *et al.*, 2002).

In addition to the immune reaction, a bacterial infection of the mammary gland brings change to several other processes such as milk production, involution and apoptosis (Bannerman, 2009), increasing the complexity of identifying the processes and proteins involved in the development of the infection. Several proteins are members of multiple signal transduction pathways. As more interactions between these signalling pathways are identified, it became clear that signalling does not necessarily occur through parallel, linearly independent processes (Hornberg *et al.*, 2006). Interactions can occur at many hierarchical levels and

signalling proteins from different pathways can influence each other, which leads to unexpected behaviour (Bhalla & Ravi Iyengar, 1999).

These interactions give rise to an overwhelmingly complex dynamic system with proteins involved in signalling pathways and gene network regulation controlled by multiple factors. The quantification of the protein concentration or gene expression provides no information on the kinetics of the signalling processes. Therefore, we lack the understanding of the dynamics of the development of the disease. In signalling pathways, behaviour involving oscillatory patterns can play a role in the establishment of the disease (Nelson *et al.*, 2004). The downstream detection of a signalling protein is not always in the amplitude, represented by the concentration of the protein, but can be in the frequency of the protein detection (Kell, 2005).

Graphical models or a verbal description of the events can be used to visualize the interactions in a complex system. However, in order to identify the real strength of the influence of the different components on each other, verbal description and graphical representation is no longer sufficient. We need mechanistic and quantitative understanding of the functionalities of the proteins and their kinetic implications in the disease outcome to be able to answer questions such as: are these proteins involved in the initiation, differentiation or attenuation of the disease? Does a small change in the concentration of a protein have a measurable or negligible effect? Or can we change the concentration of a particular protein to a large extent without effects? Is the amplitude or the frequency of a particular protein important?

Systems biology is a research discipline that uses an integrative approach to address questions of the complex biological processes in a rich network of genetic and metabolic pathways (Suresh Babu *et al.*, 2006). Systems biology has the potential to address questions about the quantitative and qualitative functioning of biological systems, which are not the central focus of other areas of biology. Quantitative reasoning based on mathematical modelling has had a strong influence on biology in the past (Wingreen & Botstein, 2006). A systems biology approach assumes that the majority of genes and proteins function through biological networks. In an extraordinarily complex nonlinear network of interacting components, proteins and genes work together to ensure an appropriate response is elicited to a particular pathogen (Callard & Yates, 2005). Through mathematical modelling and *in silico* simulations, systems biology investigates the functional and dynamic behaviour of all elements in a particular network quantitatively and qualitatively (Ideker *et al.*, 2001). Signalling events within cells are well-known to be complex and dynamic, often containing oscillatory components. This approach is therefore useful in explaining complex dynamics in the innate

immune system reaction to mastitis. A systems biology approach allows for systems-level understanding of disease to provide potential targets for the development of vaccines and bio markers (Friboulet & Thomas, 2005).

In order to achieve a qualitative and/or quantitative level of understanding of the interactions in disease, a systems biology approach, using mathematical modelling, is used in cancer research (Hornberg *et al.*, 2006). The approach has led to invaluable progress in those fields. A systems biology approach for the development of cancer treatments identified the role of proteins in signalling pathways that were not considered earlier from biological experiments. The concentrations of these proteins did not differ extensively between the diseased and non diseased state, however, modelling identified a significant sensitivity resulting in mechanistic differences as a result of minor concentration changes. The identification of these proteins resulted in new areas of research not considered previously with the classical biological experimentation (Schoeberl *et al.*, 2009). A systems biology approach in diseases related to farm animals is only at its beginning (Cassar-Malek *et al.*, 2008). Mastitis is also a complex disease dependent on dynamic interactions of proteins in signalling and gene regulation pathways. Therefore, a systems biology approach to mastitis is a particularly suitable introduction of a systems biology approach in veterinary science and the dairy industry.

## 1.2 Modelling in the dairy industry, a historical background

The dairy industry is familiar with modelling, and modellers familiar with modelling cows and other aspects of the dairy industry. The ‘spherical cow’ is a metaphor for highly simplified models of reality, is a mathematical joke told in many variants (Harte, 1988). The metaphor highlights the fact that modellers reduce a problem to its simplest form in order to make calculations feasible. At the moment the combinatorial explosion of interactions in modelling the whole cow or even the mammary gland or a cell in detail, force modellers to reduce the problem to a small subset of the reactions that take place (Aldridge *et al.*, 2006).

Several types of modelling are available. Here an overview is given of different types of models and illustrate them with their applications in the dairy industry. The most common model is a graphical model, cartoon, of the process. Cellular signalling pathways are often presented as a graphical model. Although informative, these models do not identify the kinetics of the components and are therefore not considered here. In this thesis I will

concentrate on dynamical models that allow simulation of input data to identify scenarios of the process modelled.

Coarse grained, also known as simple models are abstract models investigating the overall dynamics of a biological process while ignoring the details of the process. Their components and parameters often do not correspond directly to well-defined physical quantities, nonetheless they can provide insight into the behaviour of a system and drive experimental and detailed modelling research (Goldstein *et al.*, 2004). There are several coarse grained models investigating economic aspects of performance in the dairy industry. A well known coarse grained model is Molly, a dynamic, mechanistic computer simulation model of a dairy cow developed to gain information on ruminant digestion (Baldwin, 1995). This model predicts milk production based on the nutritional state and condition of the cow. The model does not take all aspects in consideration, e.g. weather conditions, walking distance to the dairy shed, all having an influence on the milk production are not considered. Even so, it is very informative to gain an understanding of the relation between nutrition and milk production.

### 1.2.1 Previous models of mastitis

Coarse grained, abstract, models of mastitis in dairy cows have been developed from 1976 onwards (Oltenacu & Natzke, 1976). Several models provide information on different aspects of the economic impact of mastitis, and assist in making decisions for the treatment of the disease. The cost of clinical mastitis was modelled using dynamic programming by Bar *et al.* (2008). The model provide a decision making tool for development of a treatment plan for mastitis and its effect on whole farm profitability. Another dynamic model was developed to predict the incidence of mastitis based on the enzyme activity of L-Lactate dehydrogenase measured during in-line milk testing (Chagunda *et al.*, 2006).

Allore *et al.* reviewed three different mathematical approaches to modelling intra-mammary infections and the relation to udder health to determine if simulations of the three approaches yield stable prevalence (1999). There was no agreement between the approaches and they concluded that more detail, such as pathogen specific information, was necessary to identify the dynamics of mastitis. The study is a good example for the need to identify the appropriate method for the hypothesis studied.

Finer grained, or detailed, models are less abstract and contain more details of the process simulated. A more detailed stochastic model developed by Østergaard *et al.* (2003) based on SIMHERD III, including 9 pathogen-specific mastitis types, both clinical and subclinical, identified that the representation of the variation of mastitis severity is important when modelling the economic impact mastitis (Østergaard *et al.*, 2005). A stochastic model to determine the economic consequences of blanket dry cow therapy on different types of pathogens involved in intra-mammary infections identified the need for even more detail and recommended to include farm-specific calculations (Huijps & Hogeveen, 2007). However, stochastic models are very costly with respect to the computing time and become quickly intractable.

Force *et al.* (2002) combined several mathematical models, using an object oriented analysis approach to conceptual modelling, into a simulation tool of livestock farming systems. The main goal of the simulator was to study and predict the consequences of mastitis occurrences on dairy herds. This model has become a decision-aid for stock breeders and farm advisors. The use of object oriented analysis in this model offers a conceptual approach combining the expertise of various domains into one view. A conceptual model takes an abstract perspective, identifying fundamental relationships. However, this type of modelling does not identify the kinetics of the interacting components in the model.

Mastitis modelling has been a successful aid for economic decisions as shown above. The models are fine grained and researched the combination of economic and biological aspects with emphasis on the economic outcome of the model. Here the biological aspects of the disease are of interest.

Modelling has been applied to a lesser extent to assist in the quest for biological insight in the disease. A predator-prey model was developed to investigate the concentration of *S. aureus* in mastitis milk (Detilleux, 2004). Bacteria were represented as the prey and the neutrophils (the most abundant type of white blood cells in mammals) as the predators. This model established that the rate of bacterial killing depends on the ratio of neutrophils to bacteria. Several logistic and exponential growth models were investigated. The smaller of the models with the least parameters gave the best fit of the observed data. For logistic regression, the generalized linear model is probably the most well known model. Logistic regression, also known as a logistic model, is used for the prediction of the chance of an occurrence of an event by fitting the data to a logistic curve. It uses several predictor variables, independent variables (e.g. number of bacteria, number of neutrophils), to predict the dependent variable (e.g. mastitis occurrence) of the model. However, the model does not account for interaction between

predator and prey and would therefore not be suitable for the study of the kinetics of the interacting components.

One of the first models to incorporate interactions between predators and prey was proposed independently in 1925 by the American biophysicist Alfred Lotka and the Italian mathematician Vito Volterra (Murray, 1989). Unlike the Logistic models used by Detilleux *et al*. (2004) in modelling *Staphylococcus aureus* concentration in mastitis milk, the Lotka-Volterra model is based on differential equations. Differential equations allow for the observation of the rate of change of the modelled concentrations at every time point, taking the interaction between the dependent variables into account. Being able to include in the model the interaction between the bacterium and the neutrophils allows for a more realistic representation of the process. Detilleux *et al.* (2006) developed a mathematical model for the acute inflammatory response to *E. coli* in the mammary gland, this time using Ordinary Differential Equations (ODE). The choice of ODE was motivated by the intention of the research to explore the *interactions* between the inflammatory cells and the bacteria (Detilleux *et al.*, 2006).

Mathematical aspects of ODEs are explained in more detail in Section 2.3.1, briefly, they are differential equations where the unknown function, the dependent variable, is a function of a single independent (often time) variable. The ODE describes a deterministic relationship involving some continuously changing (average) quantities (modelled by functions) and their rates of change (expressed as time-derivatives). ODEs are therefore particularly suited for the investigation of the interaction between components in the model. Detilleux *et al.* (2006) earlier research has concluded that the rate of bacterial killing depends on the ratio of neutrophils to bacteria. Therefore, investigating the rate of change in concentration of bacteria and neutrophils would be the next logical step in modelling. The developed model represented the experimental values well and the model sensitivity analysis identified cell-killing abilities and the flow rate from the production and storage sites into the blood compartment as the key parameters influencing the outcomes.

Model sensitivity analysis is a process of identifying the influence, both qualitative and quantitative, of variation in the input and the parameters on the outputs of the model. It is a form of validation of the outcome and often identifies the 'weak' points in a model. These points identify the most informative areas to measure in future research and are an important aspect of modelling. Sensitivity analysis can be used in medicine and biotechnology to predict the results of intervention (Ingalls, 2008). An extensive review of the use of sensitivity

analysis is beyond the scope of this thesis and refer the reader to a book by Saltelli *et al*. (2004).

## 1.3 Research focus of this study

The major research focus of this thesis is to elicit the source of the differentiation in disease outcome between *E. coli* and *S. aureus* bacterial mastitis. The main question is: How is it possible that these two bacterial species can give two different disease profiles while using the same immune system initiating the disease?

To address this question the difference in regulation of mRNA expression between *E. coli* and *S. aureus* induced mastitis is investigated. In a biological experiment, *E. coli* and *S. aureus* mastitis are simulated with bacterial challenges of mammary epithelial cells *in vitro*. The analysis of the gene expression profiles in the mammary epithelial cells is used for the investigation and development of the model.

First, the proteins with significantly different time profiles in mRNA expression between healthy and bacterial challenged cells are identified. In addition, the genes with significantly different time profiles in mRNA expression between the two bacterial challenges are identified. Secondly, a mathematical model of the signalling and gene network regulation of which the identified genes are part of is developed. This allows us to simulate and analyse, *in silico*, the time profiles of the mRNA expression levels identified in the biological experiments. None of previous studies have modelled or compared the regulation of mRNA expression over time of the identified signalling and gene network in *E. coli* and *S. aureus* induced mastitis. Thirdly, the mechanistic processes that cause the difference in expression levels between healthy and diseased cells are identified and the mechanistic properties of model analysed. The mechanistic intricacies of the processes are currently unclear.

We thus integrate our knowledge of mathematics and biology and use the result of biological experiments to construct an *in silico* deterministic model of the mRNA expression in the bacterial challenges leading to mastitis. The knowledge gained is used to develop hypotheses on the mechanistic behaviour of the model and can be used for optimum design of future biological experiments. In addition, the model can be used for the development of pharmaceutical targets, evaluation of breeding objectives and biomarkers.

**Research objectives**

1. Identify genes relevant to the innate immune system response to a bacterial infection representing significantly different time profiles in mRNA expression between healthy and diseased cells and between *E. coli* and *S. aureus* induced mastitis in mammary epithelial cells.
2. Develop a predictive *in silico* deterministic mathematical model to simulate the regulation of the mRNA expression of the identified genes over time. This model will form the basis for the identification/prediction of the mechanistic difference in mRNA regulation between the two different bacteria invoking mastitis studied in this thesis.
3. Elicit the underlying mechanistics of the gene regulation through sensitivity analysis of the model developed with experimental data from the *E. coli* mastitis.
4. Identification of the most informative future biological experiments.
5. Identification of the model parameters with experimental data from *S. aureus*, mastitis.
6. Identification of the robustness of the model to elicit the influence of the variation in bacterial load on the model output.

## 1.4 Summary of achievements and contributions

The main contributions of the thesis can be summarized as follows:

- Microarray time series data analysis (Chapter 3)
    - A cluster of immune system related genes, including the cytokine RANTES, with significantly distinct expression time profiles between diseased and healthy cells and between *E. coli* and *S. aureus* bacterial challenges in time series microarray experiments is identified.
    - The signalling pathway, Toll Receptor Signalling pathway, responsible for the relocation of the transcription factor, NFκB, from the cell to the nucleus, is identified as the main pathway involved in the development of mastitis. The relocation of the transcription factor initiates the mRNA expression of the cytokines such as RANTES, IL8 and TNFα, which are responsible for the different gene expression time profiles between the two bacterial challenges.

- Development of a mathematical model representing the *E. coli* challenge in mammary epithelial cells (Chapter 5)
    - A mathematical model is developed, estimating parameters to represent mRNA expression of the cytokines RANTES, IL8 and TNFα expressed in *E. coli* bacterial challenge of mammary epithelial cells. The model can be used to develop understanding of the reaction of the immune system in mastitis, the differentiation in the two types of mastitis and to test pharmaceutical targets.
    - A method to convert microarray relative expression values to mRNA concentrations is adjusted. As a result microarray data can be used in mathematical modelling.
- Sensitivity analysis of the *E. coli* model (Chapter 6)
    - The optimal time for measurement of biological values to fine tune model parameters is established.
    - The model identified that the optimal measuring time is different for each cytokine.
    - Sensitivity analysis identified that reduction of cytokine expression can only be achieved by regulating the levels of the transcription factor NFκB. Due to the pleiotropic nature of this transcription factor, reduction has been shown to have unfavourable side effects. Therefore, other avenues for the adjustment of cytokine expression need to be evaluated.
    - The model is sensitive to changes of different parameters for each of the cytokine mRNA expression levels. Indicating that future pharmaceutical product testing needs to consider all cytokine expression levels for the evaluation of the product and that cytokine levels can be manipulated individually.
- Findings based on the *S. aureus* model development (Chapter 7)
    - Expression values from the *S. aureus* biological experiment can not be explained with the model developed in this thesis. Additional pathways and processes are possibly involved in the process and need to be investigated further. This indicates that different pathways in the immune system are involved in the two bacterial infections.

- Robustness analysis of the *E. coli* model (Chapter 8)
    - The result of the robustness analysis of the model output for input variation show a lack of robustness for variation in the bacterial load:
        - Cytokine expression levels of IL8 and TNFα are not robust to variation in bacterial load at 360 minutes of the simulation. Robustness for variation in bacterial load at 360 minutes was found in biological experiments. We hypothesize that robustness to synthesis and degradation parameter variation in TNFα could play a role.
        - Cytokines expression levels of RANTES, IL8 and TNFα are neither robust to variation in the time profile of the input, representing the variation in bacterial load during the time of simulation. Variation in the time profile of the input changes the time profile of the cytokine mRNA expressions, with each cytokine showing individual variation.

## 1.5 Roadmap of the thesis

The thesis is an example of interdisciplinary work, where systems biology combines biology and mathematical modelling. I have provided an extended and more detailed introduction into the biological and mathematical modelling aspects of the work. In Chapter 2, Section 2.1 will give an overview of the biological aspects of mastitis, Section 2.2 will introduce systems biology and Section 2.3 will give an overview of the mathematical algorithms used in this thesis and Section 2.4 gives an overview of the microarray analysis and clustering methods used. Chapter 3 analyses the microarray time series data from the biological experiments and identifies the model and the model focus. Chapter 4 explains a mathematical NFκB regulation model, which is a key component of the mastitis model developed in Chapter 5. In this chapter, a model for the signalling and gene network regulation of cytokines in mastitis is developed. Chapter 6 discusses the sensitivity analysis of the *in silico* simulations of the developed *E. coli* mastitis model to elicit the influence of the parameter and initial value variation on the model output. With this, the variation in the model output due to the biological aspects and mathematical modelling aspects can be separated. Chapter 7 discusses the model characteristics in relation to experimental data from the time series microarray *S. aureus* challenge. In Chapter 8 the robustness of the model with respect to the variation in

bacterial load is analysed to identify the source of robustness to variation in bacterial load identified in biological experiments. In the last chapter summary and future directions are given.

Figure 1-1 gives a graphical outline of the roadmap of the chapters in this thesis.

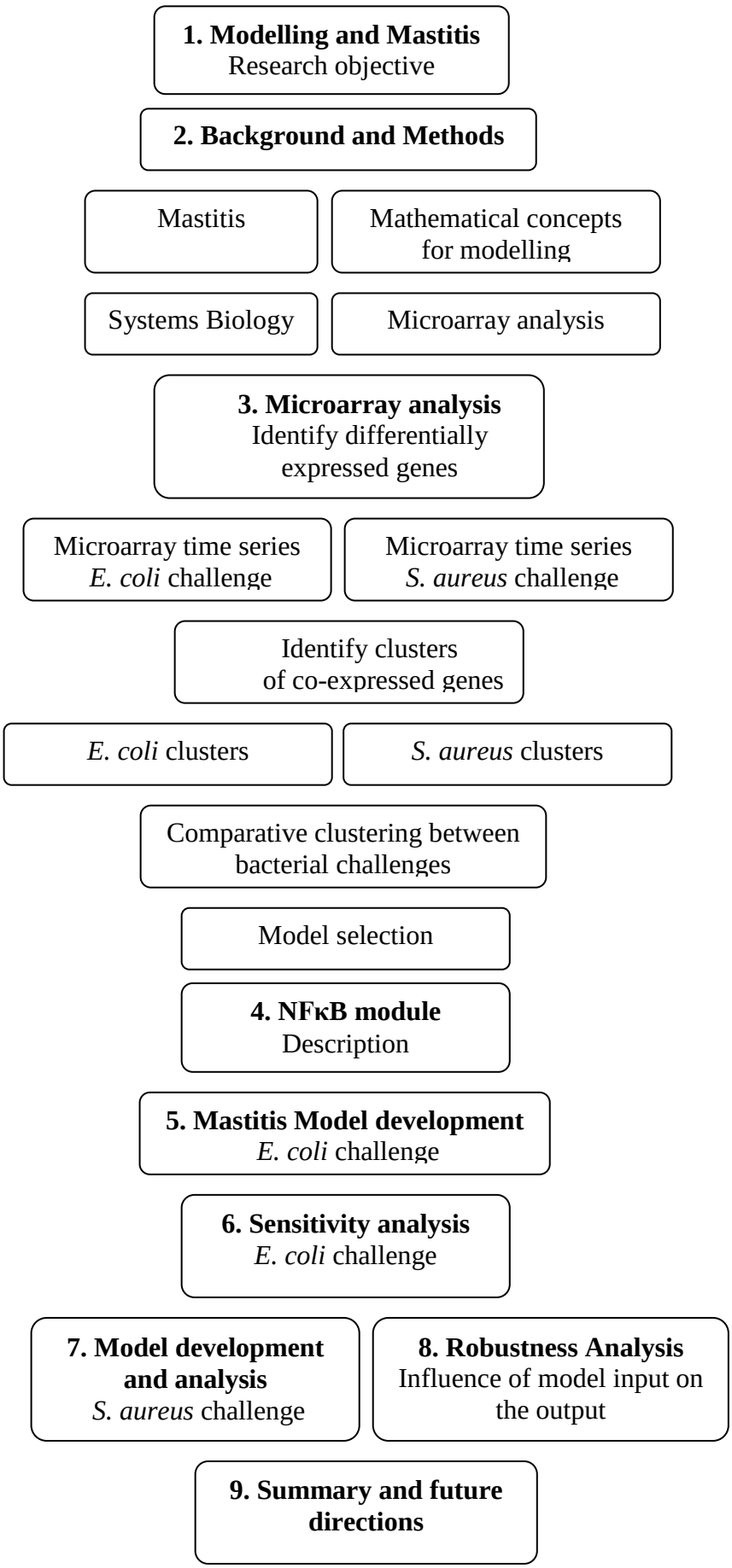


Figure 1-1 Graphical outline of the roadmap of the chapters in this thesis

# Chapter 2
# Background and Methods

***"Every object that biology studies is a system of systems."***

***Francois Jacob (1974)***

*The first Section in this chapter introduces mastitis, gives a literature review of the relevant biology of signalling pathways and gene expression identified in mastitis and explains why mastitis should be studied with a novel approach; systems biology. The second Section 2.2 introduces systems biology, a systems science with a holistic approach to biology and describes the first dogma in molecular biology. The general framework of systems biology is then related to the more specific aspects of this thesis; signalling and gene network regulation modelling. Section 2.3 introduces the methods and mathematical concepts used for modelling, analysing the sensitivity and robustness of signalling and gene network regulation in this thesis. Since a combination of signalling and gene network regulation modelling is introduced we will motivate the demand for a systems biology approach in this work and its challenges. Section 2.4 gives a short overview of the methods in microarray analysis and clustering techniques used for the analysis of the biological data. The last Section explains the conversion of microarray data to a suitable format for modelling.*

## 2.1 Mastitis an infection in the mammary gland

Mastitis is the result of an inflammatory event in the mammary gland, usually caused by a variety of bacteria. Bovine mastitis is one of the major diseases in the Dairy industry world wide and causes distress for the animal as well as a cost to the dairy farmer (de Ketelaere *et al.*, 2006). The economic impact stems from two sources, the cost of control of the disease and the cost of reduction in production (Seegers *et al.*, 2003). In the US mastitis is estimated to cost the industry US$2 billion annually (Sordillo & Streicher, 2002) while the costs world wide are US$25 billion per annum (Pareek *et al.*, 2005). In humans mastitis is associated with increased transmission of bacterial infections (Wang *et al.*, 2007) and Human Immunodeficiency Virus (HIV) passing from mother to child (John *et al.*, 2001). A recent

study by Scott *et al.* reported that 18% of women experienced at least one episode of mastitis in the 26 weeks following childbirth (2008). This thesis concentrates on bovine mastitis. Nevertheless, the increased understanding of the development and cause of the disease is also invaluable for humans and other species such as pigs.

### 2.1.1 Mastitis, cytokines and gene expression

During milking or in between milkings, bacteria can enter the teat into the glandular tissue and to the alveoli in the mammary gland. In between milkings the milk is stored in the alveoli of the mammary gland (Figure 2-1). Bacteria can reproduce in the milk and move to alveoli. Alveoli are small microscopic sacs lined with milk producing epithelial cells. The epithelial cells elicit an immune reaction to the bacterial invasion (Dogan *et al.*, 2005). It is the immune reaction and the gene expression as a result of this immune reaction that is modelled in this thesis. However, not all bacteria elicit the same immune reaction. Some bacteria cause an acute infection while others elicit a chronic infection, despite the fact that they encounter the same immune system that evokes cell signalling and gene expression. It is believed that there is a difference in the dynamics of the signalling. Comparing the difference in the dynamics of the signalling and resulting gene expression profiles between bacterial challenges is the focus of this thesis.

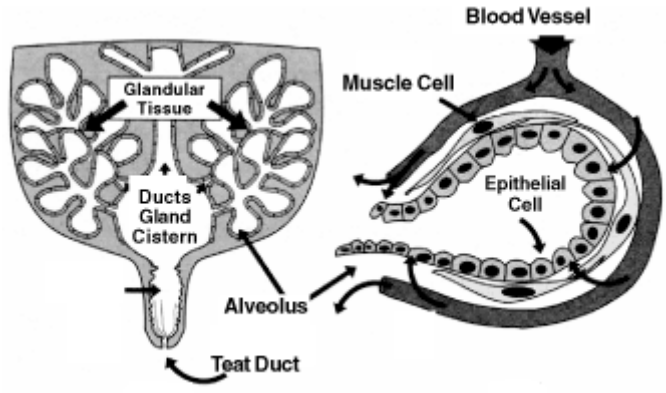


Figure 2-1 Cross section of the mammary gland showing the teat, gland cisterns, and glandular tissue. Glandular tissue is made up of small microscopic sacs, alveoli that are lined with milk producing epithelial cells.[1]

[1] http://www.ag.ndsu.edu/pubs/ansci/dairy/as1129w.htm

The main mastitis pathogens, bacteria, can be grouped in two types; gram positive bacteria and gram negative bacteria. Of the gram positive bacteria *S. aureus* and *S. uberis* are the most prevalent, cause sub clinical (persistent) mastitis while from the gram negative bacteria, *E. coli* is the most prevalent, causing transient clinical mastitis (Bannerman *et al.*, 2004). Both clinical and sub clinical mastitis change the chemical, physical and microbiological characteristics of the mammary gland and the milk; however, they do so with different severity. Clinical mastitis is characterized by observable physical changes in the udder and milk. Clots appear and the colour of the milk changes. The udder is often swollen. These effects make it easy to detect clinical mastitis. Acute clinical mastitis is caused by the gram negative bacteria *E. coli* and can have severe consequences with the animal dying or losing parts of the mammary gland. The benefits of antibiotic therapy have not been shown in clinical trials or experimental studies, while vaccines have only reduced the severity and number of incidences of clinical *E. coli* mastitis (Burvenich *et al.*, 2007).

Sub clinical mastitis, caused by the gram positive bacteria such as *S. aureus*, cause a change in milk composition and decrease milk yield. As a result, there will be a loss in revenue for the farmer. Sub clinical mastitis often causes less severe physical changes, however, the disease can turn into a chronic infection (Riollet *et al.*, 2000). Since there are no prevalent physical changes, sub clinical mastitis is more difficult to detect and regularly goes undetected for a long time. Many different strains of S. *aureus* exist, and because several strains are resistant to antibiotic treatment, successful treatment is difficult (Barkema *et al.*, 2006).

Gram positive and gram negative bacteria each produce unique toxins. Each toxin causes a specific disease profile because there is a different reaction of the innate immune system depending on the type of toxin. The innate immune system represents the first line of defence in the host response to infection.

As a result of the innate immune system's reaction of the epithelial cells, cytokines, such as RANTES, IL8 and TNFα, are secreted (Pareek *et al.*, 2005). Cytokines are a family of small proteins that carry signals between cells and play a pivotal role in the activation and regulation of the innate immune response (Zhu *et al.*, 2007). RANTES plays an active role in recruiting leukocytes (a type of white blood cells) into inflammatory sites, while IL8 attracts neutrophils (the most abundant type of white blood cells) to the site (Wellnitz & Kerr, 2004). TNFα induces inflammation and cell death (Pareek *et al.*, 2005). The precise regulation of cytokine expression is essential for the regulation of the response to the infection. Lack of regulation can lead to severe diseases and sepsis (Liew *et al.*, 2005). Different cytokine

expression profiles are responsible for the various clinical presentations in mastitis (Bannerman *et al.*, 2004). Therefore, the detailed knowledge of the mechanistics of the dynamics responsible for the initiation of cytokine expression profiles plays an important role in the understanding of the development of the disease. A detailed description of the specific function of each cytokine is beyond the scope of this thesis and for an extensive review of the bovine innate immune response of the mammary gland the reader is referred to Rainard & Riollet (2006) and De Schepper *et al.* (2008).

### 2.1.2 Toll receptor signalling and differently expressed cytokines in mastitis

The ability of the innate immune system to react to a variety of bacterial pathogens in different ways is facilitated by the ability to detect highly conserved molecular patterns on bacterial cell walls. Lypopolysaccharide (LPS) is a highly conserved pathogen-associated molecular pattern (PAMP) on the cell wall of Gram negative bacteria such as *E. coli,* while Gram positive bacteria, *S. aureus,* share LipoTeichoic Acid (LTA) on the cell wall.

On the cell membrane of mammary epithelial cells are Toll like receptors (TLR). The Toll like receptors on the cell wall of mammary epithelial cells initiates a signalling cascade that results in cytokine expression following a bacterial infection (Figure 2-2). The cytokines form the primary line of defence against invading pathogens (Doyle & O'Neill, 2006). Toll like receptors recognize the individual patterns, PAMPs, and play an important role in triggering the immune responses such as cytokine expression (Akira *et al.*, 2006). Toll like receptors are members of a large super family of interleukin1-receptors (IL1-R) that signal via a partly shared downstream signalling pathway to initiate mRNA expression. This is shown in Figure 2-2, which shows the Toll like receptor pathway as presented by the Kyoto Encyclopaedia of Genes and Genomes (KEGG).

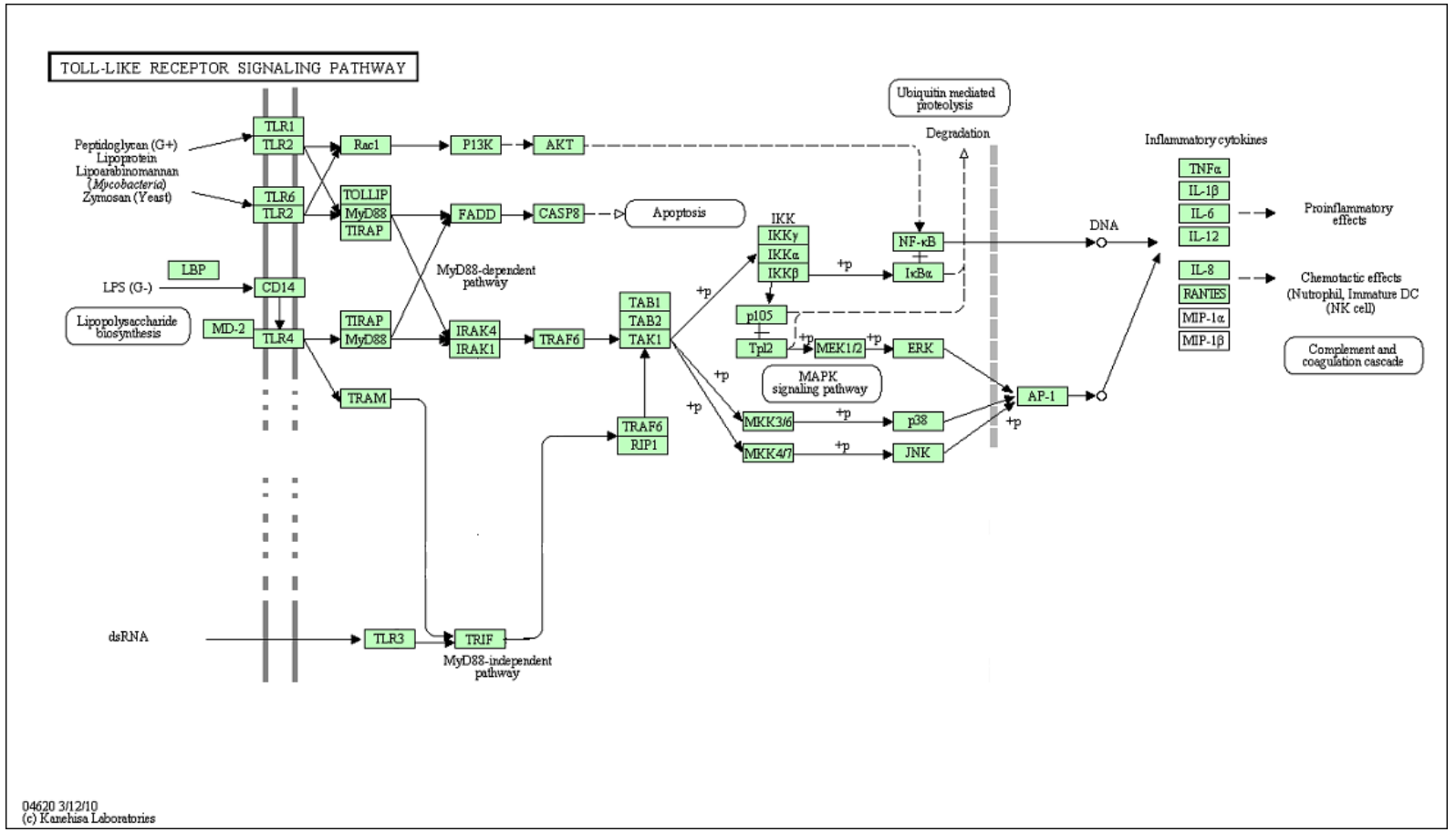


Figure 2-2 Bovine Toll receptor signalling pathway adapted from KEGG[2]

[2] Kyoto Encyclopedia of Genes and Genomes http://www.genome.jp

Multiple members of the Toll like receptor family have been identified in mammals (Doyle & O'Neill, 2006) with ten identified in cattle (Menzies & Ingham, 2006). Each individual Toll like receptor has a number and identifies a specific type of bacteria or virus (Sabroe *et al.*, 2008).

TLR2 and TLR4 receptors, used for LPS and LTA recognition respectively, and the downstream signalling pathway are expressed in mammary epithelial cells (Strandberg *et al.*, 2005). TLR2 and TLR4 activation lead to the activation of several signalling molecules that release the transcription factor Nuclear Factor-kappa-B (NFκB) (Strandberg *et al.*, 2005). Although the two bacterial infections invoke different signalling pathways, TLR2 and TLR4 respectively, it is the dynamics of the translocation of NFκB to the nucleus that influences the cytokine gene expression profiles. NFκB is a principal transcription factor in mammalian inflammatory signalling (Cheong *et al.*, 2008). In mammary epithelial cells the transcription factor NFκB binds to the upstream region of large number of genes regulating cytokine expression and other immune reactions such as inflammation, cell proliferation and apoptosis (Viatour *et al.*, 2005). The transcription factor NFκB regulates a pleiotrope of genes who play important roles in inter- and intra-cellular signalling, cellular stress response, cell growth, survival and apoptosis (Hoffmann *et al.*, 2006). Several diseases, including diabetics (Bragt *et al.*, 2009) cancer, and chronic inflammation (Fraser, 2008) have been related to the impairment of the NFκB regulation that results of a signal response.

### 2.1.3 NFκB regulation

NFκB does not require protein synthesis to activate, allowing for fast reaction, within minutes, to inflammation (Hoffmann & Baltimore, 2006). In the cytoplasm NFκB is inactive as an IκB-NFκB heterodimer (Figure 2-3).

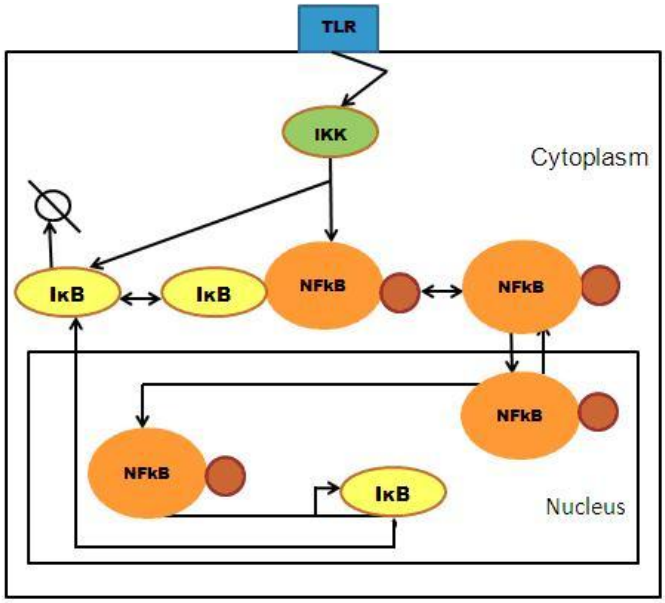


Figure 2-3 Conceptual model of TLR-IKK-NFκB signalling. The TLR receptor on the cell membrane recognizes the bacterial challenge. The signalling pathway activates the kinase IKK which breaks the IκB-NFκB dimer. As a result, the transcription factor NFκB translocates to the nucleus initiating gene expression. Among the genes expressed are the IκB isoforms which bind with NFκB in the cytoplasm to prevent translocation of NFκB to the nucleus. This process creates a negative feedback loop for the translocation of NFκB to the nucleus.

NFκB activity is largely controlled by IκB isoforms, which bind to NFκB preventing transport of NFκB to the nucleus (Hoffmann *et al.*, 2002a). TLR signals result in IκB kinase (IKK) activity. Kinases are enzymes which covalently attach phosphate groups to substrate molecules, such as IκB-NFκB heterodimer, and phosphorylate the substrate. IKK phosphorylate IκB which results in degradation of the IκB-NFκB heterodimer and free NFκB. NFκB can then transport to the nucleus and bind to DNA to function as a transcription factor. Signalling pathways determine actual cellular IKK activity profiles which originate from receptors, such as TLR, that allow for stimulus specific signal processing (Werner, 2005). The IKK initiated phosphorylation of the heterodimer IκB-NFκB activates the translocation of NFκB to the nucleus. In the nucleus NFκB functions as a transcription factor for cytokine gene expression.

Despite the fact that different bacterial challenges use the same NFκB signalling pathway, the dynamics of the translocation of the transcription factor NFκB to the nucleus, as a result of IKK activation representing the stimulus as a result of the challenge, are unique for each challenge. The patterns and timing of the translocation of NFκB to the nucleus lead to different transcriptional outputs in NFκB regulated genes (Sillitoe *et al.*, 2007). Different subsets of NFκB target genes are activated by changes in the time-dependent kinetic profile of

NFκB signalling (Vanden Berghe *et al.*, 2006). NFκB has been shown to exhibit decaying oscillatory behaviour following TNFα stimulus (Hoffmann *et al.*, 2002a), while Covert *et al.* reported a stable and consistent NFκB response to LPS (2005). NFκB signal dynamics therefore play an important role in determining cellular response such as cytokine gene expression.

Dynamics play a key role in several cellular molecular processes. The dynamics of biological networks are difficult to identify with *in vivo* or *in vitro* experiments (Thakar *et al.*, 2007). For example, some signalling pathways encode information not just as protein concentrations or location, but via changes in the dynamics of those concentrations (Kell, 2005; Nelson *et al.*, 2004). Dynamic modelling approaches describing and analyzing these processes are essential for our understanding of cellular functions. The analysis of these models facilitate more rapid testing of biological hypotheses and provide insight in aspects that might otherwise not easily be accessible with classical biological experiments (Wolkenhauer *et al.*, 2009). The analysis of a model can also assist in the design of novel biological experiments to test hypotheses that are formulated from modelling predictions.

While molecular biology is involved in the characterizing molecular mechanisms quantitatively in biology, systems biology is especially suited to investigate the mechanistics of signalling pathways and gene network regulation.

## 2.2 Systems Biology: Modelling signalling and gene network regulation

Systems biology is a holistic approach to biology and is aimed at system-level understanding of biology, understanding biological systems as a dynamic system of interactions between the different components; e.g. receptors, signalling molecules and genes. The key to systems biology is the construction and analysis of a model that is based on a number of interacting components that are each known from reductionist's studies of the subsystems. The interaction between the known subsystems can then lead to emergent behaviour of the whole system that can not be predicted from the subsystem in isolation. Systems biology is therefore an interdisciplinary field of research spanning a large area of science, attracting ideas from many different disciplines (Figure 2-4). The discipline addresses the missing links between molecules and physiology by investigating how dynamic interactions result in functionality of the cell (Bruggeman & Westerhoff, 2007). The contribution of systems sciences and the role

of mathematical modelling distinguish systems biology from other areas such as bioinformatics (Klauschen *et al.*, 2007; Wolkenhauer & Mesarovic, 2005).

Systems biology in the context of this work is a combination of life, information and systems science. In this thesis mathematical modelling (systems science) is applied to the results of biological experiments (life science) and together with available biological knowledge of the components (information science) mathematical tools are used from systems sciences to analyze the models. From the analysis knowledge is gained of the intricacies of the mechanistics of the model components which represent the cell components that determine the functionality of the cell (Figure 2-4). Systems biology's ultimate objective is, explaining how the components within a cell, receptors, signalling molecules and genes, interact dynamically and produce the observed organization and function of the cells (Wolkenhauer & Mesarovic, 2005).

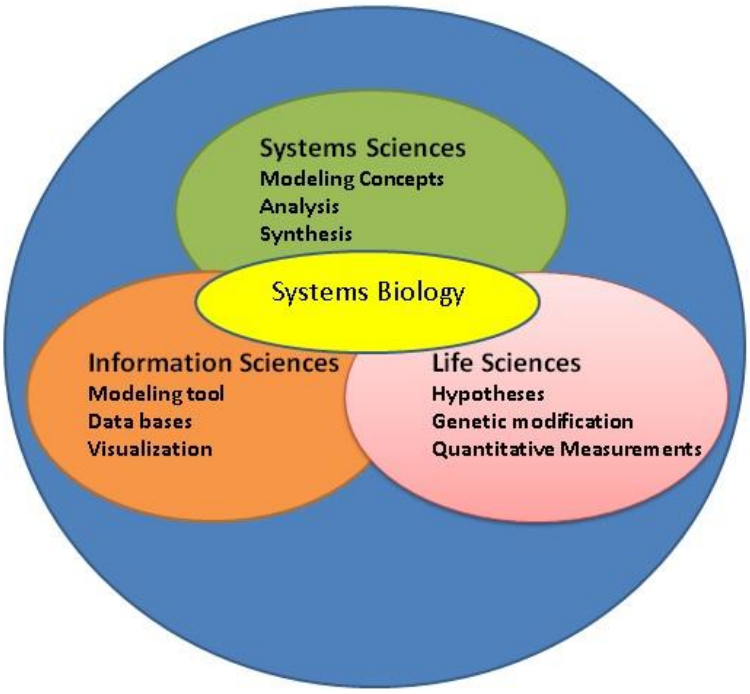


Figure 2-4 Systems biology and the relationship with other science disciplines

### 2.2.1 The principal unit of life

In order to understand a biological system as a dynamic system of interactions between components we go back to the principal unit of life; the cell. In the cell thousands of reactions and transformations are carried out to allow for survival and reproduction of the physiological entity. Cells can be grouped into tissues which form organs and organs make up living species. Components in the cell are organized in organelles separated by membranes. One of these is the nucleus where deoxyribonucleic acid (DNA), our genome, is a large component.

DNA contains genes and encodes for proteins; the basic components of life. Proteins consist of amino acids. This flow of information from genes, the genetic code of life, to proteins, is often referred to as the central Dogma of molecular biology (Figure 2-5).

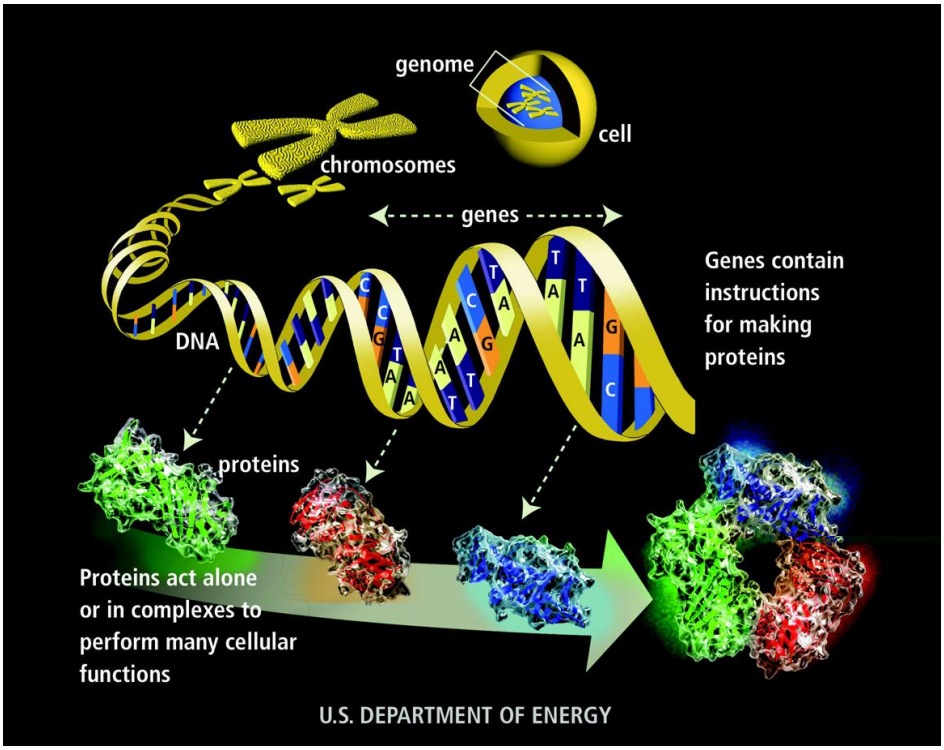


Figure 2-5 Central dogma of molecular biology. DNA codes for proteins which are the building blocks of life.[3]

The base pairs of DNA contain three letter codes for amino acids. There are twenty different amino acids and a string of amino acids form a protein. A string of three letter codes is transcribed into a string of messenger ribonucleic acid (mRNA), and translated into protein. Proteins have a wide variety of functions and can act as receptors, signalling molecules,

[3] http://genomics.energy.gov

enzymes and transcription factors. Signalling molecules receive, integrate and transduce signals that regulate cellular functions.

### 2.2.2 Signalling pathways and gene network regulation

Biological signal pathways transduce external signals and coordinate life processes in the organism. The transduction, integration and processing of signals is a complex dynamic process that leads to the activation of a gene regulatory network. A gene regulatory network is a collection of genes, DNA segments, interacting through their protein expression products and molecules in the cell in a coherent network, thereby regulating the rate of gene expression into mRNA of these and other genes (Figure 2-6). mRNA is translated into proteins. Proteins play a major role in biological processes and therefore the regulation of the network of genes as the result of the signalling process influences the phenotype of the organism.

A gene consists of two parts, a coding and non coding region. The coding region is a group of base pairs that code for the string of amino acids that form a single protein. The non coding region, containing the cis-regulatory part, plays a role in the rate of expression of the gene through a variety of regulatory elements, small molecules known as transcription factors. Gene expression is therefore regulated through a network of regulatory systems between DNA, mRNA, proteins and transcription factors (de Jong, 2002).

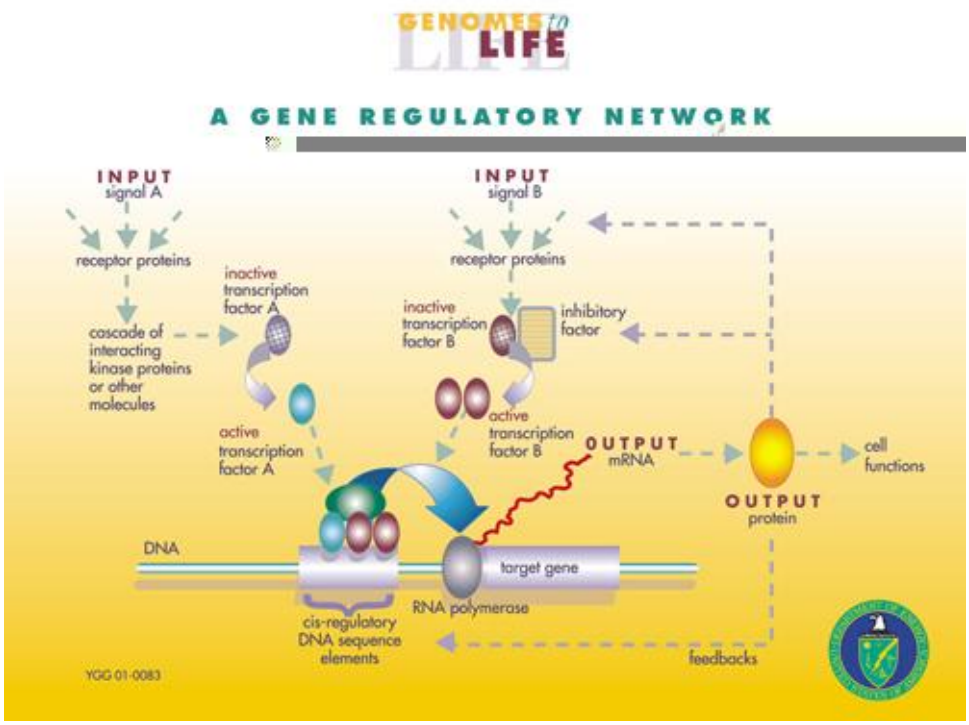


Figure 2-6 A signalling pathway and gene regulatory network[4]. An input signal, e.g. bacterial challenge is recognised by the receptor protein. The receptor protein starts the signalling cascade which results in the translocation of the transcription factor to the nucleus. The transcription factor binds to the non-coding region of the gene and results in mRNA transcription. mRNA is translated into protein and contributes to the cell function.

In order for a DNA sequence to be transcribed into mRNA, transcription factors bind to the cis-regulatory DNA, the non coding part of the gene, and influence the rate of gene transcription in a positive or negative way. These transcription factors are proteins resulting from mRNA transcription and translation regulated by other proteins themselves and can initiate or inhibit gene transcription. The transcription factors are activated by the signalling pathway, and the signalling pathways initiated by the receptor protein recognising a challenge. The signalling cascade together with the gene network in the nucleus creates a signalling and gene regulatory network as shown in Figure 2-6 (Styczynski & Stephanopoulos, 2005).

[4] http://genomics.energy.gov

### 2.2.3 Feedback loops in gene network regulation

Initiation and inhibition of gene expression is regulated by feedback loops. Feedback loops are common regulatory structures in biological systems, especially in signalling pathways and have been observed for more than 130 years (Brandman & Meyer, 2008). Feedback means that the information, on which a decision is based, is derived from the result of the output of the system. Feedback loops are necessary to introduce a shift in behaviour. The signalling and gene network regulation is shaped by positive and negative feedback loops.

The most common form of the negative feedback loop consists of a transcriptional interaction where transcription factors repress gene transcription. Negative feedback loops can stabilize signals, limit maximal signalling output, enable adaptive responses or create transient signal responses (Brandman & Meyer, 2008). Therefore, negative feedback loops can allow for adaptive behaviour to changes in the input, rather than absolute amount of input signal. Especially in a biological situation where a change in bacterial load needs to elicit a response from the immune system but not lead to sepsis, regulation is important. For instance, a strong negative feedback loop that is triggered by another negative feedback loop after a delay, can convert a constant input into a transient output signal.

Contrary to a negative feedback loop that restricts the output, positive feedback increases the output of the signal and is therefore often associated with an uncontrolled, runaway process (Brandman & Meyer, 2008). Positive feedback loops can amplify the signal, change the timing of the signalling response and create bistable switches. In a bistable switch below a certain threshold the signal remains near basal state, above critical threshold the system increases to high active state (Brandman & Meyer, 2008). With two negative feedback loops, the bistable system can be forced back into inactive state and create a pulse in the output with fixed amplitude and duration. Therefore, a combination of negative and positive feedback loops determines the dynamics and robustness of the system.

If the loops are nonlinear and show redundancy, they can add to the robustness of the system (Werner, 2005). Robustness is essential for consistent performance under a wide range of perturbations (Aldana *et al.*, 2007). It is therefore of vital importance for the understanding of a model representing a biological system to investigate the role of the feedback loops and robustness in the model.

### 2.2.4 Modelling signalling and gene network regulation

The concept of mathematical modelling of gene network regulation was introduced by Kauffman *et al.* (1995). The ideas of system level understanding are not new to biology and dates back to the 1960s (Wolkenhauer, 2001). With the remarkable progress in molecular biology in the 20$^{th}$ century, genome sequencing and high throughput applications such as microarrays (See Section 2.4.1) systems biology has been able to apply systems theory and mathematical modelling to a molecular-level. The human genome project therefore marked the beginning of the next level of understanding. The letters, genetic code (DNA), and words, the proteins (transcribed from the mRNA), of the story of life have been discovered. However, details of the dynamics of the words, ascribing a molecular function to the proteins and therefore writing the book of life remains elusive.

Systems biology has made remarkable progress but there are still significant challenges (Aderem, 2005; Wolkenhauer & Mesarovic, 2005). Although systems biology is aimed at understanding systems as a whole, the complexity intrinsic to biological systems such as cells in mammals does not allow a detailed dynamic description of the cellular system as a whole at the moment. However, subsystems and simple functional models can be identified and isolated (Kitano, 2002).

Simple models have been shown to be valuable to give insight in the qualitative behaviour of biological systems (van Riel, 2006). The challenges of modelling biological systems lie in the decision of the appropriate abstraction level to focus on and the technique to use (Szallasi *et al.*, 2006). Qualitative aspects of the system are represented by abstract models identifying key components, while quantitative aspects are represented in mathematical models identifying mechanism in the regulation of the model (Ideker & Lauffenburger, 2003). In "Therefore all models are wrong… some more then others" Wolkenhauer *et al.* explains that it is a means of reducing complexity that motivates modelling (2007). Even though a model does not reproduce every piece of knowledge of the biological system, the subsystem can be open to mathematical modelling and reveal new insights. The analysis of the model of the subsystem can explain emergent properties of the biological system not accessible with *in vivo* or *in vitro* experiments and give insight in the complexity of the complete biological system.

For instance, perturbation studies can simulate the model with different inputs, drug combinations or knockouts, by removing or changing specific components of the model.

Biological processes are robust against perturbations which is also supported by the analysis of a variety of mathematical models (Stelling *et al.*, 2004). The non-linearity of the loops complicates the identification and quantification of signalling and gene regulatory network models intuitively, and can therefore not be deeply understood by qualitative representations, drawing pictures such as shown in Figure 2-6. The level of understanding that allows predictions requires quantitative analysis of the mathematical models which represent the dynamics of the system.

Compensation mechanisms complicate the identification of the underlying source of the change in physiological behaviour by measuring components with *in vivo* or *in vitro* experiments. Mathematical models and *in silico* simulation of these models assist in the analysis of the model and allow for the understanding of adaptations with compensation mechanisms, biological switches (bi-stable systems) or rhythms (Tyson *et al.*, 2003). Modelling intrinsic dynamical systems, investigating kinetics such as amplification (Vera *et al.*, 2008) and input-output responses (Schoeberl *et al.*, 2009) have led to new biological insights.

Mathematical models representing the current knowledge of biological networks can be validated with experimental data and allow for the expansion of these networks (Aggarwal & Lee, 2003). Modelling and computer simulations can therefore contribute to the understanding of the dynamics of the regulatory processes and support in the conceptual clarification of the networks (Klipp, 2005). Simulation also makes it possible to carry out virtual experiments replacing those that might be dismissed for being impossible, unethical, expensive or time consuming (Wolkenhauer *et al.*, 2009). The kinetics insights gained from the analysis of the models can also offer guidance in the design of future studies.

#### *2.2.4.1 Dynamic modelling approaches*

A large array of mathematical methods is available to study different levels of kinetic aspects of signalling and gene network regulation (Styczynski & Stephanopoulos, 2005). An overview of the properties of different modelling formalisms and methods is beyond the scope of this thesis and the reader is referred to de Jong (2002). Briefly, mathematical techniques to describe dynamics in signalling and gene networks, started with Boolean logic introduced by Liang et al. (1998) in the algorithm REVEAL (de Jong, 2002). Boolean logic represents an abstract model in the form of undirected graphs and is suited for simple on/off

switches and therefore not informative for the study of the oscillatory behaviour in the NFκB model proposed in this thesis. Boolean models were followed by Bayesian networks, conditionally modelling directed graphs (Hartemink *et al.*, 2002). However, Bayesian networks do not allow for the inclusion of negative feedback loops, essential for the understanding of the NFκB model (van Someren *et al.*, 2002). Ordinary Differential Equations is a mathematical algorithm used in modelling capable of describing the dynamics of quantitative and qualitative aspects of signalling pathways and gene network regulation (de Jong & Ropers, 2006). Ordinary differential equations will be explained in detail in Section 2.3.1 and are the classical formalism for modelling the behaviour of natural systems, rest on a well-established theoretical framework, mathematically robust and therefore form the most prominent approach for the qualitative modelling of signalling and gene network regulations.

## 2.3 Methods and mathematical concepts in signalling and gene network regulation modelling

As described in the previous section, cells transmit external stimuli through signal transduction to the nucleus where gene expression takes place. Different stimuli create a wide variety of activity in signalling pathways activating transcription factors, which through gene regulatory networks induce or repress gene expression patterns. The use of mathematical modelling is important for elucidating the time dependent interaction of proteins that result in behaviour not seen when looking at the proteins in isolation. The complexity of Toll receptor and NFκB signalling that leads to cytokine expression as described in 2.1.3 is a challenging and exciting field to apply these methods/ideas which has not been modelled before and can lead to new insights.

Signalling pathways and gene regulatory network models can visually be represented by graphs composed of nodes, characterizing proteins, mRNA and genes. Edges symbolise the regulatory relationships between the nodes.

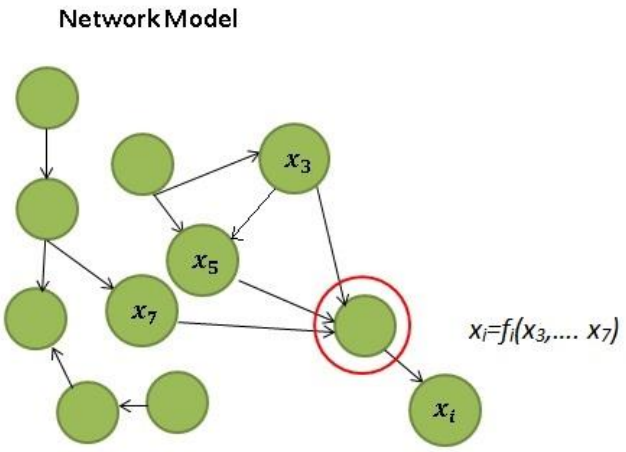


Figure 2-7 Gene network models are represented as directed graphs describing the influence of the levels of one set of transcripts (the inputs) on the level of another transcript (the output). The relation between inputs and outputs is specified by an interaction function ($f_i$) and can be described with ordinary differential equations.

A directed graph (See Figure 2-7) is the most straight forward way to visualize signalling and gene network regulation (de Jong, 2002). However, this will not give information on the dynamics of the network. The time dependent dynamics of the networks can be investigated by translating the directed graph into mathematical formalisms which allows the study of the time dependent dynamics, a process used in systems biology.

### 2.3.1 Ordinary differential equations

Time dependent models require the formulation of differential equations (Chou & Voit, 2009). There are two types of differential equations: ordinary differential equations, describing changes over time, and partial differential equations, describing changes over time and space (Wolkenhauer *et al.*, 2005). While partial differential equations are more appropriate to model intra cellular processes, they require mathematical tools and experimental data not available in most practical cases. Therefore, the focus is on Ordinary differential equations for the simulation and development of the model. Ordinary differential equations arise in many areas of science and technology. The equations are used to describe a deterministic relationship involving continuously changing quantities, and their rates of change, through variables of the equations on a continuous timescale (Klipp, 2005).

If you have a rate of production $\theta$ that increases the concentration of component *X*, where [*X*] measures the concentration of the protein, mRNA or gene, then the change in concentration of *X* is influenced by the parameter $\theta$, also identified as rate coefficient or reaction rate constant, which defines the rate of the reaction $\xrightarrow{\theta} X$ . The rate of change of the concentration of *X* is proportional to the product of concentration of X over time and the rate constant $\theta$. The change of X over time can be represented by the ordinary differential equation $\frac{d}{dt}[X] = \theta X(t)$.

A set of ODEs; one for each of the *n* components, which maybe the expression level of a gene or the concentration of a protein in the model, describes signalling and gene regulation as a function of other genes through reaction rate equations expressing the concentration of mRNA, proteins and other molecules with time dependent variables.

(2-1) $$\frac{dx_i}{dt} = f_i(x_1, .....x_n, u, \theta) \quad x_i(0) = x_{i,0}$$

The components $x_i$ , represent the vector of concentrations *i*=1,…*n* of the mRNAs, proteins and molecules (the nodes in Figure 2-7) extracted from microarray and other experiments. The initial values for each component are given in $x_i(0)$ *i*=1,…*n* and $f_i$ a nonlinear function representing the relationship between the components, *u* the external perturbation of the system and $\theta$ is a set of parameters, the rate constants of the reactions, represented as the edges on the graph in Figure 2-7, describing the interactions among the components. The rate of change, $\frac{dx_i}{dt}$ expresses the change of the component $x_i$ due to phosphorylation, association, transcription, translation or other individual processes included in the nonlinear function $f_i$ as result of the changes of $x_j$ for *j*= 1,….*n* (Klipp, 2005).

Some parameter values in the vector $\theta$ can be measured in biological experiments. Time-course data is most frequently used in gene network regulation models using discrete, continuous or hybrid variables to represent experimental observations (Styczynski & Stephanopoulos, 2005). In this study the amount of time series microarray data is best used for gene network regulation modelling with the middle out approach first described by Noble (Noble, 2002). In the middle out approach modelling is started at the level where there is extensive biological knowledge available (Doyle & Stelling, 2006). We do not seek to find

new networks in this thesis but explore the influence of the kinetics of known signalling pathways with existing models, described in Chapter 4, on the regulation of gene expression in mastitis. Modelling with the middle out approach can reduce the cost and time involved in modelling and biological experiments. Extensions to the model are made with the additional values from the gene expression studies in this thesis. Parameters in a model are a combination of values previously published in the literature, experimental data and fitted values to measured observations (Appendix A 1.2).

### 2.3.2 Parameter estimation, fitting models to data

In systems biology parameter estimation is part of an iterative process to develop predictive models based on experimental data (Ashyraliyev *et al.*, 2009). Parameters that can not be measured directly with biological experiments and are unavailable in the literature, are estimated by fitting the model to input-output data, a process known as model identification, regression or model fitting (Banga & Balsa-Canto, 2008). In biological signalling and gene network models, many kinetic parameters are often unknown, parameter estimation is therefore, highly important.

Parameter estimation techniques use nonlinear optimization to minimize the distance between the model predictions and experimental data. Because of the nonlinearity, estimating parameters can be a complex and time consuming process. A wide range of literature on parameter estimation is available (Banga & Balsa-Canto, 2008; Chou & Voit, 2009; Mendes & Kell, 1998; Moles *et al.*, 2003). In addition, there are many tools and algorithms available for the estimation of parameters. Briefly, parameter estimation is performed by minimizing the cost function, a measure of the distance between the model predictions and the experimental values ( $z = \tilde{y} - y$ ). The cost function is mathematically formulated as a non-linear optimization problem (Balsa-Canto *et al.*, 2008).

Due to the nonlinear nature of the models traditional gradient methods like Levenberg-Marquardt or Gauss-Newton could fail to identify the global solution and converge to a local minimum, while a better solution exists. Therefore, the need to use of global optimization methods that provide a globally optimum solution has been recognized recently (Moles *et al.*, 2003).

In this thesis a Fast Scatter Search developed by Rodriguez-Fernandez *et al.* is used (2006b). Fast scatter search is a combination of local and global optimization techniques which aims to find the unknown parameters of the model that give the best goodness of fit to the experimental data. The goodness of fit is optimized by minimising the cost function which is based on the maximum likelihood estimator.

The maximum likelihood estimator, introduced by Fisher in 1912, is an estimator function that maximizes the probability of the observed event. Maximum likelihood estimation consists of maximizing the likelihood function $j_{ml}$ (2-2). This is the probability density of a model of the occurrence of the experimental values for the given parameters. The likelihood function is dependent on the probability of the experimental values. If these are assumed to be uncorrelated and normally distributed, then the log-likelihood function is given as

$$j_{ml}(\theta) = \frac{N}{2}\ln(2\pi) + \frac{1}{2}\sum_{i=1}^{N}\left[\ln(\sigma_i^2) + \frac{(\tilde{y}_i - y_i(\theta))^2}{\sigma_i^2}\right] \tag{2-2}$$

The log-likelihood gives the same estimate as the likelihood estimation. The maximum likelihood estimates of the parameters $\theta$ are those for which the likelihood function has its minimum for the experimental value $\tilde{y}_i$. If the noise is assumed to be Gaussian with known constant variance, minimizing $j_{ls}$ is equivalent to minimizing the function:

$$j_{ls}(\theta) = w_i\left[\tilde{y}_i - y_i(\theta)\right]^2 \tag{2-3}$$

with $w_i = \frac{1}{\sigma^2}$, which is therefore a weighted least-square estimator. It is assume that all $\sigma_i$ 's are equal, unweighted least-squares are used ( $w_i$ =1) and the maximum likelihood criterion is equivalent to the least squares. The method therefore aims to find $\hat{\theta}$ which minimizes the sum of squared residuals of all responses (Rodriguez-Fernandez *et al.*, 2006a).

Scatter search is a hybrid method using global and local search techniques therefore optimizing the parameter search. However, despite the extensive parameter estimation

technique not all parameters can be estimated uniquely with the given structure of the model and the available experimental data.

### 2.3.3 A priori identifiability analysis of the parameters

Prior to parameter estimation the structural identifiability of a model must be assessed (Jaqaman & Danuser, 2006). The question has to be raised if it is possible to uniquely identify parameters given the structure of the model and the available experimental data? Whether the parameters for a mathematical model can be estimated is the subject of a priori or identifiability analysis (Ashyraliyev *et al.*, 2008). Difficulties during parameter estimation can arise as a result of poor identifiability of the model parameters (Banga & Balsa-Canto, 2008). Prior to parameter estimation it is therefore necessary to evaluate if it is possible, given the structure of the model and the experimental data, assuming error free experimental data, to determine the parameter values (Jaqaman & Danuser, 2006). This is also known as the identifiability problem.

In order to verify the feasibility of the estimation of parameters for the differential equations with the measured data in our experiment, identifiability analysis is performed in SBtoolbox (SBtoolbox is described in more detail in Section 4.3) (Schmidt & Jirstrand, 2006) with the method explained by Jacquez & Greif (1985). A priori identifiability of the parameters for a given experimental setting identifies the correlation between parameters to be estimated with the experimental values of the time series.

Using the values of the parameter set $\theta$ as nominal values, the $N_x$ by M ($N_x$ components $X$ and $M$ parameters in $\theta$) sensitivity matrices $Q(t_i)$ are calculated with the measurements of the experiment at the different time points in the time series. Partial derivatives are used to calculate the ratio of an infinitesimally small change for each $x$ and infinitesimally small change for each individual the parameter in set $\theta$ at each time point. Changes are made for one parameter at a time and the correlation between two parameters at a time is calculated.

(2-4) $$q_{i,j}(t_l) = \left( \frac{\partial x_i(t_l)}{\partial \theta_j} \right) \quad x = x(t,\theta) \;\; l = 1,.....,n \,,\; i \in [1, N_x] ,\;\; j \in [1, M]$$

Stacking the time dependent sensitivity matrices $Q(t)$ gives matrix G

(2-5) $$G = \begin{bmatrix} Q(t_1) \\ Q(t_2) \\ . \\ . \\ Q(t_n) \end{bmatrix}$$

The covariance matrix is then calculated $C=G^{T}IG$, with I the identity matrix since all experimental values have a similar weight. Normalizing the covariance matrix C with the geometric mean of its diagonal elements gives the sensitivity dependent correlation matrix with elements

(2-6) $$r_{i,j} = \frac{c_{i,j}}{\sqrt{c_{i,i}c_{j,j}}}$$

Parameters that are identifiable have a correlation between -1 and +1 with the other parameters. Parameters that are not identifiable have a correlation of -1 or +1 with another parameter. A correlation of -1 or +1 means that the parameters influence the model output in exactly the opposite or the same manner respectively.

With this information parameters can be estimated and the model performance analysed, a process known as sensitivity analysis.

### 2.3.4 Sensitivity analysis of the model

Input factors for mathematical models such as parameters and initial conditions are often not known with a sufficient degree of confidence. Natural variation, error in the measurement or lack of techniques to measure the parameter or initial value all contribute to uncertainty. Estimated parameters are therefore evaluated with sensitivity analysis. Sensitivity analysis is a study into the variation of the critical outcomes of the model and the distribution, qualitative and quantitative, of the different sources, especially changes in parameter values, of these variations in model outputs (Varma *et al.*, 1999). Sensitivity analysis can therefore guide us in determining which parameter values have the largest influence on the model output.

Two types of sensitivity analysis are generally employed to identify the influence of parameter changes on the model output, local and global sensitivity analysis (Ingalls, 2008). Global sensitivity analysis addresses model behaviour over a wide range of parameter values, simultaneously changing parameter values, while local sensitivity analysis concentrates attention near a particular point in the parameter space, changing parameters one at a time.

The parameter estimation method described in 2.3.2 used a hybrid approach, a combination of local and global optimization methods to estimate the parameter values (Rodriguez-Fernandez *et al.*, 2006a). Global optimization methods give a better guarantee to optimal parameter values than other methods such as manual tuning or local parameter optimization methods (Xie *et al.*, 2009). Without a reasonable guarantee of optimal parameter estimation, sensitivity analysis becomes largely ambiguous (Mendes & Kell, 1998). Since a global optimization method was used it can be assumed parameter estimation was optimal and therefore local sensitivity analysis is used to identify the influence from local changes in the parameter values on the model output.

#### *2.3.4.1 Local sensitivity analysis*

In local sensitivity analysis one parameter is changed at a time while the other parameter values are kept to their nominal values. The derivative vector is computed (2-7) to obtain a set of values for the finite parameter changes δ, $s_{ij}(t)$, which allows us to compare the sensitive regions of the output of interest $X$ for each parameter $\theta$. The output of interest $X$ can be any observable such as the concentration at time t of component $X$ ([$X$]) or a combination of the concentrations of several components ([$X_1$], [$X_2$], ....[$X_n$]) at time t. δX stands for the incremental change in X due to the incremental change in $\theta$ or x(0).

(2-7) $$s_{ij}(t) = \frac{\delta(X_i(t)) / X_i(t)}{\delta(\theta_j) / \theta_j}$$

(2-8) $$s_{ij}(t) = \frac{\delta(X_i(t)) / X_i(t)}{\delta(x_j(0)) / x_j(0)}$$

**Time dependent sensitivity**

The local normalized sensitivity of $s_{ij}(t)$ is calculated for each time step *t* of the change in the $i^{th}$ component $X_i(t)$ with respect to the change in the $j^{th}$ parameter $\theta_j$ or initial value $x_j(0)$ (Ihekwaba *et al.*, 2004). Because of the interested in the fit of the model, the component *X* was chosen as the concentration of the cytokine mRNA at time *t* in the 360 minutes simulation period and evaluated for the synthesis and degradation parameter changes.

A uniform distribution of parameter values was created by changing the value of each parameter with incremental steps of 10% from the model parameter -40% to the model parameter +40% and the corresponding change in mRNA cytokine levels recorded. The value $s_{ij}(t)$ will give a sensitivity index for each time step of the model simulation. However, time independent sensitivities would allow us to identify parameters with the highest influence on the cytokine mRNA levels for the total simulation period.

**Time independent sensitivity**

Integration of the sensitivities $s_{ij}(t)$ gives a time-independent value that allows ranking of the individual sensitivities of each cytokine as a result of parameter changes (2-9). *T* is the final time point and absolute value of the integrand prevents positive and negative values cancelling to zero under the integral $x_j(t)$ (Chen *et al.*, 2009). The quantity $S_{ij}$ measures the change in the concentration of the $i^{th}$ component with respect to the $j^{th}$ parameter normalized by *T* and therefore captures variations in concentration level between parameter changes over time.

(2-9) $$S_{ij} = \frac{1}{T}\int_0^T dt|S_{ij}(t)|$$

## 2.4 Methods for microarray analysis: analysing gene expression levels and clustering

It is believed that the difference between individuals is more in the expression of the genes than in the difference between the genomes (Bendixen *et al.*, 2005). With the sequence of the genome available researchers have changed the emphasis from sequence analysis to functional gene analysis. Research into the difference in gene expression in a variety of environments is developing rapidly. In addition, it is becoming clear that genes do not work in isolation and clusters of genes expressed concurrently elicit information on the controlling mechanisms of gene regulation. Therefore, genome wide investigation of gene expression will elicit additional information above the investigation of the expression levels of individual genes.

In the mid 1990s Stanford University published a paper introducing a new technology allowing the quantitative simultaneous monitoring of the expression of thousands of known genes using DNA microarrays (Afshari, 2002). Microarrays are used to compare genome wide gene expression levels between diseased and non-diseased tissues and have become an essential tool for the simultaneous analysis of several thousand genes. Designed to compare difference in gene expression between two treatments or periods in time, microarray data is used to classify cancers, identify the underlying genetic cause of diseases and, recently, define genetic pathways and their regulation. In addition, the expression data is used by systems biologists to develop models of gene network regulation.

### 2.4.1 Microarray analysis

Several different types of arrays are available and a commonly used array is high density oligonucleotide microarray, referred to as Affymetrix arrays. Affymetrix arrays are less noisy and more standardized than the earlier developed cDNA microarrays. The arrays are based on probe pairs of short oligonucleotides, small single-stranded segments of DNA typically 20-30 nucleotide bases in size which are synthesized in vitro to the experimental sample. Each probe pair has a perfect match (PM) and a mismatch (MM) probe that is different in the middle nucleotide from the PM probe. Typically 11-20 of these probe pairs interrogate a different part of the sequence of the gene. Together they form a probe set (Bolstad *et al.*, 2003). The

mRNA of the experimental sample is converted to biotinylated cRNA and only one target, experiment or control, is hybridized to the probes on the array (Figure 2-8). As a result only single colour fluorescence is used in Affymetrix arrays (Allison *et al.*, 2006). The intensity of the fluorescent image can then be analysed.

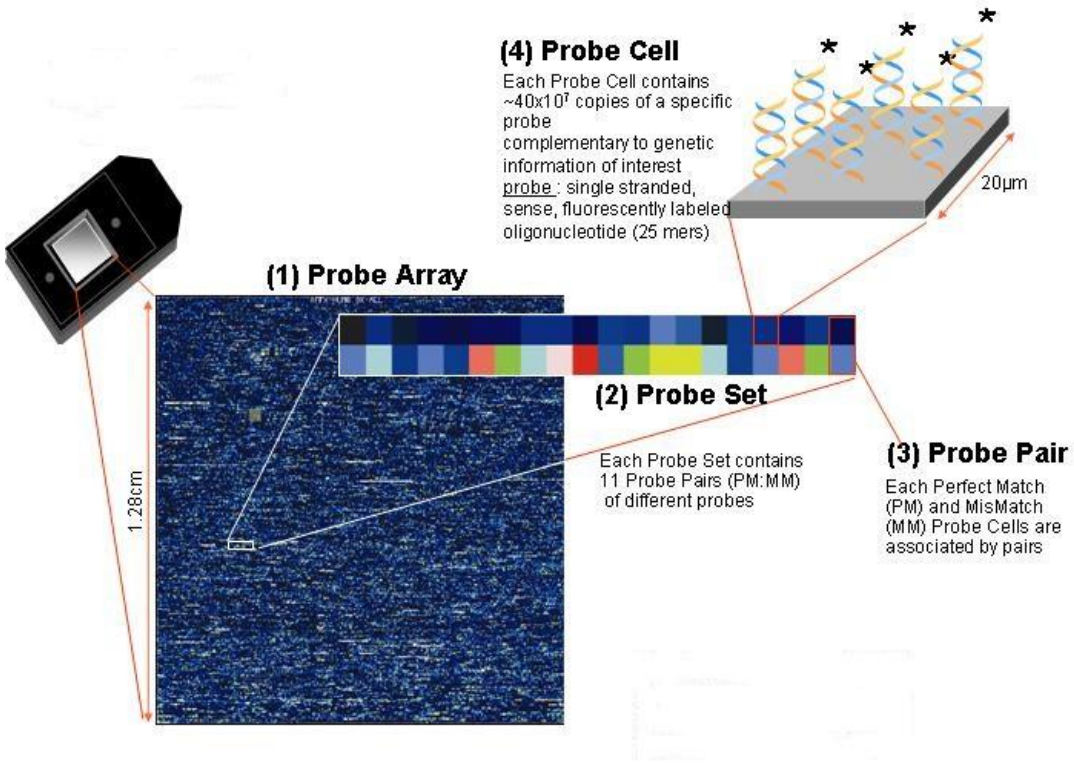


Figure 2-8 Schematic representation of the Affymetrix GeneChip® mRNA expression analysis system. The Probe Array contains ~22,000 Probe Sets on a surface of ~ 1.2 $cm^2$ [5]

Following hybridization, the image is captured and processed for data acquisition. The data is normalized and differentially expressed genes identified as show in Figure 2-9.

[5] Adapted from http://www.weizmann.ac.il/home/ligivol/research_interests.html

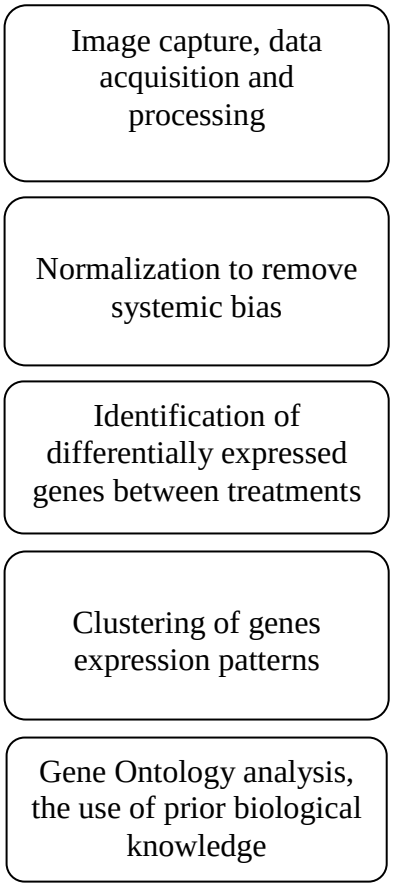


Figure 2-9 Overview of the steps involved in Affymetrix microarray analysis

#### *2.4.1.1 Image analysis*

Image analysis remains an active area of research and many image processing approaches have been developed (Allison *et al.*, 2006). The outcome of the image analysis can have a potentially large impact on the subsequent analysis such as clustering and the identification of differentially expressed genes (Yang *et al.*, 2001). The different processing methods estimate the amount of mRNA from the fluorescent array images, while attempting to reduce variation that can occur due to technical differences between the arrays. Microarrays are inherently noisy technology and replication is used to reduce variability between arrays (Armstrong & van de Wiel, 2004; Seo *et al.*, 2004).

Both open and commercial software, such as Genepix or Imagene (Shippy *et al.*, 2004), are available for the array image analysis. A large, but not complete, sample of possible image software can be found at http://www.dnamicroarrays.info/Image_software.html. These programs use different algorithms to process the scanned images. The analysis involves

gridding or addressing to assign the coordinates of each spot, segmentation to define the foreground and background areas of each spot and intensity extraction (Yang *et al.*, 2001).

#### *2.4.1.2 Normalization*

Normalization is the process that is necessary to allow the comparison of data between and within arrays and is based on the assumption that a subset of genes is expressed at constant rate (Li & Wong, 2001). Normalization removes systematic bias caused by technical variation which does not represent biological variation (Armstrong & van de Wiel, 2004; Yang *et al.*, 2002). The process adjusts and balances the hybridization intensities so that a meaningful biological comparison can be made (Quackenbush, 2002). Following normalization differentially expressed genes can be selected.

Specific packages and modules for the different steps of the microarray analysis allow for the use of different algorithms valid for the evaluation of the hypothesis explicit to the research question. The list of possible software solutions is overwhelming and it would be beyond the scope of this thesis to discuss all packages. Here BRB Array Tools[6] is used. BRB Array Tools is an integrated package for the visualization and statistical analysis of microarray gene expression data using Excel as a front end with analysis models based on R statistical packages developed by Dr. Richard Simon and Amy Peng Lam (Simon *et al.*, 2007). The software allows us to use advanced analysis facilities and intensity dependent non-parametric normalization techniques and identify differentially expressed genes.

Following the identification of the differentially expressed genes, clustering of genes is used to identify additional information.

### 2.4.2 Clustering

Clustering is the assignment of a set of genes into subsets (clusters) so that the genes in the same cluster are similar in some way. Mathematical algorithms provide the option to identify clusters of genes with similar time expression profiles based on mathematical properties. Following normalization, clustering of genes has the potential to reveal meaningful biological

[6] http://linus.nci.nih.gov/BRB-ArrayTools.html

patterns (Bar-Joseph, 2004). Many different clustering methods such as K-means clustering, hierarchical clustering and supervised clustering can be used to identify clusters of co-regulated genes and have been used with gene expression data (Allison *et al.*, 2006).

The existing literature is rich in papers relating to different clustering methods, algorithms and their applications (Draghici, 2003). The two techniques commonly applied to microarray analysis are unsupervised learning and classification, also known as supervised learning or discriminant analysis.

**Unsupervised clustering**

Clustering is unsupervised when the clusters are formed based on mathematical algorithms without the use of biological knowledge. Unsupervised clustering is popular despite the fact that little is known about the validity of this process to support biological interpretation (Allison *et al.*, 2006; Armstrong & van de Wiel, 2004). Neither can these pure mathematical methods capture the biological fact that many gene products are part of more than one biological process (Fang *et al.*, 2006). Unsupervised clustering relies on genes that have discriminatory power, show different expression levels, over the samples or experiments (Armstrong & van de Wiel, 2004). The process is highly dependent on the distance metric used and the same algorithm applied to the same data may produce different results (Draghici, 2003).

In contrast to pattern discovery of unsupervised clustering, supervised learning or classification techniques, also known as discriminant analysis, are designed to classify genes into known groups such as diseases like cancer or biological processes (Armstrong & van de Wiel, 2004). It has been found that supervised learning is more reliable than unsupervised learning (Fang *et al.*, 2006). To overcome this problem Fang *et al.* (2006) combined Gene Ontology (GO) with the mathematical methods of clustering making the analysis of the clusters stable and biological meaningful.

**Gene Ontology**

Gene Ontology provides a formal representation of the knowledge and relationships of the gene properties in three domains; the cellular components, the molecular function and the biological process. Gene Ontology and existing knowledge of biological pathways can be used as prior knowledge in supervised clustering.

**Supervised clustering of short time series**

The incorporation of multi-source information in the form of prior knowledge, such as Gene Ontology, with objective mathematical techniques, can also overcome the problem of oversampling and is used to enhance the supervised clustering of genes in time profiles (Wang *et al.*, 2008). However, not all approaches are suitable for the analysis of short, also known as sparse, between three and eight time points, series (Ernst *et al.*, 2005). In animal studies the high cost of acquiring biological samples and microarrays limits the number of time-points and samples for which data is collected. Limited sampling and the high dimensionality of microarrays can lead to model over fitting (Wang *et al.*, 2008). In addition, noise from the experimental data and microarrays increases the difficulty of differentiating between real and random patterns. This has a greater influence on the analysis of short time-series analysis than on long time series (Ernst *et al.*, 2005).

Ernst *et al.* (2006) developed a tool specific for the clustering of short time series to overcome the restrictions of limited sampling and therefore allow the extraction of meaningful information for further investigation (Ernst & Bar-Joseph, 2006). Their algorithm, Short Time Expression Miner (STEM), is specifically designed to cluster short time expression series. The program selects a set of potential expression profiles representing a unique temporal expression pattern. Each gene is assigned to one of these profiles which represent the different clusters. Predefining the temporal patterns of gene expression is a simplification method that has, as a side benefit, noise reduction in the original data. Therefore, the subsequent clustering in STEM is more robust to noise (Wang *et al.*, 2008).

Ernst *et al.* developed an algorithm, implemented in STEM, to select a set of potential profiles which describe the direction and magnitude of the gene expression with respect to time, differentiating between patterns arising from random noise and patterns arising from biological response (2005). Following the assignment of the genes to the profiles, depending on direction and magnitude of gene expression, STEM identifies the enrichment of genes in each profile based on Gene Ontology which is computed to determine profile significance (Ernst & Bar-Joseph, 2006).

## 2.5 Methods for data processing prior to parameter estimation

Microarray data is increasingly available, however, not extensively used in conjunction with a systems biology modelling approach because microarray analysis results in fold changes. The fold changes give a relative change which compares the change in mRNA expression between diseased and non-diseased cells and therefore does not measure absolute concentration levels in the diseased cell. Ordinary differential equations in the model simulate absolute concentration levels of mRNA expression. To be able to fit the model parameters, the concentration levels from the microarray experiments need to be extracted.

To quantify the concentration levels, a method described by Hekstra *et al.* (2003) was adjusted. The concentration of the expression levels are calculated from the intensity of the fluorescence levels. Fluorescence levels change with the level of hybridization of fluorescently labelled mRNA to the probes on the microarray. The hybridization of the labelled mRNA on oligonucleotide microarrays have also been shown to be affected by sequence of the probe and the chemical saturation properties (Hekstra *et al.*, 2003). Hekstra *et al.* developed a model, using Langmuir absorption and the sequence composition of the microarray probes, which predicts the absolute mRNA concentrations. Additionally, the model accounts for chemical saturation, reducing the compressive bias of differential expression estimates which normally occur at high concentrations.

To implement Hekstra's model, probe nucleotide sequence for bovine Affymetrix ® microarray were extracted from the manufacturer's website http://www.affymetrix.com. Each cytokine is measured on the microarray by 11 perfect match (PM) probes. For each probe the number of A, C and G nucleotides were calculated. With the number of nucleotides in the probe the parameters *a*, *b* and *d* in Equation (2-10) can be calculated. The dependence of the fluorescence is described by *a*, while *d* is the non specific background of the array and *b* can be interpreted as the concentration at which half of the probes are saturated with the complementary RNA if there was no non-specific hybridization (Hekstra *et al.*, 2003).

(2-10)
$$\begin{pmatrix} \ln a \\ \ln b \\ \ln d \end{pmatrix} = \begin{pmatrix} \gamma_A^a & \gamma_C^a & \gamma_G^a \\ \gamma_A^b & \gamma_C^b & \gamma_G^b \\ \gamma_A^d & \gamma_C^d & \gamma_G^d \end{pmatrix} . \begin{pmatrix} n_A \\ n_C \\ n_G \end{pmatrix} + \begin{pmatrix} C^a \\ C^b \\ C^d \end{pmatrix} + \vec{\varepsilon}$$

Where $n_L$ is the number of nucleotides in the sequence of a probe with L= A, C or G, $\gamma_s$ are the nucleotide specific susceptibilities, $C^S$ are the intercepts corresponding to the estimates for *a*, *b* and *d* when the probe sequence would be composed of Ts only and $\vec{\varepsilon}$ is an error term. The total number of nucleotides must add up to 25, the probe length; therefore the number of T nucleotides does not have to be taken into consideration in (2-10). The coefficients $\gamma_C^b$ can be interpreted as the change in $\ln b$ when a C nucleotide is substituted by a T. The values for $\gamma_s$ and $C^S$ were calculated with a calibration data set produced by Affymetrix® by Hekstra *et al.* (2003) and taken from Table 1 in this publication.

Table 2-1 Parameters for the calculation of mRNA concentration (2-10) calculated by Hekstra *et al.* (2003) with calibration data set produced by Affymetrix®. $C^S$ (S is *a*, *b* or *d*) are the intercepts corresponding to the estimates for *a*, *b* and *d* when the probe sequence would be composed of Ts. You can interpret $\gamma_C^b$ as the change in $\ln b$ when a C nucleotide is substituted by a T.

| PM | $C^S$ | $\gamma_A$ | $\gamma_C$ | $\gamma_G$ |
|---|---|---|---|---|
| $\ln a$ | 6.617 | 0.08 | 0.219 | 0.195 |
| $\ln b$ | 0.768 | 0.154 | 0.206 | 0.377 |
| $\ln d$ | 2.533 | -0.305 | 0.035 | 0.168 |

When *x* is a specific target RNA concentration, the fluorescence intensity *I* is given by

(2-11) $$I = a\frac{x}{x+b} + d$$

The intensities *I* for the perfect matching probes from the microarray experiment were extracted from the .CEL Affymetrix intensity files generated in our experiment which will be described in Chapter 3.

From (2-11) the concentration for each probe *p* can be estimated with the calculated parameters *a*, *b* and *d* for each probe.

(2-12) $$x_p = b\frac{I-d}{a+d-I}$$

Probes with $I > a+d$ or $I < d$ will be excluded because they have intensity less than the background intensity or an intensity higher than the saturation level (Hekstra *et al.*, 2003).

Eleven probes form a perfect matching probe set representing a specific gene. The probe set concentration is then estimated by (2-13) where (‘) means the probe set with the probes where $I < a+d$ or $I > d$ have been removed and n’ the number of the probes included in the new set.

(2-13) $$\log(x_{probeset}) = \frac{1}{n'}\sum_{p}\log(x_p)$$

# Chapter 3
# *E. coli* and *S. aureus* mastitis microarray gene expression analysis

*In this chapter the microarray analysis of the two bacterial challenges on mammary epithelial cells is described. The first Section describes the experimental setup and the microarray analysis identifying the differentially expressed genes between diseased and non diseased state. This is followed by clustering of the genes for each bacterial challenge and a comparison of the genes in the clusters between the two bacterial challenges. The comparison is necessary to elicit the clusters and the genes in the clusters which identify the difference in regulation between the two bacterial challenges. From these genes the most likely candidates that will lead to the differentiation in disease presentation between the two challenges are chosen. In the last section the genes of interest for the model are identified and the results discussed.*

## 3.1 Microarray analysis

Scanned Affymetrix microarray data files were made available to us by Professor H-M Seyfert from the Research Institute for the Biology of Farm Animals (FBN) in Dummerstorf, Germany. The microarray experiments are part of the EADGENE (European Animal Disease Genomics Networks of Excellence for Animal Health and Food Safety) network studies in mastitis and the experimental setup is described in full in Petzl *et al.* (2008). Briefly, mammary tissue samples from three healthy cows were taken. First tissue cultures of samples of primary bovine Mammary Epithelial Cells (pbMEC) were grown in a medium as described by Yang *et al.* (2006). Secondly the cultures were challenged with *E. coli* and *S. aureus* bacteria in two different experiments. Samples were collected 0, 1, 3, 6 and 24 hours after the challenge for each bacterium. mRNA was then extracted and applied to the Affymetrix microarrays according to the manufacturer's instruction. The Microarrays were scanned at 1.56 micron resolution using the GeneChip Scanner 3000 (Affymetrix).

The analysis was applied to the provided Affymetrix microarray scanned CEL files. CEL files contain the fluorescence intensity of the scanned microarrays. The result of the analysis of the

time series microarray chips is described below and is then used for the development of the proposed model. In addition to the identification of differentially regulated genes, the use of standard bovine Affymetrix microarrays facilitates pathway analysis and the conversion of fluorescence intensity to concentration levels which is described in Section 2.5. Concentration levels of mRNA over time are used in gene network regulation models and are therefore important for the development of the mastitis model in our study.

### 3.1.1 Identifying differentially regulated genes

The first objective was to establish a list of genes that are differentially expressed between challenged and non challenged mammary epithelial cells. Scanned microarray data was imported in BRB Array tools. BRB Array Tools 3.5.1 is used to normalize the 30 Affymetrix bovine microarray chips and identify the differentially regulated genes (Simon *et al.*, 2007). The analysis of the microarrays for the three cows in each challenge identified 1960 genes with significant different expression (fold change > 1.5, $p<0.01$) at one or more time points for each of the bacterium.

The large number of genes can be explained by the fact that more than one function changes as a result of the bacterial challenge. Apoptosis, involution and the immune reaction all induce gene expression in the bacterial challenge (Viatour *et al.*, 2005).

### 3.1.2 Clustering of the differentially expressed genes

The microarray analysis described in the previous section produced a list of differently expressed genes. To identify clusters of significantly different time profiles between the two bacterial challenges, the experiments were clustered separately for each bacterium, followed by a comparison of the two bacterial challenges. Two pre-processed data-sets of the *E. coli* and *S. aureus* challenge, with the earlier identified 1960 differentially expressed genes, were submitted to STEM (Ernst & Bar-Joseph, 2006). The STEM clustering method (described in more detail in Section 2.4.2) with a maximum number of 50 profiles was used. The maximum unit change in the model profile between the change of the maximum and minimum of the two time points with a significance of $p <= 0.05$ and Bonferroni correction was applied.

Clustering identified eight statistically significant time profiles representing 566 genes in the *E. coli* microarrays (Figure 3-1). The remaining genes could not be assigned to a profile with statistical significance.

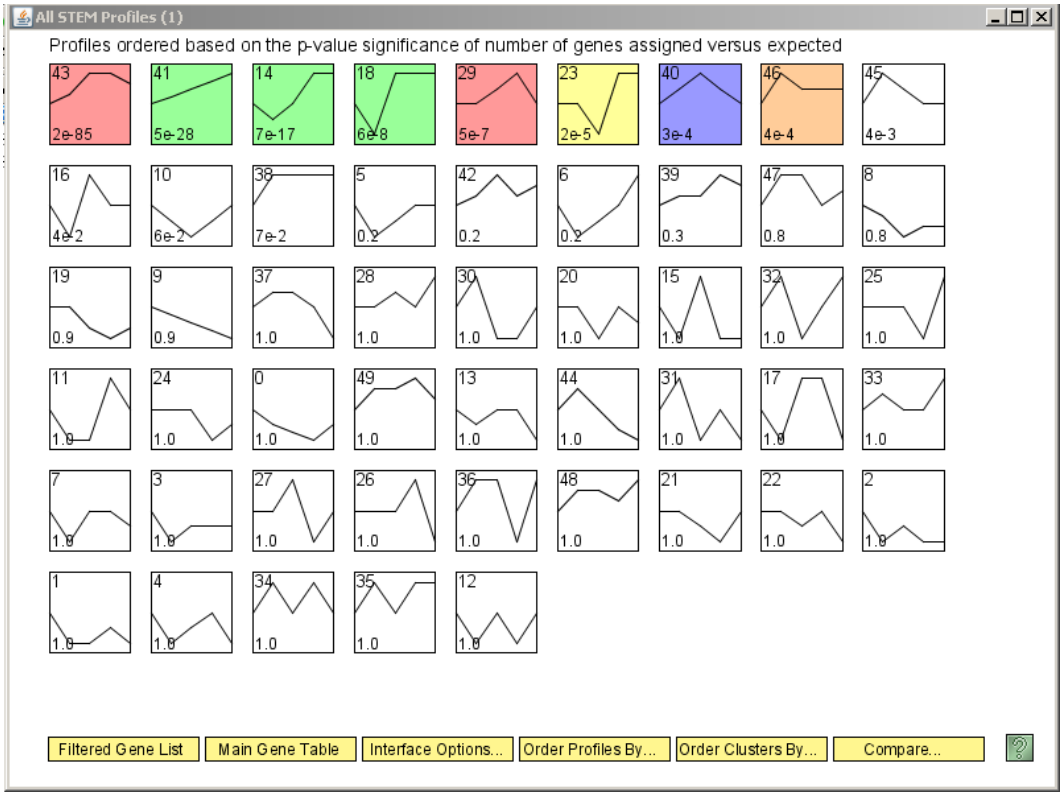


Figure 3-1 The clustering results of the STEM (Short time expression mining) algorithm for the time profiles in the *E. coli* challenge. In the top left corner of each profile is the profile number, and on the bottom the p-value for the significance of the number of genes assigned. Colored blocks represent (arbitrarily numbered) profiles with a significant number of genes assigned to the profile, while white blocks contain profiles without a significant number of genes. The colors represent the trend of the time profile.The x-axis represents the time while the y-axis represents the expression level.

Clustering the genes in time profile narrowed the possible genes of interest down to 64 genes in three time profiles in the *S. aureus* experiment (Figure 3-2).

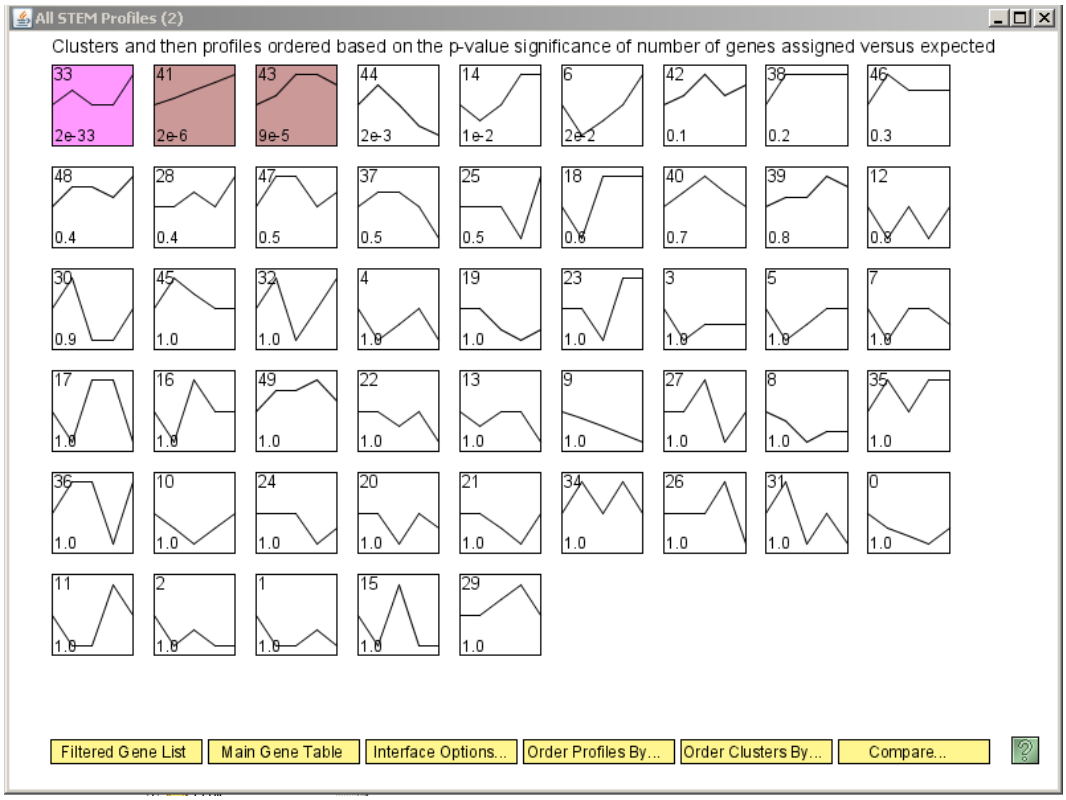


Figure 3-2 The results of STEM(Short time expression mining) clustering of the time profiles in the *S. aureus* challenge. In the top left corner of each profile is the (arbitrary assigned) profile number, and on the bottom the p-value for the significance of the number of genes assigned. Colored blocks represent profiles with a significant number of genes assigned to the profile, while white blocks contain profiles without a significant number of genes. The colors represent the trend of the time profile. The x-axis represents the time while the y-axis represents the expression level.

The clustering results from STEM left us with more than 500 genes in six different time profiles (profile 41 and 43 are represented in both bacteria) to investigate. The lack of differential regulation in *S. aureus* could mean a difference in regulation responsible for the differentiation in the disease profile and can therefore not automatically be excluded from the analysis.

### 3.1.3 Comparative clustering

Unlike other available methods, STEM supports the comparison of multiple data sets (Ernst & Bar-Joseph, 2006). Mathematical comparison without the use of prior biological information for the two experiments identified three sets of time profiles Figure 3-3.

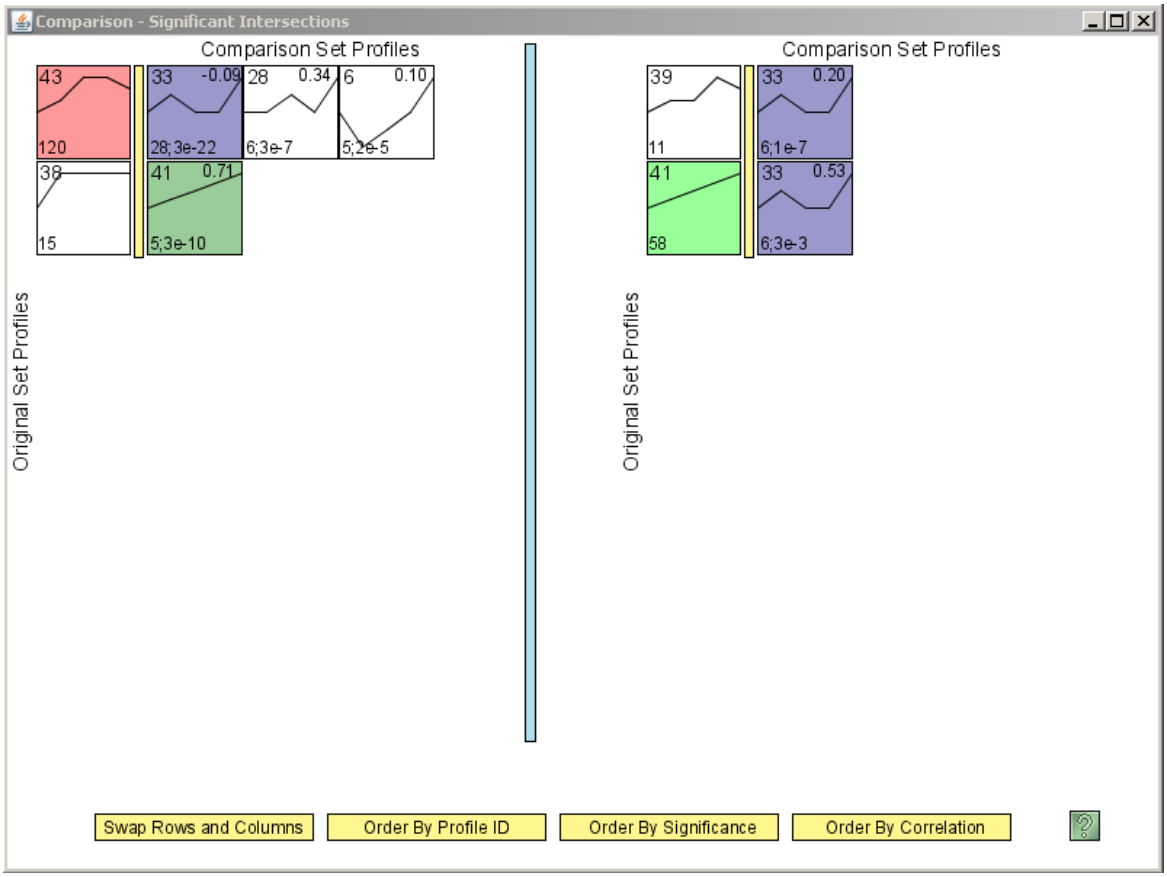


Figure 3-3 In order to identify genes with significantly different time profiles between the two bacterial challenges, comparisons of the allocation of genes to the clusters between the bacterial challenges are performed in STEM. Clusters with significantly different allocation of genes are presented in this figure. In the two blocks on the far left: genes allocated to profile 43 for the *E. coli* experiment are identified since the same genes are allocated to cluster 33 in the *S. aureus* challenge. In the two blocks on the far right: genes significantly differently expressed in the *S. aureus* challenge are allocated to profile 33, while the same genes are allocated to profile 41 in the *E. coli* challenge. The x-axis represents the time while the y-axis represents the expression level.

The identified difference in clusters of gene expression included 75 genes for the *E. coli* challenge, cluster 43, and 6 genes for the *S. aureus* challenge, cluster 33. Of these, 6 genes appear in the intersection of the genes in the clusters, indicating a difference in time profile between the two bacterial challenges for the expression for these genes. This is a notable reduction in potential candidates. This leaves still a large number of genes to investigate. Prior biological knowledge of the scientists involved in a study is always used to narrow down the focus of an experiment or results. There is a danger of focussing only on the area established in earlier research. In this study, prior biological knowledge represents the use of large datasets (Gene Ontology) containing an amalgamation of biological knowledge from different research as explained in Section 2.4.2.

The result for the STEM analysis of profile 43 are shown in Table 3-1 with the most significant group of genes ($p<0.001$) differentially expressed from the expected value is a group of five genes in the immune response (GO:0006955) category. The genes represented in this category are listed in Table 3-2.

Table 3-1 GO Results for STEM Profile 43 in the *E. coli* challenge based on the actual number of genes assigned to the profile (GO Gene Ontology).

| Category ID | Category Name | #Genes Category | #Genes Assigned | #Genes Expected | #Genes Enriched | Corrected p-value |
|---|---|---|---|---|---|---|
| GO:0006955 | immune response | 48 | 13 | 2.9 | 10.1 | <0.001 |
| GO:0006915 | apoptosis | 17 | 6 | 1 | 5 | 0.022 |
| GO:0012501 | programmed cell death | 17 | 6 | 1 | 5 | 0.022 |
| GO:0008219 | cell death | 18 | 6 | 1.1 | 4.9 | 0.028 |
| GO:0016265 | death | 18 | 6 | 1.1 | 4.9 | 0.028 |
| GO:0004872 | receptor activity | 41 | 9 | 2.5 | 6.5 | 0.032 |
| GO:0048869 | cellular developmental process | 27 | 7 | 1.7 | 5.3 | 0.036 |
| GO:0030154 | cell differentiation | 27 | 7 | 1.7 | 5.3 | 0.036 |
| GO:0048468 | cell development | 20 | 6 | 1.2 | 4.8 | 0.038 |

Table 3-2 Five identified genes in the intersection between STEM profile 43 (*E. coli* challenge) and 33 (*S. aureus* challenge) of the GO category GO:0006955 with distinctly different time profiles between the *E. coli* and *S. aureus* challenge (Bt.60918 previously Bt9296). (UG Uni Gene, GB accession Gene Bank accession)

| UG | Name | GB accession |
|---|---|---|
| Bt.20891 | OAS1 | CK960499 |
| Bt.24855 | tumor necrosis factor (ligand) superfamily, member 13b | BE753440 |
| Bt.4675 | interferon-induced GTP-binding protein Mx1 | NM_173940.2 |
| Bt.552 | chemokine (C-C motif) ligand 5 (RANTES) | NM_175827.2 |
| Bt.60918 | similar to Interferon- induced guanylate-binding protein 1 (GTP-binding protein 1) (Guanine nucleotide-binding protein 1) (HuGBP-1) | CK957199 |

Comparing the time profiles of the five genes between the two bacterial challenges in Figure 3-4 shows that both were elevated at 24 hours. Gene expression in the *E. coli* challenge had increased in the first 6 hours, returning to lower values 24 hours after the challenge. In contrast, the gene expression in the *S. aureus* challenge did not show an increase in the first 6 hours and increased in expression between 6 and 24 hours.

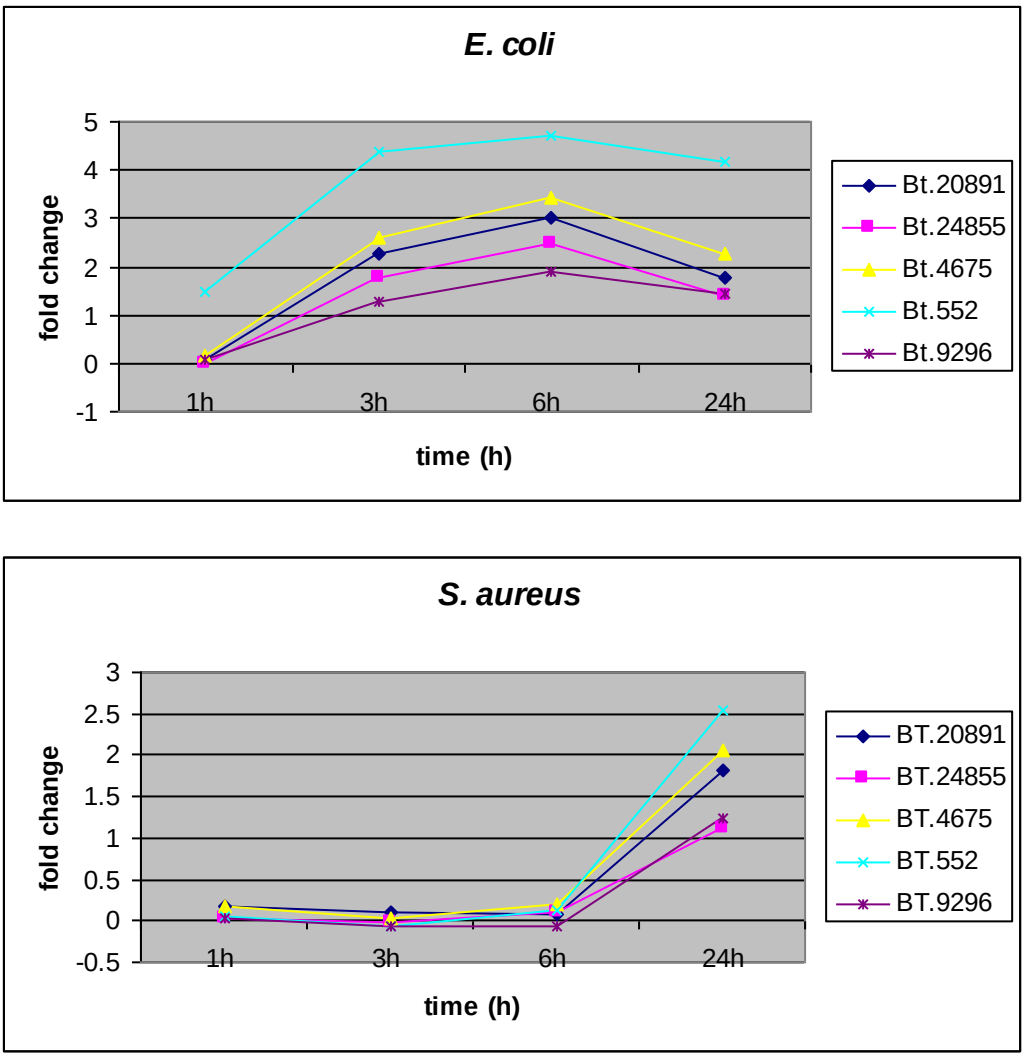


Figure 3-4 Time profile of the 5 genes in the *E. coli* and *S. aureus* challenge in the intersection of STEM profile 43(*E. coli*) and 33 (*S. aureus*). These genes are identified as having significantly different time expression profiles between the two bacterial challenges in mammary epithelial cells.

All differentially expressed genes identified in our initial microarray analysis in Section 3.1.1 from the *E. coli* challenge were submitted to the Toll receptor signalling pathway (See Figure 3-5) and compared with the differentially expressed genes in the *S. aureus* challenge (See Figure 3-6). A markedly different level of mRNA expression in the Toll Receptor signalling pathway between the two bacterial challenges can be seen.

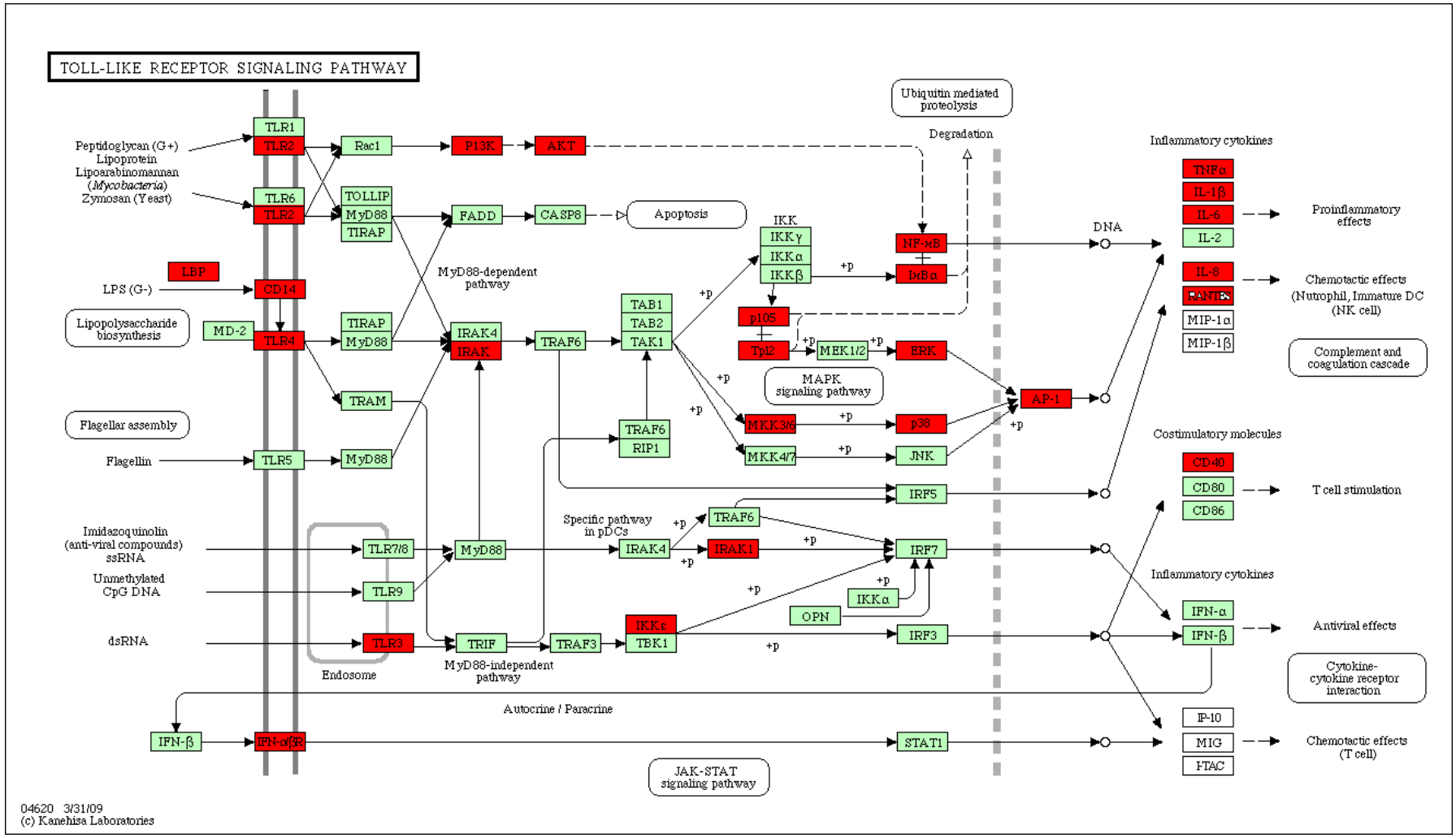


Figure 3-5 Bovine Toll-like receptor signalling pathway adapted from KEGG with in red the genes identified as differentially regulated (fold change > 1.5, p <0.01) from healthy cells in the *E. coli* challenge at any time point in the BRB Array Tools analysis.

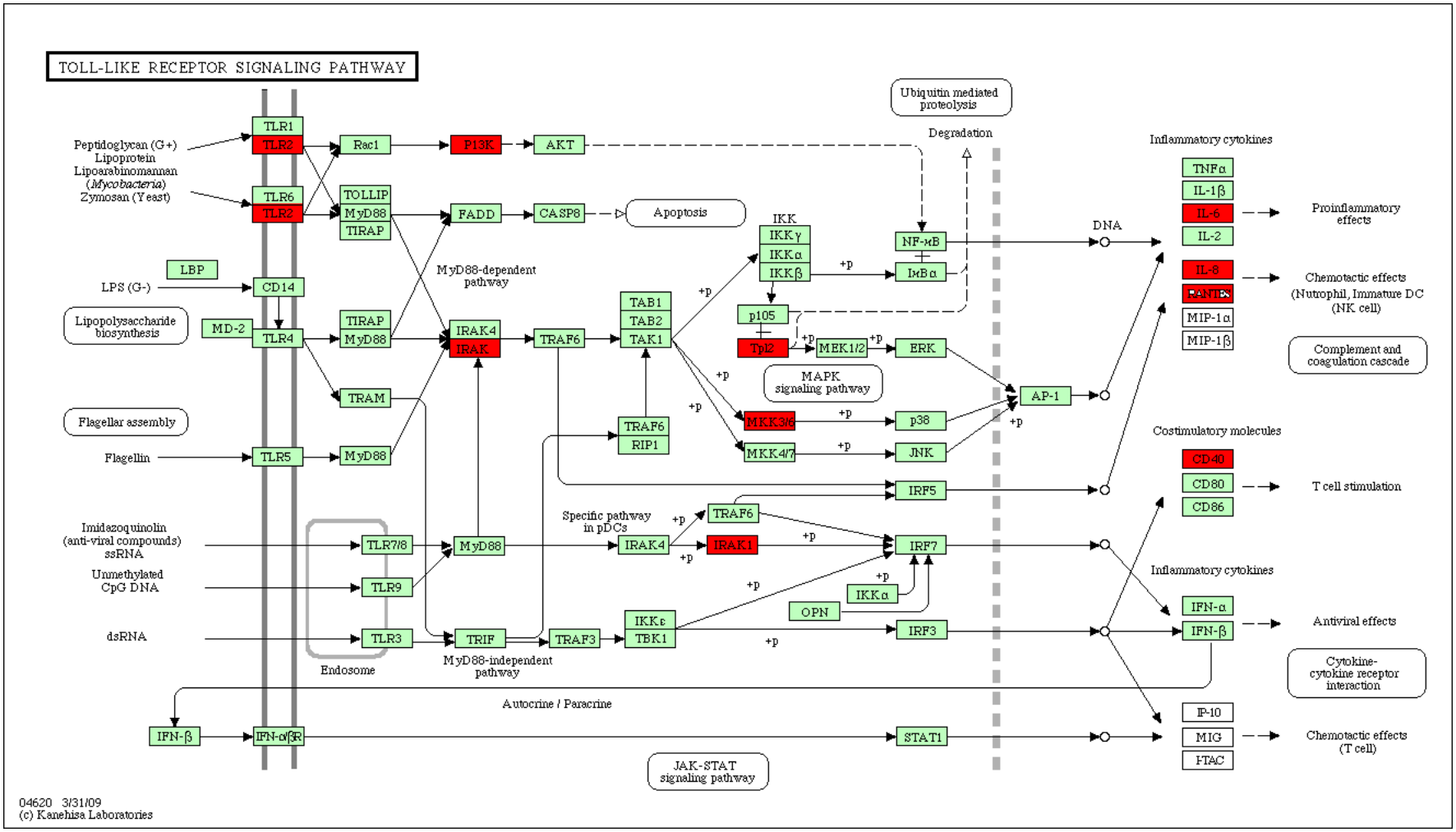


Figure 3-6 Bovine Toll-like receptor signalling pathway adapted from KEGG with in red the genes identified as differentially regulated (fold change > 1.5, p <0.01) from healthy cells in the *S. aureus* challenge at any time point in the BRB Array Tools analysis.

The cytokines RANTES, IL8 and TNFα are differentially expressed between the two bacterial challenges. Differential cytokine induction between *E. coli* and *S. aureus* mastitis in milk is believed to be responsible for the differentiation in the disease profile (Bannerman *et al.*, 2004; Riollet *et al.*, 2000).

### 3.1.4 Cytokine expression levels

RANTES, IL8 and TNFα have a common transcription factor, NFκB, which initiates the gene expression of these cytokines (See Figure 3-5). The transcription factor NFκB is the most important *cis*-regulatory element controlling TNF-induced RANTES expression (Casola *et al.*, 2002). IκBα expression is also regulated by NFκB and forms a feedback loop on the NFκB translocation to the nucleus. Therefore the expression level of IκBα mRNA was also investigated.

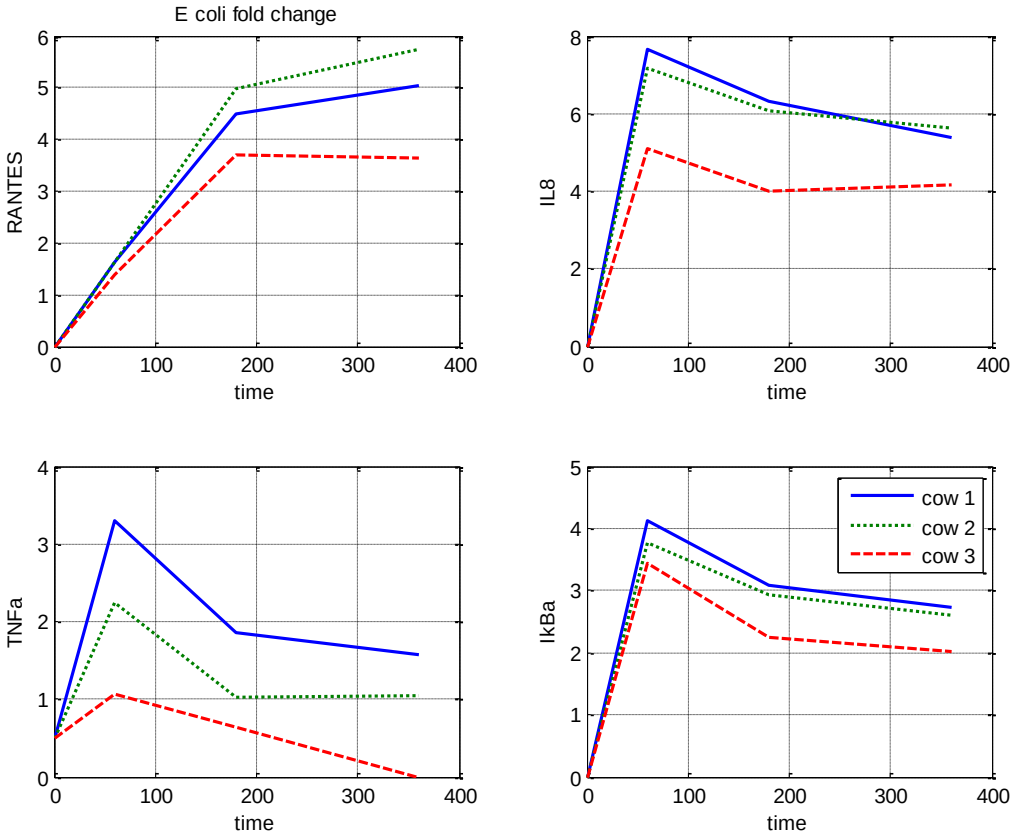


Figure 3-7 Relative fold changes(log2) of microarray mRNA expression levels between no infection and infection for three different cows as result of *E. coli* challenge.

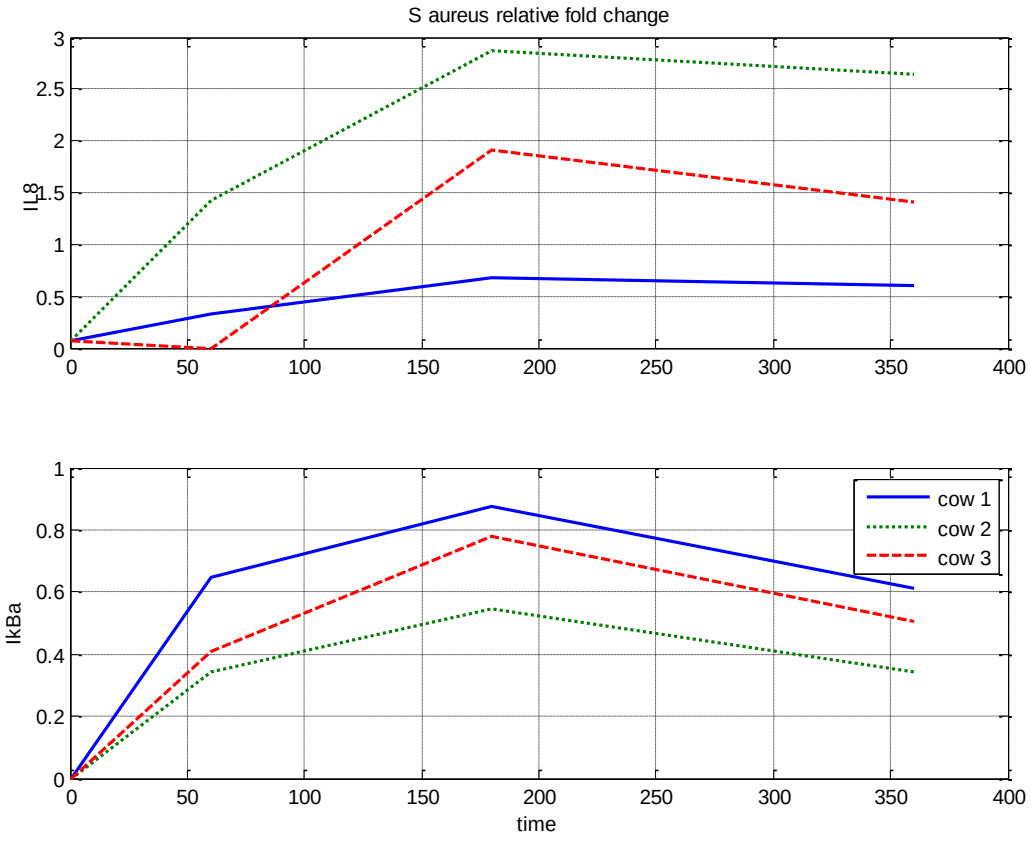


Figure 3-8 Relative fold changes(log2) between no infection and infection of microarray mRNA expression analysis for three different cows as the result of *S. aureus* challenge

The cytokines RANTES, IL8 and TNFα were expressed in *E. coli* challenge Figure 3-7), while the *S. aureus* challenge only identified differentially expressed IL8 mRNA levels (Figure 3-8). There was also a clear difference in expression level and pattern of IκBα between the two bacterial challenges. While the *E. coli* challenge elicit a sharp increase in IκBα in the first hour followed by a reduction in the IκBα expression levels, the *S. aureus* bacterial challenge showed a rise in fold change from the first to the third hour in the mammary epithelial cells.

## 3.2 Discussion

In this chapter the genes differentially expressed in the epithelial cells between the healthy and diseased cells and the genes differentially expressed between the two bacterial challenges were identified. Identifying the genes differentially expressed in the epithelial cells between the two bacterial challenges leads us to the identification of the signalling pathway and gene network that contributes to the gene expression in the disease differentiation. This signalling pathway and gene network regulation can be modelled and interrogated with a systems biology approach to identify the underlying mechanistics of the differentiation.

Investigating gene expression time-series analysis of cDNA microarray in *E. coli* mammary infection has been performed in a previous study on an existing set of cDNA microarrays by van Loenen-den Breems *et al.* (2008). In this study a pipe line of bioinformatics tools was applied, using Gene Ontology and clustering to a set of differentially expressed genes in the mammary gland to cluster gene expression time profiles and identify biological pathways involved in the disease. The study identified four pathways to be involved in *E. coli* mastitis. Modelling the interaction of the four pathways would lead to a very complex model and requires extensive biological experiments which are not feasible in this thesis. In addition, the experiments were performed on the mammary tissue, and as identified in Section 2.1.1 not only an inflammatory response, but apoptosis, milk production and other functions are performed in the mammary gland. The experimental setup therefore did not facilitate the separation of pathway involvement between the different functions of the mammary gland.

To separate the pathway involvement and identify the most important pathway and genes in the inflammatory response we therefore set out to identify the difference in regulation between two types of mastitis, gram positive and gram negative, *E. coli* and *S. aureus,* mastitis in mammary epithelial cells. In our knowledge, comparative studies with genome wide gene expression profiles resulting from gram negative and gram positive bacterial challenges of mammary epithelial cells, over several time steps have not been performed before.

Rather than looking at lists of genes, clusters of genes with specific functionality defined in Gene Ontology groups that differed in expression time profile between the two bacterial challenges were identified. This resulted in the identification of five genes of the immune response category (GO:0006955). These genes are believed to be regulated by the IFNα/β (Noppert *et al.*, 2007). The IFNα/β receptor is also involved in STAT5 signalling which is

suggested to play a role in mastitis in neutrophils in milk (Boutet *et al.*, 2004). However, the work in this thesis involves mammary epithelial cells with the focus to identify one signalling pathway in the differentiation between two bacterial challenges.

RANTES, one of the five identified genes in the cluster, had been identified earlier as up regulated with LPS challenged mammary epithelial cells (Pareek *et al.*, 2005). LPS, as explained in Section 2.1.2, is found on the cell wall of *E. coli* bacteria and used to simulate bacterial infection in cell cultures. Pareek *et al.* indicated that the mammary epithelial cells are the source of RANTES expression in a LPS challenge (2005), which was confirmed in our experiment.

RANTES is expressed as the result of the signalling process of the Toll receptor signalling pathway and the transcription factor NFκB (See also Section 2.1.2). The Toll receptor signalling pathway was identified as one of the four signalling pathways in mastitis by us (van Loenen-den Breems *et al.*, 2008). The involvement of Toll like receptors in the innate immune defence in the udder against *E. coli* and *S. aureus* mastitis was later confirmed in other biological experiments after our microarray studies by Petzl *et al.* (2008). These studies confirmed the findings of Rainard & Riollet (2006) and De Schepper *et al.* (2008) of the involvement of pro-inflammatory cytokines, such as TNFα, IL-1, IL-6, the chemokines IL8 and RANTES and Toll receptor signalling in mastitis. In more recent studies, also performed after our experiments, RANTES has been reported as differentially expressed between *E. coli* and *S. aureus* challenges of mammary epithelial cells (Griesbeck-Zilch *et al.*, 2008). The role of cytokines and mammary epithelial cells in the immune defence of the mammary gland was emphasized in studies by Lahoussa *et al.* (2007).

Variance in cytokine expression is believed to be responsible for the different clinical profiles in mastitis (Bannerman *et al.*, 2004). However, it had not been shown what caused the difference in the expression time profile of RANTES between *E. coli* and *S. aureus* epithelial challenges. LPS on the *E. coli* cell membrane initiates TLR4 signalling (Figure 3-5). *S. aureus*, as explained in Section 2.1.2, has LTA on the bacterial cell wall and initiates TLR2 signalling (Figure 3-6). TLR signalling, TLR2 and TLR4, regulates NFκB transcription factor translocation to the nucleus. NFκB is a transcription factor which initiates cytokine gene expression. NFκB has been recognized as the 'master switch' in regulating the expression of various cytokines in the immune defence response (Hayden *et al.*, 2006). The activation of NFκB has been linked with mastitis (Connelly *et al.*, 2010).

The NFκB activation of cytokine expression in mastitis is sustained with LPS but not with LTA and the role of NFκB in this regulation is unclear. The cause of the difference in expression of RANTES, IL8 and TNFα between *E. coli* and *S. aureus* challenged mammary epithelial cells has not been identified at this stage. Therefore, the results of our analysis indicate the need for further investigation into the effect of NFκB regulation on cytokine expression as result of the Toll receptor signalling in mastitis. Differentiation in cytokine expression causes differentiation in disease profile.

Describing the regulation of NFκB on the cytokines gene expression levels can not be achieved with gene expression or protein concentration lists at different time points alone. Feedback loops, such as the negative feedback loop initiated by IκBα expression, and compensation mechanisms are involved in NFκB activation. Therefore, the effect of the NFκB regulation on the gene network regulation in mastitis should be modelled with a systems biology approach. In Section 2.2 the use of mathematical modelling was introduced. In the following chapters a model is developed to represent and analyse the cytokine mRNA expression dynamics in mammary epithelial cells as a result of the bacterial challenges.

# Chapter 4
# NFκB signalling model

*In this thesis the mechanistics responsible for cytokine expression in mammary epithelial cells are under investigation. Cytokine expression is initiated by the NFκB transcription factor in the nucleus of the cell. Understanding the regulation of the translocation of the NFκB transcription factor from the cytoplasm to the nucleus and its influence on cytokine expression is therefore of particular interest to us. While Section 2.1.3 described the biology of NFκB regulation, this chapter introduces a mathematical model previously developed to investigate the regulation of the translocation of the NFκB transcription factor between the cytoplasm and nucleus. NFκB models have been developed in the past and using an existing model reduces time and cost. The described model will become a part of our model for cytokine expression in mastitis, which will be developed in Chapter 5.*

*In Section 4.1 the conceptual model is explained. Section 4.2 describes the special features of the model; the input function used to represent the different bacterial challenges, the model output, feedback loops and highlights assumptions of the model. Our implementation of the model is described in Section 4.3. This implementation performed identically to the published model.*

## 4.1 Mathematical modelling of NFκB regulation

The transcription factor NFκB is a central mediator in inflammatory response and involved in several diseases such as mastitis (Boulanger *et al.*, 2003; Boutet *et al.*, 2007; Connelly *et al.*, 2010; Notebaert *et al.*, 2008a; Notebaert *et al.*, 2008b), cancer, diabetics and arthritis (Bragt *et al.*, 2009; Cheong & Levchenko, 2008; Kumar *et al.*, 2004). As a result and the nonlinearity of the interactions responsible for NFκB regulation, information gained from biological experiments is often limited and therefore there has been a high interest in mathematical modelling of NFκB regulation (Cheong *et al.*, 2008).

The conceptual model for NFκB regulation described in Section 2.1.3 is shown in Figure 4-1. The model was first implemented by Hoffmann *et al.* in (2002a). A mathematical model was implemented to investigate the dynamical control of NFκB regulation and the role of the IκB

on the signalling process. Since then several other researchers have used and extended this model in a wide variety of studies (Cheong *et al.*, 2008; Cheong *et al.*, 2006; Kearns & Hoffmann, 2008; Lipniacki *et al.*, 2004; Werner *et al.*, 2005).

In this thesis the work is based on the model extensions and parameter values developed by Werner *et al.* (2005). The model included feedback loops and was calibrated against LPS challenge. In this thesis cytokine mRNA expression as a result of the LPS challenge in mammary epithelial cells is investigated. The model developed by Werner *et al.* (2005) is based on experimental values in similar experiments and therefore the model was most suited for our investigations.

## 4.2 Model description

Based on the conceptual model in Figure 4-1 the scope of the model in terms of the reaction components and reactions are described. First the model components are described (Section 4.2.1). In addition to the components the model reactions are defined and together form the model. The reactions were formulated as uni-, bi- and tri-molecular processes according to the law of mass action based on the biochemical reactions that are linked together. An equation for the rate of change is written for each component. The equation can have many terms, depending on the number of reactions in which the component participates. The law of mass action is based on diffusion of components (in the cytoplasm and nucleus), collisional interaction, and binding and unbinding, such that effective rates of production or degradation are proportional to the concentration of each component that contributes to the reaction.

The reactions of the IκB isoforms and all complexes with IκB (Section 4.2.2) are presented. In Section 4.2.3 we will present the IKK reactions which play an important role in the model input, in Section 4.2.4 nuclear NFκB, the model output and in Section 4.2.5 the reactions involved in the feedback loops in the model are discussed. The complete list of mass action equations can be found in the supplementary material (Table A- 1), and is compiled from previously published work (Hoffmann *et al.*, 2002a; Werner *et al.*, 2005).

The nomenclature of reaction rates use the same format of those proposed in (Werner *et al.*, 2005). They are of the form X_Y_Z, with X the action; pd is protein degradation, ps protein synthesis, a association, d degradation, Y the location of the reaction; c cytoplasm, n nucleus,

and Z the component involved; i for IKK, n for NFκB and a, e, b the three IκB isoforms; IκBα, IκBβ and IκBε.

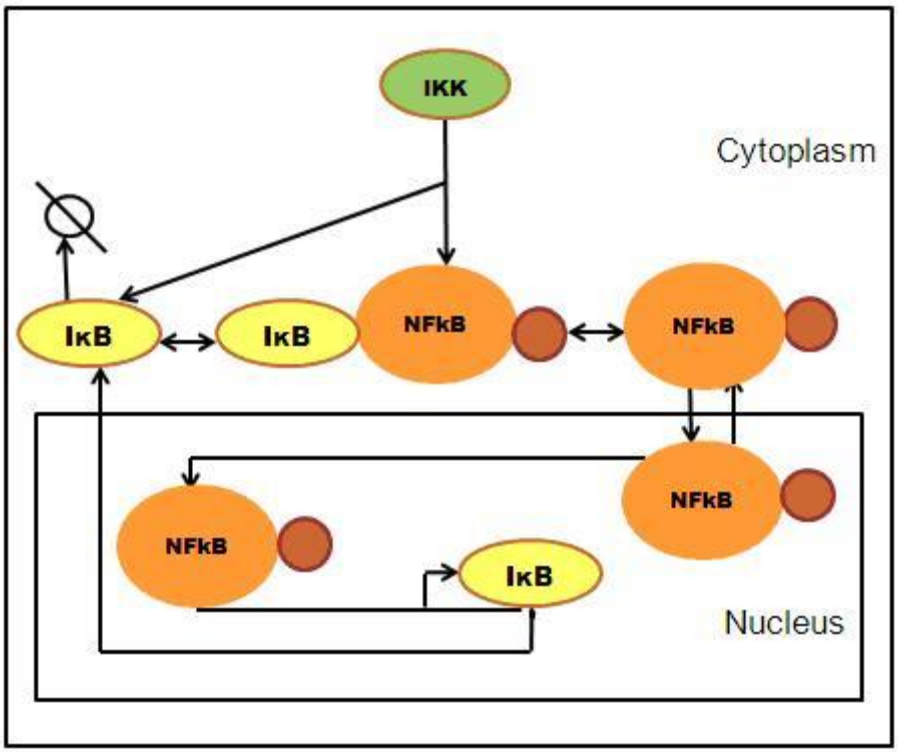


Figure 4-1 Conceptual model of NFκB signalling implemented by Hoffmann *et al.* (2002a).The activated kinase IKK breaks the IκB-NFκB dimer. As a result the transcription factor NFκB translocates to the nucleus. Gene expression is initiated. Among the genes expressed are the IκB isoforms which bind with NFκB in the cytoplasm to prevent translocation of NFκB to the nucleus. This process creates a negative feedback loop for the translocation of NFκB to the nucleus.

### 4.2.1 Model components

The model includes 24 proteins which are changing dynamically and their concentrations are the modelled components (Table 4-1). The model is divided in two compartments, representing cytoplasm and nucleus (Figure 4-1). Compartmentalization was achieved by representing a single protein as multiple components, one for each compartment. Each component is represented by their molecular name in the cytoplasm, e.g. IκBα, and their molecular name followed by an n, IκBαn, representing the protein form in the nucleus or followed by a t, representing the mRNA of this molecule in the nucleus (Table 4-1). Protein

transport was modelled as movement of components between the compartments with first order kinetics making the process computationally tractable.

Table 4-1 Reaction components and their location in the NFκB model implemented by Werner *et al.* in 2005.

| component | location |
|---|---|
| IκBα | cytoplasm |
| IκBαIKK | cytoplasm |
| IκBαIKKNFκB | cytoplasm |
| IκBαNFκB | cytoplasm |
| IκBαNFκBn | nucleus |
| IκBαn | nucleus |
| IκBαt | nucleus |
| IκBβ | cytoplasm |
| IκBβIKK | cytoplasm |
| IκBβIKKNFκB | cytoplasm |
| IκBβNFκB | cytoplasm |
| IκBβNFκBn | nucleus |
| IκBβn | nucleus |
| IκBβt | nucleus |
| IκBε | cytoplasm |
| IκBεIKK | cytoplasm |
| IκBεIKKNFκB | cytoplasm |
| IκBεNFκB | cytoplasm |
| IκBεNFκBn | nucleus |
| IκBεn | nucleus |
| IκBεt | nucleus |
| IKK | cytoplasm |
| NFκB | cytoplasm |
| NFκBn | nucleus |

### 4.2.2 Model reactions of IκB isoforms

Reactions which are represented with the component IκB, or a complex with IκB, are a representation of the reactions of all three isoforms of IκB (IκBα, IκBβ and IκBε) (Figure 4-2). In the model the reactions are implemented in triplicate, one for each isoform. Here we show one form for clarity.

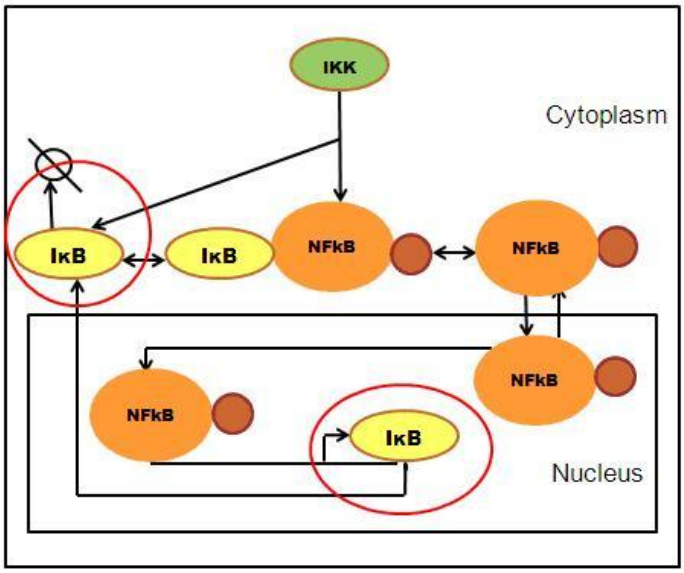


Figure 4-2 Conceptual model of NFκB signalling. The model reactions of the IκB isoforms are circled in this figure. The IκB isoforms influence the rate of translocation of NFκB to nucleus with a negative feedback loop and the reactions involved are discussed in this section.

The rate of change in the concentration of free IκB isoforms in the cytoplasm is modelled as:

$$\begin{aligned}\frac{d[IkB]}{dt} = &+ ps\_c\_a[IkBt] \\ &- a\_c\_an[IKB][NFkB] \\ &+ d\_c\_an[IkBNFkB] \\ &- a\_c\_ai[IkB][IKK] \\ &+ d\_c\_ai[IkBIKK] \\ &- in\_a[IkB] \\ &+ ex\_a[IkBn] \\ &- pd\_c\_a[IkB]\end{aligned}$$

The rate of change in the concentration of the IκBIKK complex in the cytoplasm is modelled as:

$$\begin{aligned}\frac{d[I\kappa BIKK]}{dt} = &+a\_c\_ai[I\kappa B][IKK]\\ &-d\_c\_ai[I\kappa BIKK]\\ &-a\_c\_2ain[I\kappa BIKK][NF\kappa B]\\ &+d\_c\_2ain[I\kappa BIKKNF\kappa B]\\ &-pd\_c\_2ai[I\kappa BIKK]*ikkm(t)\end{aligned}$$

The rate of change in the concentration of nuclear IκB is modelled as:

$$\begin{aligned}\frac{d[I\kappa Bn]}{dt} = &-a\_n\_an[I\kappa Bn][NF\kappa Bn]\\ &+d\_n\_an[I\kappa BNF\kappa Bn]\\ &+in\_a[I\kappa B]\\ &-ex\_a[I\kappa Bn]\\ &-pd\_n\_a[I\kappa Bn]\end{aligned}$$

The rate of change in the concentration of IκB mRNA in the nucleus is modelled as:

$$\begin{aligned}\frac{d[I\kappa Bt]}{dt} = &+rsu\_a\\ &+rsr\_an[NF\kappa B(t-\tau)]^{h\_an\_n}\\ &-rd\_a[I\kappa Bt]\end{aligned}$$

The equations above of the transcription of IκBα, IκBβ and IκBε ([IκBt]) are the only mathematical equations which differ between the three isoforms. IκBα and IκBε mRNA transcript level, IκBαt and IκBεt, are dependent on NFκB initiated transcription, degradation and residual transcription of IκBt. IκBβ mRNA is not initiated by NFκB and therefore described by residual transcription and degradation rates of IκBβt and h_an_n set to zero. IκBα is translated without a delay in the model, $\tau = 0$, while there is a delay of $\tau = 45$ minutes for IκBε.

### 4.2.3 Model input: IKK

NFκB is a pleiotropic transcription factor that responds to numerous intra and intercellular signalling events. Experimentally measurable input and output activities were selected as the model boundary. The majority of the upstream signalling events lead to the activation of IκB kinase complex IKK (See also Figure 2-2 for the location of IKK in the TLR signalling process), therefore IKK activity is used as the model input, while the concentration of nuclear NFκB is defined as model output.

In order to facilitate modelling of arbitrary or observed IKK profiles, active IKK is represented in the input signal. The IKK input is solved numerically, by a piecewise linear input function, ikkm(t) (See Figure A-1), rather than analytically and based on experimental values of the LPS challenge (Werner *et al.*, 2005).

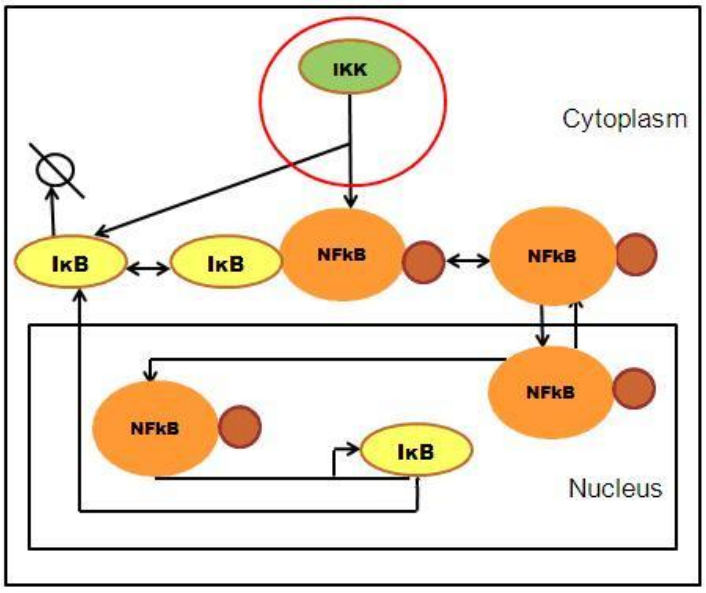


Figure 4-3 Conceptual model of NFκB signalling. The model reactions of the IKK, the model input, are circled in this figure. The signalling pathway activates the kinase IKK which breaks the IκB-NFκB dimer. IKK is seen as the input of the model representing the bacterial challenge and the reactions involved are discussed in this section.

There are 15 mass action kinetic reactions (Table A- 1 in A.1.1) that remove or add active IKK from free and complex proteins in the system. The rates modify degradation rates proportionally for each complex of IκBIKK and IκBIKKNFκB proteins. Complex proteins

IκBIKK and IκBIKKNFκB are modelled to represent the phosphorylation of NFκB bound proteins, targeting them for proteolysis through the ubiquintin-proteasome pathway (Ghosh *et al.*, 1998).

The rate of change in the concentration of free IKK in the cytoplasm is modelled as:

$$\begin{aligned}\frac{d[IKK]}{dt} = & -a\_c - ai[I\kappa B][IKK] \\ & + d\_c\_ai[I\kappa BIKK] \\ & - a\_c\_2ani[I\kappa BNF\kappa B][IKK] \\ & + d\_c\_2ani[I\kappa BIKKNF\kappa B] \\ & + pd\_c\_2ai[I\kappa BIKK]*ikkm(t) \\ & + pd\_c\_3ain[I\kappa BIKKNF\kappa B]*ikkm(t)\end{aligned}$$

### 4.2.4 Model output: NFκB

The model output is defined as the nuclear NFκB ([NFκBn]) concentration in response to the LPS challenge over time. The output is therefore not defined as the concentration of nuclear NFκB with the model in steady state, but as the change in concentration as a function of time.

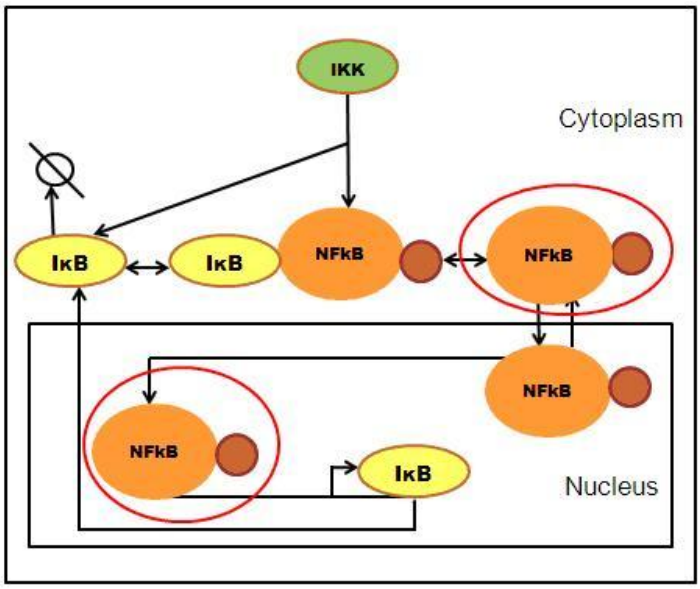


Figure 4-4 Conceptual model of NFκB signalling. The model reactions of the cytoplasmic and nuclear NFκB are circled in this figure. NFκB is a key transcription factor and the mechanistics of the translocation to the nucleus as result of the IKK activation play an important role in the immune reaction. Nuclear NFκB concentration is the output of the model and the reactions are discussed in this section.

The rate of change in the concentration of nuclear NFκB is modelled as:

$$\begin{aligned}\frac{d[NF\kappa Bn]}{dt} = & -a\_n\_an[I\kappa Bn][NF\kappa Bn] \\ & +d\_n\_an[I\kappa BNF\kappa Bn] \\ & +in\_n[NF\kappa B] \\ & -ex\_n[NF\kappa Bn] \\ & +pd\_n\_2an[I\kappa BNF\kappa Bn]\end{aligned}$$

Nuclear NFκB, NFκBn, is depleted as the result of the association with IκB and export of NFκB into the cytoplasm. An increase of nuclear NFκB is the result of disassociation and protein degradation of NFκBIκB complex and import of NFκB from the cytoplasm. The nuclear NFκB and the NFκB in the cytoplasm form the total free NFκB in the model.

The rate of change in the concentration of NFκB in the cytoplasm is modelled as:

$$\begin{aligned}\frac{d[NF\kappa B]}{dt} = & -a\_c\_an[I\kappa B][NF\kappa B] \\ & +d\_c\_an[I\kappa BNF\kappa B] \\ & -a\_c\_2ain[I\kappa BIKK][NF\kappa B] \\ & +d\_c\_2ain[I\kappa BIKKNF\kappa B] \\ & -in\_n[NF\kappa B] \\ & +ex\_n[NF\kappa Bn] \\ & +pd\_c\_2an[I\kappa BNF\kappa B] \\ & +pd\_c\_3ain[I\kappa BIKKNF\kappa B]*ikkm(t)\end{aligned}$$

Cytoplasmic NFκB is depleted due to the formation of IκBNFκB and IKKIκBNFκB complexes and transport of free NFκB to the nucleus. Degradation of these complexes and disassociation due to phosphorylation by IKK and transport of nuclear NFκB into the cytoplasm increases the concentration of cytoplasmic NFκB.

### 4.2.5 Feedback

A feedback loop is a closed cycle of components each affecting the concentration or activity of the next component with activation or inhibition (Mengel *et al.*, 2010). Feedback mechanisms prevent the translocation of NFκB to the nucleus influencing the temporal dynamics of NFκB and the response to the bacterial challenge. There are two parts to the feedback loop. Firstly, NFκB activates the IκBα mRNA expression and secondly IκBα forms a dimer with NFκB in the cytoplasm sequestering it in the cytoplasm. In the second feedback loop is similar: the dimer of IκBε with NFκB in the cytoplasm prohibits the translocation of NFκB to the nucleus but IκBε mRNA expression is activated by NFκB with a delay (See Section 4.2.2). The third IκB isoform IκBβ forms a dimer with NFκB in the cytoplasm and prevents the translocation to the nucleus but mRNA expression of IκBβ is not initiated by NFκB. IκBβ is therefore not part of a feedback loop but influences the outcome of the immune reaction.

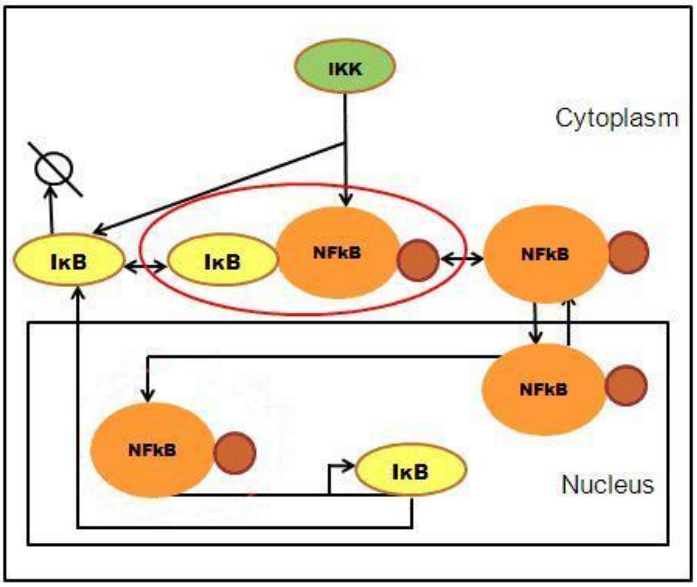


Figure 4-5 Conceptual model of NFκB signalling. The kinase IKK breaks the IκB-NFκB dimer. The model reaction of the IκBNFκB components are circled in this figure. They are the heart of the feedback mechanism for the translocation of NFκB and discussed in this section.

The rate of change in the concentration of IκBNFκB complex is modelled as:

$$\begin{aligned}\frac{d[I\kappa BNF\kappa B]}{dt} &= +a\_c\_an[I\kappa B][NF\kappa B] \\ &\quad -d\_c\_an[I\kappa BNF\kappa B] \\ &\quad -a\_c\_2ani[I\kappa BNF\kappa B][IKK] \\ &\quad +d\_c\_2ani[IKKI\kappa BNF\kappa B] \\ &\quad -in\_2an[I\kappa BNF\kappa B] \\ &\quad +ex\_2an[I\kappa BNF\kappa Bn] \\ &\quad -pd\_c\_2an[I\kappa BNF\kappa B]\end{aligned}$$

The rate of change in the concentration of nuclear IκBNFκB complex is modelled as:

$$\begin{aligned}\frac{d[I\kappa BNF\kappa Bn]}{dt} &= +a\_n\_an[I\kappa Bn][NF\kappa Bn] \\ &\quad -d\_n\_an[I\kappa BNF\kappa Bn] \\ &\quad +in\_2an[I\kappa BNF\kappa B] \\ &\quad -ex\_2an[I\kappa BNF\kappa Bn] \\ &\quad -pd\_n\_2an[I\kappa BNF\kappa Bn]\end{aligned}$$

The rate of change in the concentration of the IκBIKKNFκB complex is modelled as:

$$\frac{d[I\kappa BIKKNF\kappa B]}{dt} = +a\_c\_2ani[I\kappa BNF\kappa B][IKK] \\ -d\_c\_2ani[I\kappa BIKKNF\kappa B] \\ +a\_c\_2ain[I\kappa BIKK][NF\kappa B] \\ -d\_c\_2ain[I\kappa BIKKNF\kappa B] \\ -pd\_c\_3ain[I\kappa BaIKKNF\kappa B]*ikkm(t)$$

### 4.2.6 Assumptions of the model

Each model has several assumptions. Detail of the model needs to be limited in line with the experimental data and a more elaborate model would make parameter estimation and model analysis intractable.

**Parameters**

Ideally all parameters would be measured however, this is not always possible. Due to the rich literature of biochemical rate constants derived from *in vitro* measurements and quantitative cell biology, one third of the parameters were known with high degree of confidence, one third was significantly constrained by the literature and the remaining third was estimated in parameter fitting with experimental data (Kearns & Hoffmann, 2008).

**Equal distribution of molecules**

The signalling process can be described with ODE if the diffusion process is fast and the molecules equally distributed. Diffusion coefficients of proteins are variable and differ from 0.05μm$^2$/s for trans membrane receptors, up to 0.5 μm$^2$/s for membrane bound proteins and more than 10 μm$^2$/s for proteins in the cytoplasm (Arrio-Dupont *et al.*, 2000; Niv *et al.*, 1999). The average distance *s* for a protein to travel can be calculated from the diffusion coefficient D and the time t (4-1).

(4-1) $$s = \sqrt{4*D*t/\pi}$$

A protein in the cytoplasm with diffusion coefficient of 10 $\mu m^2/s$ diffuses on average 3.5μm/s (Teruel & Meyer, 2000). Trans-membrane proteins can be regionally localized but cytoplasmic proteins diffuse rapidly. The rapid diffusion permits us to consider the proteins in the cytoplasm as proteins in a well stirred medium. Therefore, the use of ODE is sufficient to describe the dynamics of intracellular reactions. This facilitates the systems to be analysed with nonlinear systems theory. Differential equations have been used with great effect in the NFκB pathway models (Cheong & Levchenko, 2008).

**Stochasticity**

Many organisms are phenotypically variable as a result of stochastic gene expression. Differential equations model the system deterministically and continuously assuming a well stirred environment with unlimited availability of the components of the system (Materi & Wishart, 2007). Gene expression is stochastic or noisy. Noise plays an important role in biological networks, increasing sensitivity (Paulsson *et al.*, 2000), driving oscillations (Vilar *et al.*, 2002) and timing gene activities (Amir *et al.*, 2007). The stochasticity stems from two sources: intrinsic and extrinsic noise (Cheong *et al.*, 2010). Intrinsic noise is confined in the system, availability of the components, while extrinsic noise is caused by changes in the surrounding environment (Swain *et al.*, 2002).This variation, "noise" in protein expression is thought to play a key role in the differentiation of transcriptional activation (Mettetal & van Oudenaarden, 2007). The stochastic approach is much more computationally expensive and the analysis of the underlying dynamics of the system difficult (Doyle & Stelling, 2006). Stochastic simulation techniques are therefore often used because they are closer to reality than deterministic models for single cell measurements.

Observations on population levels present the average response of the cells to external perturbations. For the given model with fixed parameters and initial conditions the time evolution of the components is fixed, i.e. deterministic and can therefore be approximated by a deterministic process adequately representing the stochastic influences of the individual cells on the cell population. Therefore, the Ordinary Differential Equations represent the time evolution of the mean concentration values of the population of cells.

In addition, it has been shown that extrinsic noise dominates the intrinsic noise (Raser & O'Shea, 2005). A model with Ordinary Differential Equations and parameter estimations

based on average cell population measurements will still be informative and able to indicate further biological experiments.

**NFκB heterodimer**

NFκB is a protein complex and the complicated kinetics of its formation is not modelled. NFκB is a heterodimer composed of RelA(p65) and NFκB1 (p50). RelA is synthesized as a mature product. The second product has a large precursor p105 and requires post translational modification dependent on NFκB. However, the synthesis of the crucial NFκB component, RelA, appears to be constant and signal independent. Therefore, it is expected that the production of NFκB heterodimers is constant can be balanced by degradation in the model (Lipniacki *et al.*, 2004). In addition, no specific data is available to justify increasing the detail of the model.

**Multiple transcription factors**

Limited data prevents modelling multiple transcription factors, however, transcriptional nonlinearity, such as cooperative binding and multiple transcription factors have been represented with the coefficient of 3 (h_an_n) in NFκB induced transcription of IκBα and IκBε (IκBt in Section 4.2.2).

**IKK**

IKK phosphorylates each IκB isoform. Due to the lack of biochemical data it was assumed that ubiquitination and proteolysis of IκB isoforms follows the specific phosphorylation event of IκB by IKK immediately. Therefore, the interaction of IKK and IκB isoforms proceed as a single enzyme degradation scheme and can be represented by the following reactions:

$$IKK + I\kappa B \underset{disassociation}{\overset{association}{\rightleftarrows}} IKKI\kappa B \xrightarrow{protein\,deg} IKK$$

$$IKK + I\kappa BNF\kappa B \underset{disassociation}{\overset{association}{\rightleftarrows}} IKKI\kappa BNF\kappa B \xrightarrow{protein\,deg} IKK + NF\kappa B$$

If IKK represents the enzyme, IκB the substrate and IKKIκB or IKKIκBNFκB the enzyme-substrate complex, the reaction scheme can be represented by differential equations. The differential equations describe the rate of change of the concentrations of IKK, IKKIκB, IκBNFκB, IKKIκBNFκB and IκB. Where the association of IKK with IκB represents the start

of the signalling event, the disassociation represents the stability of the complex. The rate of protein degradation is dependent on the input function, unique for each bacterial challenge, and changes over time in the model.

Free cytoplasmic IKK can then be represented by the reactions

$$I\kappa B + IKK \xrightarrow{a\_c\_ai} IKKI\kappa B$$

$$IKKI\kappa B \xrightarrow{d\_c\_ai} IKK + I\kappa B$$

$$IKKI\kappa B \xrightarrow{pd\_c\_2ai} IKK$$

$$I\kappa BNF\kappa B + IKK \xrightarrow{a\_c\_2ani} IKKI\kappa BNF\kappa B$$

$$IKKI\kappa BNFkB \xrightarrow{d\_c\_2ani} IKK + I\kappa BNF\kappa B$$

$$IKKIkBNFkB \xrightarrow{pd\_c\_3ain} IKK + NF\kappa B$$

For each IκB represented in the equations above there are three mass action equations, one for each isoform IκBα, IκBβ and IκBε.

In order to allow the model to be applied to a variety of signalling cascades as a result of different stresses, IKK is represented as a single entity. Therefore, the model does not separate between IKK1/IKK2 (IKKα/IKKβ) heterodimer scaffolded by NEMO (IKKγ). The single entity IKK represents active IKK. Different receptors on the cell membrane, such as TLR4 or TNFα lead to different IKK heterodimer activation. The use of the input function ikkm (Section 4.2.3) facilitates the different activation rates depending on the bacterial challenge.

## 4.3 Implementation of the model

The model described by Werner *et al.* (2005) was implemented in SBtoolbox (Schmidt & Jirstrand, 2006) (See Appendix B). SBtoolbox is a systems biology toolbox in MATLAB ("MATLAB® ", R2007a ). The toolbox is an open and extendible environment with a large number of analysis tools such as deterministic simulation. The toolbox uses the MATLAB numerical differential equation solver, ode15s, to solve the equations. The solution to the equations, the time course for each component, can then be compared with the experimental values

The simulations were performed with the system of ODE describing the biochemical reactions involving in signal transduction between IKK and nuclear NFκB activity described

in Section 4.1. Initial values were calculated by running the model with a basal input level (0.1μM) until no more changes in concentration could be detected. Our implementation of the model created the same model behaviour as the implementation from Werner *et al.* (2005).

## 4.4 Summary

In this chapter we explained the concepts and highlighted the features of the model for the translocation of the NFκB transcription factor from the cytoplasm to the nucleus. The model was developed by Hoffmann *et al.* (2002a) and extended by Werner *et al.* (2005) and used in several applications. Our implementation of the model in MATLAB performed identically to the published model. The model will become part of the model which represents cytokine mRNA expression in mammary epithelial cells described in Chapter 5. The model is chosen to reduce time and cost in the development of the mastitis model.

# Chapter 5
# Mastitis model development

***Models should be as simple as possible, but not simpler***

***Albert Einstein***

*This study aims to evaluate the effect of the dynamics of the translocation of the transcription factor NFκB to the nucleus on the mechanistics of the cytokine mRNA expression in mastitis. The signalling and gene network regulation as a result of the bacterial challenges are investigated to see if this explains the mechanistics of the cytokine expression profiles. As described in the last chapter, several studies have developed mathematical models to explain the translocation of the transcription factor NFκB from the cytoplasm to the nucleus. The transcription factor NFκB plays and important role in the cytokine expression. In this chapter, a mathematical model representing signalling and gene network regulation of cytokine mRNA expression in mammary epithelial cells is developed. The model consists of two modules; the first module is described in detail in the previous chapter representing the signalling and NFκB translocation, while the second module, the gene network regulation of cytokines as a result of the NFκB translocation, is described in detail in this chapter.*

*In the first section of this chapter the selection of a conceptual model based on the microarray analysis results described in Chapter 2 is discussed. In the second section the parameter estimation for the module, representing cytokine mRNA expression in mammary epithelial cells, is described. In the third section sensitivity analysis of the module for cytokine mRNA expression is performed to evaluate the influence of the parameter values, estimated in this chapter, on the model output.*

## 5.1 Model selection

The biological complexity and limited quantitative measurements impose major challenges for model selection from experimental time-series data (Cho *et al.*, 2003; Kutalik *et al.*, 2004). Due to the high cost of microarray experiments, especially time series microarray experiments, data points are often limited. The available experimental data in this thesis does

not allow for the identification of the structure of the model and prior biological knowledge as described in Section 3.1.3 is used to identify the model structure. Based on the prior biological knowledge and molecular basis of cytokine mRNA expression described in Chapter 2 and Chapter 3 the topological model with system components and schematic regulatory connections between components is derived and presented in Figure 5-1.

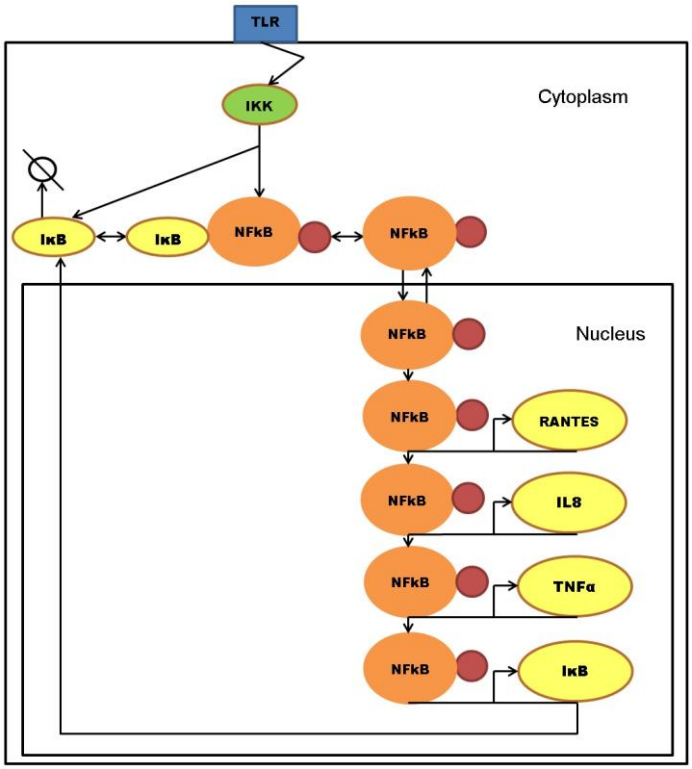


Figure 5-1 Stimulus specific conceptual model of TLR-IKK-NFκB signalling in mastitis. The TLR receptor on the cell membrane recognizes the bacterial challenge. The signalling pathway activates the kinase IKK which breaks the IκB-NFκB dimer. As a result, the transcription factor NFκB translocates to the nucleus initiating gene expression. The transcription factor NFκB initiates the expression of three cytokines, RANTES, IL8 and TNFα in mastitis. In addition, the IκB isoforms which bind with NFκB in the cytoplasm to prevent translocation of NFκB to the nucleus are expressed. This process creates a negative feedback loop for the translocation of NFκB to the nucleus.

Model development can be time consuming and biological experiments costly. Therefore, we choose a modular approach where an existing model constitutes a part of the new model. This reduces the time and cost of additional biological experiments and model development. We chose the model, developed by Werner *et al.* (2005) described in Chapter 4, to represent the TLR-NFκB signalling and translocation of NFκB to the nucleus.

In our model the nuclear NFκB activity, the output of the model developed by Werner *et al.* (2005), is incorporated in a system of ODE's representing the cytokine mRNA expression levels in mastitis.

### 5.1.1 Module reactions for cytokine mRNA expression

The conceptual diagram in Figure 5-2 describes the reactions of the cytokine mRNA expression levels of RANTES, IL8 and TNFα initiated by the transcription factor NFκB as result of bacterial challenge to mammary epithelial cells.

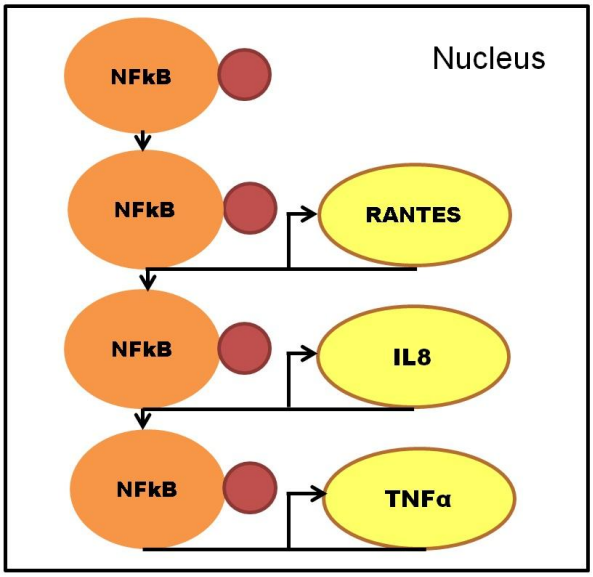


Figure 5-2 Conceptual diagram for cytokine mRNA expression in the nucleus in mammary epithelial cells. The transcription factor NFκB initiates the expression of the cytokine RANTES, IL8 and TNFα in the nucleus.

The schematic diagram in Figure 5-2 allows us to set up the reactions for cytokine mRNA expression in mastitis. The same nomenclature as described in Section 4.1 is used to describe the rate constants and components. The reactions for synthesis and degradation of the cytokines are described in (5-1)-(5-6) with the rate constants for synthesis, rsr_xn and degradation, d_n_x (x depends on the cytokine, 8 for IL8, TNFα for TNFα, r for RANTES) are shown below. The suffix _xn in the synthesis parameter indicates the association of NFκB with the gene x during the synthesis followed by the release of NFκB when the synthesis of mRNA is completed. In RANTESt, IL8t and TNFαt the t at the end represent the concentration of the mRNA of the cytokines RANTES, IL8 and TNFα respectively in line

with the nomenclature of the first model. While in NFκBn the additional n following NFκB indicates the nuclear form of NFκB as described in Section 4.1.

(5-1) $3NF\kappa Bn \xrightarrow{rsr\_rn} RANTESt + 3NF\kappa Bn$

(5-2) $RANTESt \xrightarrow{d\_n\_r} \text{sink}$

(5-3) $3NF\kappa Bn \xrightarrow{rsr\_8n} IL8t + 3NF\kappa Bn$

(5-4) $IL8t \xrightarrow{d\_n\_8} \text{sink}$

(5-5) $3NF\kappa Bn \xrightarrow{rsr\_TNF\alpha n} TNF\alpha t + 3NF\kappa Bn$

(5-6) $TNF\alpha t \xrightarrow{d\_n\_TNF\alpha} \text{sink}$

Based on the molecular details of cytokine mRNA expression described in Section 2.1.2 and the law of mass action we can derive the molecular balance for each cytokine, which results in three ODEs representing the mRNA expression levels of RANTES, IL8 and TNFα (5-7)-(5-9). The mRNA concentration for each cytokine is represented as the name of the cytokine followed by a t, [RANTESt] and is then the component representing the concentration of RANTES mRNA, [IL8t] is the component representing the concentration of IL8 mRNA while [TNFαt] is the component representing the concentration of TNFα mRNA.

(5-7) $$\frac{d[RANTESt]}{dt} = +rsr\_rn[NF\kappa Bn(t)]^{h\_an\_r} - rd\_r[RANTESt]$$

(5-8) $$\frac{d[IL8t]}{dt} = +rsr\_8n[NF\kappa Bn(t)]^{h\_an\_8} - rd\_8[IL8t]$$

(5-9) $$\frac{d[TNF\alpha t]}{dt} = +rsr\_TNF\alpha n[NF\kappa Bn(t)]^{h\_an\_TNF\alpha} - rd\_TNF\alpha[TNF\alpha t]$$

Table 5-1 Parameter description for synthesis, degradation and the Hill coefficient with x replaced by r (RANTES), 8 (IL8) or TNFα (TNFα).

| Parameter | description |
|---|---|
| rsr_ xn | nuclear NFκB induced mRNA synthesis |
| d_n_x | degradation of m RNA |
| h_an_x | Hill coefficient |

The ODEs for cytokine mRNA expressions are incorporated with the model described in Chapter 4. Together the two modules form the model representing cytokine mRNA expression in mammary epithelial cells. The total model consists of 27 ODEs and 89 reaction rates and a full description of the ODE, initial values and parameters can be found in Appendix A.

## 5.2 Parameter estimation

Parameters for degradation and synthesis for the equations in (5-7) - (5-9) were estimated to fit experimental values from Chapter 3. Synthesis and degradation rates for cytokine mRNA expression are not available, however, we are able to quantify mRNA concentrations from microarray experiments described in Chapter 3 and estimate synthesis and degradation rates to fit experimental values. In addition, initial values are estimated.

### 5.2.1 Prior identifiability analysis for parameter estimation

To estimate n parameters at least n data points need to be available. Over fitting of the model needs to be carefully considered; if too many, more than n, parameters are estimated with a limited number of experimental values, n, several combinations of parameters could fit the experimental data. To prevent over fitting we limited parameter estimation to the degradation and synthesis parameters for the mRNA cytokine expression levels. Using prior identifiability analysis, described in Section 2.3.3, we will show that the experimental data for the chosen model structure limits unique parameter identification for synthesis and degradation for each individual cytokine. However, the experimental data allows for the unique identification of the parameters between cytokines and qualitative analysis of the model behaviour.

The priori identifiability analysis as described in Section 2.3.3 was used to identify possible correlations between the parameters that we need to estimate with the available experimental values over the different time points (0, 60 , 180 and 360 minutes). The method is implemented in the SBtoolbox (Schmidt & Jirstrand, 2006) in Matlab ("MATLAB® ", R2007a ). The correlation between the parameters to be estimated for the model is shown in

Figure 5-3. The correlation ranges between 0, black boxes with no correlation between the parameters, to 1, white boxes, with total correlation between the parameters. Elements on the diagonal represent the correlations of the parameters on it self and have an expected correlation of 1.

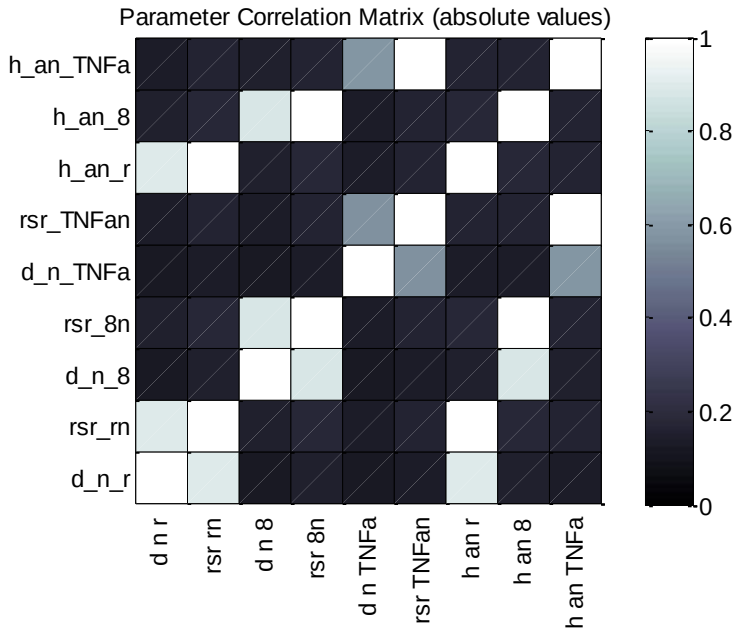


Figure 5-3 In order to establish identifiability of the parameters prior to parameter estimation the correlation between degradation, synthesis and Hill coefficients parameters estimated with the experimental values is calculated. The lighter the colour, the higher the correlation between the parameters is. A high correlation between the parameters indicates non-identifiability of the parameters with these experimental values, while low correlation indicates that the parameters can be estimated with the experimental values.

The parameters for degradation (d_n_r, d_n_8 and d_n_TNFα) and NFκB induced synthesis (rsr_rn, rsr_8n and rsr_TNFαn) between cytokines do not correlate. The low correlation indicates that the parameters responsible for the NFκB induced mRNA expression and the degradation of the mRNA can be identified independently for each cytokine. However, the parameters for the synthesis of the mRNA and the Hill coefficient for each individual cytokine correlate positively with a value of 1 and unique determination of the individual parameters may not be possible with the experimental values. One way to reduce the correlation between parameters is to set a parameter to the nominal value. We therefore set the Hill coefficient to 3, the value used for similar reactions in the first model by Werner *et al.* (2005).

The identifiability is recalculated with the reduced parameter set where the Hill coefficient is set to the nominal value of 3. Figure 5-4 shows the correlation between the synthesis and degradation coefficients.

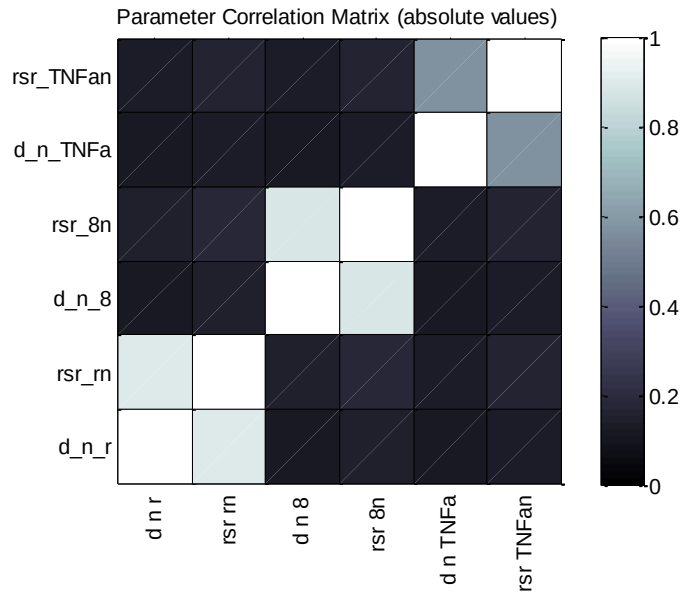


Figure 5-4 Parameter correlation matrix of the parameters estimated in the model with the Hill coefficient set to nominal value. The lighter the colour, the higher the correlation between the parameters is. A high correlation between the parameters indicates non-identifiability of the parameters with these experimental values, while low correlation indicates that the parameters can be estimated with the experimental values. The correlations between parameters are less than 1 and therefore these experimental values are sufficient to identify the synthesis and degradation parameters.

The correlations between the synthesis and degradation parameters are less than 1 and therefore these experimental values are sufficient to identify the synthesis and degradation parameters.

### 5.2.2 Initial value estimation

In a model of ODE, initial values need to be estimated or measured to allow numerical analysis. Werner *et al.* (2005) established initial values for the first module by running the model with a basal input of 0.1 μM IKK until equilibrium was achieved. Initial values are established before the bacterial challenge is applied. Equilibrium is defined as the state in the

model when changes of concentrations are less than 1% over a period of time for the component. To estimate the initial values of the combined model initial values were set to 0.1 μM for IKK and nuclear NFκB and 0 for the other components. The model was run in Matlab ("MATLAB® ", R2007a ) using the ode15s routine for numerical solutions of the equations.

Initial values for the components in the model described by Werner *et al.* (2005) were not affected by the addition of the ODE for cytokine mRNA expression levels and were kept the same as published previously (See A.1.3). Initial values for components representing cytokine mRNA concentration were estimated at 0 μM. Cytokine expression does not eventuate in healthy cells. The values at equilibrium reflect therefore the levels of each cytokine over baseline levels prior to the pathway activation by the *E. coli* challenge and were used as initial values for the model.

### 5.2.3 Data processing prior to parameter estimation

Prior to parameter estimation we converted the fold changes calculated in Chapter 3 with the microarray analysis to concentration levels of mRNA expression over time.

The method from Hekstra *et al.* (2003) was implemented in ("MATLAB® ", R2007a ) as described in Section 2.5. The concentration levels for the expressed mRNA for each cytokine from the microarray experiments for each time point were extracted with this implementation.

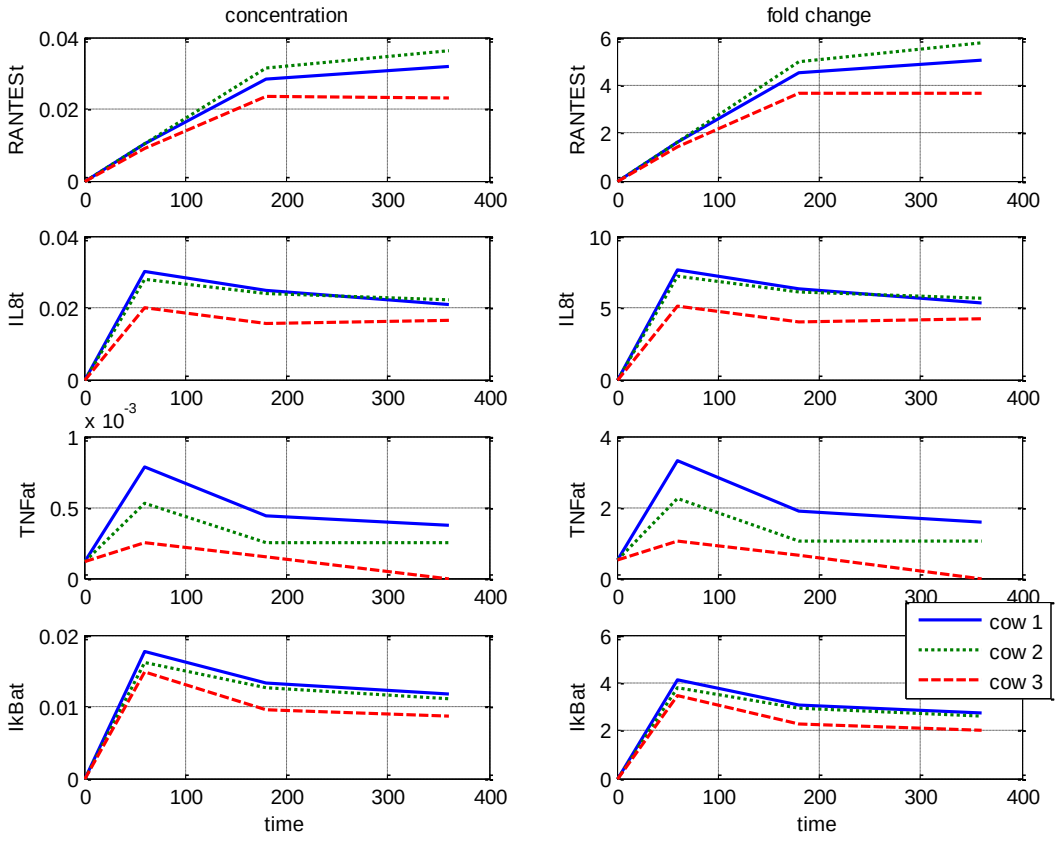


Figure 5-5 Experimental mRNA fold change expression levels converted to concentration levels for use in the model. Comparison of the cytokine concentration (μM) on the left of *E. coli* challenged mammary epithelial cells, and mRNA fold changes, on the right hand side show same time profile.

Relative fold changes, calculated in Chapter 3, for each component were normalised between 0 and 1 and multiplied with the max concentration level for each component calculated with the method described above. Converted mRNA cytokine and IκBα concentration levels showed the same trend, same relative pattern of rising and falling of concentration levels, as the calculated fold changes (Figure 5-5).

Converted mRNA expression levels of IκBα mRNA (IκBαt) from the Bovine Affymetrix® microarray experiments used in our study show the same trend, relative rising and falling of concentration levels, at the times of the measurements in the experiment as the expression levels of IκBαt in the model and experimental values challenged with LPS by Werner *et al.* (2005) (Figure 5-6).

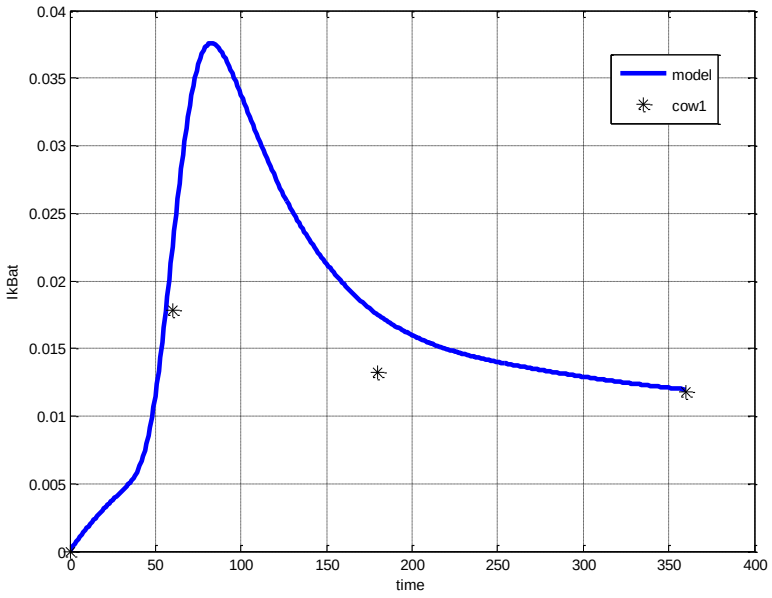


Figure 5-6 Converted mRNA expression levels (cow1) and model predictions of IκBα mRNA in our model implementation of the model developed by Werner *et al.* (2005). The x-axis represent the time (min) and the y-axis the concentration (µM).

The concentration levels of IκBα mRNA expression in the model by Werner *et al.* (2005) are arbitrary concentrations. Therefore, relative but no absolute information can be extracted from the model as will be shown in Section 5.3.

Although it has not been validated experimentally that the parameters in Table 2-1 can be transferred across different microarray platforms (Hekstra *et al.*, 2003), we proceeded with the use of the converted concentrations in our model. This implicates that we can only infer qualitative and not quantitative conclusions from the model.

### 5.2.4 Cytokine synthesis and degradation parameter estimation

The parameters representing the rate constants for the degradation and synthesis of mRNA for the ODE representing cytokine mRNA expression needed to be fitted against the mRNA concentrations calculated in the previous Section. Parameter estimations for models that include delay functions require extensive computer time. To minimize the computer time we therefore took the following steps:

(i) Parameters for each cytokine were estimated in individual estimation runs with the fast scatter search implemented in the SBtoolbox (Rodriguez-Fernandez *et al.*, 2006a) and described in Section 2.3.2. Equations (5-1) to (5-6) were fit one at a time. Synthesis and degradation parameters for each specific cytokine would be estimated while the synthesis and degradation parameters for the other cytokines were set to default values or the outcome of the previous estimation runs. Since the ODE for the cytokine concentrations are not coupled, the transcription factor NFκB is the only protein modelled in the ODE, separating parameter estimation for each cytokine reduces the parameter search area without compromising the accuracy. Biological knowledge was used to identify the boundary of the parameters to set limitations to the search area.

(ii) Following the estimation for each individual cytokine, the model was simulated with the estimated parameters and the model output compared with the experimental measurements for goodness of fit.

(iii) After the reduction of the parameter search areas, iteratively the parameters were estimated, using the fast scatter search, with the values of the simulations of the model that incorporated the estimated parameter values until no further optimisation of the parameter values could be achieved.

Parameter estimation and simulations for this model were performed using SBToolbox2 (Schmidt & Jirstrand, 2006) in MATLAB 7.4.0 (R2007a). In this study we tested a number of local and global estimation algorithms. Several algorithms converged to a similar solution as the fast scatter search method described in Section 2.3.2. Scatter search is an evolutionary global optimization method. The method incorporates strategic responses that take into account evaluations and history to generate the estimates of the parameters (Egea *et al.*, 2007; Rodriguez-Fernandez *et al.*, 2006b). The fast scatter search used the lowest computational time. Therefore the fast scatter method was used to estimate the parameters as described above to fit the converted microarray experimental values calculated in Section 5.2.3, followed by manual tuning.

#### *5.2.4.1 Results of parameter estimation with fast scatter search*

The estimated parameters used for the model simulations are listed in Table 5-2. Calculations are performed in μM per min with the experimental values of cow1 (arbitrarily chosen).

Table 5-2 Parameter values fitted in this study for the differential equations of cytokine mRNA expression.

| Parameter | value | units | description |
|---|---|---|---|
| d_n_r | 0.00039365 | $min^{-1}$ | degradation RANTES |
| rsr_rn | 5.28555 | $\mu M^{-2}\ min^{-1}$ | NFκB induced RANTES mRNA synthesis |
| h_a_r | 3 | | Hill coefficient |
| d_n_8 | 0.00175918 | $min^{-1}$ | degradation IL8 |
| rsr_8n | 5.28555 | $\mu M^{-2}\ min^{-1}$ | NFκB induced IL8 mRNA synthesis |
| h_a_8 | 3 | | Hill coefficient |
| d_n_TNFα | 0.020602 | $min^{-1}$ | degradation TNFα |
| rsr_TNFαn | 1.67 | $\mu M^{-2}\ min^{-1}$ | NFκB induced TNFα mRNA synthesis |
| h_a_TNFα | 3 | | Hill coefficient |

### 5.2.5 Qualitative comparison of the model with experimental data

It is important to evaluate the model and to check the model with experimental data not used in the parameter estimation process. In this section, therefore, an evaluation and a qualitative comparison of the model predictions with the additional experimental observations, which had not been included in the parameter estimation, was carried out (See Figure 5-7). We simulated the model for a time frame of 360 minutes, beginning from 0.

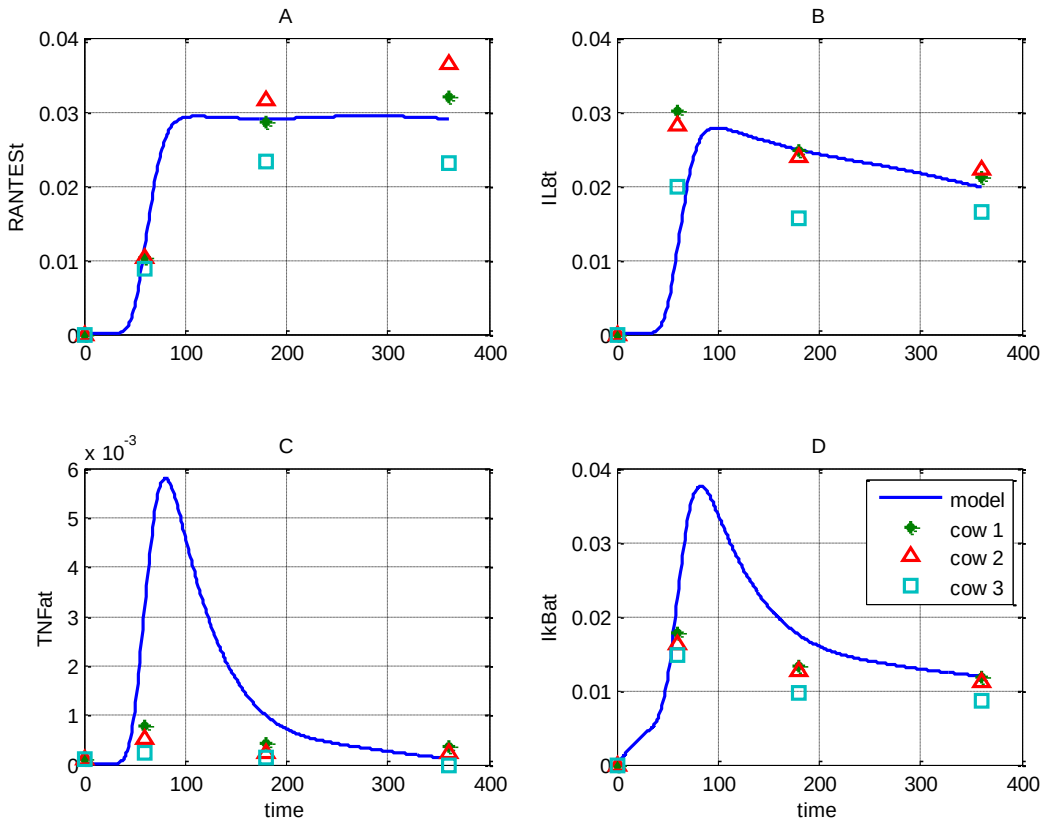


Figure 5-7 Comparison of the experimental values with the model values. The outcome of the model predictions and the experimental values are shown for the three cows (+,Δ, □). Estimation was performed with data from cow 1; the model was simulated for 360 minutes and the model predictions qualitatively compared with experimental data from cow 2(Δ) and 3(□). Solid lines represent the model outputs and (+) represent cow 1. The x-axis represent the time (min) and the y-axis the concentration (µM).

In Chapter 3 we described the replication of our microarray experiments with epithelial cells for three different cows. Data from the first cow, arbitrarily chosen, was used for parameter estimation, leaving the option to use data from the second and third cow to evaluate the model. The general behaviour of the mRNA expression for TNFα and IκBα mRNA are similar for all three cows (Figure 5-7 C and D). The general of behaviour of the mRNA expression for RANTES and IL8 is reproduced for the values of cow 2 (Figure 5-7 A and B). The third data set (cow 3) indicates a lower expression level for RANTES and IL8 than predicted by the model. However, the levels of mRNA expression follow the same trend in all three cows.

## 5.3 Sensitivity analysis of cytokine synthesis and degradation parameter changes on the model output

Sensitivity analysis is performed to identify the influence of parameter and initial value variation on the model output, understand the rate determining steps in the model and separate the biological and mathematical influence on the model output. In this Section the focus is on the synthesis and degradation parameters for the cytokine mRNA expression. Because global parameter estimation methods were used, local sensitivity analysis, described in Section 2.3.4, is used to identify the model sensitivities. Both time dependent and time independent sensitivities are investigated.

### 5.3.1 Time independent sensitivities of cytokine synthesis and degradation parameter changes on cytokine mRNA expression

The time independent local sensitivities of cytokine mRNA expression levels for changes in the parameters for synthesis and degradation of the cytokines mRNA expression levels are presented in Figure 5-8. Parameter changes showed a linear increase in sensitivity, therefore sensitivity of parameter increases and decreases with 40% were considered for further evaluation. Sensitivity towards changes in the degradation parameter was higher than sensitivity towards NFκB induced synthesis parameter for each cytokine mRNA expression level, with TNFα showing the highest sensitivity for changes in the degradation and synthesis parameter (Figure 5-8 (A)).

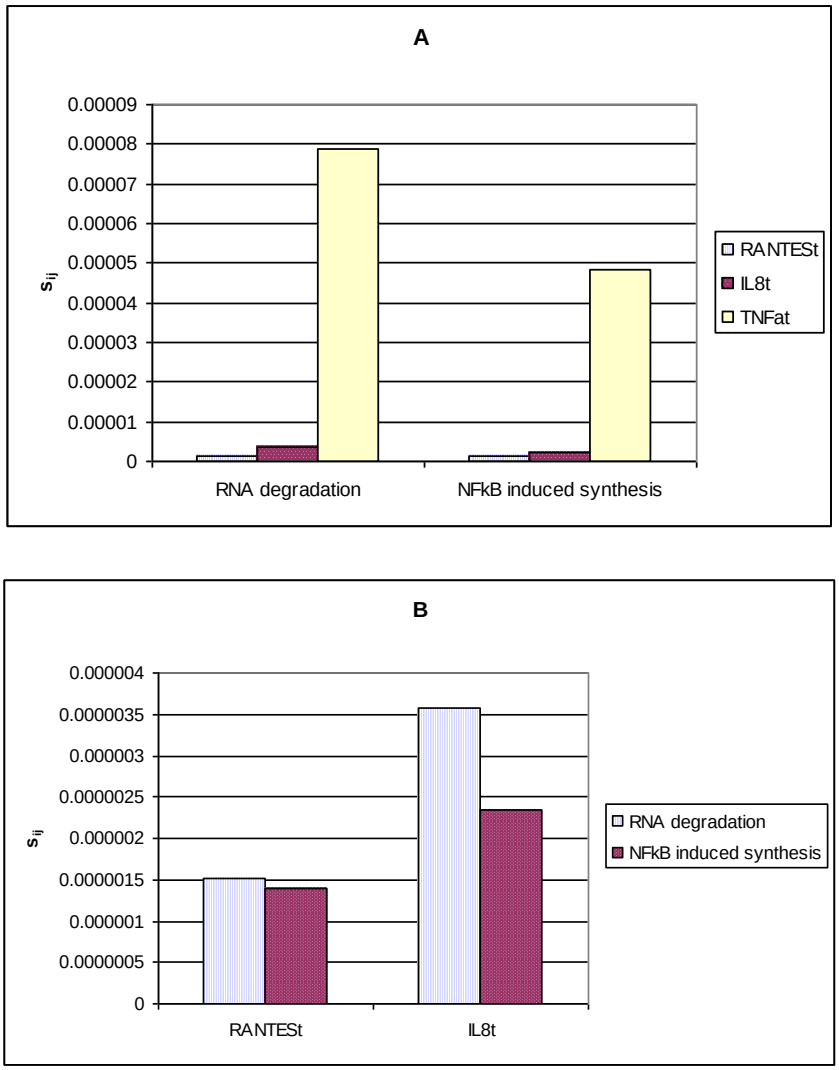


Figure 5-8 Time independent sensitivities of the model parameters for degradation and synthesis of the cytokine mRNA expression levels with parameter increase or decrease of 40%. Model predictions with the estimated parameters were compared with model predictions of parameters increased or decreased by 40% and time independent sensitivity calculated. (A) TNFα shows the highest sensitivity of the three cytokines. TNFα is more sensitive to changes in parameters for degradation than NFκB induced synthesis. (B) The expression of IL8 shows a higher sensitivity to degradation than to NFκB induced synthesis of mRNA, while in RANTES changes in either parameter have a similar influence on the expression levels.

The rate of change in the concentration for cytokine expression is described in Section 5.1.1. Looking at the general form (5-10) we can see that the influence of nuclear NFκB on the rate of change of the cytokine mRNA expression levels is cubed as a result of the Hill coefficient h_an_ set to 3.

(5-10) $$\frac{d[cytokine]}{dt} = +k_{syn}[NF\kappa B]^3 - k_{deg}[cytokine]$$

NFκB values ranges from 0 to 0.05 µM (Figure 5-10) while cytokine levels range approximately from 0-0.04 µM for RANTES and IL8 mRNA and 0-0.02 µM TNFα (Figure 5-5).The degradation rate is influencing the changes in the cytokine expression in linear relation with the cytokine levels.

TNFα and IL8 are more sensitive to changes in degradation rate than synthesis rate, while RANTES show similar sensitivity to both rates.

### 5.3.2 Time dependent sensitivities of cytokine synthesis and degradation parameter changes on cytokine mRNA expression

Time dependent sensitivities calculate the sensitivity of the model for parameter changes in each time step (Section 2.3.4.1). This will allow us to identify variation in the sensitivity over time. In addition, this section investigates the time dependent sensitivities of synthesis and degradation parameter changes on the variation in concentration of cytokine mRNA expression to evaluate the influence of the variation in sensitivities on the concentrations.

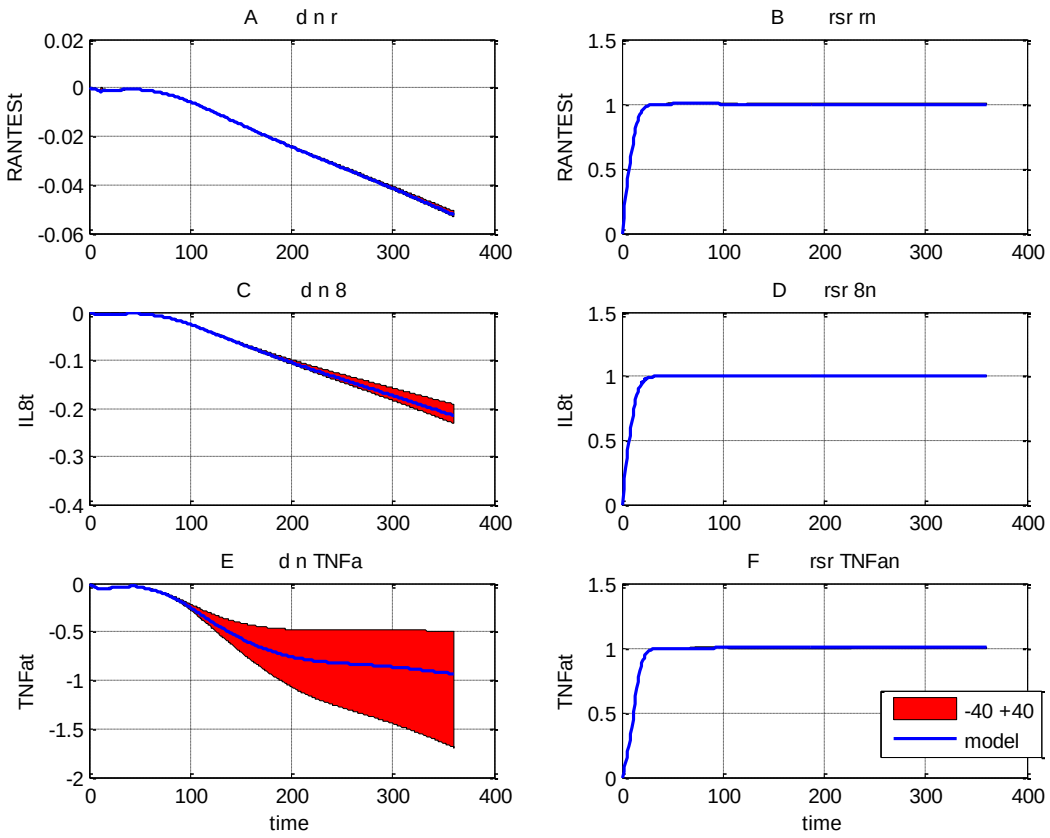


Figure 5-9 Time dependent sensitivities of model parameters for degradation and synthesis of mRNA cytokine expression levels. Time dependent parameter sensitivities for degradation (d_n) (A, C, E) and synthesis (rsr_) (B, D, F) of mRNA cytokine expression levels were calculated for parameter changes from -40% to +40% and the gradual change over the range is shown in the shaded areas. Sensitivity as result of changes in degradation parameters increases over model simulation time (A, C, E), while sensitivity as result of change in synthesis parameters stays constant(B, D, F). TNFα shows the largest variation in model sensitivity for the degradation parameter changes and the highest sensitivity values for the model (E). The x-axis represent the time (min) and the y-axis the concentration (µM).

Sensitivities for changes in parameters for synthesis are constant in time dependent sensitivity analysis (See Figure 5-9 B, D and F). Sensitivities for changes in the parameters for degradation rate vary over time (See Figure 5-9 A, C and E). Especially for TNFα, the range in sensitivity for the degradation rate changes from -40% to +40% increases towards the end of the simulation, while early in the simulation, less than 100 minutes, the sensitivity is the same for the complete range of changes in the parameter. Variations in nuclear NFκB concentration level reduce towards the end of the model simulation (Figure 5-10) and therefore the influence of the nuclear NFκB concentration becomes more stable towards the end of the simulation.

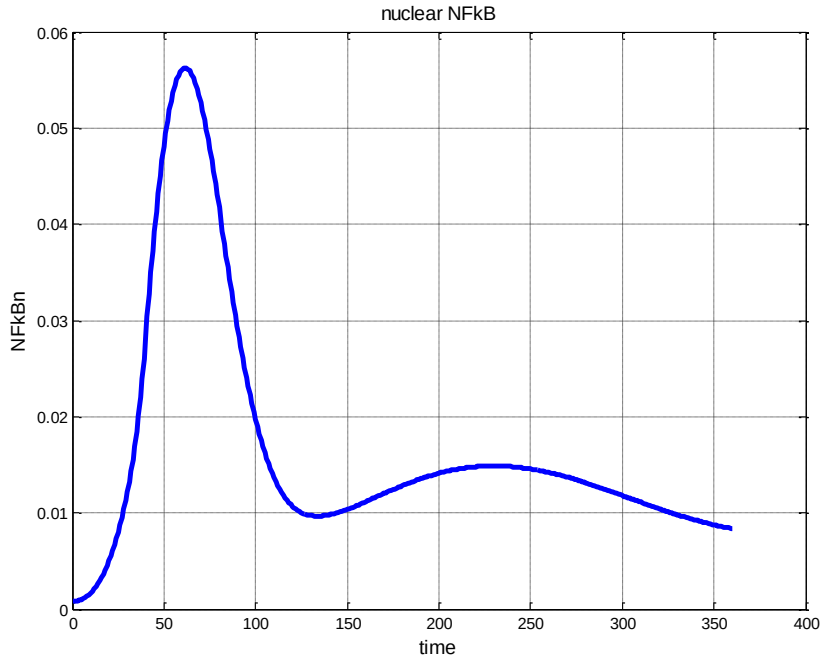


Figure 5-10 Predicted values for the nuclear NFκB during the 360 minutes simulation period of the model. The nuclear NFκB is not affected by the parameter changes of the degradation and synthesis of cytokine mRNA. The x-axis represent the time (min) and the y-axis the concentration (µM).

Parameter changes for TNFα degradation show the largest variation in sensitivity over time, which is reflected in the time independent sensitivity. Each degradation parameter change increases the influence of the parameter on the mRNA cytokine levels over time and has the highest influence at 360 minutes of model simulation.

### 5.3.3 Effect of cytokine synthesis and degradation parameter changes on mRNA cytokine concentration

Time dependent sensitivity analysis indicated an increasing influence on the mRNA cytokine concentration levels of the changes in degradation parameter values towards 360 minutes of model simulation, while synthesis parameters show a consistent influence during model simulation. While this evaluation gives an indication on the relative sensitivity, it does not give information on the absolute changes in concentration as a result of the parameter

changes. The absolute changes can assist in the identification of the optimum time for a biological experiment.

A plot of the change in concentration over 360 minutes of simulation time for the changes of the synthesis and degradation parameters clearly shows a changing influence on the cytokine mRNA concentration levels as result of the parameter changes, especially in TNFα concentration (Figure 5-11).

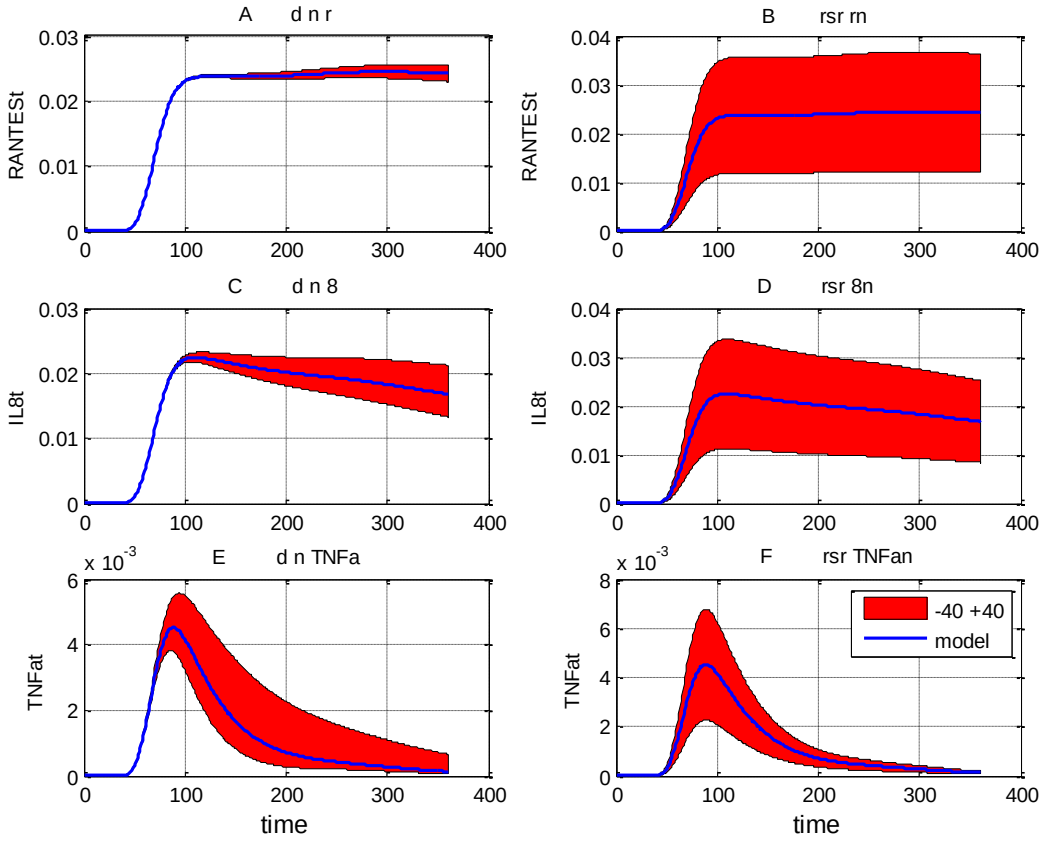


Figure 5-11 Predicted values (μM) for cytokine mRNA expression levels with degradation (A, C and E) and synthesis (B, D and F) parameter changes from -40% to +40%. The gradual change over the range is shown in the shaded areas. The x-axis represent the time (min) and the y-axis the concentration (μM).

TNFα synthesis and degradation parameters have a large influence at 90 minutes while the parameter changes have less influence on the change in concentration levels at 360 minutes. RANTES degradation parameters have a small influence over this range on the concentration. The influence increases towards 360 minutes simulation predictions, while synthesis rates have larger but stable influence from 100 minutes onwards. For the IL8 mRNA cytokine,

changes in degradation rate increases their influence towards 360 minutes, while changes in synthesis parameters show a stable influence from 75 minutes onward.

The model did not show sensitivity towards the initial values of the cytokines if changed with an increase of 40%. Initial values are established before the model is exposed to the bacterial challenge and therefore the lack of sensitivity is in line with biological knowledge.

### 5.3.4 Influence of variation in parameter values for cytokine synthesis and degradation on the model fit

To identify the ranges of the parameters for which the model output predicts the experimental values we simulated the model repeatedly with different parameter values, one at a time. We identified the parameter value ranges that would perform similar to the chosen model with less than 1% change in the cost function, the sum of squares. A 1% range was chosen because parameter estimation had shown to be the best fit for the combined parameter values.

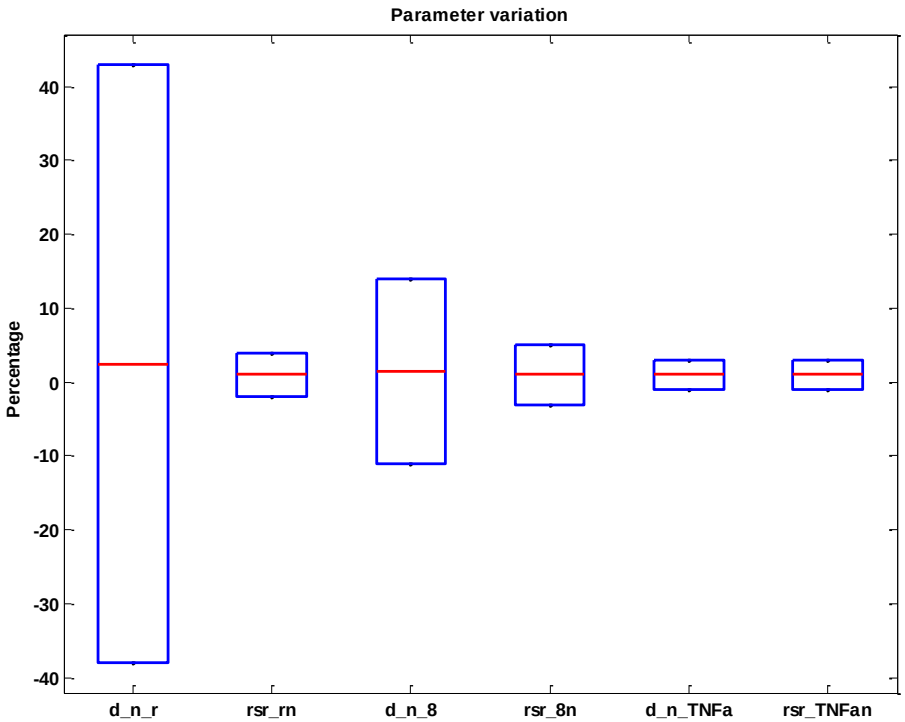


Figure 5-12 Percentage of change in parameter value that creates less than 1% change in Sum of Squares between the model prediction and the experimental values

We simulated the model 1800 times changing each parameter *i* from 1/100 of the model value to twice the model value with incremental steps of 1% Table 5-3.

Table 5-3 Simulation values for parameter range analysis. Parameters were varied from 1/100 of the model value to twice the model value with incremental steps of 1%.

| Parameter | Min value | Model value | Max value |
|---|---|---|---|
| d_n_r | 3.94E-06 | 0.000394 | 0.000787 |
| rsr_rn | 0.052856 | 5.28555 | 10.5711 |
| d_n_8 | 1.76E-05 | 0.001759 | 0.003518 |
| rsr_8n | 0.052856 | 5.28555 | 10.5711 |
| d_n_TNFα | 0.000206 | 0.020602 | 0.041204 |
| rsr_TNFαn | 0.0167 | 1.67 | 3.34 |

With the predicted outcomes of the model simulations we calculated the objective function $f(k)$, the sum of the sum of squares for each time point, 60, 180 and 360 minutes (N=3) of the difference between the simulated model output and the experimental values (5-11). The objective function describes how much the model prediction deviates from the observed data as a result of the variation in parameters.

(5-11) $$f_i(k) = \sum_{i=1}^{N} (f_{\exp}(i) - f_{per}(i,k))^2$$

We set a threshold value of 1% change in the objective function and then identified the $i^{th}$ change of the $k^{th}$ parameter value $\theta_{i,k}$ (5-12), the minimum, and $j^{th}$ change of the $k^{th}$ parameter $\theta_{j,k}$ (5-13), the maximum, for which the model would predict the concentration levels at 60, 180 and 360 minutes with less than 1% change in the objective function of the model.

(5-12) $$\theta_{i,k} = \min\{\theta_{i,k}\} \left| \frac{f_{i,k} - f_{\text{model}}}{f_{\text{model}}} \right| < 0.01$$

(5-13) $$\theta_{j,k} = \max\{\theta_{j,k}\} \left| \frac{f_{j,k} - f_{\text{model}}}{f_{\text{model}}} \right| < 0.01$$

As predicted by the sensitivity analysis in Section 5.3.1, change in the degradation parameter for TNFα causes the largest variation in the concentration levels and therefore have the highest restriction on parameter change.

Table 5-4 Minimum and Maximum parameter values that will fit the model predictions with the experimental data with less the 1% difference between the sum of squares of the model predictions and the experimental data.

| Parameter | min | model value | max | parameter function |
|---|---|---|---|---|
| d_n_r | 0.000244 | 0.000394 | 0.000563 | degradation RANTES |
| rsr_rn | 5.179839 | 5.28555 | 5.496972 | synthesis RANTES |
| d_n_8 | 0.001566 | 0.001759 | 0.002005 | degradation IL8 |
| rsr_8n | 5.126984 | 5.28555 | 5.549828 | synthesis IL8 |
| d_n_TNFα | 0.020396 | 0.020602 | 0.02122 | degradation TNFα |
| rsr_TNFαn | 1.6533 | 1.67 | 1.7201 | synthesis TNFα |

## 5.4 Summary and discussion

In this chapter we developed the module for the cytokine mRNA expression levels in mastitis and integrated the module in our model. A mathematical model is necessary because the nonlinear behaviour of some of the components in the pathway that leads to cytokine expression. The developed model can be used to investigate the mechanistics of the cytokine expression levels in mastitis and the differentiation of the cytokine expression levels between the two bacterial challenges which are believed to cause differentiation in the disease profile. We have thus developed a model which links the extra cellular stimulus representing the bacterial challenge to the signalling pathway response in the cytoplasm, which initiates the translocation of the NFκB transcription factor to the nucleus which then initiates the cytokine mRNA expression in the nucleus.

**Synthesis and degradation parameters**

We have chosen to include separate descriptions of synthesis and degradation representing mRNA concentration levels. Although specific data for synthesis and degradation rates are not available in this study, they are increasingly available with the evolvement of molecular techniques. In addition, in diseases, such as multiple sclerosis, degradation rates for cytokines such as RANTES have been changed from non disease levels (Li & Bever, 2001). Therefore, the influence of the synthesis and degradation rates is of interest in disease modelling. Separating synthesis and degradation rates allows us to study the influence of both parameters on the model dynamics. The concentration of mRNA expression measured in our experiments for the cytokines RANTES, IL8 and TNFα can be described by the difference between the mRNA synthesis and degradation of each individual cytokine.
Constitutive mRNA synthesis is not modelled since cytokines are expressed as result of the innate immune reaction but not expressed in healthy cells.

**Motivation for using Hill coefficient of 3**

Hill coefficients are exponents which traditionally quantify the cooperative binding of multiple proteins (Aldridge *et al.*, 2006). In this model the coefficient is modelled without the representation of saturation and can increase exponentially without upper bound. No new NFκB is generated in the model, we therefore restrict the exponential increase by keeping the total concentration, in the cytoplasm and nucleus, of NFκB constant.

The model is very sensitive to changes in the Hill coefficient. However, if we included the Hill coefficient in the parameter estimation, allowing the synthesis and degradation parameters to be fit in combination with the Hill coefficient, the fit did not improve (data not shown). This is expected from the prior identifiability analysis because of the correlation of 1 between the Hill coefficient and synthesis parameter. In addition, we do have experimental data for the concentration of the cytokines but no experimental data relating to the concentration of NFκB or other transcription factors. Therefore, based on our biological insight and the prior identifiability analysis, we chose to use the same Hill coefficient as the Hill coefficient in the module for reactions describing mRNA synthesis of the other components induced by NFκB.

With the Hill coefficient set to 3 the remaining estimated parameters for the model are identifiable and will capture experimental values of the combined synthesis and degradation. Ideally one would aspire to know all parameters with high accuracy, however, in practise this

is usually not possible and therefore we have to deal with uncertainty in parameter values. Highly correlated parameters, identify nearly linearly dependent results of the sensitivity functions (partial derivatives of the measured components with respect to the parameters), but do not indicate that the model is not identifiable (Banga & Balsa-Canto, 2008). The high correlation is not a serious problem if the main purpose of a model is to predict the dynamical behaviour of the system, and little significance is attributed to parameter values. Since our main interest in this study is the dynamical properties of the model we proceeded to estimate the synthesis and degradation parameters. Further experimental values to uniquely identify degradation and synthesis parameters for the individual cytokines are informative because they can lead to unique parameter values. Unique parameter values would allow for quantitative studies.

**Model assumptions**

The model uses the model assumptions from Werner *et al.* (2005) as described in Section 4.2.6 . In addition, we used the same value for the kinetic rate constants for mammary epithelial cells as the values published in the earlier model which was based on experimental values of mouse embryonic fibroblasts. Mouse embryonic fibroblast are healthy cells and express the cytokines investigated in this work (Hoffmann *et al.*, 2006). However, we did not include parameters from HEK cells, a cancer cell line, in the model. In cancer cells disruption of the NFκB regulation is believed to be one of the reasons for the development of cancer and the NFκB regulation is different from healthy cells. Mammary epithelial cell lines are healthy cell lines and therefore the NFκB regulation is not comparable with NFκB regulation in cancer cell lines. Additional experiments to confirm the assumptions of comparability between the mouse embryonic fibroblast and mammary epithelial cells were beyond the scope of this thesis but need to be performed to validate our assumptions.

Experimental microarray data from cell cultures allow us to study the expression levels specific to the mammary epithelial cells as opposed to the expressions in the mammary gland which contains several different types of cells. Epithelial cells initiate cytokine expressions, which are signalling molecules that evoke reactions in the blood, milk and lymph system, assisting in the development of diseases such as mastitis in the mammary gland. Cell cultures do not include interactions of processes in the body from additional sources, such as blood and lymph systems, of the innate immune reaction. Therefore, the model represents the actions of the epithelial cells but not the interactions between the other innate immune

components, such as blood, lymph system, with the epithelial cells. A time frame of six hours was chosen because other mechanisms, such as blood and lymph systems, not included in the model, would influence the experimental data at time periods longer than six hours (Rangamani & Sirovich, 2007). Model predictions for longer periods are not of interest in this study where we identify the mechanistic properties of cytokine expression in the epithelial cells.

We were able to estimate the parameters from microarray experiments because we modified an algorithm for the estimation of concentration levels of mRNA from microarray experiments. We also showed how these values can be used to estimate parameters in signalling- gene network regulation models. Microarray values are relative but the conversion allowed us to estimate absolute concentration levels. The estimated parameters represented the experimental values well. The method has not been evaluated with biological experiments validating our results. Therefore, the conversion model needs to be validated in the future. It is of great importance to validate this method since it would allow the use of the vast array of microarray experiments currently available.

We can not speculate on the value of the experimental values between the measured points of our experiment. Since the time points are relatively wide apart compared with the time frame of molecular interactions we can only predict the model performance based on the assumption that the model behaviour of IκBαt in the module from Werner *et al.* (2005) is representative for the results of the microarray trend in this study.

**Multiple transcription factors**

It is known that multiple transcription factors in addition to NFκB are involved in the expression of the cytokines (Ghosh & Hayden, 2008). To our knowledge, experimental data for the multiple transcription factors in bovine mammary epithelial cells challenged with LPS is currently not available. Promoter deletion and mutagenesis experiments indicate that the nuclear factor NFκB site is the most important *cis*-regulatory element controlling TNFα induced RANTES transcription in alveolar epithelial cells (Casola *et al.*, 2002). In our model we therefore modelled mRNA synthesis to be initiated by NFκB dimerisation as the result of LPS challenge (Ghosh & Hayden, 2008). The NFκB transcription factor in the model is therefore the biological representation of several transcription factors. We represent the involvement of other transcription factors in the transcription of the cytokines with a Hill

coefficient of 3 for nuclear NFκB, similar to the coefficient for mRNA synthesis in the first module by Werner *et al.* (2005) in an elementary chemical reaction.

**Model behaviour**

The model predictions shown in Figure 5-7(A) show a build up of RANTES mRNA, which quickly rises when the nuclear NFκB concentration levels have reached a peak level (Figure 5-10). Although RANTES mRNA expression has been reported as a late gene in TNFα challenges of mouse embryonic fibroblasts, our experimental data indicates that mammary epithelial cells increase expression levels of RANTES mRNA as early as 60 minutes after LPS challenge.

For the first 40 minutes the model does not show an increase in mRNA concentration of the cytokines. This delay in the change of concentration represents the biological aspects of cytokine mRNA expression, where the model simulates the time necessary to build up nuclear NFκB levels to sufficient concentrations. In addition, transcription of a gene takes approximately 30 minutes in mammalians (Alon, 2007). Allocating transcription factors to the gene is part of this process and the delay is therefore acceptable.

For IL8 the rapid build up of mRNA concentration levels also starts after the initial lag representing the build up of nuclear NFκB and the time to transcribe a gene (Figure 5-7 (B)). However, following the peak, levels of IL8 mRNA expression slowly decrease in line with the experimental data. Similar expression levels of IL8 in mammary epithelial cells have been seen in other experimental studies (Strandberg *et al.*, 2005).

The model predicts a quick surge of TNFα mRNA concentration peaking at 100 minutes followed by a reduction in expression levels. Although no expression levels are measured in this experiment at 100 minutes, similar surges in raised TNFα mRNA concentration have been shown in other experimental studies (Strandberg *et al.*, 2005) and therefore the model predictions do not conflict with prior biological knowledge. The experimental data gives us no information on the peak in TNFα mRNA concentration. The experimental data predicts a higher concentration of TNFα at 1 hour than at 3 hours, which is confirmed in other experiments and depended on the bacterial load (Günther *et al.*, 2010). However, to our knowledge there is no experimental information on the concentration values in between the time points and the values need to be confirmed in biological experiments.

Model predictions of IκBα mRNA expression levels and the experimental values show a good fit at 60, 180 and 360 minutes (Figure 5-7 D). In our microarray experiment we measured expression levels at 60, 180 and 360 minutes, therefore no model predictions outside the data points can be compared with experimental data from the microarray experiments. Werner *et al.* (2005) measured IκBα degradation profiles at 0, 5, 10, 15, 30, 45, 60, 90 and 120 minutes and incorporated these values in the parameter estimation. The IκBα mRNA expression levels in our model are similar to the model predictions in Werner *et al.* (2005) for the time points that were measured. Therefore, the model is reliable to predict experimental values accurately during the simulation time.

**Comparison with additional experimental values**

While the general behaviour of the mRNA expression for TNFα and IκBα is similar for all three cows, the general of behaviour of the mRNA expression for RANTES and IL8 is different for the third data set (cow 3). Individual differences between cows can result in individual differences of cytokine mRNA expression levels and, as a result, mastitis resistance (Burvenich *et al.*, 2003; Paape *et al.*, 2002). Genetically determined differential expression levels of RANTES to pathogens between mastitis resistant and non resistant cows have been indicated earlier (Griesbeck-Zilch *et al.*, 2009). The difference between cows in RANTES expression levels has been indicated as possible selection indication for mastitis resistant animals. It is therefore valid to use the data of individual cows, rather than the average of a small dataset. In addition, the trend of the expression levels is the same and therefore the model can supply qualitative information on the underlying kinetics of the mRNA expression levels.

**Model fit for ranges of parameter values**

The analysis of the model fit (5.3.4) based on the three experimental values for the estimated parameters clearly indicate that the accuracy of model fit is highly dependent on the accuracy of the synthesis and degradation rates of TNFα. The accuracy of the degradation rates for RANTES and IL8 do not influence the model fit to the same degree. The model fit is not dependent on high accuracy of these parameters and the predictions for RANTES are informative. However, since the model fit for IL8 and especially TNFα are dependent on higher accuracy of the synthesis and degradation parameters for these cytokines and model

predictions should take the sensitivity of the model for changes in these parameters in consideration.

**Sensitivity and concentration**

The change in relative sensitivity values over time for RANTES and IL8 are reflected in the change in concentration levels over the simulation time (Figure 5-9 (A-D) and Figure 5-11 (A-D)). Increasing variation in sensitivity over time for degradation shows increasing variation for the concentration levels. A stable sensitivity for synthesis parameter changes shows a stable variation for concentration for RANTES and IL8.

For TNFα this is not the case. While the sensitivity of degradation parameter changes over time the variation in the concentration decreases (Figure 5-9 (E) and Figure 5-11 (E)). The sensitivity for synthesis is constant but the variation in concentration decreases over time (Figure 5-9 (F) and Figure 5-11 (F)). The findings for the lack of variation in the concentration of TNFα mRNA at 360 minutes are in line with findings in biological experiments testing the influence of variation in the bacterial load on the TNFα mRNA expression (Günther *et al.*, 2010) and will be further discussed in Chapter 8.

**Optimum time for experimental measurements**

The lack of influence of the parameter changes in the first 50 minutes is directly related to the changes in nuclear NFκB. Nuclear NFκB peaks at 70 minutes and has a second lower peak at 230 minutes (Figure 5-10). While the second peak of nuclear NFκB attenuate the increase in RANTES and IL8 it decreases the influence on the expression levels of TNFα to the value predicted with the model parameters.

The sensitivity analysis of parameter variation on cytokine mRNA concentration indicated the optimum time for experimental measurements (Figure 5-11). While TNFα mRNA concentration levels are most informative between 100 and 150 minutes, RANTES and IL8 mRNA concentration levels are more informative between 250 and 360 minutes.

There also is difference in the optimum time for measuring the mRNA concentration rate of the cytokines for the estimation of synthesis and degradation rates. The optimum time to measure cytokine concentration for the estimation of the degradation rates for RANTES and IL8, mRNA concentration is between 250 and 360 minutes in future biological experiments,

while TNFα concentration values are more informative between 100 and 200 minutes. To estimate synthesis rates measurements for concentration levels of mRNA should be done between 100 and 360 minutes for RANTES and IL8, while TNFα concentration is most informative between 75 and 150 minutes. The model simulations and sensitivity analysis have therefore shown that the timing of experimental values is of high importance and need to be carefully planned to insure the accuracy of the model development and the conclusions that can be drawn from the model simulations.

# Chapter 6
# Sensitivity analysis of parameter changes other than the synthesis and degradation parameters of the cytokines on the model output

*This chapter investigates the effects variation in all model parameters and initial values on the model output. The results of the analysis can be used for the design of future biological experiments and analysis of pharmaceutical targets.*

*The sensitivity analysis applied in Section 5.3 to the synthesis and degradation parameters of the cytokines in the model is thus extended to variation in all parameters and initial values of the model on cytokine mRNA expression levels. The sensitivity analysis will give an insight into the variation of the influence of different components in the TLR-IKK-NFκB signalling on the model output. The model parameters, other than the parameters estimated in the previous chapter, are a mix of parameters that are estimated, measured or retrieved from the literature with biological experiments on fibroblasts. In this work mammary epithelial cells are used for the biological experiments. It is important to evaluate the sensitivity of the model output to initial value and parameter changes when parameters are estimated from biological experiments with other cell types.*

*In the first Section we identify the time independent sensitivity of the initial values and parameters. Time independent sensitivity analysis assists in the identification of the parameters and initial values for which the model output has the highest sensitivity. This is followed by a time dependent sensitivity analysis of the parameters and initial values for which the model is highly sensitive. Time dependent sensitivity identifies the change in sensitivity over the model simulation time. The result of the time dependent sensitivity leads us to an investigation into the change in nuclear and cytoplasmic ratio of NFκB over the simulation time. We identify the difference of this regulation for each individual cytokine.*

*In the last Section in silico knockout simulations identify the importance of the negative feedback regulation of the IκB on NFκB regulation in the cytokine mRNA expression. We also highlight the value of modelling prior to the design of experiments and identify the significance of the difference in most informative time point in experimental measurements for each individual cytokine.*

## 6.1 Motivation for sensitivity analysis of all model parameters and initial values

Sensitivity analysis allows us to quantify the dependence of the system's behaviour on the parameters and initial values that affect the process dynamics (Rodriguez-Fernandez & Banga, 2009). In the previous chapter we extended a model to simulate cytokine mRNA concentrations and investigated sensitivity of the model output for the variation in synthesis and degradation cytokine parameters and initial values. The model captures qualitative and semi-quantitative data generated as result of *E. coli* challenged mammary epithelial cells.

As identified in Section 4.2.6, in the part of the model simulating the NFκB regulation to the nucleus, one third of the parameters are estimated, while others are bound by literature and experimental values. The parameters were estimated or measured for mouse embryonic fibroblasts as opposed to mammary epithelial cells used in our experiments. We have assumed that the same parameter values can be applied to mammary epithelial cells. Since we lack experimental data to verify this, it becomes necessary to investigate the qualitative behaviour of the model; to analyse the effect on the model output to changes in initial conditions and parameters and evaluate the effect of the changes on the model output. With the analysis we can thus establish the need for verification with biological experiments. The higher the sensitivity of the model for the parameter value changes, the higher the need for experimental verification of the parameter values. Parameters identified in the sensitivity analysis which are estimated and are not based on experimental values also need re-evaluating. The sensitivity analysis will thus assist us in the experimental design of future experiments and identify the components whose experimental values lead to maximum amount of information for parameter estimation and optimal model identification.

Parameter and initial value changes in the model influence the nuclear NFκB concentration and therefore the cytokine mRNA levels. In a linear system one would expect that parameters which change the concentration of nuclear NFκB are of particular interest. Since this is a nonlinear system dependencies are not always obvious. Therefore, we use sensitivity analysis on all parameters to show that parameters with an indirect influence on the nuclear NFκB concentration influence the model output to a larger extent than parameters with a direct influence on the NFκB concentration.

## 6.2 Sensitivity analysis

The sensitivity analysis applied in this work is outlined in Section 2.3.4. The analysis is used to study the variation in the model output as a result of variation in remaining initial values and parameters of the model implemented in Chapter 5.

The time independent sensitivity analysis is described in Section 2.3.4.1 is first applied. Briefly, initial values and kinetic parameters for the model are changed with incremental steps of 10% from -40% to +40% and the model simulated. For each component and parameter and the time independent values are calculated and ranked. The time independent sensitivity analysis identifies the parameters for which the model is highly sensitive. This is followed by the time dependent sensitivity analysis of the parameters and initial values for which the model output has shown high sensitivity.

### 6.2.1 Sensitivity of the model output for initial value changes of components other than the cytokines

Changes in initial values can change the model output. We determined the initial values by setting the values of NFκB and IKK to 0.1 and the remaining components to 0 and run the model with a basal input function, no bacterial challenge, until the model is in steady state as described in Section 5.2.2. To identify the highest sensitivity of the model output for the initial values of the components we rank the time independent and time dependent model sensitivities for the initial values.

#### *6.2.1.1 Time independent sensitivity of model output for initial value changes of components other than the cytokines*

The magnitude of the change in initial value showed a linear relationship between the change in the initial value and the sensitivity (results not shown), therefore an increase of 40% of the initial value is chosen for further evaluation. Exceptionally high sensitivity of the model output is recorded for changes in IKKIκBαNFκB initial values. TNFα, IL8 and RANTES mRNA expression all showed substantially higher sensitivity for the change in initial value of IKKIκBαNFκB than any of the other components (Table 6-1).

Table 6-1 Time averaged normalized sensitivities for change of initial value with a 40% increase are calculated and ranked. RANTES, TNFα and IL8 are highly sensitive to change in initial value of IκBαIKKNFκB.

| Components | RANTES Sensitivities | IL8 | TNFα | Rank | RANTES Sensitivity ranks | IL8 | TNFα |
|---|---|---|---|---|---|---|---|
| IκBαIKKNFκB | 2.1537 | 2.1372 | 2.3405 | | 1 | 1 | 1 |
| IκBαNFκB | 0.2645 | 0.2611 | 0.2548 | | 2 | 2 | 2 |
| IKK | 0.148 | 0.1483 | 0.1929 | | 4 | 4 | 3 |
| IκBεIKKNFκB | 0.1115 | 0.1115 | 0.143 | | 5 | 5 | 4 |
| IκBαt | 0.2169 | 0.2111 | 0.1226 | | 3 | 3 | 5 |
| IκBβIKKNFκB | 0.0733 | 0.0736 | 0.1033 | | 7 | 7 | 6 |
| IκBαNFκBn | 0.0899 | 0.0887 | 0.0862 | | 6 | 6 | 7 |
| IκBεNFκB | 0.0624 | 0.0623 | 0.0774 | | 8 | 8 | 8 |
| IκBβNFκB | 0.0519 | 0.0523 | 0.0762 | | 10 | 10 | 9 |
| IκBαIKK | 0.0322 | 0.0325 | 0.0467 | | 12 | 12 | 10 |
| NFκBn | 0.0608 | 0.0606 | 0.0427 | | 9 | 9 | 11 |
| IκBεNFκBn | 0.0211 | 0.0211 | 0.0259 | | 16 | 16 | 12 |
| IκBεt | 0.0376 | 0.0369 | 0.0247 | | 11 | 11 | 13 |
| IκBβt | 0.0302 | 0.0297 | 0.0225 | | 13 | 13 | 14 |
| IκBα | 0.0239 | 0.0237 | 0.0217 | | 14 | 15 | 15 |
| IκBαn | 0.0239 | 0.0239 | 0.0202 | | 15 | 14 | 16 |
| TNFαt | 0 | 0 | 0.019 | | 27 | 27 | 17 |
| IκBβNFκBn | 0.0036 | 0.0036 | 0.0051 | | 18 | 18 | 18 |
| IκBβIKK | 0.0015 | 0.0015 | 0.0022 | | 23 | 23 | 19 |
| IκBεIKK | 0.0013 | 0.0013 | 0.002 | | 24 | 24 | 20 |
| IκBε | 0.0023 | 0.0022 | 0.0018 | | 19 | 19 | 21 |
| IκBβ | 0.0018 | 0.0018 | 0.0014 | | 20 | 20 | 22 |
| NFκB | 0.0018 | 0.0018 | 0.0014 | | 21 | 21 | 23 |
| IκBεn | 0.0017 | 0.0017 | 0.0013 | | 22 | 22 | 24 |
| IκBβn | 0.0006 | 0.0006 | 0.0005 | | 25 | 25 | 25 |
| RANTESt | 0.012 | 0 | 0 | | 17 | 26 | 26 |
| IL8t | 0 | 0.0119 | 0 | | 26 | 17 | 27 |

#### *6.2.1.2 Time dependent sensitivity of the model output for initial value changes of components other than the cytokines*

While time independent sensitivity analysis gives us a tool to investigate the influence of changes in initial values on the model output over the total simulation time, investigation into time dependent sensitivities indicated a change of the influence over time (See Figure 6-1).

All three cytokine mRNA expression levels have indicated high sensitivity for the initial value of the component IκBIKKNFκB. The sensitivity of the model output is increasing for the first 45 minutes of the simulation and then decreases to a stable influence from 75 minutes onward for RANTES and IL8, however, sensitivity for TNFα mRNA expression increase again after 200 minutes (Figure 6-1).

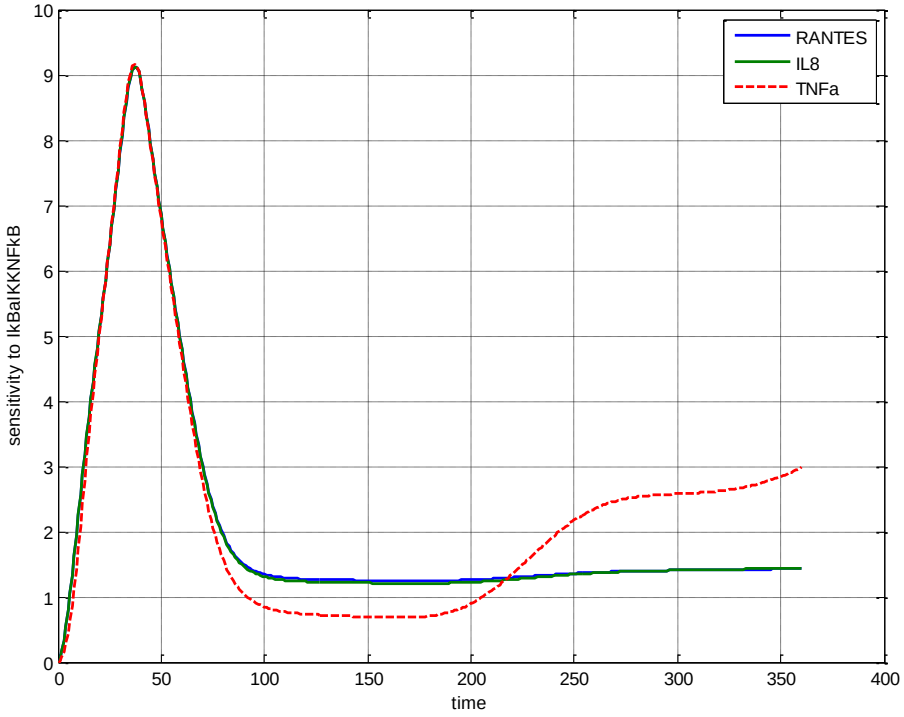


Figure 6-1 Sensitivity over time for the 40% increase in the initial value of IκBαIKKNFκB. This sensitivity is increasingly prevalent in the first 75 minutes of the model. Sensitivity of TNFα but not RANTES or IL8 to IκBαIKKNFκB increases again after 200 minutes. The x-axis represent the time (min) and the y-axis the concentration (μM).

### 6.2.2 Sensitivity of the model output for parameter changes of parameters other than synthesis and degradation parameters for cytokine expression

The model output is sensitive to the changes in parameters, but not equally sensitive to all parameters in the model. In order to rank the parameters for sensitivity on the model output we first investigate time independent sensitivities of the model output as described in 2.3.4. This facilitates ranking of the parameters in order of sensitivity for the model output. This is

followed by time dependent sensitivity on the parameters ranked for highest sensitivity on the model output (described in 2.3.4).

#### *6.2.2.1 Time independent sensitivity analysis of model output for parameter changes*

Time independent sensitivity analysis allows us to rank the parameters in order of sensitivity to the model output independent of time (Chen *et al.*, 2009). Ranking identifies the top 20 parameters, whose changes have the largest influence on the mRNA concentration of the cytokines over the 360 minutes simulation period (Figure 6-2).

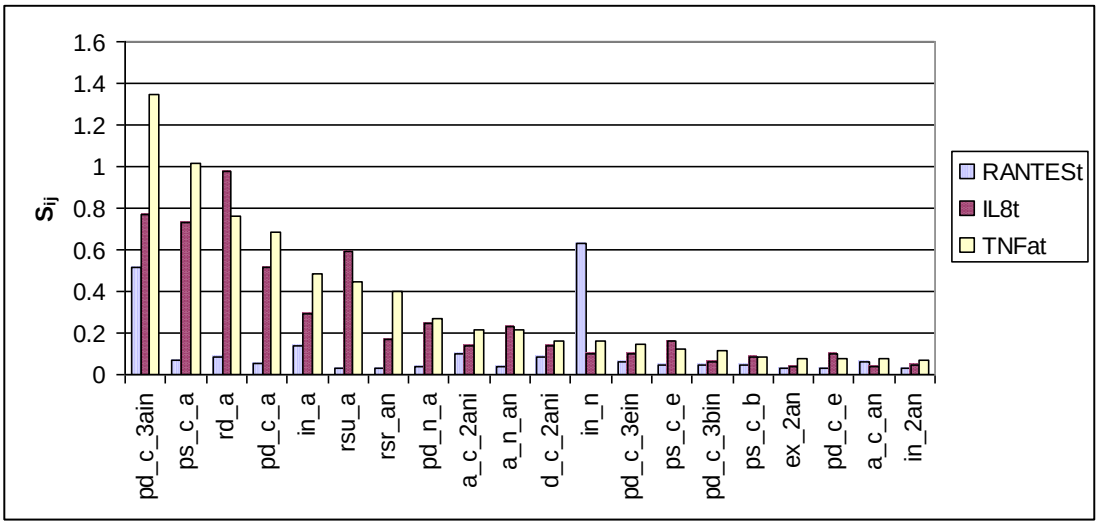


Figure 6-2 Time independent sensitivities for the 40% variation in the top 20 parameters with the highest influence on the RANTES, IL8 and TNFα mRNA expression levels.

Since the cytokine expression is dependent on the nuclear NFκB concentration, we also considered the sensitivity for the model output of nuclear NFκB to evaluate if factors influencing nuclear NFκB would explain sensitivity for mRNA cytokine expression levels. It might be expected that all three cytokines show similar sensitivity to the changes in nuclear NFκB levels, however this is not the case.

Table 6-2 Ranking of time independent parameter sensitivity for the model output of RANTES, IL8, TNFα mRNA cytokine expression levels and nuclear NFκB. Each parameter is ranked for all three cytokines and nuclear NFκB (RR rank RANTES, RI rank IL8, RT rank TNFα, RNn rank nuclear NFκB).

| Parameter | RANTESt | IL8t | TNFαt | NFκBn | RR | RI | RT | RNn | Reaction | | | |
|---|---|---|---|---|---|---|---|---|---|---|---|---|
| pd_c_3ain | 0.514921 | 0.772747 | 1.348037 | 1.925736 | 2 | 2 | 1 | 2 | IκBαIKKNFκB | => | IKK + NFκB | protein degradation |
| ps_c_a | 0.065551 | 0.731161 | 1.016088 | 1.229843 | 7 | 3 | 2 | 3 | | => | IκBα | protein synthesis |
| rd_a | 0.084081 | 0.97667 | 0.765133 | 2.248255 | 6 | 1 | 3 | 1 | IκBαt | => | | RNA degradation |
| pd_c_a | 0.05229 | 0.51537 | 0.687101 | 1.141565 | 11 | 5 | 4 | 4 | IκBα | => | | protein degradation |
| in_a | 0.141784 | 0.294533 | 0.481989 | 0.611404 | 3 | 6 | 5 | 6 | IκBα | => | IκBαn | import Cytoplasm->Nucleus |
| rsu_a | 0.030366 | 0.592339 | 0.443582 | 0.784223 | 24 | 4 | 6 | 5 | | => | IκBαt | constitutive RNA synthesis |
| rsr_an | 0.029787 | 0.167645 | 0.397572 | 0.40115 | 26 | 9 | 7 | 8 | | => | IκBαt | NFκB induced RNA synthesis |
| pd_n_a | 0.038653 | 0.244195 | 0.269018 | 0.440502 | 17 | 7 | 8 | 7 | IκBαn | => | | protein degradation |
| a_c_2ani | 0.100004 | 0.137585 | 0.217971 | 0.283192 | 4 | 12 | 9 | 10 | IκBαNFκB+IKK | => | IκBαIKKNFκB | association |
| a_n_an | 0.035567 | 0.233075 | 0.211935 | 0.338122 | 20 | 8 | 10 | 9 | IκBαn+NFκBn | => | IκBαNFκBn | association |
| d_c_2ani | 0.084734 | 0.135727 | 0.159476 | 0.229501 | 5 | 13 | 11 | 13 | IκBαIKKNFκB | => | IKK + IκBαNFκB | dissasociation |
| in_n | 0.633307 | 0.098388 | 0.157964 | 0.215763 | 1 | 18 | 12 | 14 | NFκB | => | NFκBn | import Cytoplasm->Nucleus |
| pd_c_3ein | 0.063983 | 0.100374 | 0.146605 | 0.192289 | 8 | 17 | 13 | 16 | IκBεIKKNFκB | => | IKK + NFκB | protein degradation |
| ps_c_e | 0.048143 | 0.161559 | 0.12461 | 0.257851 | 12 | 10 | 14 | 11 | | => | IκBε | protein synthesis |
| pd_c_3bin | 0.046429 | 0.061163 | 0.115105 | 0.129704 | 14 | 24 | 15 | 21 | IκBβIKKNFκB | => | IKK + NFκB | protein degradation |
| ps_c_b | 0.044232 | 0.085209 | 0.088157 | 0.152894 | 15 | 21 | 16 | 19 | | => | IκBβ | protein synthesis |
| ex_2an | 0.033019 | 0.035038 | 0.078989 | 0.087337 | 21 | 36 | 17 | 28 | IκBαNFκBn | => | IκBαNFκB | export Nucleus->Cytoplasm |
| pd_c_e | 0.029514 | 0.101408 | 0.077794 | 0.18142 | 27 | 15 | 18 | 17 | IκBε | => | | protein degradation |
| a_c_an | 0.06216 | 0.041896 | 0.076054 | 0.088746 | 10 | 29 | 19 | 27 | IκBα+NFκB | => | IκBαNFκB | association |
| in_2an | 0.031638 | 0.044048 | 0.067095 | 0.085575 | 23 | 28 | 20 | 29 | IκBαNFκB | => | IκBαNFκBn | import Cytoplasm->Nucleus |

TNFα mRNA expression shows the highest sensitivity to protein degradation of IKKIκBαNFκB (Table 6-2). In addition, TNFα mRNA expression showed sensitivity to initial concentration of this component (Table 6-1). IL8 mRNA expression is sensitive to protein degradation of IκBα mRNA. RANTES mRNA expression showed high sensitivity to changes in parameters influencing NFκB import into the nucleus, followed by the sensitivity to protein degradation of IκBα in the cytoplasm and transport of IκBα into the nucleus.

#### *6.2.2.2 Time dependent sensitivity analysis of model output for parameter changes*

To investigate if the sensitivity of parameter changes on the model output is time dependent we calculated the sensitivity for each time step as described in Section. The sensitivity was calculated for each cytokine with changes in the parameter values with the highest rank identified in Section 6.2.2.1.

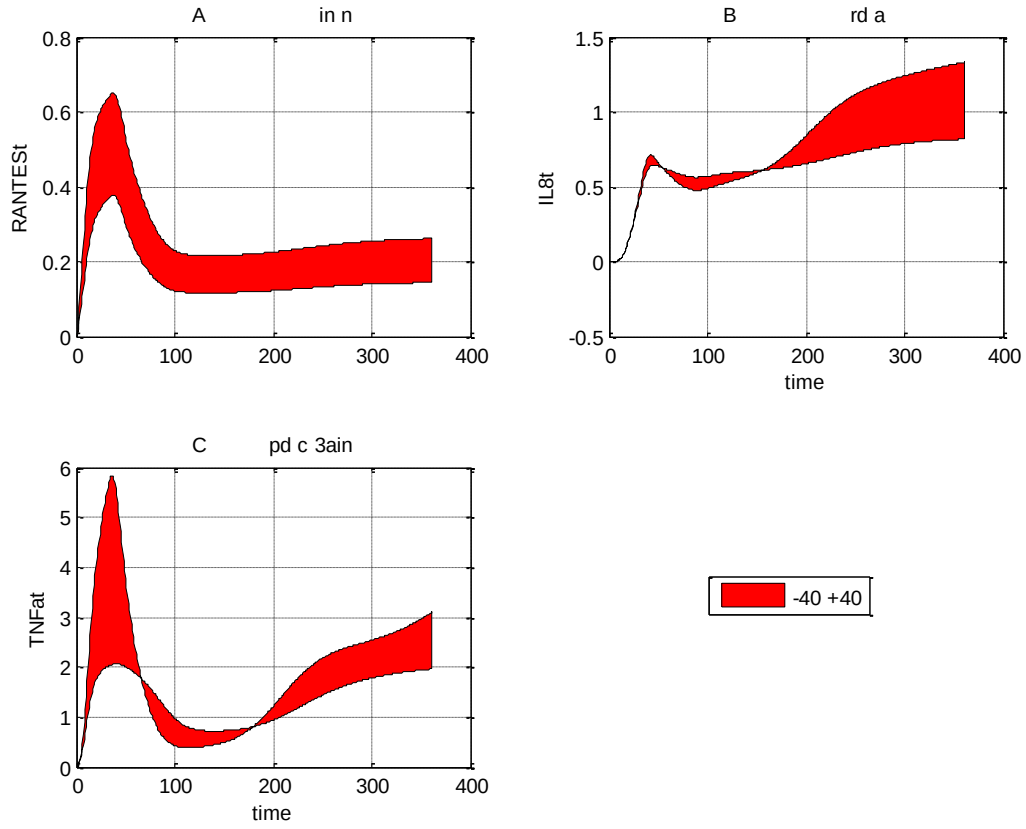


Figure 6-3 Time dependent sensitivity. The model was simulated with parameter values decreasing and increasing from -40% to +40% from the model values and sensitivity for each time step is calculated for parameters that indicated highest model sensitivity in the time independent analysis. (A) RANTES mRNA shows sustained sensitivity for in_n, NFκB nuclear import, over 360 minutes of simulation (B) IL8 mRNA sensitivity for degradation of IκBα increases toward the end of the simulation time (C) TNFα mRNA sensitivity for protein degradation of IKKIκBαNFκB indicates changing sensitivity overtime with increased sensitivity at 45 minutes. TNFα shows the highest sensitivity values and RANTES the lowest.

As can be seen in Figure 6-3, the range of the sensitivity coefficient for the parameters varies over time for IL8 and TNFα, while the coefficient is stable for RANTES during the time of simulation. This indicates that RANTES concentration over 360 minutes of simulation is sensitive to changes in NFκB nuclear import over the total simulation time. In contrast, sensitivity for the parameters influencing the IL8 concentration during the 360 minutes simulation increased after 180 minutes of simulation, indicating a change in sensitivity after 180 minutes. Sensitivity for TNFα concentration for parameter changes has a peak at 45

minutes and then is increasing after 200 minutes of simulation with the TNFα concentration less sensitive between 60 and 200 minutes.

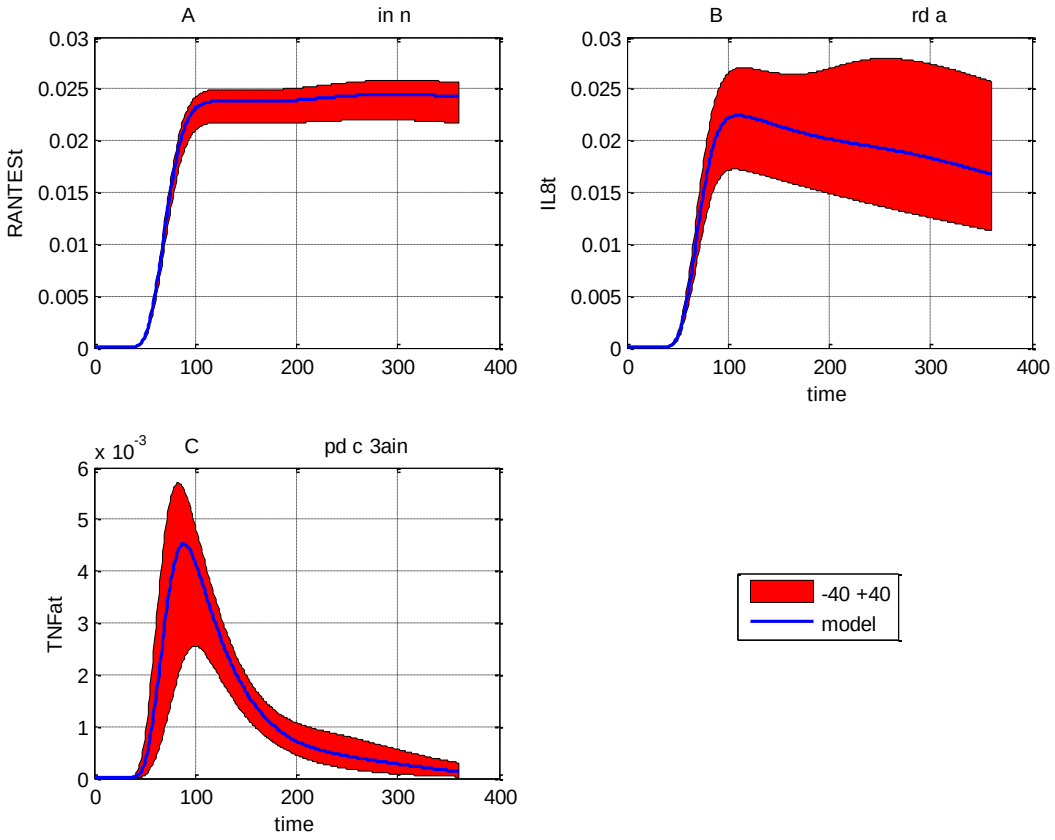


Figure 6-4 Variation in cytokine mRNA concentration(μM) as the result of 360 minutes of simulation with varying parameter values from -40% to +40% from the nominal value. The model output was indicated as highly sensitive for the parameters in the sensitivity analysis. (A) RANTES mRNA concentration show sustained change in concentration for parameter change influencing the transport of NFκB into the nucleus (in_n). (B) IL8 mRNA concentration changes with the change in parameter influencing the mRNA degradation of IκBα, specifically after 200 minutes (rd_a). (C) TNFα mRNA concentration changes as a result of the parameter changes influencing the IKK mediated protein degradation in the first 60 minutes of the model (pd_c_3ain). The x-axis represent the time (min) and the y-axis the concentration (μM).

When the effect on the concentration of the cytokine for variations in the parameters on the individual cytokines is studied over time, a distinct difference in the effect at varying times on each cytokine concentration is noticed (Figure 6-4). RANTES mRNA expression is sensitive during the entire simulation time for the translocation of NFκB into the nucleus, however, the change in concentration levels is only prevalent after 75 minutes of simulation (Figure 6-4).

TNFα is sensitive early in the simulation and towards the end of the simulation and the largest change in concentration can be found in the peak around 100 minutes. Sensitivity of IL8 increased after 200 minutes of simulation, changes in concentration level as an effect of the parameter changes can already be seen after 100 minutes and are the largest at 240 minutes. This indicates that biological experiments need to be carefully planned to optimize the information from the experimental values.

#### *6.2.2.3 Time dependent sensitivities for parameter changes on nuclear NFκB*

Although our interest is in the mRNA concentrations of the cytokines, the highest ranked parameters all have an influence on the nuclear NFκB concentration. In addition, it has been suggested that pharmaceutical products modulate NFκB concentration to treat the infection and modulate cytokine expression levels. It would therefore be of great value to evaluate the influence of variation in NFκB concentration on cytokine expression levels with the model. The effect of variation in highest ranked parameters on nuclear NFκB concentration is investigated. With this, the relationship between nuclear NFκB concentration and the cytokine concentrations and possible use of nuclear NFκB concentration for cytokine synthesis and degradation parameter estimation is evaluated.

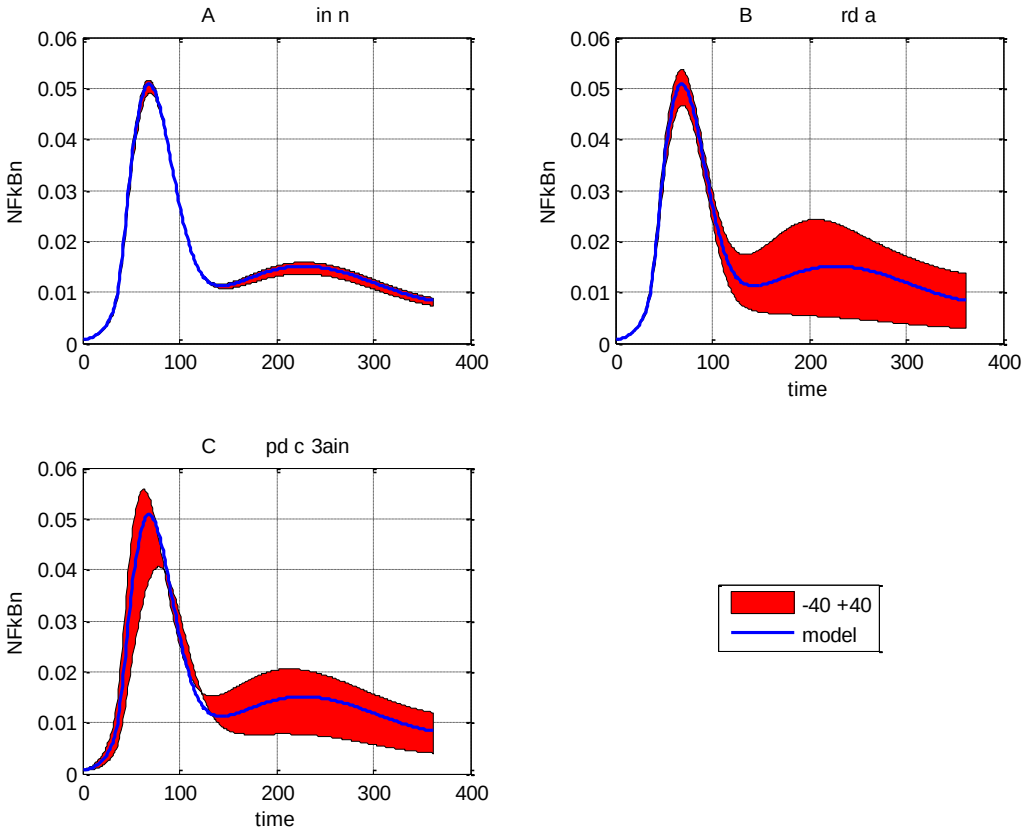


Figure 6-5 Nuclear NFκB concentration changes for simulation of parameter changes from -40% to +40% in: NFκB import (in_n), IκBα mRNA degradation (rd_a) and IKKIκBαNFκB protein degradation (pd_c_3ain). The x-axis represent the time (min) and the y-axis the concentration (μM).

Changes in protein degradation parameters for IκBα (rd_a) show an increasing change in nuclear NFκB after 100 minutes, peaking at 200 minutes (Figure 6-5 (B)). This change is related to the change in the IL8 concentration level (Figure 6-4 (B)). Experimental measurements of nuclear NFκB levels would assist in the identification of the correct parameter values for IL8 concentration. Nuclear NFκB levels with parameter changes for IKK mediated protein degradation (pd_c_3ain) do not follow the pattern of TNFα concentration levels (Figure 6-4(C) and Figure 6-5 (C)) and therefore would not be informative for parameter estimation of TNFα. Changes in nuclear import parameters (in_n) (Figure 6-5 (A)) do not influence the concentration of nuclear NFκB. Nuclear NFκB concentration is therefore not indicative for parameter estimation of RANTES concentration values.

The findings indicate that nuclear NFκB levels could be further explored with biological experiments as an indicator for synthesis and degradation parameter estimation in IL8 expression levels. Nuclear NFκB concentration level variation is insufficiently related to RANTES or TNFα mRNA concentration.

We also investigated the change in cytoplasmic NFκB concentration as a result of the change in the highest ranked parameters (Figure 6-6).

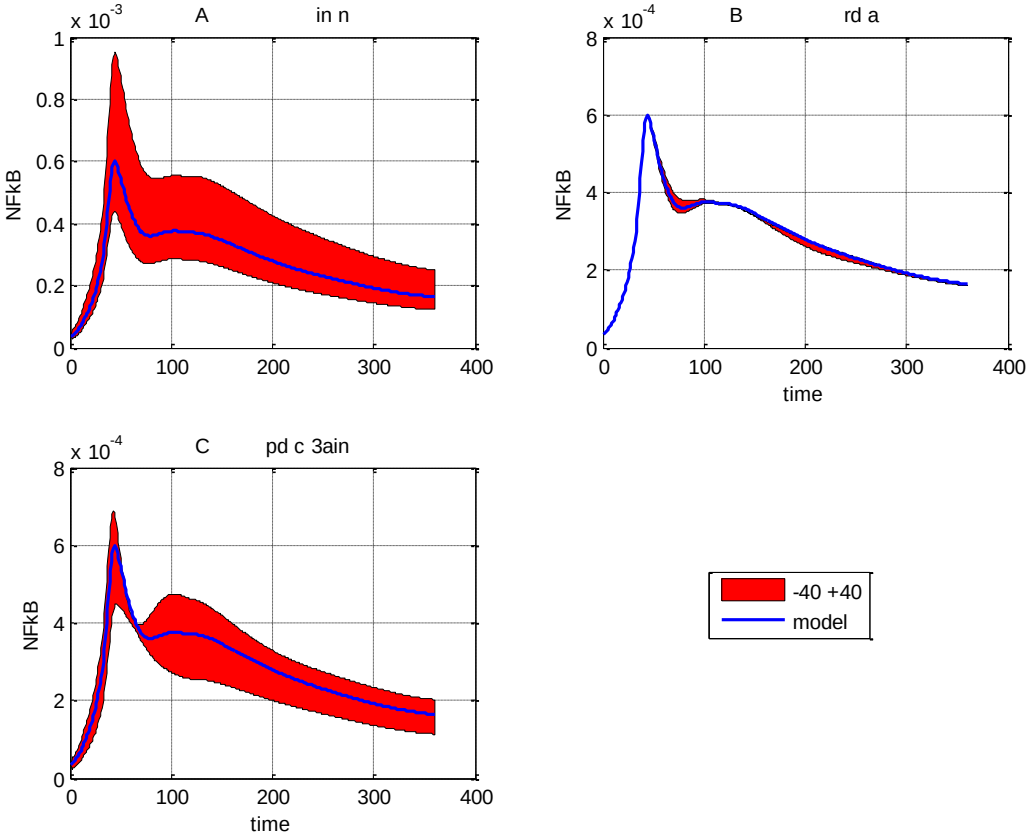


Figure 6-6 Cytoplasmic NFκB concentration changes for the model simulation of parameter variation from -40% to +40% in: NFκB import (in_n), IκBα mRNA degradation (rd_a) and IKKIκBαNFκB protein degradation (pd_c_3ain). While parameter changes in NFκB import (in_n) and IKKIκBαNFκB protein degradation (pd_c_3ain) change the concentration, variation in IκBα mRNA degradation parameter (rd_a) does not influence the cytoplasmic NFκB concentration. The x-axis represent the time (min) and the y-axis the concentration (μM).

While parameter changes in NFκB import (in_n) and IKKIκBαNFκB protein degradation (pd_c_3ain) change the concentration, variation in IκBα mRNA degradation parameter (rd_a) does not influence the cytoplasmic NFκB concentration. The relationship between cytoplasmic NFκB, RANTES and TNFα is clearer than the relationship between nuclear NFκB and the cytokines RANTES and TNFα. There is no relationship between cytoplasmic NFκB and IL8.

#### 6.2.2.4 Changes in the ratio of cytoplasm to nucleus NFκB as a result of parameter changes

Experimentally it is not always possible to separate the nuclear and cytoplasmic concentrations of NFκB due to the fast reaction of the translocation of NFκB from the cytoplasm to the nucleus in an infection. It would be more informative and cost effective to be able to identify the model output against one measurement of NFκB. Neither did we see a clear relationship between nuclear or cytoplasmic NFκB concentrations and the cytokine expression. Therefore, the ratio between the NFκB in the cytoplasm and nucleus ([NFκB]: [NFκBn]) is investigated for the highest ranked parameters in this section.

The change in the ratio of NFκB in the cytoplasm and nucleus was plotted over time for the range of -40% to +40% for the highest ranked parameters identified in Section 6.2.2.1 (Figure 6-7).

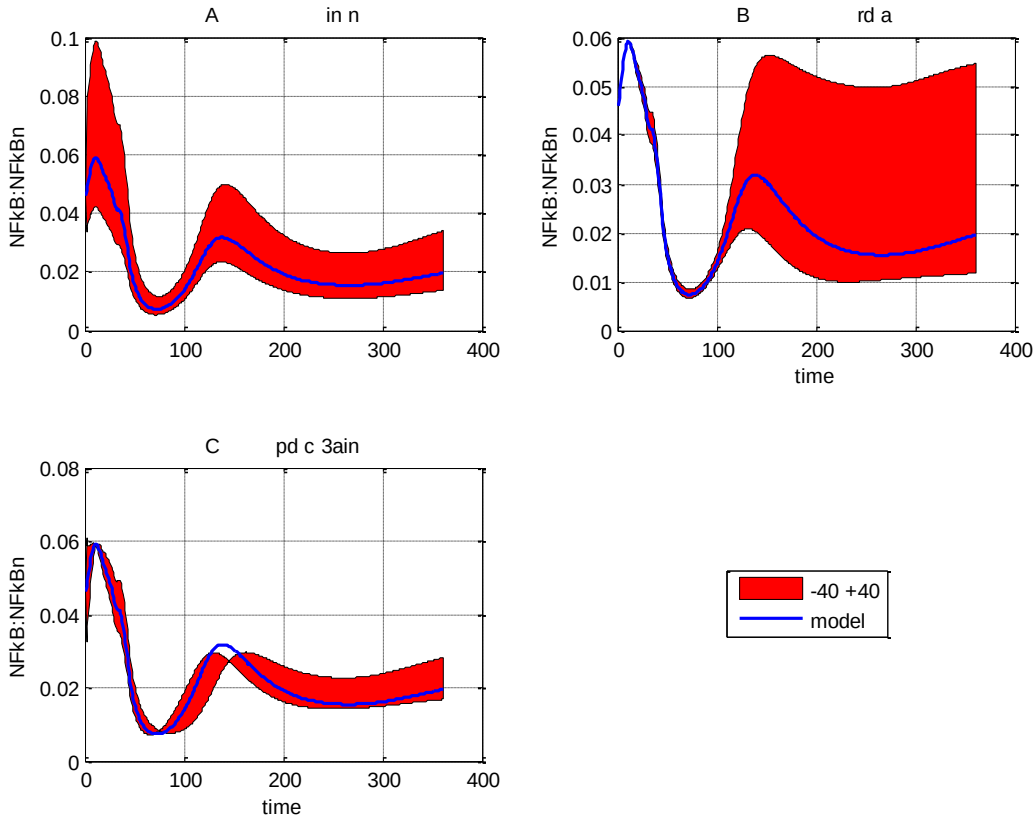


Figure 6-7 Changes in the ratio of cytoplasmic and nuclear NFκB concentration (μM) over the 360 minutes simulation period for highest ranked parameters in model sensitivity analysis. (A) NFκB ratio changes as result of parameter changes in transport of NFκB from the cytoplasm to the nucleus (in_n) are consistent over the simulation time, which is similar to the changes in the RANTES mRNA concentration. (B) The NFκB ratio shows a change from 120 minutes onward, while after 180 minutes IL8 mRNA shows a change in concentration with variation in mRNA degradation (rd_a) of IκBα. (C) A relatively small change in the ratio is shown for parameter changes in IKK mediated protein degradation of IκBα (pd_c_3ain) indicated as the parameter with the highest rank in sensitivity analysis for TNFα mRNA concentration.

Change in the ratio is very prevalent with the change in parameters with a high ranking for RANTES and IL8 mRNA, indicating a possible relationship between the NFκB ratio, the parameter values and the concentration of the mRNA expression. The change in ratio of NFκB for the parameter variation influencing TNFα is less prevalent. However, both nuclear and cytoplasmic NFκB change as result of the variation in the parameter with the highest rank for TNFα mRNA (Figure 6-5(C) and Figure 6-6(C)). Change in NFκB ratio for parameters ranked high with RANTES mRNA is attributed to a change in cytoplasmic NFκB (Figure 6-6 (A)). For IL8 mRNA the change in ratio is attributed to a change in nuclear NFκB (Figure 6-5

(B)). In addition, parameters differ in the time period where they have an influence on the change in the [NFκB]:[NFκBn] ratio for each cytokine.

RANTES shows the highest sensitivity to change in the parameter influencing the translocation of NFκB from cytoplasm to the nucleus, especially in the first 45 minutes and after 120 minutes of simulation (Figure 6-7 (A)). During these times there is a significant change in [NFκB]:[NFκBn] ratio as a result of parameter changes.

IL8 shows sensitivity to the change in the [NFκB]:[NFκBn] ratio after 120 minutes as a result of change in the parameter for RNA degradation of IκBα (Figure 6-7 (B)). During this period the ratio of [NFκB]:[NFκBn] between cytoplasm and nucleus changes significant with the parameter changes.

TNFα mRNA expression is most sensitive in the early stages of the model simulation where there is a sharp decline in the [NFκB]:[NFκBn] ratio (See Figure 6-7 (C)) as a result of the change in the parameter for IKK mediated IκBα protein degradation in the cytoplasm. TNFα mRNA expression shows a pulse like behaviour while IL8 mRNA expression is sustained over a longer period. This difference comes back in the [NFκB]:[NFκBn] ratio plots with TNFα showing sensitivity towards the change in the peak while IL8 shows sensitivity towards the parameter that influences the change in sustained change of the ratio indicating that the [NFκB]:[NFκBn] ratio influences the expression levels.

Further analysis did not indicate a specific relationship between the [NFκB]:[NFκBn] ratio and cytokine expression levels. The ratio is therefore not indicative of the cytokines mRNA expression or informative in parameter estimation. However, nuclear and cytoplasmic NFκB have been shown to influence mRNA expression in a unique way for each cytokine, therefore, the regulation of NFκB need to be investigated further.

## 6.3 Simulation of knockout models

The influence of a specific component on the model output can be investigated with knockout simulations. NFκB is controlled by IκB isoforms (2.1.3) with negative feedback loops. To separate the influence of NFκB and the role of the IκB isoforms on the cytokine expression levels we perform *in silico* knockout simulations. Biological experiments can not always simulate a total knockout, total removal of the expression of the protein, due to lethality and

redundancy. In addition, prior *in silico* simulations can reduce the number of biological experiments needed that will optimize the model output.

Investigations into the sensitivity of the model output revealed that the variation of parameters influencing the concentration of IκB isoforms and NFκB affect the mRNA expression of the cytokines. Since IκBα forms a negative feedback loop for NFκB, it is important to separate the influence of both components to identify the individual contribution to the model output.

Sensitivity analysis also identified parameters that influence IκBε and IκBβ levels have an influence on TNFα and IL8 cytokine expression, even though they are less than the influence of parameters which affect IκBα levels. Changes in IκBε and IκBβ levels showed higher sensitivity in RANTES mRNA expression. IκBε is highly NFκB inducible in TNFα challenges and mediates a functional negative feedback on NFκB activity in anti phase to IκBα (Kearns *et al.*, 2006). Interaction between IκBα and IκBε has been found to be responsible for the translocation of NFκB from the cytoplasm to the nucleus. We therefore perform *in silico* simulations of knockout models of IκBα, IκBε and NFκB to investigate the influence of each of these components on the cytokine concentrations.

### 6.3.1 Simulation of IκBα knockout model

The *in silico* IκBα, NFκB, IκBε and IκBβ knockout models were generated from the wild type model by setting the initial value and the concentration of IκBα, IκBα mRNA, NFκB, and IκBε respectively during the simulation to zero.

*In silico* simulation of the protein IκBα or the IκBα mRNA knockout model show a substantial increase of mRNA levels of RANTES, IL8 and TNFα (Figure 6-8). The NFκB in the cytoplasm is reduced as a result of the knockout of IκBα, while the nuclear NFκB increases (Figure 6-8 (D, E)). This is expected since IκBα is a negative feedback loop for the translocation of NFκB to the Nucleus (Hoffmann *et al.*, 2002a). IκBα associates with NFκB in the cytoplasm preventing the movement of NFκB from the cytoplasm to the nucleus. Reduction of IκBα therefore increases the concentration of free NFκB in the cytoplasm which results in increased movement of NFκB to the nucleus where cytokine expression is initiated.

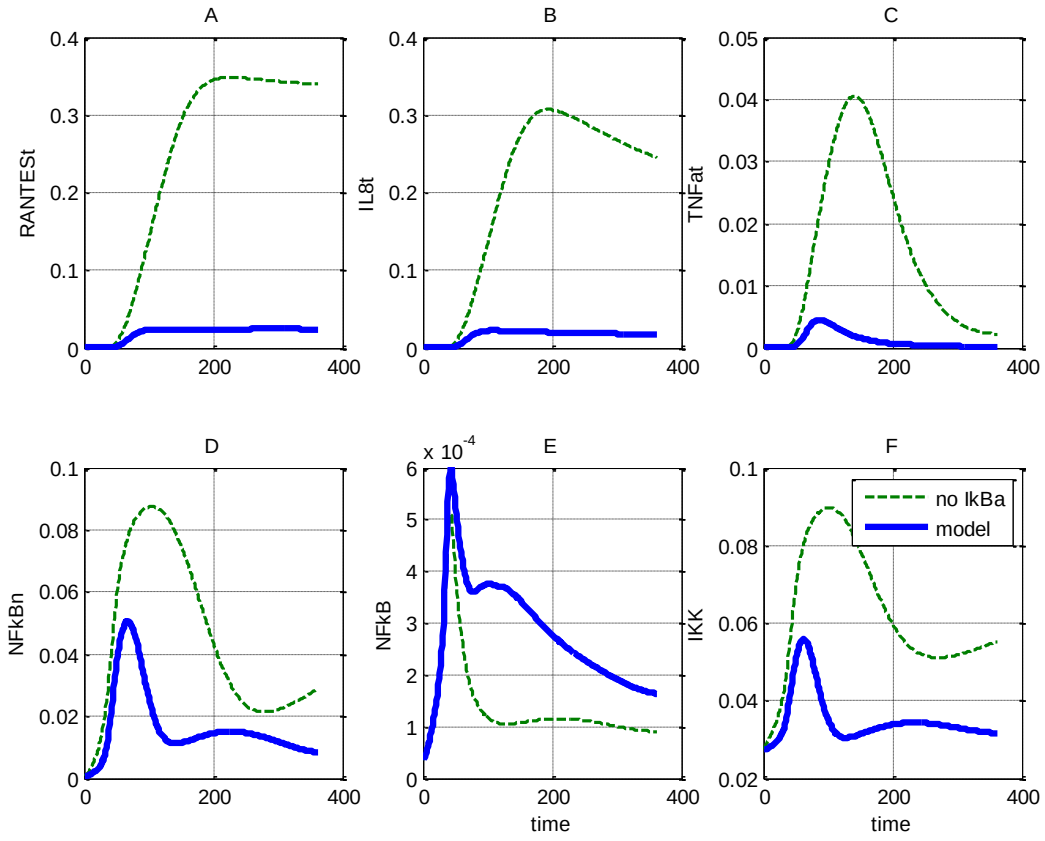


Figure 6-8 Simulations of IκBα knockout and the effect on the different components. Fig A and B, RANTES and IL8 do not return to the model values, while TNFα (Fig C) does return to the model values. While Nuclear NFκB (Fig D) is higher than the model value, cellular NFκB (Fig E) is lower than the model value. IKK (Fig F) is increased and stays at increased level. The x-axis represent the time (min) and the y-axis the concentration (μM).

RANTES expression shows a prolonged increase in mRNA expression level before the concentration stabilizes (Figure 6-8 (A)). IL8 also shows a prolonged increase but decreases toward the wild type level (Figure 6-8 (B)) while the TNFα increases with a higher peak but reduces quickly to the wild type value when the nuclear NFκB reduces (Figure 6-8 (C)).

Looking at the NFκB ratio between cytoplasm and nucleus in Figure 6-9 (C), the IκBα knockout reduces the ratio, stabilizing after 70 minutes with increased concentration of NFκB in the nucleus and reduced concentration of NFκB in the cytoplasm.

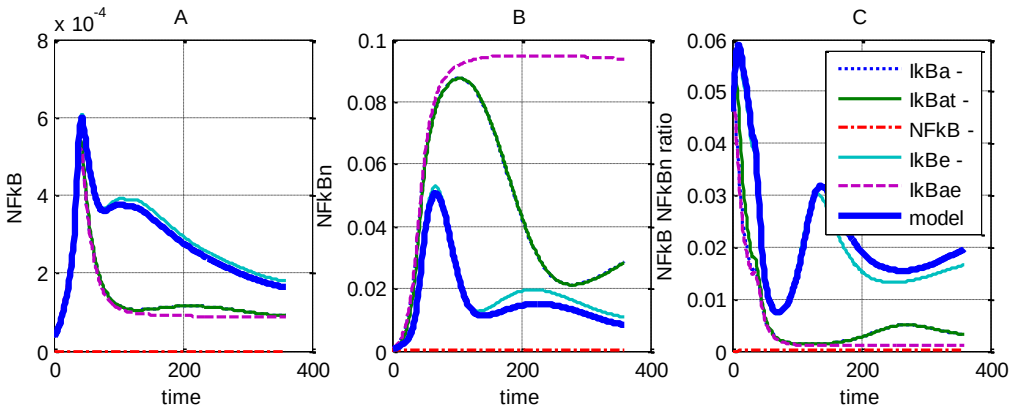


Figure 6-9 Knockout simulations of the model with IκBα, IκBα mRNA, NFκB, IκBε, and the double knockout IκBα/IκBε. (A) Cytoplasmic levels of NFκB are reduced with the knockout models after the initial peak, while IκBε knockouts do not have an effect on the cytoplasmic NFκB levels. (B) Nuclear NFκB levels increase. This highlights the function of the second feedback loop of IκBε in (C) NFκB cytoplasmic to nucleus ratio is reduced with the double knockout, all the NFκB is in the nucleus inducing increased expression levels. The x-axis represent the time (min) and the y-axis the concentration (μM).

### 6.3.2 NFκB knockout simulations

*In silico* simulation of the NFκB knockout shows a sustained sharp decrease of RANTES and IL8 mRNA (Figure 6-10 (C and D)Figure 6-11). TNFα mRNA decreases to 0 after 200 minutes (Figure 6-10 (E)). Werner *et al.* (2005) did not detect TNFα mRNA expression in biological experiments with NFκB deficient cells after LPS stimulation. However, levels in the model are so small that they could be undetectable with experimental methods using a population average. IκBα is maintained at initial value levels (Figure 6-10 (F))

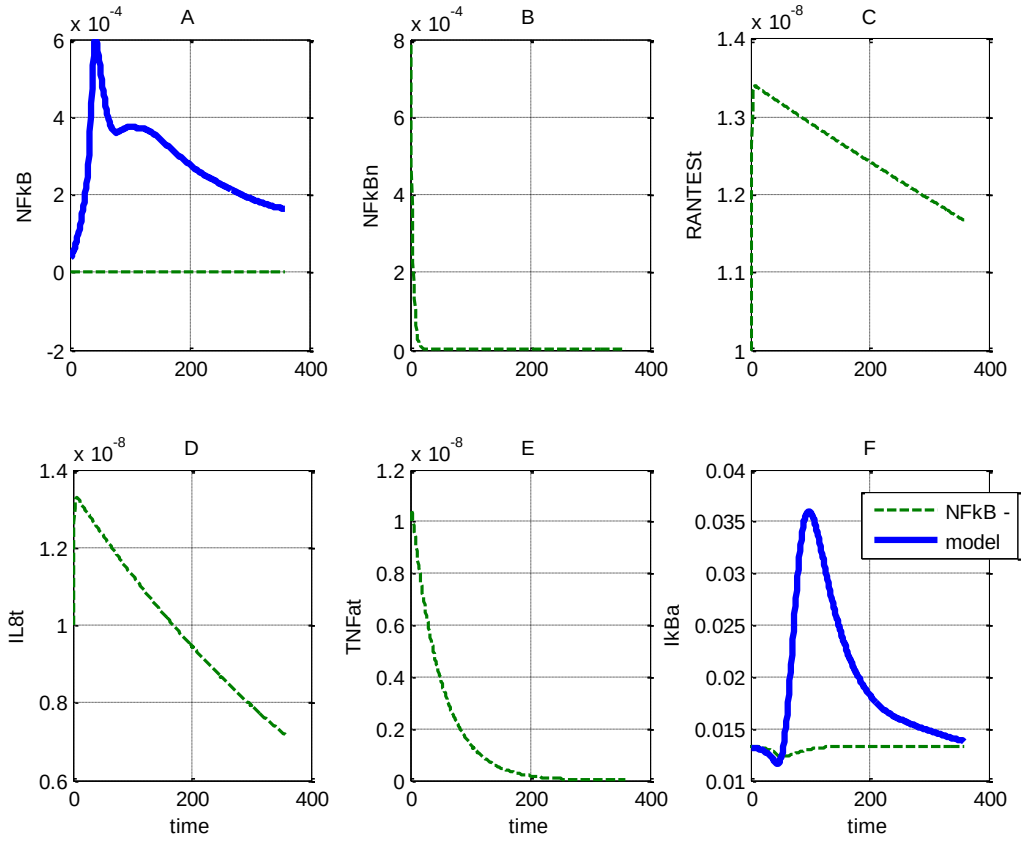


Figure 6-10*In silico* knockout simulation of NFκB. (For clarity model values of RANTES, IL8 and TNFα expression are omitted, they are substantially higher that the knockout values). (A) NFκB wild type and knockouts values (B) Nuclear NFκB is quickly reduced to zero (C-D) RANTES, IL8 is reduced over time (D) TNFα shows a different pattern indicating different regulation of the expression levels between the cytokines (F) IκBα concentration is does not show a rise as seen in wild type and is reduced to significantly low levels. The x-axis represent the time (min) and the y-axis the concentration (μM).

*In silico* simulation of the knockout of NFκB reduced the concentration of IκBα and IκBε, while it increased the concentration of IκBβ (Figure 6-11 (D-F)).

### 6.3.3 IκBε and multiple knockout simulations

As with the IκBα knockout model, the NFκB knockout indicates a different regulation for each cytokine. While IκBα knockout increases expression levels, NFκB knockout decrease expression levels. However, the complete picture is unclear and we need to look at IκBβ and IκBε and the interaction between the IκBs and their influence on the expression levels.

IκBε plays an important role in terminating inflammatory response (Kearns *et al.*, 2006) and is part of a negative feedback loop reducing NFκB translocation to the nucleus in sustained infections (Cheong *et al.*, 2008). Therefore, we investigate influence of IκBε on the cytokine mRNA expression levels with IκBε knockout models. The *In silico* simulation of the IκBε knockout models show almost no change of mRNA levels of RANTES, IL8 and TNFα (Figure 6-11 (A-C)). The knockouts increase the IκBα concentration raising the peak minimally, returning back to the wild type model values (Figure 6-11 (E)). NFκB in the cytoplasm and nucleus are marginally affected by the knockouts.

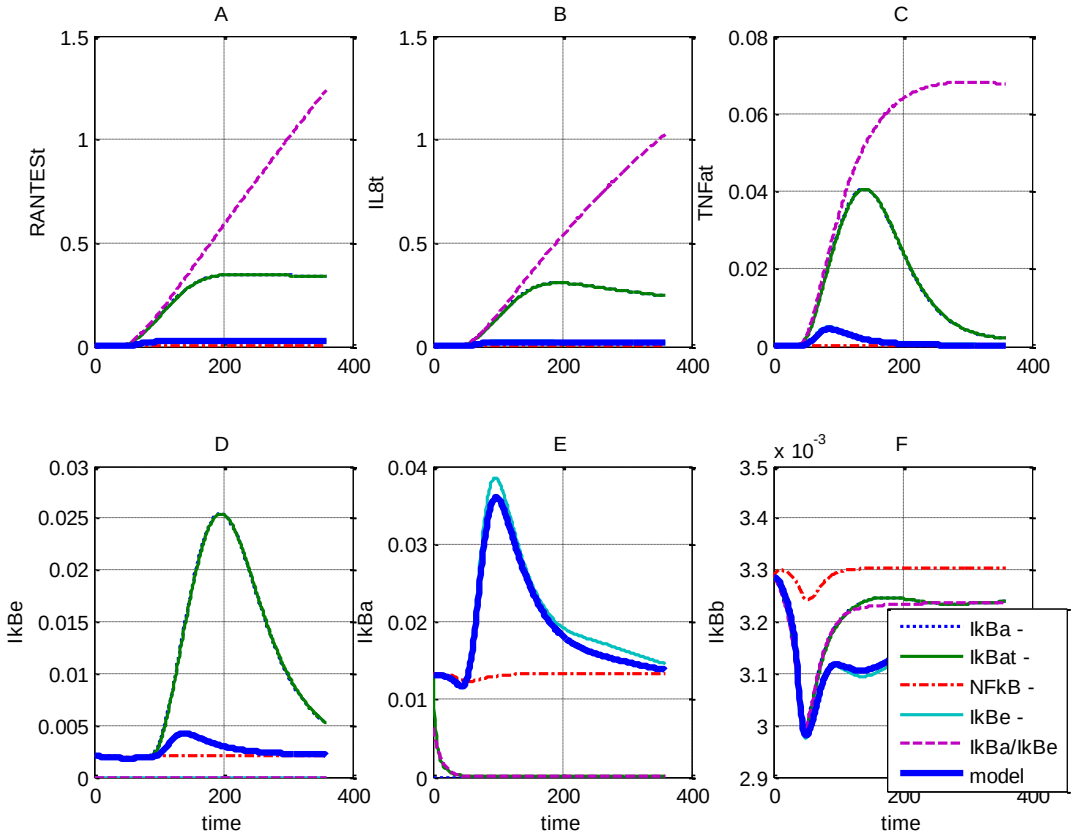


Figure 6-11 Simulations of the model with IκBα, IκBα mRNA, NFκB, IκBε, and the double knockout IκBα/IκBε. Knockout models were generated from the wild type model by setting the initial value and the rate of expression to zero (A-B) RANTES and IL8 expression levels for the knockout models showed attenuation of the IκBα/IκBε double knockout and raised levels for IκBα knockouts, while NFκB knockouts reduced the levels. (C) TNFα expression is raised with IκBα/IκBε knockouts but returns to a stable level, while IκBα knockouts are raised but return to wild type level at 360 minutes and NFκB knockouts reduces the expression levels. (D) IκBε levels are raised by IκBα and IκBαt knockouts but return to wild type level at 360 minutes of simulation (F) IκBβ levels were raised by the knockouts apart from the IκBε knockout. IκBε does not influence the level of IκBβ. The x-axis represent the time (min) and the y-axis the concentration (μM).

All three cytokines have increased expression levels as result of the IκBα/IκBε knockout. RANTES and IL8 (Figure 6-11(A-B)) continue to increase expression levels during the simulation time while TNFα reaches saturation (Figure 6-11 (C)).

The knockout of both negative feedback loops, IκBα/IκBε, lead to a decrease in cytoplasmic NFκB during the simulation period (Figure 6-12 (A)) and an increase and attenuation in the concentration of nuclear NFκB (Figure 6-12 (B)). The knockout of IκBε does not change the NFκB concentrations (Figure 6-12).

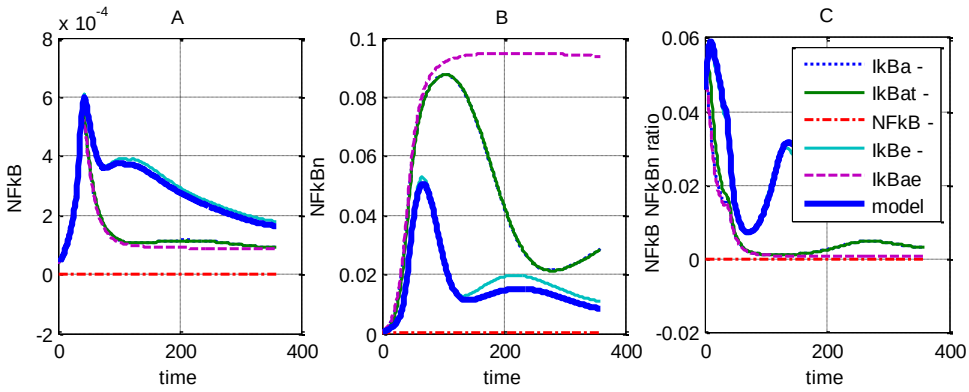


Figure 6-12 Simulations of the model with IκBα, IκBα mRNA, NFκB, IκBε, and the double knockout IκBα/IκBε. Knockout models were generated from the wild type model by setting the initial value and the rate of expression to zero. (A) NFκB in the cytoplasm does not change with the IκBε but decreseases with IκBα and IκBα/IκBε knockout. (B) Nuclear NFκB increases with IκBα/IκBε knockout and does not change with IκBε knockout. (C) The nuclear to cytoplasmic ratio of NFκB decreases with IκBα/IκBε and IκBε knockout. The x-axis represent the time (min) and the y-axis the concentration (μM).

## 6.4 Summary and Discussion

In summary, analysing the dependence of the systems behaviour for a wide range of parameter and initial value variations indicated that different parameters influence the model output for each cytokine in a distinct manner. Less than 20 parameters and one initial component value significantly influence the model output. While time independent sensitivity analysis identified that the most sensitive parameters differ between cytokines, time dependent analysis identified the importance of different measurement times between cytokines in biological experiments. Therefore, the possible pharmaceutical targets need to be

carefully evaluated for all cytokines involved and at different time steps for each parameter. Knockout models rather than sensitivity analysis highlighted the importance of interactions between IκB isoforms and the effect on the model output.

**Sensitivity analysis for the change in initial values**

Time independent sensitivity analysis of the initial values showed high sensitivity of the model output for the initial value of IKKIκBαNFκB. IKKIκBαNFκB is the component in the model that represent the process of phosphorylation followed by ubiquitination and proteolysis of IκBαNFκB which degrades IκBα and increases free NFκB in the cytoplasm (Hoffmann *et al.*, 2002a). The rate of protein degradation is changed over time with the input function as described in Section 4.2.3. It is therefore indicated by this model that cytokine mRNA expression is highly sensitive to the input function of the model. Therefore, the model reproduces the relationship between the input function, a representation of the bacterial challenge, and cytokine expression. This would indicate that the signalling pathway modelled in this work represents a mechanism that is able to differentiate the reaction to the bacterial challenges depending on the input. The influence of the input function and the robustness of the model and the model output values for the variation in the input function are further investigated in Chapter 8.

Time dependent sensitivity analysis indicated a difference in sensitivity for the initial values of IKKIκBαNFκB between the cytokines (Figure 6-1). TNFα has a different biological function from RANTES and IL8 therefore the difference in sensitivity is to be expected from a biological perspective. TNFα elicit a quick increase in expression levels which has been confirmed with biological experiments (Lahouassa *et al.*, 2007). This highly proinflammatory cytokine has both beneficial and harmful properties (Bannerman, 2009). TNFα promotes endothelial activation and the recruitment of leukocytes to the site of infection as well as the induction of fever. Although the effects are beneficial to the host, systemic TNFα is also associated with heightened inflammatory responses which can be life threatening for the host. Shock, tissue damage, vascular leakage and multi organ failure have been shown to be a result of systemic TNFα (Bannerman, 2009). Therefore, increased sensitivity after 200 minutes could be a mechanism to protect the cells from TNFα exposure over a longer period of time.

One might expect sensitivity of the model output to changes in the initial values of nuclear and cytoplasmic NFκB, but the model indicates higher sensitivity to the IκBα bound NFκB and IKK. Therefore, cytokine mRNA expression is more dependent on the result of the

stimulus, IKK, and on the available bound NFκB in cytoplasm, than on the actual NFκB in the nucleus or cytoplasm. This is in line with biological expectations; cytokine expression is only initiated after TLR signalling which increases IKK levels. In rest, the status represented in the initial value of the components, without pathway signalling, NFκB in the nucleus should not initiate cytokine mRNA expression. Free NFκB in the nucleus builds up over the first 60 minutes following the bacterial challenge (See Figure 5-10) and the increase initiates the cytokine expression levels. This free NFκB does not come from newly synthesized NFκB but from the release of bound NFκB in the cytoplasm. The mechanism supports the function of NFκB, allowing for a quick initiation of the immune system rather than a delay due to the need for protein synthesis of NFκB.

**Sensitivity analysis for changes in highest ranked parameters**

With a large number of parameters, time dependent sensitivity analysis can quickly become intractable. Using time independent sensitivity analysis to narrow down the search space for time dependent sensitivity analysis has been proven to be very efficient in the sensitivity analysis. Time independent analysis of the parameters showed a difference in ranking for the parameters between cytokines.

RANTES mRNA expression showed high sensitivity to changes in parameters influencing NFκB import into the nucleus, followed by the sensitivity to protein degradation of IκBα in the cytoplasm and transport of IκBα into the nucleus. RANTES is described as a late gene that is activated only after prolonged exposure (8 hours) to NFκB in TNFα challenges (Ting & Endy, 2002). LPS simulation of mouse embryonic fibroblast also showed an increase after 8 hours (Werner *et al.*, 2005). In our experiments we identified a small increase in fold changes 1.6 ($p<0.05$) at 60 minutes after LPS stimulus rising to 4.3 at 180 minutes and 4.8 at 360 minutes (Figure 3-4). RANTES is expressed in fibroblast and epithelial cells but it is suggested that the kinetics of RANTES differ between cell types leading to tissue specific inflammatory responses (Arima *et al.*, 2000). It can be speculated that the dissimilarity points to a difference in RANTES expression levels between mouse embryonic fibroblast and mammary epithelial cells.

TNFα shows the highest sensitivity to protein degradation of IKKIκBαNFκB (Table 6-2). In addition TNFα showed sensitivity to initial concentration of this component (Table 6-1). Earlier sensitivity studies of NFκB signalling in the first model developed by Hoffmann *et al.* as a result of TNFα challenge have identified model output, nuclear NFκB concentration,

sensitive as result of changes in the initial value and kinetic parameters for protein degradation of the component IKKIκBαNFκB (Hoffmann *et al.*, 2002a; Ihekwaba *et al.*, 2007; Yue *et al.*, 2008). NFκB is a transcription factor for TNFα and therefore similar sensitivities of the model output for NFκB and TNFα are to be expected. The sensitivity for this parameter also indicates a strong link between the model input and the TNFα mRNA expression levels.

IL8 showed the highest sensitivity to protein degradation of IκBα mRNA. Newly synthesized IκBα binds to NFκB and attenuates the pathway response, thereby functioning as a negative feedback loop in the model, preventing NFκB in the nucleus and cytoplasm to activate the cytokine expression. As shown in Section 5.2.5 IL8 expression level increases quickly. Sensitivity of IL8 expression to a change in IκBα mRNA levels can be explained as the result of a change in the negative feedback loop which modifies the nuclear NFκB level. Similar to TNFα, IL8 shows comparable ranking to nuclear NFκB and sensitivity for the initial values of IKKIκBαNFκB therefore a strong dependence between model input and IL8 levels is indicated. The parameter influencing RANTES was fitted, while the parameters influencing IL8 and TNFα are fitted with restrictions taken from the literature (Hoffmann *et al.*, 2002a). Measurements in biological experiments of these parameters can therefore optimise the model accuracy.

None of the cytokines show a similar ranking pattern for parameter sensitivity as nuclear NFκB, although IL8 and TNFα share the top three sensitive parameters with nuclear NFκB in a different order and with different magnitude. The ranking difference of the parameters influencing the nuclear NFκB concentration in the sensitivity analysis for different cytokines between the cytokines is also not expected in the first instance, since they are all dependent on nuclear NFκB input.

Although it was initially unclear why the individual cytokines were sensitive to changes in different parameters influencing the NFκB concentration (See ranking in Table 6-1) in the nucleus while they all are dependent on the nuclear concentration of NFκB (See Section 5.1.1), time dependent sensitivity analysis indicated that each cytokine was sensitive to changes in the concentration at a different time step. Different parameters influence the concentration of NFκB at different time steps; therefore each cytokine is sensitive to specific parameters influencing the NFκB concentration in the nucleus at a specific time in the simulation. Thereby indicating the importance and additional information time dependent sensitivity analysis can provide over time independent sensitivity analysis.

**Optimum experimental measurement time**

Despite the sensitivity of RANTES early in the simulation, measuring the concentration levels early, before 100 minutes, would not give us data to refine the parameter values. TNFα is sensitive early in the simulation and towards the end of the simulation. The largest change in concentration can be found in the peak around 100 minutes. Despite a substantial change in sensitivity at 50 minutes, concentration changes can only be expected at 100 minutes. Therefore, biological experiments should be designed to capture concentration levels at 100 minutes (Figure 6-4) for RANTES and TNFα.

Although the sensitivity of IL8 increased after 200 minutes of simulation, changes in concentration level as an effect of the parameter changes can already be seen after 100 minutes and are the largest at 240 minutes, indicating that any experimental measurement before 100 minutes will not give us additional information to fine tune the parameter values in the model. Measurements for this work have been taken at 60, 180 and 360 minutes. However, biological experimental values at 100 and 240 minutes would be more informative. These results clearly indicate the value of sensitivity analysis and simulation before experimental design.

**Knockout simulations**

Biological experiments can not always simulate knockout due to lethality, cost and ethical considerations. *In silico* simulations are therefore a good way to investigate the influence of specific components. IκBα knockout models showed a prolonged increase in RANTES mRNA expression before the concentration stabilizes (Figure 6-8 (A)). IL8 also shows a prolonged increase but decreases toward the wild type level (Figure 6-8 (B)) while the TNFα increases with a higher peak but reduces quickly to the wild type value when the nuclear NFκB reduces (Figure 6-8 (C)). The model therefore indicates a difference in kinetic response to the IκBα knockout between RANTES, IL8 and TNFα mRNA. TNFα resumes wild type levels during the simulation period while RANTES and IL8 do not return to wild type levels. From a biological perspective the robustness of TNFα is necessary and prevents prolonged expression of TNFα. Prolonged exposure to TNFα is linked to heightened inflammatory response which could threaten life (Bannerman, 2009).

In the IκBα knockout simulations the NFκB ratio between cytoplasm and nucleus in Figure 6-9 stabilizes after 70 minutes with increased concentration of NFκB in the nucleus and reduced concentration of NFκB in the cytoplasm. This effect can be contributed to the negative feedback function of IκBα. IκBα holds NFκB in the cytoplasm and prevents translocation to the nucleus. Reduced levels of IκBα eventually will lead to the translocation of all NFκB to the nucleus.

The difference in NFκB levels and cytoplasm and nucleus ratios between the wild type and IκBα knock out would explain the increased transcription of the cytokines as a result of the IκBα knockout but not the difference in the increase between the individual cytokines. This is similar to the earlier findings in Section 6.2.2.3 where we identified that the cytokine expression levels showed sensitivity to different parameters which represented changes in NFκB levels at different simulation times. A different effect on each cytokine is therefore to be expected. However, the mechanism is more complex and not influenced by IκBα alone. In addition to change in IκBα levels in the knockout simulation, an IKK concentration increases. Increased concentration of IKK results in increased degradation of IκBα. The increased degradation then increases concentration of NFκB in the cytoplasm free to trans-locate to the nucleus. The effect of changing the IKK profile will be further investigated in Chapter 8.

The ratio of NFκB between cytoplasm and nucleus is more stable with the IκBα knockout explaining sustained gene expression of RANTES and IL8 but not TNFα, neither does it explain the difference in the return to the wild type for IL8 and TNFα.

The NFκB knockout model indicates a different time profile for each of the mRNA cytokine expression levels as result of NFκB knockouts (Figure 6-10). Blocking NFκB with pharmaceutical product can therefore expected to have a different effect on each expression level and the effect of highly reduced, as opposed to no expression levels need to be taken into consideration and verified with biological experiments. NFκB is available in the cytoplasm for fast reaction and does not depend on protein synthesis. Experimental studies of *S. aureus* mastitis failed to identify NFκB or TNFα mRNA levels in mammary epithelial cells (Yang *et al.*, 2008). However, the pathogen causes chronic inflammation in the mammary gland and activates TLR2 and TLR4 signalling. TLR signalling leads to NFκB activation. NFκB levels as result of chronic mastitis were raised in milk (Boulanger *et al.*, 2003). Therefore, other cells in the mammary gland could be responsible for the raised NFκB levels in milk. Targeted inhibition of NFκB signalling reduced milk loss and apoptotic signalling,

which are of great concern during mastitis (Connelly *et al.*, 2010). Reducing NFκB levels in mammary epithelial cells with pharmaceuticals might not have the desired effect on the inflammation. For instance, it could still lead to chronic mastitis as seen in *S. aureus* mastitis and therefore needs further biological experimentation to verify the model prediction of NFκB knockout.

There is no difference between IκBα knockout and IκBαIκBε knockout with respect to NFκB in the cytoplasm, both reduce NFκB. The inhibitory role of IκBα and IκBε in the form of negative feedback loops for the DNA-binding activity of NFκB of the canonical (TLR activated) IκBs as result of TNFα simulation has been described earlier (Hoffmann *et al.*, 2006). IκBα provides a negative feedback loop and is responsible for down regulation following the initial induction of NFκB activation. The delayed IκBε function is in an anti-phase to IκBα. It is proposed that the anti-phase regulation stabilizes the NFκB activity without reducing the ability to terminate NFκB activation after the removal of the stimulus (Hoffmann *et al.*, 2006). The two kinases, IκBα and IκBε, work in tandem to rapidly repress NFκB translocation after TNFα stimulation. A similar effect as result of *E. coli* stimulation is seen in this study, providing evidence for the importance of IκBε in terminating the inflammatory response. IκBα and IκBε work together to ensure rapid post induction repression of NFκB, suppressing sustained oscillations. Sustained oscillations can be a shortcoming in simple linear control systems (Cheong *et al.*, 2008). In an inflammatory response these could for instance lead to an over-reaction of the immune system.

**Conclusion**

The model captures the experimental values of the cytokine expression levels for mammary epithelial cells indicating that the same model components are capable of capturing the experimental values with different kinetics in different cell types. Therefore, we could explore the kinetics of the expression and the change in sensitivity during the simulation time. This is very valuable for the future design of biological experiments.

# *Chapter 7*
# *S. aureus* model

*In the previous Chapters a model for the E. coli bacterial challenge was developed and analysis of the sensitivity of the model output for parameter changes performed. From the biological review in Section 2.1 we identified a shared signalling gene network regulation pathway used in E. coli and S. aureus bacterial infections. The signalling gene network initiates cytokine mRNA expression with a different time profile between the two bacterial challenges. The difference in time profile is the result of a variation in the input function of the model. While the input function was available from biological experiments with the E. coli challenge, no data for the input function with the S. aureus challenge is available. We therefore set out to estimate the parameters representing the input function of S. aureus challenge for the model developed in Chapter 5 and will show that this is not feasible with the available experimental data. An insight is given in the possible causes for the lack of fit. In addition, future experiments that could elicit insight in the regulation as the result of an S. aureus infection in mammary epithelial cells are discussed.*

## *7.1* Fitting the *S. aureus* experimental values to the model

The conceptual model for the *S. aureus* challenge is given in Figure 7-1. As described in Section 2.1.2 the *S. aureus* challenge invokes the same TLR-IKK-NFκB signalling pathway which results in the cytokine mRNA expression as the *E. coli* challenge. Although it invokes the same signalling pathway, the time profiles of the input representing the two bacterial challenges are different. Therefore the model developed in Chapter 5 can be used for both challenges using two different input functions. While estimating parameters for cytokine mRNA expression in the *E. coli* challenge the input function for the model (ikkm(t) described in Section 4.2.3 and Figure A-1) was based on experimental values from Werner *et al.* (2005). In contrast to the *E. coli* experiment, no input profile is available for a *S. aureus* challenge in the literature.

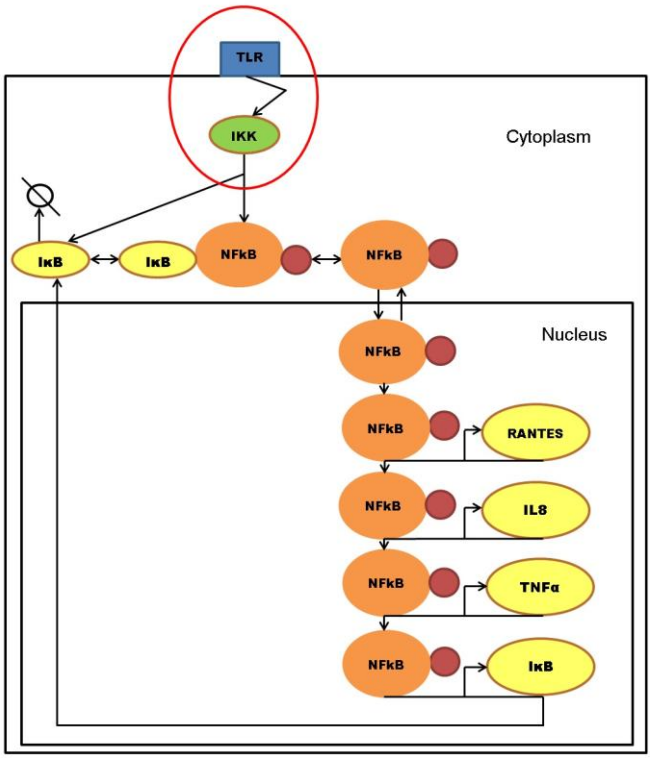


Figure 7-1 Parameters to be estimated for the *S. aureus* mastitis model are related to the input function circled in the conceptual diagram of TLR-IKK-NFκB signalling in mastitis. The TLR receptor on the cell membrane recognizes the bacterial challenge. The signalling pathway activates the kinase IKK which breaks the IκB-NFκB dimer. As a result, the transcription factor NFκB translocates to the nucleus initiating gene expression. The transcription factor NFκB initiates the expression of three cytokines, RANTES, IL8 and TNFα in mastitis. In addition, the IκB isoforms which bind with NFκB in the cytoplasm to prevent translocation of NFκB to the nucleus are expressed. This process creates a negative feedback loop for the translocation of NFκB to the nucleus.

Estimating both, parameters for the input function and parameters for the synthesis and degradation of the cytokines in the *S. aureus* challenge, would be an exercise of input-output fitting and lead to over fitting. Many parameter estimations could fit the data and insufficient experimental data is available to verify if the estimated parameters would be correct.

Thus it is assumed that the estimated parameters for cytokine mRNA synthesis and degradation in Section 5.2 for the *E. coli* challenge are correct and the same for the *S. aureus* challenge. This leaves the parameters for the input function ikkm; 8 time points and 8 levels of concentration, to be estimated with the experimental values of the *S. aureus* challenge.

As shown in Section 3.1.4 expression levels for IκBα and IL8 mRNA are significantly different in the *S. aureus* challenge, while TNFα and RANTES expression level do not differ from unchallenged cells in the experiment.

Despite the use of a variety of parameter estimation method no suitable parameter values could be identified for the input function to fit the experimental values of IκBα and IL8 mRNA concentration at the same time. In the following sections prior identifiability analysis and biological insight are used to evaluate the possible cause for the lack of suitable parameter values.

## 7.2 Prior identifiability analysis for fitting the model input parameters to *S. aureus* experimental data

Prior identifiability analysis as described in Section 2.3.3 is used to identify correlations between the parameters with the available experimental values. Parameters for the input function of the *S. aureus* challenge are estimated to fit the experimental values of IκBα and IL8 mRNA expression. The input function is a piecewise linear function with 8 time points (t1-t8) and 8 concentration levels (ikk1-ikk8) that is solved numerically (Figure A-1 and Section 4.2.3).

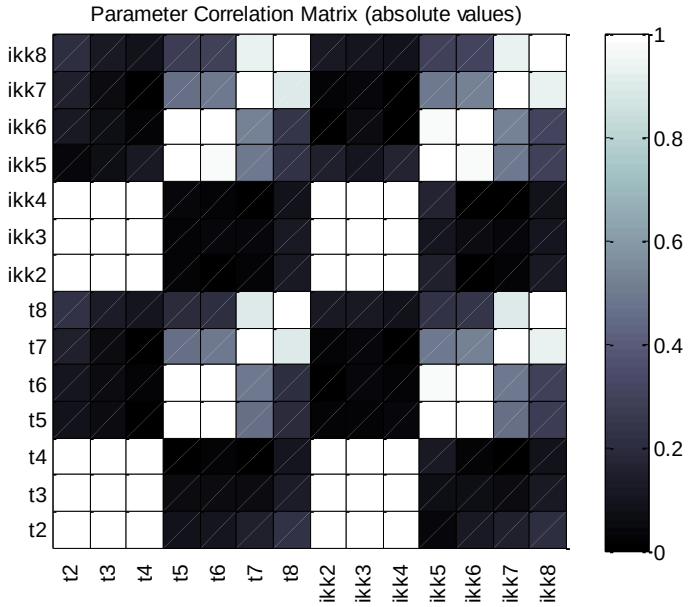


Figure 7-2 Prior identifiability analysis shows the correlation between the parameters that will be estimated using the experimental data for the *S. aureus* challenge. The input function is a piecewise linear function with 8 time points (t1-t8) and 8 concentration levels (ikk1-ikk8). The correlation between the time point and concentration is high for each pair (time, concentration). A high correlation between parameters indicates non-identifiability of the parameters with the available experimental values.

As can be seen in Figure 7-2, the correlation between each pair of parameters (time, concentration) is high and indicates no unique parameters can be estimated with the available experimental values. Nominal values can be used to reduce the correlation between parameters. However, using nominal values for the time does not reduce the correlation sufficiently as can be seen in Figure 7-3.

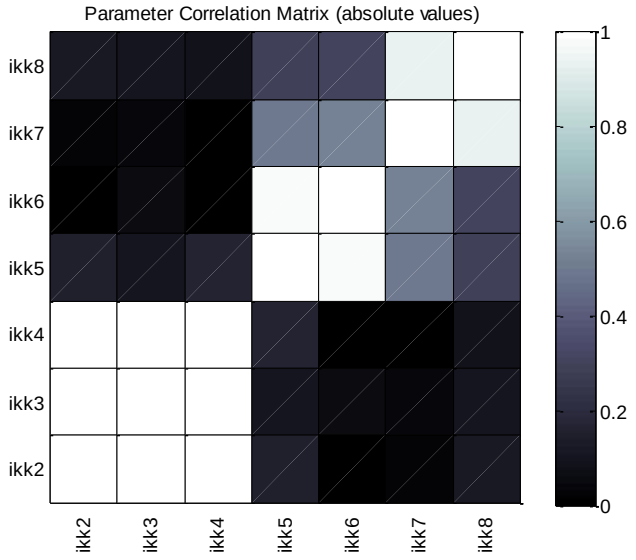


Figure 7-3 Prior identifiability analysis shows the correlation between the parameters that will be estimated using the experimental data for the *S. aureus* challenge. In this case nominal values have been used for time. High correlation between the remaining parameters indicate non identifiability of those parameters with the available experimental values.

Further reduction of the number of time points and the number of concentration levels did not reduce the correlation. Several different parameter estimation algorithms did not manage to get a solution, which was expected with the high correlation between the parameters indicating non-identifiability.

## 7.3 Discussion

In this chapter an attempt is made to estimate the input parameters of the model to fit the experimental values of the *S. aureus* bacterial challenge. Identification of the parameter values failed with the available experimental values. Close examination of the model equations (A.1.1) identifies an important aspect of the input function ikkm. In the ODEs for

IκBxIKK, IκBxIKKNFκB (x = α, β or ε) and IKK the ikkm(t) function influences the free floating concentration of IκB, IKK and NFκB. The influence results in an intrinsic link between the protein degradation parameters (pd_c_xi*, x=a, b or e, *=n or blank) and the input function. In the previous chapter it has been shown that the model is highly sensitive to changes in protein degradation parameters for the *E. coli* challenge (Section 6.2.2).

Protein degradation values for IκBα were taken from Hoffmann *et al.* (2002a) who based the values on research by Pando *et al.* (2000). The NFκB signalling component of the model consists of a combination of parameters which are estimated or based on literature and experimental data with fibroblasts. Since we use mammary epithelial cells as opposed to fibroblasts there could be a difference in the parameters due to the difference in cell type. Tissue specific regulation of cytokine expression could be a way to facilitate tissue specific immune regulation (Arima *et al.*, 2000).

To investigate a possible difference in protein degradation parameter as a result of the use of mammary epithelial cells as opposed to fibroblasts used in Hoffmann *et al.* (2002a) we investigated the protein degradation parameter values. Estimating the protein degradation parameters for IκBα in conjunction with the protein degradation parameters for the IKKIκB or IKKIκBNFκB complex (pd_c_yxi*, x=a, b or e, *=n (y=3) or blank (y=2)) to fit IκBα and IL8 mRNA expression did not lead to a fit with the experimental data for both IκBα and IL8 mRNA. While a fit for experimental values for IκBα or IL8 mRNA could be found, no fit suitable for both values with a single set of parameters using a variety of parameter estimation methods was found. Neither were parameters found that would fit both the *E. coli* and the *S. aureus* experimental values. The *S. aureus* bacterium is known to evade the immune system. Rather than a difference in parameter values due to a difference in cell type it is therefore likely that there could be other signalling and/or gene networks involved in the cytokine expression in the *S. aureus* challenge.

In the *E. coli* model the role of NFκB in the differentiation of the cytokines was investigated. This model was chosen since the transcription factor NFκB is the most important *cis*-regulatory element controlling TNFα-induced RANTES expression (Casola *et al.*, 2002). Cytokines have been identified to be responsible for the variation in clinical profiles of mastitis (Bannerman *et al.*, 2004). The cytokine RANTES is one of the five genes in the cluster identified as regulated with a significantly different time profile between the two bacterial challenges (Section 3.1.3). The dynamic behaviour of the translocation of NFκB from the cytoplasm to the nucleus is different between several challenges and the difference in temporal dynamics is believed to be the source of the variation in gene regulation (Cheong

& Levchenko, 2008). Therefore the influence of NFκB on RANTES expression in an *E. coli* challenge was modelled. While the model is able to reproduce the experimental values in the *E. coli* challenge indicating that RANTES and IL8 expression can be explained by the role of the dynamics in NFκB translocation in the model, this does not apply to the IL8 expression in the *S. aureus* challenge.

Looking at the cluster with differentially regulated genes between the two bacterial challenges in Table 3-2, five genes are seen which are regulated by IFNα/β (Noppert *et al.*, 2007). The IFNα/β receptor is also involved in STAT5. The STAT5 signalling pathway has been suggested to play in role in sub clinical mastitis (Boutet *et al.*, 2004#372) and milk production (Khatib *et al.*, 2008). The STAT5 transcription factors have been linked to LPS (Kimura *et al.*, 2008) and reduction of casein protein in *E. coli* infected quarters but not in subclinical *S. aureus* (Vanselow *et al.*, 2006). This indicates a different role of STAT5 in *E. coli* and *S. aureus* mastitis. However, the relation with cytokine expression is unclear.

In this study IFNα/β is up-regulated in the *E. coli* but not in the *S. aureus* challenge. *S. aureus* does not invoke the MyD88 independent pathway (See Figure 3-6). The cytokine IFN-β has been identified as the signature molecule for MyD88-independent TLR4 signalling as a result of *E. coli* stimulation in macrophages (Thomas *et al.*, 2006). IFN-β is recognized by IFNα/β and activates STAT1 containing DNA binding complexes that participate in the induction of genes not expressed in response to TLR2 (Toshchakov *et al.*, 2003). Jones *et al.* proposed that IFNα/β might provide the missing signal that underlies the differential patterns of cytokine production induced by TLR2 and TLR4 in macrophages (Jones *et al.*, 2001). Therefore, the cytokine expression could be differentiated by IFNα/β rather than, or in addition to, a difference in NFκB regulation.

It can be speculated that NFκB might not be the most important transcription factor in the *S. aureus* challenge of mammary epithelial cells for IL8. In conjunctival cells loss of function of the NFκB site does not influence the expression of IL8 (Venza *et al.*, 2007). Other transcription factors such as JNK, P38 and AP-1 also contribute to IL8 gene expression (Hoffmann *et al.*, 2002b). P38 is very well studied MAPK kinase in terms of anti-inflammatory drug target (Han & Ulevitch, 2005). AP-1 is a MAPK induced transcription factor (Sun *et al.*, 2008). The cis-elements for NFκB and AP-1 are located in close proximity of the IL8 promoter, which suggest the formation of a higher-order nucleo-protein, a transcriptional enhanceosome. The transcriptional enhanceosome provides a multi-protein surface that facilitates maximal gene transcription. A closer look at the expressed mRNA in *E. coli* (Figure 3-5) and *S. aureus* (Figure 3-6) in our experiments indicated the expression of

NFκB, p38 and AP-1 in *E. coli* but not in *S. aureus.* Our experimental data therefore supports the activation of MAPK signalling pathways in both *S. aureus* and *E. coli* challenges, while the NFκB signalling pathways is only activated in *E. coli.* Crosstalk between the MAPK and NFκB signalling pathways exists and the experimental data indicates a difference in regulation in the crosstalk between the two bacterial challenges.

NFκB regulation is influenced by IκBα. IκBα regulation is different between the two bacterial challenges as can be seen in Figure 3-7 and Figure 3-8. However, IκBα does not influence the MAPK signalling pathway responsible for JNK, p38 and AP-1 activation (See Figure 3-5). A combination of the activation of the NFκB and MAPK signalling pathways are essential for the IL8 activation.

In the *E. coli* challenge both pathways have increased mRNA expression levels, indicating that both pathways are activated. Our method of using the Hill factor of three for NFκB (See Section 5.1.1) was sufficient to represent both pathways in the *E. coli* model. In contrast, in the *S. aureus* challenge the NFκB does not show a change in expression indicating a lack of activation of the NFκB pathway while the MAPK pathway is activated since the precursors AP-1 shows increased expression in the *S. aureus* challenge.

The importance of AP-1 in mastitis has been identified by us earlier (van Loenen-den Breems *et al.*, 2008). In this study AP-1 was identified as a component of a unique expression profile in *E. coli* mastitis in the udder. In conjunctival cells, Venza *et al.* concluded that the AP-1 binding site alone was required for optimal IL8 *S. aureus* induced promoter activity while the loss of function in the NFκB site did not affect IL8 promoter activation (2007). The fact that the IL8 mRNA expression in the *S. aureus* challenge could not be explained by the NFκB regulation alone could be attributed to a similar mechanism in mammary epithelial cells.

In order to verify the conclusions we propose to perform biological experiments identifying the AP-1 and p38 transcription factor activity. With these experimental values the model can be extended, including the cross signalling of the NFκB and MAPK signalling pathways and exploring the *S. aureus* expression profile in the mammary epithelial cells. The model interrogation of the interaction between the MAPK and NFκB signalling pathways could well shed light on the difference in regulation between *E. coli* and *S. aureus* mastitis.

# Chapter 8
# Robustness of the cytokine expression to input variations

*This Chapter investigates the robustness of the model for the variation in the model input. The model input represents the bacterial load causing the infection in mastitis. Robustness is an important property of biological systems regulating over and under reaction to external perturbations of the biological process. In the first Section the definition of robustness relevant to cytokine expression in mastitis used in this thesis is described. The Section 8.2 the input variation representing the bacterial load is described and in Section 8.3 the results of the simulations with the different input profiles are given. The last section discusses the effect of the input variation on the cytokine expression levels, the output of the model. We speculate that the robustness for TNFα mRNA expression observed in biological experiments at 360 minutes is not caused by robustness to the variation in nuclear NFκB time profile but by robustness to variation in synthesis and/or degradation parameter values.*

## 8.1 Robustness in biological systems

Robustness is a key property of biological systems and refers to the ability of a biological system to maintain its functionality while exposed to perturbations in operating conditions (Stelling *et al.*, 2004). In this thesis robustness is defined as the ability of a system to maintain its functions despite input perturbations. The input perturbations represent a change in bacterial load on the mammary epithelial cell, while the functionality is the time profile of the cytokine mRNA expression levels, representing the immune system reaction to the bacterial infection.

While total robustness to the input variation would make a biological system insensitive to the environment and imply a lack of communication with the environment, lack of robustness could cause an over reaction of the system to the perturbation such as a bacterial infection. However, robustness to common perturbations such as temperature or light changes is necessary to maintain functionality and performance. Extraordinary robustness to uncommon perturbations can be catastrophic; for an infection such as mastitis total robustness to the

bacterial infection could lead to sepsis and death due to the lack of the immune reaction, while extreme sensitivity would influence the performance such as milk production. From an evolutionary point, milk production is essential for the survival of the species and reduction of milk production can not be sustained for a longer period. Therefore, biological networks often exhibit extraordinary robustness to common perturbations in their environment such as temperature change and less robustness to uncommon perturbations such as a bacterial infection. Subsequently a biological trade-off can be expected between robustness and sensitivity to input variations that maintain the performance. Elucidating this trade-off between robustness and sensitivity is often the key to understanding the complexity of the biological network (Csete & Doyle, 2002; El-Samad *et al.*, 2005; Stelling *et al.*, 2004). Robustness plays a role in the design of pharmaceutical targets, influencing the efficiency of the product.

### 8.1.1 Robustness to the variation in bacterial infections for cytokine expression in mastitis

Cytokine mRNA expression levels are an indicator of the effect of the bacterial infection on the immune system reaction in mastitis. Cytokine expression levels in milk varied due to a change in severity of *E. coli* mastitis (Vangroenweghe *et al.*, 2004; Werner-Misof, 2007). Increase of the bacterial load changed the time profile of the cytokine expression levels and therefore the reaction of the immune system to the infection. Vangroenweghe *et al.* concluded that a higher bacterial load in *E. coli* mastitis resulted in an earlier increase in IL8 in milk samples (2004). However, neither the mechanism nor the component in the network which is responsible for the increase in IL8 is known.

A biological study of mammary epithelial cells challenged with different concentrations of *E. coli* indicated that the concentration of the pathogens is recognised by the cells and as a result cytokine expression levels are changed (Günther *et al.*, 2010). Relative mRNA copy number varied 180 minutes after stimulation of the mammary epithelial cells with *E. coli* for IL8 but not for TNFα with a positive correlation to the bacterial load, while there was no correlation with the bacterial load after 360 minutes, indicating robustness for the variation in bacterial load at 360 minutes. However, it is unclear which changes in the network cause these variations in expression levels.

As discussed in more detail in Section 2.1.2, *E. coli* bacteria are recognised by Toll Receptors on the cell membrane. Toll Receptor signalling then results in the translocation of NFκB to the nucleus, which then regulates cytokine mRNA expression levels. Earlier studies concluded that RANTES mRNA expression as result of TNFα challenge is primarily controlled by the transcription factor NFκB (Casola *et al.*, 2002). NFκB has also been shown to play an indispensable role in IL8 mRNA expression in mastitis (Boulanger *et al.*, 2003). It has been proposed that IL8 could play a key role in the modulation of *E. coli* mastitis (Alluwaimi, 2004). Therefore, the transcription factor NFκB plays an important role in the cytokine mRNA expression in mastitis. In Section 6.3.2 NFκB knockout simulations identified a different effect for each cytokine when NFκB is blocked. Blocking NFκB is often suggested as a treatment in infections but has been shown to lead to sepsis (Liew *et al.*, 2005).

A bacterial infection load changes over time, due to the effects of milking and the immune system reactions. The input is thus not an on/off signal but represented by a variety of time profiles indicating the severity of the bacterial load. Therefore, investigating the effect of the variation in the nuclear NFκB time profile, on the cytokine mRNA expression with *in Silico* simulation can identify the effect of nuclear NFκB variation on cytokine mRNA expression and identify the level of robustness to the nuclear NFκB variation.

## 8.2 Input variation to represent variation in the bacterial infection

In order to vary the nuclear NFκB time profile, the input profile of the model, described in Section 4.2.3, need to be varied. With the variation in the input of the model the variation of the bacterial load in mastitis is simulated. To create a set of diverse input profiles a computer program was developed to generate experiment files described in Section 4.3. The experiment files contain the input (ikkm, Section 4.2.3) profiles for the simulation of the model. Each profile contains a rising phase (a in Figure 8-1), a first plateau (b in Figure 8-1) and a second plateau (c in Figure 8-1) with varying time levels (x and y in Figure 8-1). During a total simulation time of 360 minutes the duration of the rising phase was simulated for 0, 60, 120 and 240 minutes. The rise of the first plateau (x) was simulated with 0.04, 0.12, 0.34 and 1.01 µM. The duration of the first plateau (b) was 0, 5, 15, 30, 60 or 120 minutes. The falling phase (c) had duration of 0, 60, 120 or 240 minutes. The second plateau was equal or lower than the first plateau and varied between 0.01, 0.04, 0.12, 0.34 and 1.01 µM. This algorithm has also been used by Werner *et al.* (2005) who ran the simulation for 240 minutes and

identified 36 different nuclear NFκB time profiles. The simulation ran for 360 minutes. However, increasing the range of values for the times (a, b and c in Figure 8-1) or concentration levels (x and y in Figure 8-1) creating more than 2500 different ikkm profiles did not increase the coverage of the input space or the number of different nuclear NFκB time profiles.

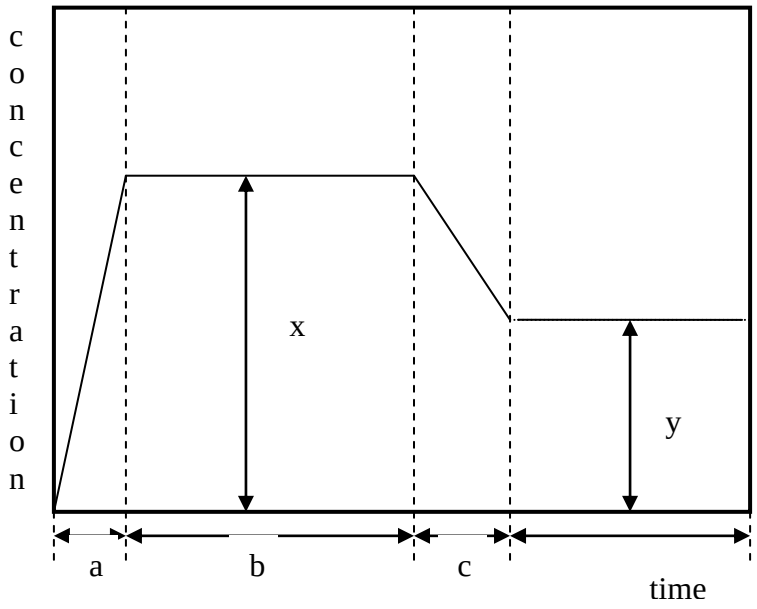


Figure 8-1 A set of input profiles was generated varying the time of the rising, first plateau and falling phase (a, b and c with $a \leq b \leq c$) and the concentration in the first and second plateau (x and y with $x \geq y$).

Clustering the IKK time profiles with the κ- means clustering algorithm implemented in the Matlab Statistics Toolbox with standard squared Euclidian distance measure identified 36 clusters of IKK time profiles (Table 8-1) that produce distinct nuclear NFκB time profiles. Using the representations of the clustered IKK profiles distinctly different nuclear NFκB profiles can be generated. These clusters cover the input space for the identification of the robustness of the cytokine expression with respect to nuclear NFκB time profiles.

Table 8-1 IKK input profiles generating **36** different nuclear NFκB time profiles. For the original value (See A.1.4). (a = rising phase, b = first plateau, c = falling phase, x = concentration first plateau, y = concentration second plateau in Figure 8-1)

| | a | b | c | x | y | | a | b | c | x | y |
|---|---|---|---|---|---|---|---|---|---|---|---|
| **1** | 60 | 5 | 120 | 0.34 | 0.01 | **19** | 60 | 5 | 5 | 0.34 | 0.12 |
| **2** | 60 | 5 | 5 | 0.34 | 0.01 | **20** | 0 | 5 | 120 | 0.12 | 0.04 |
| **3** | 0 | 5 | 60 | 0.12 | 0.04 | **21** | 60 | 5 | 5 | 1.01 | 0.34 |
| **4** | 60 | 120 | 5 | 0.34 | 0.01 | **22** | 120 | 5 | 60 | 0.34 | 0.12 |
| **5** | 0 | 5 | 240 | 0.34 | 0.01 | **23** | 0 | 5 | 60 | 0.12 | 0.01 |
| **6** | 120 | 5 | 5 | 0.34 | 0.34 | **24** | 60 | 5 | 5 | 1.01 | 1.01 |
| **7** | 120 | 5 | 5 | 1.01 | 1.01 | **25** | 0 | 5 | 60 | 0.34 | 0.01 |
| **8** | 0 | 5 | 5 | 0.12 | 0.12 | **26** | 60 | 30 | 60 | 1.01 | 0.01 |
| **9** | 0 | 5 | 5 | 1.01 | 1.01 | **27** | 60 | 5 | 5 | 1.01 | 0.12 |
| **10** | 60 | 5 | 120 | 1.01 | 0.34 | **28** | 60 | 5 | 5 | 1.01 | 0.01 |
| **11** | 0 | 5 | 240 | 0.04 | 0.01 | **29** | 60 | 5 | 5 | 0.12 | 0.12 |
| **12** | 60 | 5 | 120 | 1.01 | 0.01 | **30** | 120 | 15 | 5 | 0.34 | 0.12 |
| **13** | 60 | 5 | 60 | 0.12 | 0.01 | **31** | 120 | 5 | 5 | 0.12 | 0.01 |
| **14** | 60 | 30 | 60 | 1.01 | 0.34 | **32** | 60 | 60 | 60 | 1.01 | 0.01 |
| **15** | 0 | 5 | 5 | 0.34 | 0.34 | **33** | 0 | 5 | 60 | 0.34 | 0.12 |
| **16** | 0 | 5 | 5 | 0.04 | 0.04 | **34** | 60 | 5 | 120 | 0.34 | 0.12 |
| **17** | 60 | 5 | 5 | 0.34 | 0.34 | **35** | 120 | 5 | 5 | 0.12 | 0.12 |
| **18** | 120 | 5 | 60 | 1.01 | 0.34 | **36** | 0 | 60 | 120 | 0.34 | 0.01 |

The 36 input profiles are used for the *in Silico* simulations. The model ran with the input profiles for 360 minutes described in Section 4.3.

## 8.3 Cytokine expression levels as a result of variation in bacterial infection

Because biological experiments indicated robustness to variation in bacterial load at 360 minutes, the simulations are clustered for the nuclear NFκB concentration at 360 minutes with the κ- means clustering algorithm implemented in the Matlab Statistics Toolbox is used. The clustering identified 6 clusters with different NFκB concentration at 360 minutes (Figure 8-2 to Figure 8-7).

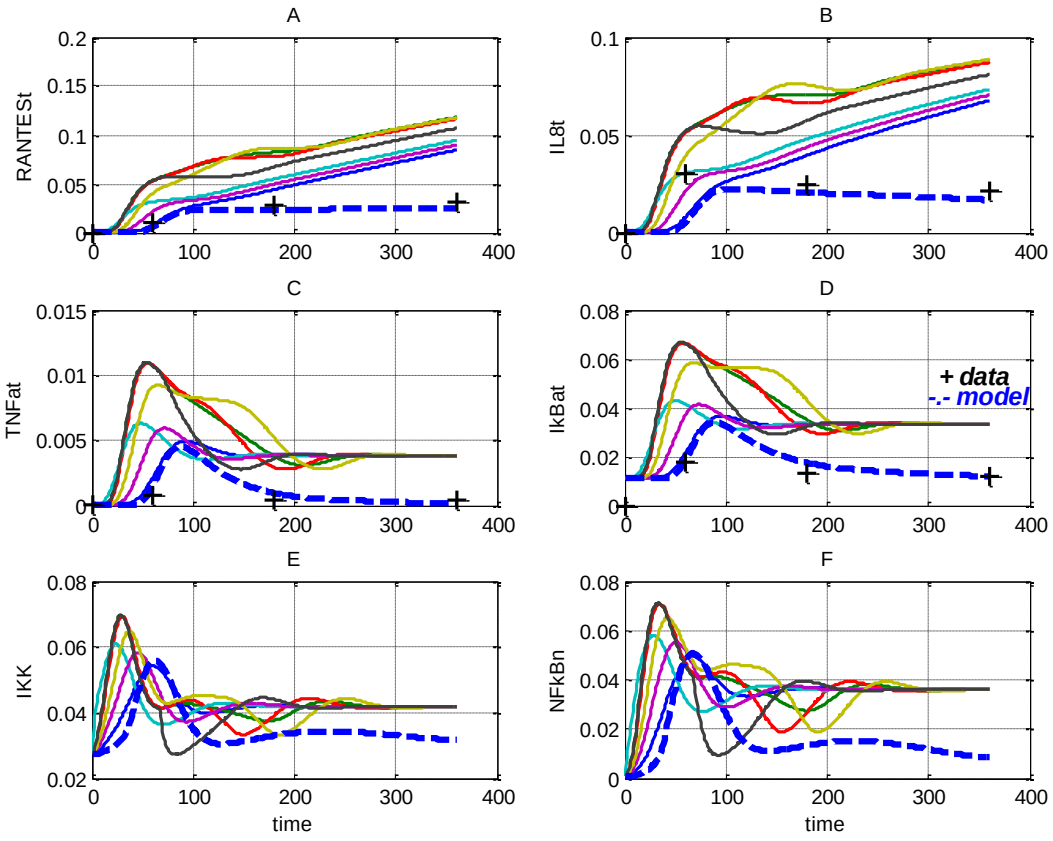


Figure 8-2 First cluster. Simulations with input profile 6, 10, 14, 15, 17, 18 and 21 (Table 8-1) for (A) RANTES mRNA, (B) IL8 mRNA, (C) TNFα mRNA, (D) IκBα mRNA, (E) IKK and (F) nuclear NFκB are shown. The x-axis represent the time (min) and the y-axis the concentration (μM).

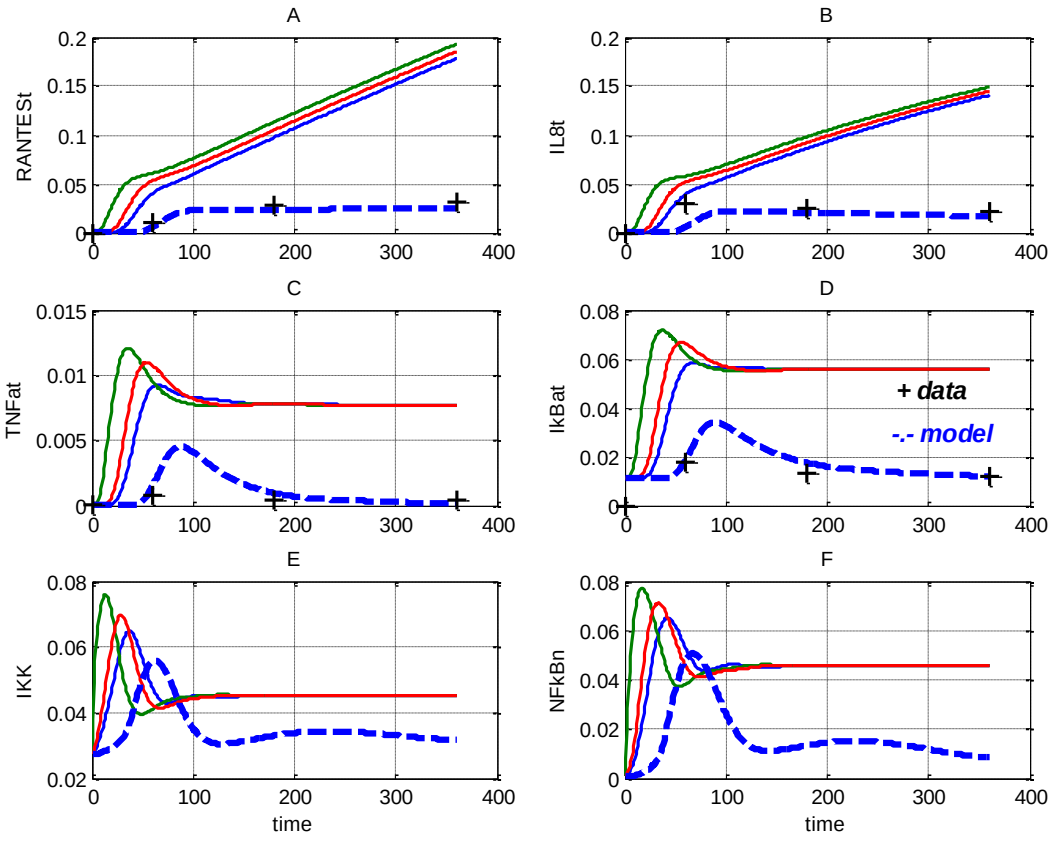


Figure 8-3 Second cluster. Simulations with input profiles 7, 9 and 24 (Table 8-1) for (A) RANTES mRNA, (B) IL8 mRNA, (C) TNFα mRNA, (D) IκBα mRNA, (E) IKK and (F) nuclear NFκB are shown. The x-axis represent the time (min) and the y-axis the concentration (μM).

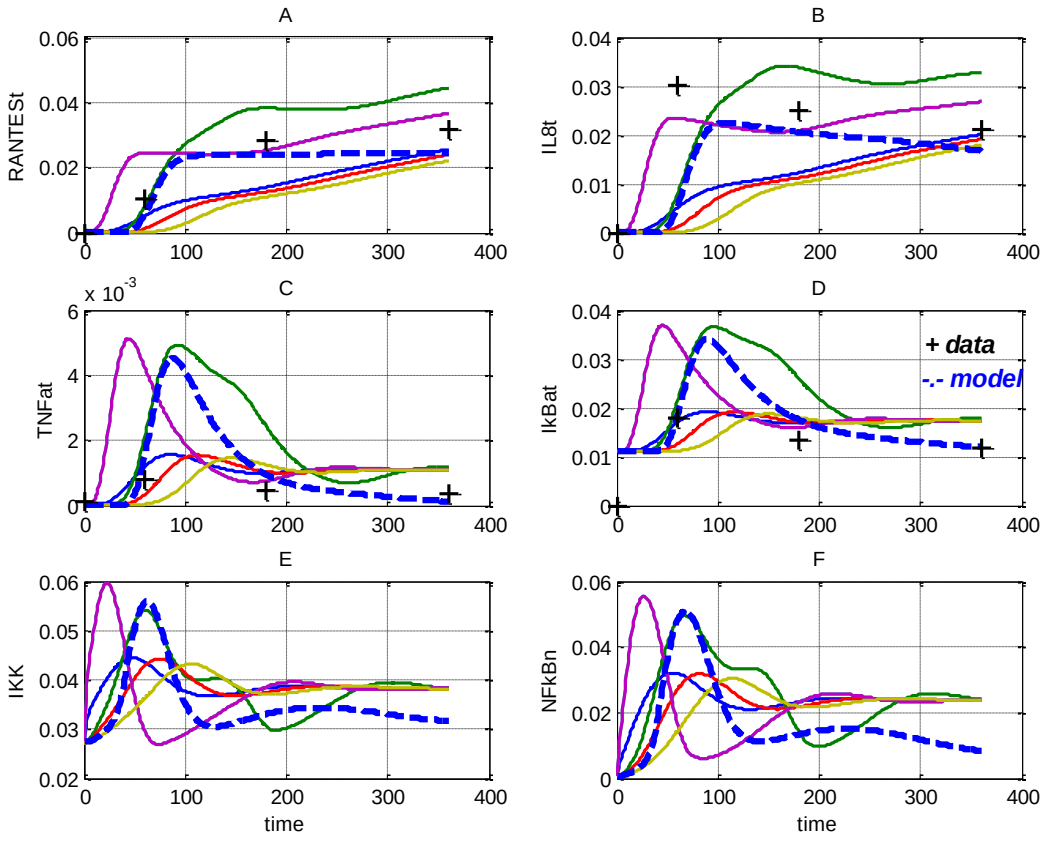


Figure 8-4 Third cluster. Simulations with input profiles 8, 22, 29, 32, 33 and 35 (Table 8-1) for (A) RANTES mRNA, (B) IL8 mRNA, (C) TNFα mRNA, (D) IκBα mRNA, (E) IKK and (F) nuclear NFκB are shown.The x-axis represent the time (min) and the y-axis the concentration (μM).

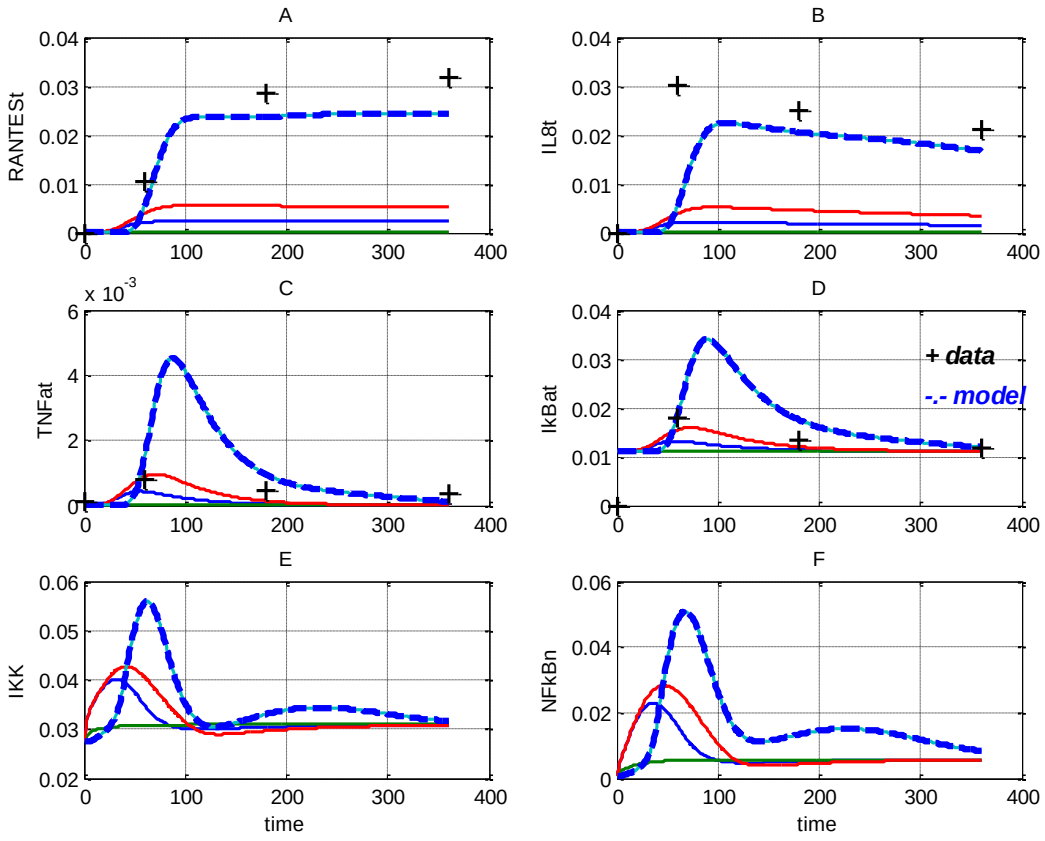


Figure 8-5 Fourth cluster. Simulations with input profiles 3, 16, 20, 38 (Table 8-1) for (A) RANTES mRNA, (B) IL8 mRNA, (C) TNFα mRNA, (D) IκBα mRNA, (E) IKK and (F) nuclear NFκB are shown. The x-axis represent the time (min) and the y-axis the concentration (μM).

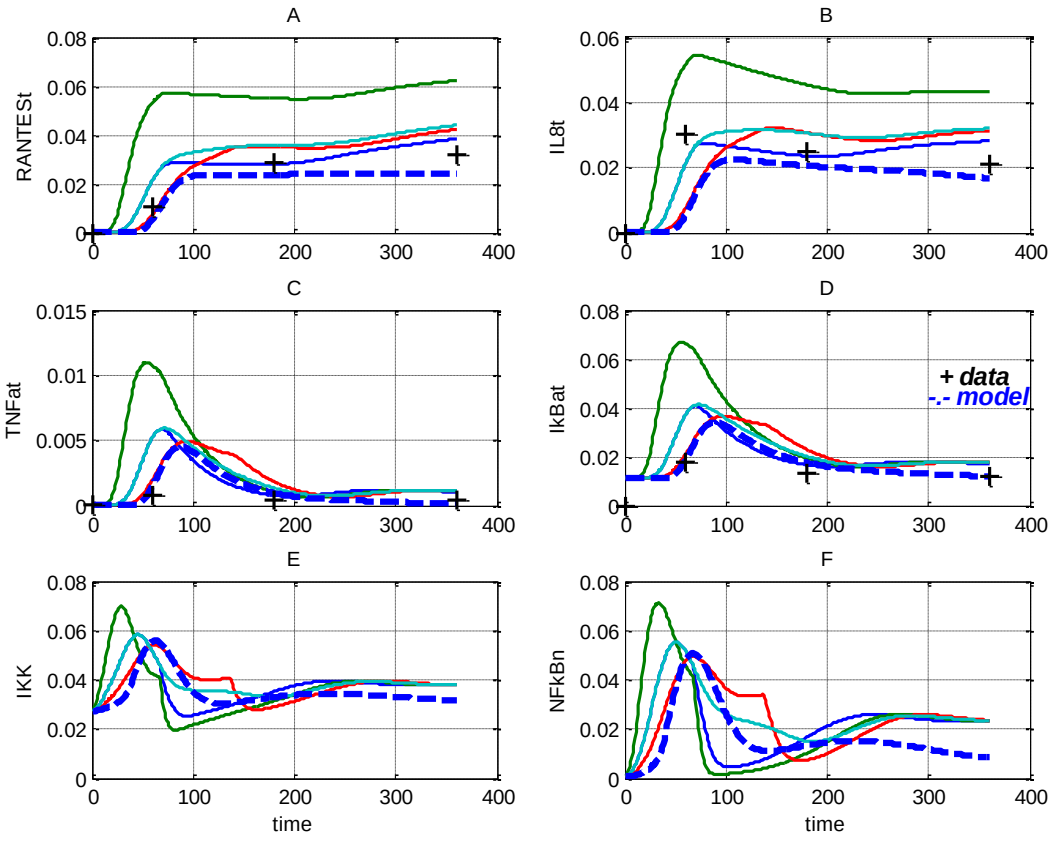


Figure 8-6 Fifth cluster. Simulations with input profiles 19, 27, 30 and 34 (Table 8-1) for (A) RANTES mRNA, (B) IL8 mRNA, (C) TNFα mRNA, (D) IκBα mRNA, (E) IKK and (F) nuclear NFκB are shown. The x-axis represent the time (min) and the y-axis the concentration (μM).

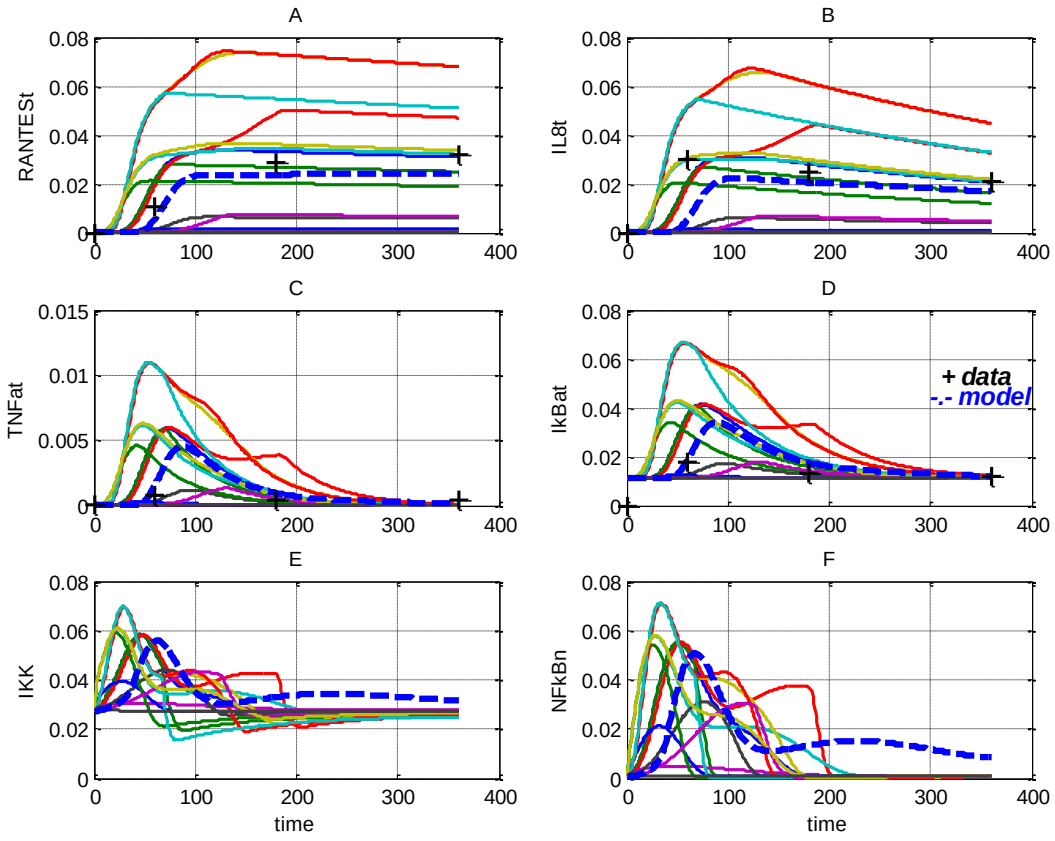


Figure 8-7 Sixth cluster. Simulations with the input profiles 1, 2, 4, 5, 11, 12, 13, 23, 25, 26, 28, 31 and 36 (Table 8-1) for (A) RANTES mRNA, (B) IL8 mRNA, (C) TNFα mRNA, (D) IκBα mRNA, (E) IKK and (F) nuclear NFκB are shown. This cluster included the model simulations with the original input functions (--).The x-axis represent the time (min) and the y-axis the concentration (μM).

The clusters show a clear relationship between the concentration of nuclear NFκB, IκBαt, IKK and TNFα mRNA at 360 minutes. If the concentration of the nuclear NFκB at 360 minutes increases with respect to the model, the concentration of the IκBαt, IKK and TNFα mRNA at 360 minutes increases. If the concentration of the nuclear NFκB at 360 minutes decreases with respect to the model, the concentration of the IκBαt, IKK and TNFα mRNA at 360 minutes decreases. The in- and de-creases are the same for the simulations in the clusters; therefore the concentration of the nuclear NFκB at 360 minutes can be used as a predictor for the concentration of IκBαt, IKK and TNFα mRNA at 360 minutes. However, the model does not show robustness to the variation in nuclear NFκB at 360 minutes for TNFα mRNA expression.

The concentrations of RANTES and IL8 mRNA at 360 minutes are also related to the concentration of the nuclear NFκB at 360 minutes but not as clear as the concentration of

TNFα mRNA is related to nuclear NFκB at 360 minutes. While TNFα mRNA at 360 minutes merges to a specific value for each cluster similar as nuclear NFκB at 360 minutes merges to a specific value in each cluster, IL8 and RANTES mRNA do not merge to a specific value. However, if the nuclear NFκB concentration at 360 minutes is equal or less than the model value, IL8 and RANTES mRNA time profiles show a decrease in concentration after the peak (Figure 8-8). If the nuclear NFκB concentration at 360 minutes is higher than the model value, IL8 and RANTES mRNA values continue to increase (Figure 8-9). Therefore the model does not show robustness for nuclear NFκB concentration changes in IL8 and RANTES mRNA expression either.

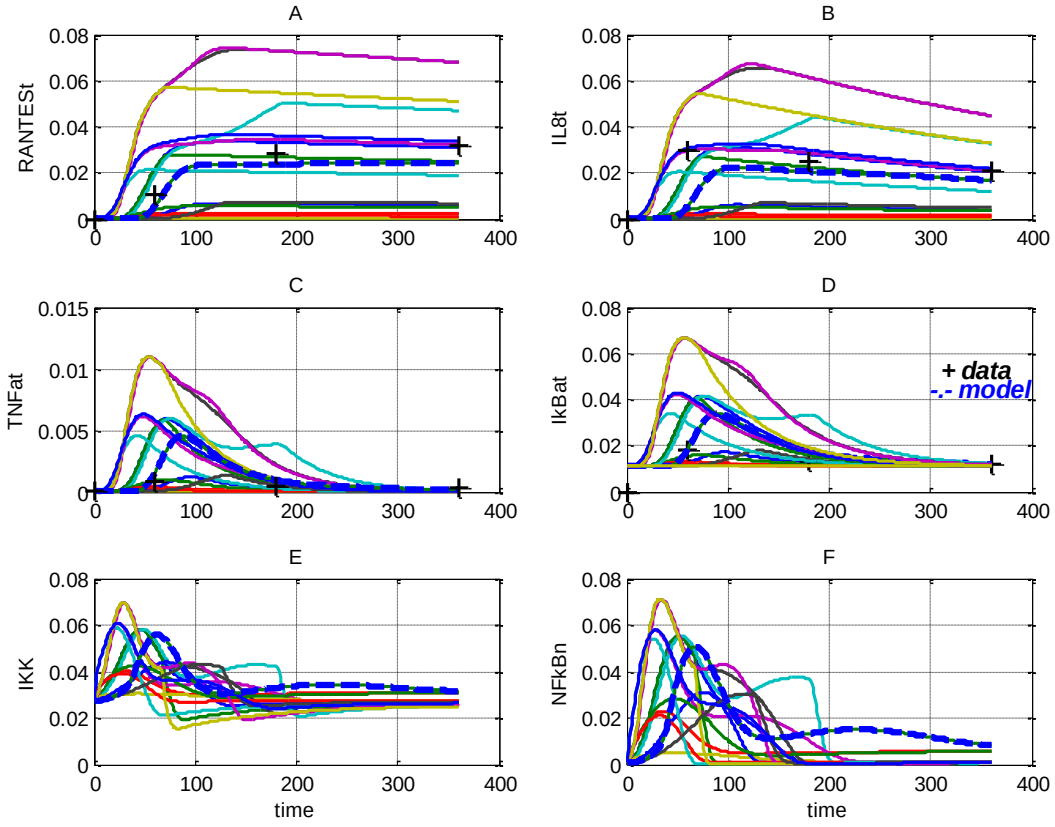


Figure 8-8 Simulations of (A) RANTES mRNA, (B) IL8 mRNA,(C) TNFα mRNA,(D) IκBα mRNA,(E) IKK and (F) nuclear NFκB with the input profiles (1 2 3 4 5 11 12 13 20 23 25 26 28 31 36 38) are shown. Simulations show IκBα mRNA and nuclear NFκB values lower or equal than the model value. IL8 and RANTES mRNA show a decrease after the peak value. The x-axis represent the time (min) and the y-axis the concentration (μM).

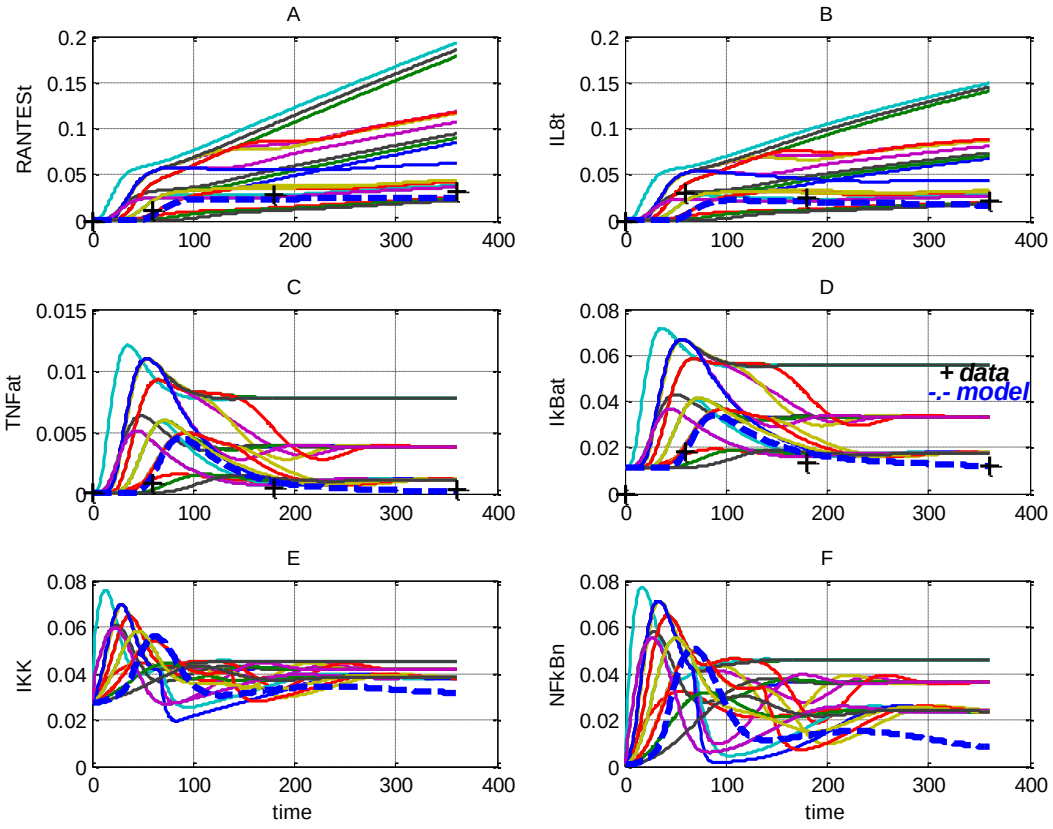


Figure 8-9 Simulations of (A) RANTES mRNA, (B) IL8 mRNA,(C) TNFα mRNA,(D) IκBα mRNA,(E) IKK and (F) nuclear NFκB with the input profiles (6 7 8 9 10 14 15 16 17 18 19 21 22 24 27 29 30 32 33 34 35 37) are shown. Simulations show IκBα mRNA and nuclear NFκB values higher than the model value. IL8 and RANTES mRNA show a continued increase of concentration during the simulation period. The x-axis represent the time (min) and the y-axis the concentration (μM).

The difference between Figure 8-8 and Figure 8-9 is not only in the difference of the simulation value with the model value but also in the oscillation of nuclear NFκB. For the simulations in Figure 8-8 nuclear NFκB shows none or minimal oscillations, while in the simulations in Figure 8-9 nuclear NFκB show clear oscillations. As a result of the nuclear NFκB oscillations, IL8 and RANTES mRNA continue to increase and are therefore not robust to the change in nuclear NFκB oscillations.

No relationship between the time of the IL8 mRNA expression peak and nuclear NFκB could be found.

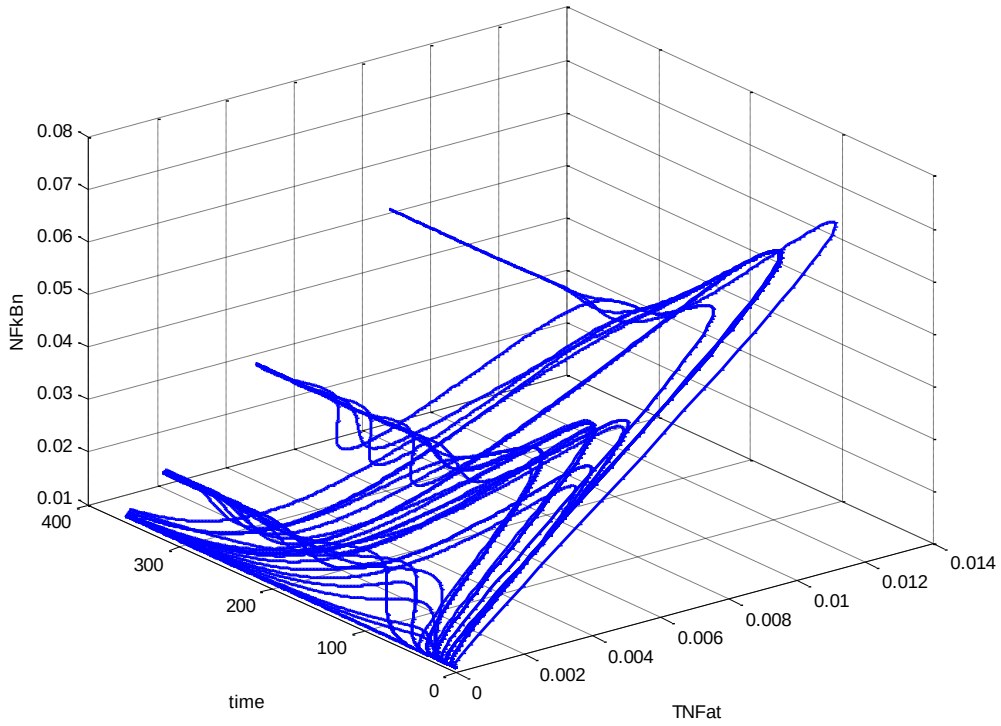


Figure 8-10 Increase in the maximum concentration (µM) of nuclear NFκB (NFκBn) shows an increase in the maximum concentration (µM) of TNFα mRNA expression at 360 min of the simulation.

With an increase in the maximum concentration of nuclear NFκB the maximum concentration of TNFα increased (Figure 8-10). This indicates a direct relationship between the maximum concentration of nuclear NFκB and the maximum concentration of TNFα. It also indicates that TNFα mRNA expression is not robust for an increase in the maximum concentration of nuclear NFκB.

## 8.4 Summary and discussion

In this chapter the robustness of the model output with several different nuclear NFκB time profiles was evaluated. The different nuclear NFκB time profiles represent different bacterial loads which develop mastitis. In milk samples, a higher bacterial load increased the IL8 concentration and the time of the peak was earlier (Vangroenweghe, 2004). With the developed model no relationship between the maximum concentration of nuclear NFκB or the steepness of the increase in nuclear NFκB and the time of the maximum IL8 mRNA

expression could be identified. From this, it can not be concluded that there is a lack of a relationship between nuclear NFκB expression in mammary epithelial cells and IL8 concentration in the milk. The relationship between mRNA expression levels in mammary epithelial cells and milk concentrations levels of the protein IL8 have not been established. The relationship is not necessarily a linear relationship. Several processes follow mRNA expression in mammary epithelial cells to produce the protein IL8 in the milk and therefore the concentration of IL8 in the milk can not be predicted from the mRNA expression levels in the mammary epithelial cells alone. As a result of these processes it is still possible that there is a nonlinear relationship between nuclear NFκB and IL8 concentration in the milk. In order to identify this relationship, further biological experiments investigating the relationship between mRNA expression in mammary epithelial cells and IL8 concentration in milk need to be performed. With those results the relationship between nuclear NFκB in mammary epithelial cells and IL8 concentration in milk can be investigated. However, we can conclude that the model is not robust for the time of the IL8 mRNA expression peak in relation to changes in the nuclear NFκB time profile.

IL8 and RANTES mRNA expression levels are influenced by nuclear NFκB. Oscillations of nuclear NFκB cause a continuation in the increase in IL8 and RANTES mRNA expression levels while lack of oscillations reduce the IL8 and RANTES mRNA levels. Therefore, it can be concluded that the model supports the theory that nuclear NFκB has a defining role in the expression levels of IL8 and RANTES mRNA in the LPS challenge. A similar conclusion can be drawn for the importance of nuclear NFκB in the LPS challenge on TNFα mRNA expression levels. TNFα mRNA appears to have a closer relationship with nuclear NFκB than IL8 and RANTES. However, the cytokine expression levels are not robust at 360 minutes of the simulation in relation to changes in the nuclear NFκB time profile.

In Section 5.3.3 we compared the relative sensitivity of synthesis and degradation parameter changes (Figure 5-9 (E and F)) with the change in concentration values for TNFα mRNA expression (Figure 5-11 (E and F)). The results were discussed in and Section 5.4 and although the sensitivity for parameter values increased, the concentration returned to the model levels, especially for variation in synthesis parameters at 360 minutes. It can be speculated that the robustness for variation in the synthesis and degradation rates for TNFα mRNA in the mammary epithelial cells influences the robustness to variation in bacterial load at 360 minutes. It is thus possible that the robustness for synthesis and/or degradation parameter changes, rather that the robustness for change in NFκB regulation is the cause for robustness at 360 minutes observed in biological experiments. Changes in cytokine

degradation rates as a result of disease have been seen earlier in other cells (Li & Bever, 2001). Robustness to variation in synthesis and degradation parameter variation does not apply to IL8 mRNA expression (See Section 5.4 and Figure 5-11 C and D) and other mechanisms must be involved in regulating IL8 mRNA expression robustness at 360 minutes.

Other commonalities of the nuclear NFκB time profile such as peak height, time of the first peak, concentration at 60 minutes or 180 minutes did not reveal a relationship with the cytokine expression level or robustness to changes in these values for cytokine expression levels. It can be concluded that robustness at 360 minutes and the lack of positive correlation between bacterial load and cytokine expression as found in the biological experiment is not originated in the nuclear NFκB concentration. Additional processes, such as cross pathway signalling, need to be investigated to identify the mechanism of this robustness.

Since the effect of a change in the nuclear NFκB time profile differs between the cytokines, changing the time profile with pharmaceutical applications need to be carefully considered for the effect on all cytokines.

# Chapter 9
# Conclusions and Future work

*In the last chapter of this work an overview of the work, the contributions and an insight in future research areas are given. Section 9.1 summarizes the findings presented is this thesis and discusses selected aspects. Section 9.2 outlines the possible future areas of research and extensions of the model.*

## 9.1 Summary

The overall theme of the study conducted in this thesis is about the application of systems biology, specifically mathematical modelling, to mastitis. The main goal of this work was to obtain a deeper understanding of the origin and mechanistics of the difference in gene regulation in two disease presentations; acute and chronic mastitis as introduced in Chapter 1. Chapter 2 gives a background into mastitis and discusses the methods used in the thesis.

The first focus of the work, discussed in Chapter 3, was to identify a gene network of genes significantly differentially expressed in the two clinical representations of mastitis that are caused by two different types of bacteria. To fulfil this goal a large number of microarrays from two bacterial challenges in mammary epithelial cells at different time points were analysed. From the analysis genes differentially expressed from healthy cells for each bacterium were identified. The genes were clustered into groups with similar mRNA expression time profiles for each bacterium. The genes in the clusters were compared between the two bacterial challenges and those with a difference in time profiles between the two bacterial challenges identified as our focus for further study.

Our approach proved successful in the identification of a cluster of immune system related genes with significantly distinct gene expression time profiles between the two bacterial challenges. The cluster included a cytokine not previously identified as a gene with different expression time profiles in epithelial cells between two bacterial challenges. Using biological knowledge from the literature and pathway databases we identified a specific signalling pathway and gene network responsible for the expression of the identified cytokine. We thus exposed the most likely signalling pathway and gene network regulation involved in the

clinical differentiation of the disease. Chapter 4 outlines a mathematical model for part of the identified signalling pathway.

The second focus was the development of a mathematical model for the signalling and gene network regulation, which is described in Chapter 5. We have successfully modelled mathematically, simulated computationally, and analysed analytically, in Chapter 5 and Chapter 6, the dynamical behaviours of cytokine expression in acute mastitis caused by the *E. coli* bacterium. The model was extended with additional cytokines to the cytokine identified in Chapter 3. These cytokines are regulated by the same signalling pathway and are reported in the literature to be influential in mastitis. The cytokines were included to be able to analyse the regulation of the cytokines and compare the regulatory mechanism between the cytokines. The use of a modular approach to set up the model resulted in a reduction of time and cost for the model development.

We modified a method for the conversion of relative expression levels from microarray experiments to mRNA concentration levels. This facilitated the use of microarray data in our modelling approach (Section 5.2.3). With this method the large number of microarray data currently available in public databases and the literature could be used for modelling in the future with greater accuracy.

Our results show that the model fit the experimental data well for the *E. coli* experiment. However, no fit could be found for the *S. aureus* experimental values as described in Chapter 7. This work has therefore identified that other signalling pathways and or gene network regulations are involved in the immune reaction of the *S. aureus* infection in mammary epithelial cells and that the differentiation of the clinical profile is not solely caused by the Toll Receptor Signalling pathway and the NFκB transcription factor.

The third focus was the analysis of the model and the identification of the mechanistics responsible for the differentiation in expression between healthy and diseased cells. In addition, we analysed the regulation of additional cytokines reported in the literature as involved in mastitis to evaluate the difference in regulation between cytokines. In Chapter 6, extensive sensitivity analysis identified that there is no single regulatory mechanism responsible for the differentiation in cytokine expression but that each cytokine playing a role in the immune reaction is sensitive to different parameters in the model. Not only are the cytokines sensitive to different parameters, they also show a difference in robustness for variation in the input, the bacterial load. In Chapter 8 robustness analysis identified that the robustness of IL8 and TNFα mRNA expression to a variation of the bacterial load at 360

minutes in biological experiments could not be explained with a variation in the input profile. The input profile represents the bacterial load. This indicates that the robustness, seen in biological experiments, can not be contributed to the variation in the time profile and concentration of nuclear NFκB. Other influences, such as the interaction of multiple signalling pathways and/or variation in synthesis and degradation need to be investigated to explain the robustness observed in biological experiments.

In addition, the study highlighted the importance of modelling prior to the design of biological experiments. The analysis identified specific time frames, different for each cytokine in the model to be most informative for the model optimization. The model can be used for future evaluations of pharmaceutical targets, biomarkers and experimental design. The study highlighted that while the regulation of the cytokines appear to be uniformly originating from one source, either the input or the transcription factor, the effect of changing the input or the regulation of this transcription factor is not uniform among the cytokines regulated by these functions. Pharmaceutical targets therefore need to be evaluated for all aspects of the immune reaction to prevent undesirable side effects.

## 9.2 Future Directions

The described work in this thesis can not be considered complete and suggests several directions of future work. Necessary for modelling analysis, assumptions had to be made based on critical evaluation of the current literature. Some important predictions and assumptions need to be validated with experimental data. But the model also suggests areas of extension that will increase our understanding of cytokine expression in mastitis and the differentiation between the two clinical presentations.

### 9.2.1 Biological experiments

**Experimental verification**

The work described above is based on the conversion of the relative expression levels in microarray experiments into concentration levels of mRNA. Further experimental validation with bovine microarray and mammary epithelial cells are necessary.

**Relationship between bacterial load, robustness and synthesis and degradation parameters**

In Chapter 8 it is speculated that the robustness of TNFα to variation in bacterial load at 360 minutes could be explained with the robustness to variation in synthesis and degradation parameters. This would be based on the assumption that the variation in bacterial load changes the synthesis and/or degradation parameters. Variation in cytokine degradation parameter values have been seen in other diseases (Li & Bever, 2001). To confirm the hypothesis, biological experiments need to measure the relationship between synthesis and degradation parameters and the bacterial load.

### 9.2.2 Extension of the model

Model extensions can be diverse and extensive but extensions should be guided by the research questions and available experimental data. Following the model developed in this work some insights in future extensions are given.

**Separation between active and inactive IKK**

As described in Section 4.2.6 the model in this work represents only active IKK. No equations are included to model the transformation of inactive IKK to active IKK. Lipniacki *et al.* constructed a model with two regulatory feedback loops, IκBα and the zinc-finger protein A20 (2004). IKK inactivation is controlled by A20 and the bovine forebrain zinc finger protein A20 has been indicated to be related to mastitis resistance (Sugimoto *et al.*, 2006). Therefore, it would be of interest to investigate the influence of activation of inactive IKK to active IKK due to the activity of A20 in the model. The zinc-finger protein A20 is a NFκB induced protein that uses the inactivation of active IKK into inactive IKK as a negative feedback loop for NFκB induced gene expression. Although Lipniacki *et al.* developed a model that represented the negative feedback regulation of A20 (2004) the exact mechanism of A20 has not been resolved and this model does not take the IκBε and IκBβ regulatory effects on IKK into account. Neither could the precise regulation of A20 be validated in experimental settings (Cheong *et al.*, 2006). Since we do not have data for A20 regulation or activity of A20 as a transcription factor, inclusion of this feedback loop would result in further speculation and over fitting with our limited experimental dataset. However, since the bovine

forebrain zinc finger protein A20 has been indicated as playing a role in mastitis resistance, modelling the mechanistic properties of this protein and the influence on cytokine expression levels with future biological data would be informative and could lead to further biological questions.

**Multiple signalling pathways**

In Chapter 7 we showed that the cytokine expression of the *S. aureus* challenge could not be modelled with the current model of one signalling pathway. IκBα and IL8 expressions are different between the two bacterial challenges (Figure 3-7 and Figure 3-8). A combination of the activation of the NFκB and MAPK signalling pathways are essential for the IL8 activation. MAPK signalling causes AP-1 activation. In conjunctival cells, Venza *et al.* concluded that the AP-1 binding site alone was required for optimal IL8 *S. aureus* induced promoter activity while the loss of function in the NFκB site did not affect IL8 promoter activation (2007). In the *E. coli* challenge both pathways, MAPK and NFκB have increased mRNA expression levels, indicating that both pathways are activated (Figure 3-5). In contrast, in the *S. aureus* challenge NFκB does not show a change in expression indicating a lack of activation of the NFκB pathway while the MAPK pathway is activated (Figure 3-6). Adding the MAPK pathway to the model and the interrogation of the MAPK and NFκB signalling pathways could well shed light on the difference in regulation between *E. coli* and *S. aureus* mastitis.

In Chapter 8 the robustness for the variation in the bacterial load reported in biological experiments at 360 minutes (Günther *et al.*, 2010) could not be reproduced by the model. This is also an indication that multiple signalling pathways are involved in the immune reaction for the *E. coli* infection at 360 minutes and needs to be verified with experimental values and a model extension including multiple signalling pathways.

**Modelling multiple transcription factors**

In the current model the transcription factors are modelled as acting one transcription factor activated by one signalling pathway. Above we indicated the need for an extension of the model with multiple signalling pathways. The multiple signalling pathways initiate different transcription factors. It is known that multiple transcription factors in addition to NFκB are involved in the expression of the cytokines (Ghosh & Hayden, 2008). Separating the

mechanistics of the transcription factors could lead to a further insight in the mechanistics of cytokine expression levels. Activator protein-1 was identified by us in earlier studies to be differentially regulated in *E. coli* mastitis (van Loenen-den Breems *et al.*, 2008). AP-1 is activated by the MAPK signalling pathway. The role of AP-1 as a transcription factor has been identified in LPS challenged cells (Vora *et al.*, 2004) and is involved in cytokine mRNA expression. As described above the AP-1 transcription factor alone was required for optimal IL8 *S. aureus* induced promoter activity while the loss of function in the NFκB site did not affect IL8 promoter activation in conjunctival cells (Venza *et al.*, 2007). Therefore, separating the transcription factors could lead to an insight in the difference in cytokine expression between the two bacterial challenges. In addition, p38 and ERK expressed in the *E. coli* but not in the *S. aureus* challenges are factors involved in cytokine expression. Separating the mechanistics of the transcription factors can lead to a further insight in the mechanistics of cytokine expression levels.

# References


Aderem, A. (2005). Systems Biology: its practice and challenges. *Cell, 121*(4), 511-513.

Afshari, C. A. (2002). Perspective: microarray technology, seeing more than spots. *Endocrinology, 143*(6), 1983-1989.

Aggarwal, K., & Lee, H. K. (2003). Functional genomics and proteomics as a foundation for Systems Biology. *Briefings in Functional Genomics and Proteomics, 2*(3), 175-184.

Akira, S., Uematsu, S., & Takeuchi, O. (2006). Pathogen recognition and innate immunity. *Cell, 124*(4), 783-801.

Aldana, M., Balleza, E., Kauffman, S., & Resendiz, O. (2007). Robustness and evolvability in genetic regulatory networks. *Journal of theoretical biology, 245*(3), 433-448.

Aldridge, B. B., Burke, J. M., Lauffenburger, D. A., & Sorger, P. K. (2006). Physicochemical modelling of cell signalling pathways. *Nat Cell Biol, 8*(11), 1195-1203.

Allison, D. B., Cui, X., Page, G. P., & Sabripour, M. (2006). Microarray data analysis: from disarray to consolidation and consensus. *Nature review genetics, 7*(1), 55-65.

Allore, H. G., & Erb, H. N. (1999). Approaches to modeling intramammary infections in dairy cattle. *Prev Vet Med, 39*(4), 279-293.

Alluwaimi, A. M. (2004). The cytokines of bovine mammary gland: prospects for diagnosis and therapy. *Research in veterinary science, 77*(3), 211-222.

Alon, U. (2007). *An introduction to Systems Biology: design principles of biological circuits*. Boca Raton, Florida, USA: Chapman & Hall/CRC.

Amir, A., Kobiler, O., Rokney, A., Oppenheim, A. B., & Stavans, J. (2007). Noise in timing and precision of gene activities in a genetic cascade. *Molecular Systems Biology, 3*, 1-10.

Arima, K., Nasu, K., Narahara, H., Fujisawa, K., Matsui, N., & Miyakawa, I. (2000). Effects of lipopolysaccharide and cytokines on production of RANTES by cultured human endometrial stromal cells. *Mol Hum Reprod, 6*(3), 246-251.

Armstrong, N. J., & van de Wiel, M. A. (2004). Microarray data analysis: from hypotheses to conclusions using gene expression data. *Cellular Oncology, 26*(5-6), 279-290.

Arrio-Dupont, M., Foucault, G., Vacher, M., Devaux, P. F., & Cribier, S. (2000). Translational diffusion of globular proteins in the cytoplasm of cultured muscle cells. *Biophysical Journal, 78*(2), 901-907.

Ashyraliyev, M., Jaeger, J., & Blom, J. (2008). Parameter estimation and determinability analysis applied to *Drosophila* gap gene circuits. *BMC Systems Biology, 2*(1), 83.

Ashyraliyev, M., Fomekong-Nanfack, Y., Kaandorp, J. A., & Blom, J. G. (2009). Systems Biology: parameter estimation for biochemical models. *FEBS Journal, 276*(4), 886-902.

Baldwin, R. L. (1995). *Modeling ruminant digestion and metabolism*. Padstow, Cornwall, Great Britain: Chapman & Hall.

Balsa-Canto, E., Peifer, M., Banga, J. R., Timmer, J., & Fleck, C. (2008). Hybrid optimization method with general switching strategy for parameter estimation. *BMC Systems Biology, 2*, 26.

Banga, J. R., & Balsa-Canto, E. (2008). Parameter estimation and optimal experimental design. *Essays Biochem, 45*, 195-209.

Bannerman, D. D. (2009). Pathogen-dependent induction of cytokines and other soluble inflammatory mediators during intramammary infection of dairy cows. *Journal of animal science, 87*(13_suppl), 10-25.

Bannerman, D. D., Paape, M. J., Lee, J. W., Zhao, X., Hope, J. C., & Rainard, P. (2004). *Escherichia coli* and *Staphylococcus aureus* elicit differential innate immune responses following intramammary infection. *Clinical and diagnostic laboratory immunology, 11*(3), 463-472.

Bar-Joseph, Z. (2004). Analyzing time series gene expression data. *Bioinformatics, 20*(16), 2493-2503.

Bar, D., Tauer, L. W., Bennett, G., Gonzalez, R. N., Hertl, J. A., Schukken, Y. H., Schulte, H. F., Welcome, F. L., & Grohn, Y. T. (2008). The cost of generic clinical mastitis in dairy cows as estimated by using dynamic programming. *Journal of dairy science, 91*(6), 2205-2214.

Barkema, H. W., Schukken, Y. H., & Zadoks, R. N. (2006). Invited review: The role of cow, pathogen, and treatment regimen in the therapeutic success of bovine *Staphylococcus aureus* mastitis. *Journal of Dairy Science, 89*(6), 1877-1895.

Bendixen, C., Hedegaard, J., & Horn, P. (2005). Functional genomics in farm animals - Microarray analysis. *Meat Science, 71*(1), 128-137.

Bhalla, & Ravi Iyengar, U. S. (1999). Emergent properties of networks of biological signaling pathways. *Science (New York, N.Y, 283*(5400), 381-387.

Bolstad, B. M., Irizarry, R. A., Astrand, M., & Speed, T. P. (2003). A comparison of normalization methods for high density oligonucleotide array data based on variance and bias. *Bioinformatics, 19*(2), 185-193.

Boulanger, D., Bureau, F., Melotte, D., Mainil, J., & Lekeux, P. (2003). Increased nuclear factor kappaB activity in milk cells of mastitis-affected cows. *Journal Dairy Science, 86*(4), 1259-1267.

Boutet, P., Boulanger, D., Gillet, L., Vanderplasschen, A., Closset, R., Bureau, F., & Lekeux, P. (2004). Delayed neutrophil apoptosis in bovine subclinical mastitis. *Journal of Dairy Science, 87*(12), 4104-4114.

Boutet, P., Sulon, J., Closset, R., Detilleux, J., Beckers, J. F., Bureau, F., & Lekeux, P. (2007). Prolactin-induced activation of nuclear factor kappaB in bovine mammary epithelial cells: role in chronic mastitis. *Journal of dairy science, 90*(1), 155-164.

Bragt, M., Plat, J., Mensink, M., Schrauwen, P., & Mensink, R. (2009). Anti-inflammatory effect of rosiglitazone is not reflected in expression of NFkappaB-related genes in peripheral blood mononuclear cells of patients with type 2 diabetes mellitus. *BMC Endocrine Disorders, 9*(1), 8.

Brandman, O., & Meyer, T. (2008). Feedback loops shape cellular signals in space and time. *Science (New York, N.Y, 322*(5900), 390-395.

Bruggeman, F. J., & Westerhoff, H. V. (2007). The nature of Systems Biology. *Trends in Microbiology, 15*(1), 45-50.

Burvenich, C., van Merris, V., Mehrzad, J., Diez-Fraile, A., & Duchateau, L. (2003). Severity of *E. coli* mastitis is mainly determined by cow factors. *Veterinary research, 34*(5), 521-564.

Burvenich, C., Bannerman, D. D., Lippolis, J. D., Peelman, L., Nonnecke, B. J., Kehrli, M. E., Jr., & Paape, M. J. (2007). Cumulative physiological events influence the inflammatory response of the bovine udder to *Escherichia coli* infections during the transition period. *Journal of dairy science, 90 Suppl 1*, E39-54.

Callard, R. E., & Yates, A. J. (2005). Immunology and mathematics: crossing the divide. *Immunology, 115*(1), 21-33.

Casola, A., Henderson, A., Liu, T., Garofalo, R. P., & Brasier, A. R. (2002). Regulation of RANTES promoter activation in alveolar epithelial cells after cytokine stimulation. *American journal of physiology, 283*(6), L1280-1290.

Cassar-Malek, I., Picard, B., Bernard, C., & Hocquette, J. (2008). Application of gene expression studies in livestock production systems: a european perspective. *Australian Journal of Experimental Agriculture, 48*(7), 701-710.

Chagunda, M. G. G., Friggens, N. C., Rasmussen, M. D., & Larsen, T. (2006). A model for detection of individual cow mastitis based on an indicator measured in milk. *Journal of dairy science, 89*(8), 2980-2998.

Chen, W. W., Schoeberl, B., Jasper, P. J., Niepel, M., Nielsen, U. B., Lauffenburger, D. A., & Sorger, P. K. (2009). Input-output behavior of ErbB signaling pathways as revealed by a mass action model trained against dynamic data. *Mol Syst Biol, 5*

Cheong, R., & Levchenko, A. (2008). Wires in the soup: quantitative models of cell signaling. *Trends Cell Biol, 18*(3), 112-118.

Cheong, R., Hoffmann, A., & Levchenko, A. (2008). Understanding NF-kappaB signaling via mathematical modeling. *Mol Syst Biol, 4*

Cheong, R., Paliwal, S., & Levchenko, A. (2010). Models at the single cell level. *Wiley Interdiscip Reviews: Systems Biolgy and Medicine, 2*(1), 34-48.

Cheong, R., Bergmann, A., Werner, S. L., Regal, J., Hoffmann, A., & Levchenko, A. (2006). Transient IkappaB kinase activity mediates temporal NF-kappaB dynamics in response to a wide range of tumor necrosis factor-alpha doses. *J Biol Chem, 281*(5), 2945-2950.

Cho, K. H., Kolch, W., & Wolkenhauer, O. (2003). Experimental Design in Systems Biology, Based on Parameter Sensitivity Analysis Using a Monte Carlo Method: A Case study for the TNFa-Mediated NFkB Signal Transduction Pathway. *Simulation, 79*(12), 726-739.

Chou, I. C., & Voit, E. O. (2009). Recent developments in parameter estimation and structure identification of biochemical and genomic systems. *Mathematical Biosciences, 219*(2), 57-83.

Connelly, L., Barham, W., Pigg, R., Saint-Jean, L., Sherrill, T., Cheng, D.-S., Chodosh, L. A., Blackwell, T. S., & Yull, F. E. (2010). Activation of nuclear factor kappa B in mammary epithelium promotes milk loss during mammary development and infection. *Journal of Cellular Physiology, 222*(1), 73-81.

Covert, M. W., Leung, T. H., Gaston, J. E., & Baltimore, D. (2005). Achieving stability of lipopolysaccharide-induced NF-kappaB activation. *Science (New York, N.Y, 309*(5742), 1854-1857.

Csete, M. E., & Doyle, J. C. (2002). Reverse engineering of biological complexity. *Science (New York, N.Y, 295*(5560), 1664-1669.

de Jong, H. (2002). Modeling and simulation of genetic regulatory systems: a literature review. *Journal of computational biology, 9*(1), 67-103.

de Jong, H., & Ropers, D. (2006). Qualitative approaches to the analysis of genetic regulatory networks. In Z. Szallasi (Ed.), *Systems Modeling in Cellular Biology* (pp. 125-147). Cambridge, USA: MIT.

de Ketelaere, A., Goossens, K., Peelman, L., & Burvenich, C. (2006). Technical note: validation of internal control genes for gene expression analysis in bovine polymorphonuclear leukocytes. *Journal of dairy science, 89*(10), 4066-4069.

de Schepper, S., de Ketelaere, A., Bannerman, D. D., Paape, M. J., Peelman, L., & Burvenich, C. (2008). The toll-like receptor-4 (TLR-4) pathway and its possible role in the pathogenesis of *Escherichia coli* mastitis in dairy cattle. *Veterinary research, 39*(1), 5.

Detilleux, J. C. (2004). Neutrophils in the war against *Staphylococcus aureus*: Predator-prey models to the rescue. *Journal of dairy science, 87*(11), 3716-3724.

Detilleux, J. C., Vangroenweghe, F., & Burvenich, C. (2006). Mathematical model of the acute inflammatory response to *Escherichia coli* in intramammary challenge. *Journal of dairy science, 89*(9), 3455-3465.

Dogan, B., Klaessig, S., Soimpson, K., Oliver, S., A;, e., R, & Schukken, Y. (2005). Pathogeneis of chronic intramammary Escherichia coli infections. In H. Hogeveen (Ed.), *Mastitis in dairy production current knowledge and future solutions* (pp. 131-136). Wageningen: Wageningen Academic Publishers.

Doyle, F. J., & Stelling, J. (2006). Systems interface biology. *Journal of the Royal Society Interface, 3*(10), 603-616.

Doyle, S. L., & O'Neill, L. A. (2006). Toll-like receptors: from the discovery of NFkappaB to new insights into transcriptional regulations in innate immunity. *Biochemical Pharmacology, 72*(9), 1102-1113.

Draghici, S. (2003). *Data analysis tools for DNA microarrays*. Boca Raton, USA: Chapman & Hall/CRC.

Egea, J., Rodríguez-Fernández, M., Banga, J., & Martí, R. (2007). Scatter search for chemical and bio-process optimization. *Journal of Global Optimization, 37*(3), 481-503(423).

El-Samad, H., Kurata, H., Doyle, J. C., Gross, C. A., & Khammash, M. (2005). Surviving heat shock: control strategies for robustness and performance. *Proceedings of National Acadamy of Sciences, 102*(8), 2736-2741.

Ernst, J., & Bar-Joseph, Z. (2006). STEM: a tool for the analysis of short time series gene expression data. *BMC Bioinformatics, 7*, 191.

Ernst, J., Nau, G. J., & Bar-Joseph, Z. (2005). Clustering short time series gene expression data. *Bioinformatics, 21 Suppl 1*, i159-i168.

Fang, Z., Yang, J., Li, Y., Luo, Q., & Liu, L. (2006). Knowledge guided analysis of microarray data. *Journal of Biomedical Informatics, 39*(4), 401-411.

Force, C., Pérochon, L., & Hill, D. R. C. (2002). Design of a multimodel of a dairy cows herd attacked by mastitis. *Simulation Modelling Practice and Theory, 10*(8), 543-554.

Fraser, C. C. (2008). G Protein coupled receptor connectivity to NF-kappaB in inflammation and cancer. *International Reviews of Immunology, 27*(5), 320 - 350.

Friboulet, A., & Thomas, D. (2005). Systems Biology-an interdisciplinary approach. *Biosensors and Bioelectronics, 20*(12), 2404-2407.

Ghosh, S., & Hayden, M. S. (2008). New regulators of NFkappaB in inflammation. *Nature Reviews Immunology, 8*(11), 837-848.

Ghosh, S., May, M. J., & Kopp, E. B. (1998). NF-kappaB and Rel proteins: evolutionarily conserved mediators of immune responses. *Annu Rev Immunol, 16*, 225-260.

Goldstein, B., Faeder, J. R., & Hlavacek, W. S. (2004). Mathematical and computational models of immune-receptor signalling. *Nature Reviews Immunology, 4*(6), 445-456.

Griesbeck-Zilch, B., Meyer, H. H., Kuhn, C. H., Schwerin, M., & Wellnitz, O. (2008). *Staphylococcus aureus* and *Escherichia coli* cause deviating expression profiles of cytokines and lactoferrin messenger ribonucleic acid in mammary epithelial cells. *Journal of dairy science, 91*(6), 2215-2224.

Griesbeck-Zilch, B., Osman, M., Kuhn, C., Schwerin, M., Bruckmaier, R. H., Pfaffl, M. W., Hammerle-Fickinger, A., Meyer, H. H. D., & Wellnitz, O. (2009). Analysis of key molecules of the innate immune system in mammary epithelial cells

isolated from marker-assisted and conventionally selected cattle. *Journal of dairy science, 92*(9), 4621-4633.
Günther, J., Liu, S., Esch, K., Schuberth, H.-J., & Seyfert, H.-M. (2010). Stimulated expression of TNFalpha and IL-8, but not of lingual antimicrobial peptide reflects the concentration of pathogens contacting bovine mammary epithelial cells. *Veterinary immunology and immunopathology, 135*(1-2), 152-157.
Han, J., & Ulevitch, R. J. (2005). Limiting inflammatory responses during activation of innate immunity. *Nature Immunology, 6*(12), 1198-1205.
Harte, J. (1988). *Consider a spherical cow: a course in environmental problem solving*. Mill Valley, California, USA: University Science Books.
Hartemink, A., Gifford, D., Jaakkola, T., & Young, R. (2002). Combining location and expression data for principled discovery of genetic regulatory network models. *Pacific Symposium on Biocomputing*, 437-449.
Hayden, M. S., West, A. P., & Ghosh, S. (2006). NFkappaB and the immune response. *Oncogene, 25*(51), 6758-6780.
Hekstra, D., Taussig, A. R., Magnasco, M., & Naef, F. (2003). Absolute mRNA concentrations from sequence-specific calibration of oligonucleotide arrays. *Nucleic acids research, 31*(7), 1962-1968.
Hoffmann, A., & Baltimore, D. (2006). Circuitry of NF kappaB signaling. *Immunological Reviews, 210*, 171-186.
Hoffmann, A., Natoli, G., & Ghosh, G. (2006). Transcriptional regulation via the NF-kappaB signaling module. *Oncogene, 25*(51), 6706-6716.
Hoffmann, A., Levchenko, A., Scott, M. L., & Baltimore, D. (2002a). The IkappaB-NFkappaB signaling module: temporal control and selective gene activation. *Science (New York, N.Y, 298*(5596), 1241-1245.
Hoffmann, E., Dittrich-Breiholz, O., Holtmann, H., & Kracht, M. (2002b). Multiple control of interleukin-8 gene expression. *Journal of Leukocyte Biology, 72*(5), 847-855.
Hornberg, J. J., Bruggeman, F. J., Westerhoff, H. V., & Lankelma, J. (2006). Cancer: a Systems Biology disease. *Bio Systems, 83*(2-3), 81-90.
Huijps, K., & Hogeveen, H. (2007). Stochastic modeling to determine the economic effects of blanket, selective, and no dry cow therapy. *Journal of dairy science, 90*(3), 1225-1234.
Ideker, T., & Lauffenburger, D. (2003). Building with a scaffold: emerging strategies for high- to low-level cellular modeling. *Trends in Biotechnology, 21*(6), 255-262.
Ideker, T., Galitski, T., & Hood, L. (2001). A new approach to decoding life: systems biology. *Annual review of genomics and human genetics, 2*, 343-372.
Ihekwaba, A. E., Broomhead, D. S., Grimley, R. L., Benson, N., & Kell, D. B. (2004). Sensitivity analysis of parameters controlling oscillatory signalling in the NFkappaB pathway: the roles of IKK and IkappaBalpha. *Systems biology, 1*(1), 93-103.
Ihekwaba, A. E. C., Wilkinson, S. J., Waithe, D., Broomhead, D. S., Li, P., Grimley, R. L., & Benson, N. (2007). Bridging the gap between *in silico* and cell-based analysis of the Nuclear factorkappaB signaling pathway by *in vitro* studies of IKK2. *FEBS Journal, 274*(7), 1678-1690.
Ingalls, B. (2008). Sensitivity analysis: from model parameters to system behaviour. *Essays Biochem, 45*, 177-193.
Jacquez, J. A., & Greif, P. (1985). Numerical parameter identifiability and estimability: Integrating identifiability, estimability, and optimal sampling design. *Mathematical Biosciences, 77*(1-2), 201-227.

Jaqaman, K., & Danuser, G. (2006). Linking data to models: data regression. *Nature Reviews Molecular Cell Biology, 7*(11), 813-819.

John, G. C., Nduati, R. W., Mbori-Ngacha, D. A., Richardson, B. A., Panteleeff, D., Mwatha, A., Overbaugh, J., Bwayo, J., Ndinya-Achola, J. O., & Kreiss, J. K. (2001). Correlates of mother-to-child human immunodeficiency virus type 1 (HIV-1) transmission: association with maternal plasma HIV-1 RNA load, genital HIV-1 DNA shedding, and breast infections. *The Journal of infectious diseases, 183*(2), 206-212.

Jones, B. W., Heldwein, K. A., Means, T. K., Saukkonen, J. J., & Fenton, M. J. (2001). Differential roles of Toll-like receptors in the elicitation of proinflammatory responses by macrophages. *Annals of the Rheumatic Diseases, 60 Suppl 3*, iii6-12.

Kauffman, S. A., & Macready, W. G. (1995). Search strategies for applied molecular evolution. *Journal of theoretical biology, 173*(4), 427-440.

Kearns, J. D., & Hoffmann, A. (2008). Integrating computational and biochemical studies to explore mechanisms in NFkappa B signaling. *J Biol Chem,*

Kearns, J. D., Basak, S., Werner, S. L., Huang, C. S., & Hoffmann, A. (2006). IkappaBepsilon provides negative feedback to control NF-kappaB oscillations, signaling dynamics, and inflammatory gene expression. *J Cell Biol, 173*(5), 659-664.

Kell, D. B. (2005). Metabolomics, machine learning and modelling: towards an understanding of the language of cells. *Biochemical Society transactions, 33*(3), 520-524.

Khatib, H., Monson, R. L., Schutzkus, V., Kohl, D. M., Rosa, G. J. M., & Rutledge, J. J. (2008). Mutations in the STAT5A gene are associated with embryonic survival and milk composition in cattle. *Journal of dairy science, 91*(2), 784-793.

Kimura, S., Sonoda, K., Yamane, S., Maeda, H., Matsumura, K., & Hatakeyama, M. (2008). Function approximation approach to the inference of reduced NGnet models of genetic networks. *BMC bioinformatics, 9*, 23.

Kitano, H. (2002). Systems Biology: a brief overview. *Science (New York, N.Y, 295*(5560), 1662-1664.

Klauschen, F., Angermann, B. R., & Meier-Schellersheim, M. (2007). Understanding diseases by mouse click: the promise and potential of computational approaches in Systems Biology. *Clin Exp Immunol, 149*(3), 424-429.

Klipp, E. (2005). *Systems biology in practice: concepts, implementation and application*. Weinheim, Germany: Wiley-VCH.

Kumar, A., Takada, Y., Boriek, A. M., & Aggarwal, B. B. (2004). Nuclear factor-kappaB: its role in health and disease. *Journal of Molecular Medicine, 82*(7), 434-448.

Kutalik, Z., Cho, K.-H., & Wolkenhauer, O. (2004). Optimal sampling time selection for parameter estimation in dynamic pathway modeling. *Bio Systems, 75*(1-3), 43-55.

Lahouassa, H., Moussay, E., Rainard, P., & Riollet, C. (2007). Differential cytokine and chemokine responses of bovine mammary epithelial cells to *Staphylococcus aureus* and *Escherichia coli*. *Cytokine, 38*(1), 12-21.

Li, C., & Wong, W. H. (2001). Model-based analysis of oligonucleotide arrays: expression index computation and outlier detection. *Proceedings of the National Academy of Sciences, 98*(1), 31-36.

Li, Q. Q., & Bever, C. T. (2001). Mechanisms underlying the synergistic effect of Th1 cytokines on RANTES chemokine production by human glial cells. *Int J Mol Med, 7*(2), 187-195.

Liang, S., Fuhrman, S., & Somogyi, R. (1998). Reveal, a general reverse engineering algorithm for inference of genetic network architectures. *Pacific Symposium on Biocomputing*, 18-29.

Liew, F. Y., Xu, D., Brint, E. K., & O'Neill, L. A. J. (2005). Negative regulation of Toll-like receptor-mediated immune responses. *Nature Reviews Immunology, 5*(6), 446-458.

Lipniacki, T., Paszek, P., Brasier, A. R., Luxon, B., & Kimmel, M. (2004). Mathematical model of NFkappaB regulatory module. *Journal of theoretical biology, 228*(2), 195-215.

Materi, W., & Wishart, D. S. (2007). Computational systems biology in drug discovery and development: methods and applications. *Drug Discovery Today, 12*(7-8), 295-303.

MATLAB® (Version 7.4.0). (R2007a ). Natick, Massachusetts, USA: The MathWorks, Inc. Natick, MA. Available from http://www.mathworks.com

Mendes, P., & Kell, D. (1998). Non-linear optimization of biochemical pathways: applications to metabolic engineering and parameter estimation. *Bioinformatics, 14*(10), 869-883.

Mengel, B., Hunziker, A., Pedersen, L., Trusina, A., Jensen, M. H., & Krishna, S. (2010). Modeling oscillatory control in NFkappaB, p53 and Wnt signaling. *Curr Opin Genet Dev, 20*(6), 656-664.

Menzies, M., & Ingham, A. (2006). Identification and expression of Toll-like receptors 1-10 in selected bovine and ovine tissues. *Veterinary immunology and immunopathology, 109*(1-2), 23-30.

Mettetal, J. T., & van Oudenaarden, A. (2007). Microbiology. Necessary noise. *Science, 317*(5837), 463-464.

Moles, C. G., Mendes, P., & Banga, J. R. (2003). Parameter estimation in biochemical pathways: a comparison of global optimization methods. *Genome Res, 13*(11), 2467-2474.

Murray, J. D. (1989). *Mathematical biology* (Vol. 19). Berlin; New York, USA: Springer-Verlag.

Nelson, D. E., Ihekwaba, A. E. C., Elliott, M., Johnson, J. R., Gibney, C. A., Foreman, B. E., Nelson, G., See, V., Horton, C. A., Spiller, D. G., Edwards, S. W., McDowell, H. P., Unitt, J. F., Sullivan, E., Grimley, R., Benson, N., Broomhead, D., Kell, D. B., & White, M. R. H. (2004). Oscillations in NF-kappaB signaling control the dynamics of gene expression. *Science (New York, N.Y, 306*(5696), 704-708.

Niv, H., Gutman, O., Henis, Y. I., & Kloog, Y. (1999). Membrane interactions of a constitutively active GFP-Ki-Ras 4B and their role in signaling. Evidence from lateral mobility studies. *The Journal of Biological Chemistry, 274*(3), 1606-1613.

Noble, D. (2002). Modeling the heart-from genes to cells to the whole organ. *Science, 295*(5560), 1678-1682.

Noppert, S. J., Fitzgerald, K. A., & Hertzog, P. J. (2007). The role of type I interferons in TLR responses. *Immunology & Cell Biology, 85*(6), 446-457.

Notebaert, S., Demon, D., Vanden Berghe, T., Vandenabeele, P., & Meyer, E. (2008a). Inflammatory mediators in *Escherichia coli*-induced mastitis in mice. *Comparative immunology, microbiology and infectious diseases, 31*(6), 551-565.

Notebaert, S., Carlsen, H., Janssen, D., Vandenabeele, P., Blomhoff, R., & Meyer, E. (2008b). *In vivo* imaging of NF-kappaB activity during *Escherichia coli*-induced mammary gland infection. *Cellular microbiology, 10*(6), 1249-1258.

Oltenacu, P. A., & Natzke, R. P. (1976). Mathematical modeling of the mastitis infection process. *Journal of dairy science, 59*(3), 515-521.
Østergaard, S., Sørensen, J. T., & Houe, H. (2003). A stochastic model simulating milk fever in a dairy herd. *Preventitive Veterinary Medicine, 58*(3-4), 125-143.
Østergaard, S., Chagunda, M. G. G., Friggens, N. C., Bennedsgaard, T. W., & Klaas, I. C. (2005). A stochastic model simulating pathogen-specific mastitis control in a dairy herd. *Journal of dairy science, 88*(12), 4243-4257.
Paape, M., Mehrzad, J., Zhao, X., Detilleux, J., & Burvenich, C. (2002). Defense of the bovine mammary gland by polymorphonuclear neutrophil leukocytes. *Journal Mammary Gland Biology and Neoplasia, 7*(2), 109-121.
Pando, M. P., & Verma, I. M. (2000). Signal-dependent and -independent degradation of free and NF-kB-bound IkBa. *Journal of Biological Chemistry, 275*(28), 21278-21286.
Pareek, R., Wellnitz, O., Van Dorp, R., Burton, J., & Kerr, D. (2005). Immunorelevant gene expression in LPS-challenged bovine mammary epithelial cells. *Journal of applied genetics, 46*(2), 171-177.
Paulsson, J., Berg, O. G., & Ehrenberg, M. (2000). Stochastic focusing: fluctuation-enhanced sensitivity of intracellular regulation. *Proceedings of the National Academy of Sciences, 97*(13), 7148-7153.
Petzl, W., Zerbe, H., Gunther, J., Yang, W., Seyfert, H. M., Nurnberg, G., & Schuberth, H. J. (2008). *Escherichia coli*, but not *Staphylococcus aureus* triggers an early increased expression of factors contributing to the innate immune defense in the udder of the cow. *Veterinary research, 39*(2), 18.
Quackenbush, J. (2002). Microarray data normalization and transformation. *Nat Genet, 32 Suppl*, 496-501.
Rainard, P., & Riollet, C. (2006). Innate immunity of the bovine mammary gland. *Veterinary research, 37*(3), 369-400.
Rangamani, P., & Sirovich, L. (2007). Survival and apoptotic pathways initiated by TNF-alpha: modeling and predictions. *Biotechnol Bioeng, 97*(5), 1216-1229.
Raser, J. M., & O'Shea, E. K. (2005). Noise in gene expression: origins, consequences, and control. *Science, 309*(5743), 2010-2013.
Riollet, C., Rainard, P., & Poutrel, B. (2000). Differential induction of complement fragment C5a and inflammatory cytokines during intramammary infections with *Escherichia coli* and *Staphylococcus aureus*. *Clinical and diagnostic laboratory immunology, 7*(2), 161-167.
Rodriguez-Fernandez, M., & Banga, J. R. (2009). Global sensitivity analysis of a biochemical pathway model. In J. M. Corchado, J. F. De Paz, M. P. Rocha & F. F. Riverola (Eds.), *2nd International Workshop on Practical Applications of Computational Biology and Bioinformatics (IWPACBB 2008)* (pp. 233-242). Berlin, Germany: Springer-Verlag.
Rodriguez-Fernandez, M., Mendes, P., & Banga, J. R. (2006a). A hybrid approach for efficient and robust parameter estimation in biochemical pathways. *Bio Systems, 83*(2-3), 248-265.
Rodriguez-Fernandez, M., Egea, J. A., & Banga, J. R. (2006b). Novel metaheuristic for parameter estimation in nonlinear dynamic biological systems. *BMC Bioinformatics, 7*, 483.
Sabroe, I., Parker, L. C., Dower, S. K., & Whyte, M. K. B. (2008). The role of TLR activation in inflammation. *Journal of Pathology, 214*(2), 126-135.
Saltelli, A., Tarantola, S., Campolongo, F., & Ratto, M. (2004). *Sensitivity analysis in practice: a guide to assessing scientific models*. Hoboken, New Jersey, USA: Wiley.

Schmidt, H., & Jirstrand, M. (2006). Systems Biology toolbox for MATLAB: a computational platform for research in systems biology. *Bioinformatics, 22*(4), 514-515.

Schoeberl, B., Pace, E. A., Fitzgerald, J. B., Harms, B. D., Xu, L., Nie, L., Linggi, B., Kalra, A., Paragas, V., Bukhalid, R., Grantcharova, V., Kohli, N., West, K. A., Leszczyniecka, M., Feldhaus, M. J., Kudla, A. J., & Nielsen, U. B. (2009). Therapeutically targeting ErbB3: a key node in ligand-induced activation of the ErbB receptor-PI3K axis. *Sci Signal, 2*(77), ra31-.

Scott, J. A., Robertson, M., Fitzpatrick, J., Knight, C., & Mulholland, S. (2008). Occurrence of lactational mastitis and medical management: a prospective cohort study in Glasgow. *Int Breastfeed J, 3*(1), 21.

Seegers, H., Fourichon, C., & Beaudeau, F. (2003). Production effects related to mastitis and mastitis economics in dairy cattle herds. *Veterinary research, 34*(5), 475-491.

Seo, J., Bakay, M., Chen, Y. W., Hilmer, S., Shneiderman, B., & Hoffman, E. P. (2004). Interactively optimizing signal-to-noise ratios in expression profiling: project-specific algorithm selection and detection p-value weighting in Affymetrix microarrays. *Bioinformatics, 20*(16), 2534-2544.

Shippy, R., Sendera, T. J., Lockner, R., Palaniappan, C., Kaysser-Kranich, T., Watts, G., & Alsobrook, J. (2004). Performance evaluation of commercial short-oligonucleotide microarrays and the impact of noise in making cross-platform correlations. *BMC Genomics, 5*(1), 61.

Sillitoe, K., Horton, C., Spiller, D. G., & White, M. R. H. (2007). Single-cell time-lapse imaging of the dynamic control of NFkappaB signalling. *Biochemical Society transactions, 35*, 263-266.

Simon, R., Lam, A., Li, M.-C., Ngan, M., Menenzes, S., & Zhao, Y. (2007). Analysis of gene expression data using BRB-Array Tools. *Cancer Informatics, 2007*(3), 11-17.

Sordillo, L. M., & Streicher, K. L. (2002). Mammary gland immunity and mastitis susceptibility. *Journal Mammary Gland Biology and Neoplasia, 7*(2), 135-146.

Stelling, J., Sauer, U., Szallasi, Z., Doyle, F. J., 3rd, & Doyle, J. (2004). Robustness of cellular functions. *Cell, 118*(6), 675-685.

Strandberg, Y., Gray, C., Vuocolo, T., Donaldson, L., Broadway, M., & Tellam, R. (2005). Lipopolysaccharide and lipoteichoic acid induce different innate immune responses in bovine mammary epithelial cells. *Cytokine, 31*(1), 72-86.

Styczynski, M. P., & Stephanopoulos, G. (2005). Overview of computational methods for the inference of gene regulatory networks. *Computers & Chemical Engineering, 29*(3), 519-534.

Sugimoto, M., Fujikawa, A., Womack, J. E., & Sugimoto, Y. (2006). Evidence that bovine forebrain embryonic zinc finger-like gene influences immune response associated with mastitis resistance. *Proceedings of the National Academy of Sciences, 103*(17), 6454-6459.

Sun, L., Yang, G., Zaidi, M., & Iqbal, J. (2008). TNF-induced oscillations in combinatorial transcription factor binding. *Biochemical and biophysical research communications, 371*(4), 912-916.

Suresh Babu, C. V., Joo Song, E., & Yoo, Y. S. (2006). Modeling and simulation in signal transduction pathways: a systems biology approach. *Biochimie, 88*(3-4), 277-283.

Swain, P. S., Elowitz, M. B., & Siggia, E. D. (2002). Intrinsic and extrinsic contributions to stochasticity in gene expression. *Proceedings of the National Academy of Sciences, 99*(20), 12795-12800.

Szallasi, Z., Stelling, J., & Periwal, V. (2006). *System modeling in cell biology from concepts to nuts and bolts*. Cambridge, Massechutes, USA: MIT Press.

Teruel, M. N., & Meyer, T. (2000). Translocation and reversible localization of signaling proteins: a dynamic future for signal transduction. *Cell, 103*(2), 181-184.

Thakar, J., Pilione, M., Kirimanjeswara, G., Harvill, E. T., & Albert, R. (2007). Modeling systems-level regulation of host immune responses. *PLoS Computational Biology, 3*(6), e109.

Thomas, K. E., Galligan, C. L., Newman, R. D., Fish, E. N., & Vogel, S. N. (2006). Contribution of interferon-beta to the murine macrophage response to the toll-like receptor 4 agonist, lipopolysaccharide. *The Journal of Biological Chemistry, 281*(41), 31119-31130.

Ting, A. Y., & Endy, D. (2002). Signal transduction. Decoding NF-kappaB signaling. *Science, 298*(5596), 1189-1190.

Toshchakov, V., Jones, B. W., Lentschat, A., Silva, A., Perera, P. Y., Thomas, K., Cody, M. J., Zhang, S., Williams, B. R., Major, J., Hamilton, T. A., Fenton, M. J., & Vogel, S. N. (2003). TLR2 and TLR4 agonists stimulate unique repertoires of host resistance genes in murine macrophages: interferon-beta-dependent signaling in TLR4-mediated responses. *Journal of Endotoxin Research, 9*(3), 169-175.

Tyson, J. J., Chen, K. C., & Novak, B. (2003). Sniffers, buzzers, toggles and blinkers: dynamics of regulatory and signaling pathways in the cell. *Current Opinion in Cell Biology, 15*(2), 221-231.

van Loenen-den Breems, N. Y., Molenaar, A., Henderson, H. V., & Seyfert, H. M. (2008, 24-27th June 2008). *Use of cDNA microarrays to investigate gene regulation in mastitis as a result of Escherichia coli infection in the bovine mammary gland.* Paper presented at the The 68th Annual Conference of New Zealand Society of Animal Production (NZSAP) joint with the 27th Biennial Conference for the Australian Society of Animal Production (ASAP) University of Queensland, St Lucia Campus, Brisbane, Australia.

van Riel, N. A. W. (2006). Dynamic modelling and analysis of biochemical networks: mechanism-based models and model-based experiments. *Briefings in Bioinformatics, 7*(4), 364-374.

van Someren, E. P., Wessels, L. F., Backer, E., & Reinders, M. J. (2002). Genetic network modeling. *Pharmacogenomics, 3*(4), 507-525.

Vanden Berghe, W., Ndlovu, M. N., Hoya-Arias, R., Dijsselbloem, N., Gerlo, S., & Haegeman, G. (2006). Keeping up NF-[kappa]B appearances: Epigenetic control of immunity or inflammation-triggered epigenetics. *Biochemical Pharmacology, 72*(9), 1114-1131.

Vangroenweghe, F. (2004). *Experimentally induced Escherichia coli in lactating primiparous cows.* University of Ghent, Ghent, Belgium.

Vangroenweghe, F., Rainard, P., Paape, M., Duchateau, L., & Burvenich, C. (2004). Increase of *Escherichia coli* inoculum doses induces faster innate immune response in primiparous cows. *Journal of dairy science, 87*(12), 4132-4144.

Vanselow, J., Yang, W., Herrmann, J., Zerbe, H., Schuberth, H. J., Petzl, W., Tomek, W., & Seyfert, H. M. (2006). DNA-remethylation around a STAT5-binding enhancer in the alphaS1-casein promoter is associated with abrupt shutdown of alphaS1-casein synthesis during acute mastitis. *Journal of Molecular Endocrinology, 37*(3), 463-477.

Varma, A., Morbidelli, M., & Wu, H. (1999). *Parametric sensitivity in chemical systems*. New York, New York, USA: Cambridge University Press.

Venza, I., Cucinotta, M., Caristi, S., Mancuso, G., & Teti, D. (2007). Transcriptional regulation of IL-8 by *Staphylococcus aureus* in human conjunctival cells involves activation of AP-1. *Investigative Ophthalmology & Visual Science, 48*(1), 270-276.

Vera, J., Bachmann, J., Pfeifer, A. C., Becker, V., Hormiga, J. A., Torres Darias, N. V., Timmer, J., Klingmuller, U., & Wolkenhauer, O. (2008). A systems biology approach to analyse amplification in the JAK2-STAT5 signalling pathway. *BMC Systems Biology, 2*(1), 38.

Viatour, P., Merville, M. P., Bours, V., & Chariot, A. (2005). Phosphorylation of NFkappaB and IkappaB proteins: implications in cancer and inflammation. *Trends in Biochemical Sciences, 30*(1), 43-52.

Vilar, J. M., Kueh, H. Y., Barkai, N., & Leibler, S. (2002). Mechanisms of noise-resistance in genetic oscillators. *Proceedings of the National Academy of Sciences, 99*(9), 5988-5992.

Vora, P., Youdim, A., Thomas, L. S., Fukata, M., Tesfay, S. Y., Lukasek, K., Michelsen, K. S., Wada, A., Hirayama, T., Arditi, M., & Abreu, M. T. (2004). Beta-defensin-2 expression is regulated by TLR signaling in intestinal epithelial cells. *The Journal of Immunology, 173*(9), 5398-5405.

Wang, L. Y., Chen, C. T., Liu, W. H., & Wang, Y. H. (2007). Recurrent neonatal group B streptococcal disease associated with infected breast milk. *Clin Pediatr (Phila), 46*(6), 547-549.

Wang, X., Wu, M., Li, Z., & Chan, C. (2008). Short time-series microarray analysis: methods and challenges. *BMC Systems Biology, 2*(1), 58.

Wellenberg, G. J., van der Poel, W. H. M., & Van Oirschot, J. T. (2002). Viral infections and bovine mastitis: a review. *Vet Microbiol, 88*(1), 27-45.

Wellnitz, O., & Kerr, D. E. (2004). Cryopreserved bovine mammary cells to model epithelial response to infection. *Veterinary immunology and immunopathology, 101*(3-4), 191-202.

Werner-Misof, C. P., M.W., Bruckmaier, R.M. (2007). Dose-dependent immune response in milk cells and mammary tissue after intramammary administration of lipopolysaccharide in dairy cows. *Veterinarni Medicina - UZPI (Czech Republic), 52*(6), 231-244.

Werner, E. (2005). The future and limits of Systems Biology. *Science's STKE:signal transduction knowledge environment, 2005*(278), pe16.

Werner, S. L., Barken, D., & Hoffmann, A. (2005). Stimulus specificity of gene expression programs determined by temporal control of IKK activity. *Science (New York, N.Y, 309*(5742), 1857-1861.

Wingreen, N., & Botstein, D. (2006). Back to the future: education for systems-level biologists. *Nature Reviews Molecular Cell Biology, 7*(11), 829-832.

Wolkenhauer, O. (2001). Systems Biology: The reincarnation of systems theory applied in biology? *Briefings in Bioinformatics, 2*(3), 258-270.

Wolkenhauer, O., & Mesarovic, M. (2005). Feedback dynamics and cell function: why systems biology is called Systems Biology. *Molecular bioSystems, 1*(1), 14-16.

Wolkenhauer, O., Ullah, M., Wellstead, P., & Cho, K. H. (2005). The dynamic systems approach to control and regulation of intracellular networks. *FEBS Lett, 579*(8), 1846-1853.

Wolkenhauer, O., Ullah, M., Boogerd, F. C., Bruggeman, F. J., Hofmeyr, J. S., & Westerhoff, H. V. (2007). All models are wrong ... some more than others. In *Systems biology* (pp. 163-179). Amsterdam: Elsevier, Amsterdam, the Netherlands.

Wolkenhauer, O., Fell, D., De Meyts, P., Bluthgen, N., Herzel, H., Le Novere, N., Hofer, T., Schurrle, K., & van Leeuwen, I. (2009). SysBioMed report: advancing Systems Biology for medical applications. *IET Syst Biol, 3*(3), 131.

Xie, Z., Kulasiri, D., Samarasinghe, S., & Qian, J. (2009). An unbiased sensitivity analysis reveals important parameters controlling periodicity of circadian clock. *Biotechnology and Bioenginering, 105*(2), 250-259.

Yang, W., Molenaar, A., Kurts-Ebert, B., & Seyfert, H. M. (2006). NF-kappaB factors are essential, but not the switch, for pathogen-related induction of the bovine beta-defensin 5-encoding gene in mammary epithelial cells. *Molecular immunology, 43*(3), 210-225.

Yang, W., Zerbe, H., Petzl, W., Brunner, R. M., Gunther, J., Draing, C., von Aulock, S., Schuberth, H. J., & Seyfert, H. M. (2008). Bovine TLR2 and TLR4 properly transduce signals from *Staphylococcus aureus* and *E. coli*, but *S. aureus* fails to both activate NF-kappaB in mammary epithelial cells and to quickly induce TNFalpha and interleukin-8 (CXCL8) expression in the udder. *Molecular immunology, 45*(5), 1385-1397.

Yang, Y. H., Buckley, M. J., & Speed, T. P. (2001). Analysis of cDNA microarray images. *Briefings in Bioinformatics, 2*(4), 341-349.

Yang, Y. H., Dudoit, S., Luu, P., Lin, D. M., Peng, V., Ngai, J., & Speed, T. P. (2002). Normalization for cDNA microarray data: a robust composite method addressing single and multiple slide systematic variation. *Nucleic acids research, 30*(4), e15.

Yue, H., Brown, M., He, F., Jia, J., & Kell, D. B. (2008). Sensitivity analysis and robust experimental design of a signal transduction pathway system. *International Journal of Chemical Kinetics, 40*(11), 730-741.

Zhu, Y., Fossum, C., Berg, M., & Magnusson, U. (2007). Morphometric analysis of proinflammatory cytokines in mammary glands of sows suggests an association between clinical mastitis and local production of IL-1beta, IL-6 and TNF-alpha. *Veterinary research, 38*(6), 871-882.

# Appendix A

## A.1 NFκB signalling model

### A.1.1 Reactions

Table A- 1 ODE reactions: ikkm is the input functions representing the bacterial challenge that degrades the IκBs as described in (Werner *et al.*, 2005). The nomenclature of reaction rates use the same format of those proposed in (Werner *et al.*, 2005). They are of the form X_Y_Z, with X the action; pd is protein degradation, a association, d degradation, Y the location of the reaction; c cytoplasm, n nucleus, and Z the components involved; i for IKK, n for NFκB and a,e,b the three IκB isoforms.

| ODE | | | | | | |
|---|---|---|---|---|---|---|
| $\frac{d[I\kappa B\alpha]}{dt} =$ | + | ps_c_a | * | IκBαt | | |
| | - | a_c_an | * | IκBα | * | NFκB |
| | + | d_c_an | * | IκBαNFκB | | |
| | - | a_c_ai | * | IκBα | * | IKK |
| | + | d_c_ai | * | IκBαIKK | | |
| | - | in_a | * | IκBα | | |
| | + | ex_a | * | IκBαn | | |
| | - | pd_c_a | * | IκBα | | |
| $\frac{d[I\kappa B\alpha IKK]}{dt} =$ | + | a_c_ai | * | IκBα | * | IKK |
| | - | d_c_ai | * | IκBαIKK | | |
| | - | a_c_2ain | * | IκBαIKK | * | NFκB |
| | + | d_c_2ain | * | IκBαIKKNFκB | | |
| | - | pd_c_2ai | * | IκBαIKK | * | ikkm |
| $\frac{d[I\kappa B\alpha IKKNF\kappa B]}{dt} =$ | + | a_c_2ani | * | IκBαNFκB | * | IKK |
| | - | d_c_2ani | * | IκBαIKKNFκB | | |
| | + | a_c_2ain | * | IκBαIKK | * | NFκB |
| | - | d_c_2ain | * | IκBαIKKNFκB | | |
| | - | pd_c_3ain | * | IκBαIKKNFκB | * | ikkm |
| $\frac{d[I\kappa B\alpha n]}{dt} =$ | - | a_n_an | * | IκBαn | * | NFκBn |
| | + | d_n_an | * | IκBαNFκBn | | |
| | + | in_a | * | IκBα | | |
| | - | ex_a | * | IκBαn | | |

| | | | | | | |
|---|---|---|---|---|---|---|
| | - | pd_n_a | * | IκBαn | | |
| $\frac{d[I\kappa B\alpha NF\kappa B]}{dt} =$ | + | a_c_an | * | IκBα | * | NFκB |
| | - | d_c_an | * | IκBαNFκB | | |
| | - | a_c_2ani | * | IκBαNFκB | * | IKK |
| | + | d_c_2ani | * | IκBαIKKNFκB | | |
| | - | in_2an | * | IκBαNFκB | | |
| | + | ex_2an | * | IκBαNFκBn | | |
| | - | pd_c_2an | * | IκBαNFκB | | |
| $\frac{d[I\kappa B\alpha NF\kappa Bn]}{dt} =$ | + | a_n_an | * | IκBαn | * | NFκBn |
| | - | d_n_an | * | IκBαNFκBn | | |
| | + | in_2an | * | IκBαNFκB | | |
| | - | ex_2an | * | IκBαNFκBn | | |
| | - | pd_n_2an | * | IκBαNFκBn | | |
| $\frac{d[I\kappa B\alpha t]}{dt} =$ | + | rsu_a | | | | |
| | + | rsr_an | * | (NFκBn_delay_a^h_an_a) | | |
| | - | rd_a | * | IκBαt | | |
| | - | ps_c_a | * | IκBαt | | |
| | + | ps_c_a | * | IκBαt | | |
| $\frac{d[I\kappa B\beta]}{dt} =$ | + | ps_c_b | * | IκBβt | | |
| | - | a_c_bn | * | IκBβ | * | NFκB |
| | + | d_c_bn | * | IκBβNFκB | | |
| | - | a_c_bi | * | IκBβ | * | IKK |
| | + | d_c_bi | * | IκBβIKK | | |
| | - | in_b | * | IκBβ | | |
| | + | ex_b | * | IκBβn | | |
| | - | pd_c_b | * | IκBβ | | |
| $\frac{d[I\kappa B\beta IKK]}{dt} =$ | + | a_c_bi | * | IκBβ | * | IKK |
| | - | d_c_bi | * | IκBβIKK | | |
| | - | a_c_2bin | * | IκBβIKK | * | NFκB |
| | + | d_c_2bin | * | IκBβIKKNFκB | | |
| | - | pd_c_2bi | * | IκBβIKK | * | ikkm |
| $\frac{d[I\kappa B\beta IKKNF\kappa B]}{dt} =$ | + | a_c_2bni | * | IκBβNFκB | * | IKK |
| | - | d_c_2bni | * | IκBβIKKNFκB | | |
| | + | a_c_2bin | * | IκBβIKK | | NFκB |

| | | | | | | |
|---|---|---|---|---|---|---|
| | - | d_c_2bin | * | IκBβIKKNFκB | | |
| | - | pd_c_3bin | * | IκBβIKKNFκB | * | ikkm |
| $\frac{d[I\kappa B\beta n]}{dt} =$ | - | a_n_bn | * | IκBβn | * | NFκBn |
| | + | d_n_bn | * | IκBβNFκBn | | |
| | + | in_b | * | IκBβ | | |
| | - | ex_b | * | IκBβn | | |
| | - | pd_n_b | * | IκBβn | | |
| $\frac{d[I\kappa B\beta NF\kappa B]}{dt} =$ | + | a_c_bn | * | IκBβ | * | NFκB |
| | - | d_c_bn | * | IκBβNFκB | | |
| | - | a_c_2bni | * | IκBβNFκB | * | IKK |
| | + | d_c_2bni | * | IκBβIKKNFκB | | |
| | - | in_2bn | * | IκBβNFκB | | |
| | + | ex_2bn | * | IκBβNFκBn | | |
| | - | pd_c_2bn | * | IκBβNFκB | | |
| $\frac{d[I\kappa B\beta NF\kappa Bn]}{dt} =$ | + | a_n_bn | * | IκBβn | * | NFκBn |
| | - | d_n_bn | * | IκBβNFκBn | | |
| | + | in_2bn | * | IκBβNFκB | | |
| | - | ex_2bn | * | IκBβNFκBn | | |
| | - | pd_n_2bn | * | IκBβNFκBn | | |
| $\frac{d[I\kappa B\beta t]}{dt} =$ | + | rsu_b | | | | |
| | + | rsr_bn | * | (NFκBn_delay_b^h_an_b) | | |
| | - | rd_b | * | IκBβt | | |
| | - | ps_c_b | * | IκBβt | | |
| | + | ps_c_b | * | IκBβt | | |
| $\frac{d[I\kappa B\varepsilon]}{dt} =$ | + | ps_c_e | * | IκBεt | | |
| | - | a_c_en | * | IκBε | * | NFκB |
| | + | d_c_en | * | IκBεNFκB | | |
| | - | a_c_ei | * | IκBε | * | IKK |
| | + | d_c_ei | * | IκBεIKK | | |
| | - | in_e | * | IκBε | | |
| | + | ex_e | * | IκBεn | | |
| | - | pd_c_e | * | IκBε | | |
| $\frac{d[I\kappa B\varepsilon IKK]}{dt} =$ | + | a_c_ei | * | IκBε | * | IKK |
| | - | d_c_ei | * | IκBεIKK | | |

| | | | | | | |
|---|---|---|---|---|---|---|
| | - | a_c_2ein | * | IκBεIKK | * | NFκB |
| | + | d_c_2ein | * | IκBεIKKNFκB | | |
| | - | pd_c_2ei | * | IκBεIKK | * | ikkm |
| $\frac{d[I\kappa B\varepsilon IKKNF\kappa B]}{dt} =$ | + | a_c_2eni | * | IκBεNFκB | * | IKK |
| | - | d_c_2eni | * | IκBεIKKNFκB | | |
| | + | a_c_2ein | * | IκBεIKK | * | NFκB |
| | - | d_c_2ein | * | IκBεIKKNFκB | | |
| | - | pd_c_3ein | * | IκBεIKKNFκB | * | ikkm |
| $\frac{d[I\kappa B\varepsilon n]}{dt} =$ | - | a_n_en | * | IκBεn | * | NFκBn |
| | + | d_n_en | * | IκBεNFκBn | | |
| | + | in_e | * | IκBε | | |
| | - | ex_e | * | IκBεn | | |
| | - | pd_n_e | * | IκBεn | | |
| $\frac{d[I\kappa B\varepsilon NF\kappa B]}{dt} =$ | + | a_c_en | * | IκBε | * | NFκB |
| | - | d_c_en | * | IκBεNFκB | | |
| | - | a_c_2eni | * | IκBεNFκB | * | IKK |
| | + | d_c_2eni | * | IκBεIKKNFκB | | |
| | - | in_2en | * | IκBεNFκB | | |
| | + | ex_2en | * | IκBεNFκBn | | |
| | - | pd_c_2en | * | IκBεNFκB | | |
| $\frac{d[I\kappa B\varepsilon NF\kappa Bn]}{dt} =$ | + | a_n_en | * | IκBεn | * | NFκBn |
| | - | d_n_en | * | IκBεNFκBn | | |
| | + | in_2en | * | IκBεNFκB | | |
| | - | ex_2en | * | IκBεNFκBn | | |
| | - | pd_n_2en | * | IκBεNFκBn | | |
| $\frac{d[I\kappa B\varepsilon t]}{dt} =$ | + | rsu_e | | | | |
| | + | rsr_en | * | (NFκBn_delay_e^h_an_e) | | |
| | - | rd_e | * | IκBεt | | |
| | - | ps_c_e | * | IκBεt | | |
| | + | ps_c_e | * | IκBεt | | |
| $\frac{d[IKK]}{dt} =$ | - | a_c_ai | * | IκBα | * | IKK |
| | - | a_c_bi | * | IκBβ | * | IKK |
| | - | a_c_ei | * | IκBε | * | IKK |
| | + | d_c_ai | * | IκBαIKK | | |

| | | | | | | |
|---|---|---|---|---|---|---|
| | + | d_c_bi | * | IκBβIKK | | |
| | + | d_c_ei | * | IκBεIKK | | |
| | - | a_c_2ani | * | IκBαNFκB | * | IKK |
| | - | a_c_2bni | * | IκBβNFκB | * | IKK |
| | - | a_c_2eni | * | IκBεNFκB | * | IKK |
| | + | d_c_2ani | * | IκBαIKKNFκB | | |
| | + | d_c_2bni | * | IκBβIKKNFκB | | |
| | + | d_c_2eni | * | IκBεIKKNFκB | | |
| | + | pd_c_2ai | * | IκBαIKK | * | ikkm |
| | + | pd_c_2bi | * | IκBβIKK | * | ikkm |
| | + | pd_c_2ei | * | IκBεIKK | * | ikkm |
| | + | pd_c_3ain | * | IκBαIKKNFκB | * | ikkm |
| | + | pd_c_3bin | * | IκBβIKKNFκB | * | ikkm |
| | + | pd_c_3ein | * | IκBεIKKNFκB | * | ikkm |
| $\frac{d[NF\kappa B]}{dt} =$ | - | a_c_an | * | IκBα | * | NFκB |
| | - | a_c_bn | * | IκBβ | * | NFκB |
| | - | a_c_en | * | IκBε | * | NFκB |
| | + | d_c_an | * | IκBαNFκB | | |
| | + | d_c_bn | * | IκBβNFκB | | |
| | + | d_c_en | * | IκBεNFκB | | |
| | - | a_c_2ain | * | IκBαIKK | * | NFκB |
| | - | a_c_2bin | * | IκBβIKK | * | NFκB |
| | - | a_c_2ein | * | IκBεIKK | * | NFκB |
| | + | d_c_2ain | * | IκBαIKKNFκB | | |
| | + | d_c_2bin | * | IκBβIKKNFκB | | |
| | + | d_c_2ein | * | IκBεIKKNFκB | | |
| | - | in_n | * | NFκB | | |
| | + | ex_n | * | NFκBn | | |
| | + | pd_c_2an | * | IκBαNFκB | | |
| | + | pd_c_2bn | * | IκBβNFκB | | |
| | + | pd_c_2en | * | IκBεNFκB | | |
| | + | pd_c_3ain | * | IκBαIKKNFκB | * | ikkm |
| | + | pd_c_3bin | * | IκBβIKKNFκB | * | ikkm |
| | + | pd_c_3ein | * | IκBεIKKNFκB | * | ikkm |
| $\frac{d[NF\kappa Bn]}{dt} =$ | - | a_n_an | * | IκBαn | * | NFκBn |
| | - | a_n_bn | * | IκBβn | * | NFκBn |
| | - | a_n_en | * | IκBεn | * | NFκBn |
| | + | d_n_an | * | IκBαNFκBn | | |

| | | | | | | |
|---|---|---|---|---|---|---|
| | + | d_n_bn | * | IκBβNFκBn | | |
| | + | d_n_en | * | IκBεNFκBn | | |
| | + | in_n | * | NFκB | | |
| | - | ex_n | * | NFκBn | | |
| | + | pd_n_2an | * | IκBαNFκBn | | |
| | + | pd_n_2bn | * | IκBβNFκBn | | |
| | + | pd_n_2en | * | IκBεNFκBn | | |
| $\frac{d[RANTESt]}{dt} =$ | - | d_n_r | * | RANTESt | | |
| | + | rsr_rn | * | (NFκBn^h_an_r) | | |
| $\frac{d[IL8t]}{dt} =$ | - | d_n_8 | * | IL-8t | | |
| | + | rsr_8n | * | (NFκBn^h_an_8) | | |
| $\frac{d[TNF\alpha t]}{dt} =$ | - | d_n_TNFα | * | TNFαt | | |
| | + | rsr_TNFαn | * | (NFκBn^h_an_TNFα) | | |

### A.1.2 Parameter values

Table A- 2 Parameter values of the equations in Table 2-1

| | Parameter | Reaction | Category | Location | Value | Units | source |
|---|---|---|---|---|---|---|---|
| 1 | a_c_2ain | IKKIκBα+NFκB=>IKKIκBαNFκB | Association | Cytoplasm | 30 | $\mu M^{-1}min^{-1}$ | (Werner *et al.*, 2005) |
| 2 | a_c_2ani | IκBαNFκB+IKK=>IKKIκBαNFκB | Association | Cytoplasm | 11.1 | $\mu M^{-1}min^{-1}$ | (Werner *et al.*, 2005) |
| 3 | a_c_2bin | IKKIκBβ+NFκB=>IKKIκBβNFκB | Association | Cytoplasm | 30 | $\mu M^{-1}min^{-1}$ | (Werner *et al.*, 2005) |
| 4 | a_c_2bni | IκBβNFκB+IKK=>IKKIκBβNFκB | Association | Cytoplasm | 2.88 | $\mu M^{-1}min^{-1}$ | (Werner *et al.*, 2005) |
| 5 | a_c_2ein | IKKIκBε+NFκB=>IKKIκBεNFκB | Association | Cytoplasm | 30 | $\mu M^{-1}min^{-1}$ | (Werner *et al.*, 2005) |
| 6 | a_c_2eni | IκBεNFκB+IKK=>IKKIκBεNFκB | Association | Cytoplasm | 4.2 | $\mu M^{-1}min^{-1}$ | (Werner *et al.*, 2005) |
| 7 | a_c_ai | IκBα+IKK=>IKKIκBα | Association | Cytoplasm | 1.35 | $\mu M^{-1}min^{-1}$ | (Werner *et al.*, 2005) |
| 8 | a_c_an | IκBα+NFκB=>IκBαNFκB | Association | Cytoplasm | 30 | $\mu M^{-1}min^{-1}$ | (Hoffmann *et al.*, 2002a) |
| 9 | a_c_bi | IκBβ+IKK=>IKKIκBβ | Association | Cytoplasm | 0.36 | $\mu M^{-1}min^{-1}$ | (Werner *et al.*, 2005) |
| 10 | a_c_bn | IκBβ+NFκB=>IκBβNFκB | Association | Cytoplasm | 30 | $\mu M^{-1}min^{-1}$ | (Hoffmann *et al.*, 2002a) |
| 11 | a_c_ei | IκBε+IKK=>IKKIκBε | Association | Cytoplasm | 0.54 | $\mu M^{-1}min^{-1}$ | (Werner *et al.*, 2005) |
| 12 | a_c_en | IκBε+NFκB=>IκBεNFκB | Association | Cytoplasm | 30 | $\mu M^{-1}min^{-1}$ | (Hoffmann *et al.*, 2002a) |
| 13 | a_n_an | IκBαn+NFκBn=>IκBαNFκBn | Association | Nucleus | 30 | $\mu M^{-1}min^{-1}$ | (Hoffmann *et al.*, 2002a) |

| | | | | | | | |
|---|---|---|---|---|---|---|---|
| 14 | a_n_bn | IκBβn+NFκBn=>IκBβNFκBn | Association | Nucleus | 30 | $\mu M^{-1}min^{-1}$ | (Hoffmann *et al.*, 2002a) |
| 15 | a_n_en | IκBεn+NFκBn=>IκBεNFκBn | Association | Nucleus | 30 | $\mu M^{-1}min^{-1}$ | (Hoffmann *et al.*, 2002a) |
| 16 | d_c_2ain | IKKIκBαNFκB=>IKKIκBα+NFκB | Dissociation | Cytoplasm | 0.00006 | $min^{-1}$ | (Werner *et al.*, 2005) |
| 17 | d_c_2ani | IKKIκBαNFκB=>Ikk+IκBαNFκB | Dissociation | Cytoplasm | 0.075 | $min^{-1}$ | (Werner *et al.*, 2005) |
| 18 | d_c_2bin | IKKIκBβNFκB=>IKKIκBβ+NFκB | Dissociation | Cytoplasm | 0.00006 | $min^{-1}$ | (Werner *et al.*, 2005) |
| 19 | d_c_2bni | IKKIκBβNFκB=>IKK+IκBβNFκB | Dissociation | Cytoplasm | 0.105 | $min^{-1}$ | (Werner *et al.*, 2005) |
| 20 | d_c_2ein | IKKIκBεNFκB=>IKKIκBε+NFκB | Dissociation | Cytoplasm | 0.00006 | $min^{-1}$ | (Werner *et al.*, 2005) |
| 21 | d_c_2eni | IKKIκBεNFκB=>IKK+IκBεNFκB | Dissociation | Cytoplasm | 0.105 | $min^{-1}$ | (Werner *et al.*, 2005) |
| 22 | d_c_ai | IKKIκBα=>IKK+IκBα | Dissociation | Cytoplasm | 0.075 | $min^{-1}$ | (Werner *et al.*, 2005) |
| 23 | d_c_an | IκBαNFκB=>IκBα+NFκB | Dissociation | Cytoplasm | 0.00006 | $min^{-1}$ | (Hoffmann *et al.*, 2002a) |
| 24 | d_c_bi | IKKIκBβ=>IKK+IκBβ | Dissociation | Cytoplasm | 0.105 | $min^{-1}$ | (Werner *et al.*, 2005) |
| 25 | d_c_bn | IκBβNFκB=>IκBβ+NFκB | Dissociation | Cytoplasm | 0.00006 | $min^{-1}$ | (Hoffmann *et al.*, 2002a) |
| 26 | d_c_ei | IKKIκBε=>IKK+IκBε | Dissociation | Cytoplasm | 0.105 | $min^{-1}$ | (Werner *et al.*, 2005) |
| 27 | d_c_en | IκBεNFκB=>IκBε+NFκB | Dissociation | Cytoplasm | 0.00006 | $min^{-1}$ | (Hoffmann *et al.*, 2002a) |
| 28 | d_n_an | IκBαNFκBn=>IκBαn+NFκBn | Dissociation | Nucleus | 0.00006 | $min^{-1}$ | (Hoffmann *et al.*, 2002a) |

| | | | | | | | |
|---|---|---|---|---|---|---|---|
| 29 | d_n_bn | IκBβNFκBn=>IκBβn+NFκBn | Dissociation | Nucleus | 0.00006 | $min^{-1}$ | (Hoffmann *et al.*, 2002a) |
| 30 | d_n_en | IκBεNFκBn=>IκBεn+NFκBn | Dissociation | Nucleus | 0.00006 | $min^{-1}$ | (Hoffmann *et al.*, 2002a) |
| 31 | ex_2an | IκBαNFκBn=>IκBαNFκB | Export Nuc-> | Cyt | 0.828 | $min^{-1}$ | (Werner *et al.*,2005) |
| 32 | ex_2bn | IκBβNFκBn=>IκBβNFκB | Export Nuc-> | Cyt | 0.424 | $min^{-1}$ | (Werner *et al.*,2005) |
| 33 | ex_2en | IκBεNFκBn=>IκBεNFκB | Export Nuc-> | Cyt | 0.424 | $min^{-1}$ | (Werner *et al.*,2005) |
| 34 | ex_a | IκBαn=>IκBα | Export Nuc-> | Cyt | 0.012 | $min^{-1}$ | (Werner *et al.*,2005) |
| 35 | ex_b | IκBβn=>IκBβ | Export Nuc-> | Cyt | 0.012 | $min^{-1}$ | (Werner *et al.*,2005) |
| 36 | ex_e | IκBεn=>IκBε | Export Nuc-> | Cyt | 0.012 | $min^{-1}$ | (Werner *et al.*,2005) |
| 37 | ex_n | NFκBn=>NFκB | Export Nuc-> | Cyt | 0.0048 | $min^{-1}$ | (Werner *et al.*,2005) |
| 38 | in_a | IκBα=>IκBαn | Import Cyt-> | Nuc | 0.018 | $min^{-1}$ | (Werner *et al.*,2005) |
| 39 | in_b | IκBβ=>IκBβn | Import Cyt-> | Nuc | 0.018 | $min^{-1}$ | (Werner *et al.*,2005) |
| 40 | in_e | IκBε=>IκBεn | Import Cyt-> | Nuc | 0.018 | $min^{-1}$ | (Werner *et al.*,2005) |
| 41 | in_n | NFκB=>NFκBn | Import Cyt-> | Nuc | 5.4 | $min^{-1}$ | (Werner *et al.*,2005) |
| 42 | pd_c_2ai | IKKIκBα=>IKK | Prot.deg | Cytoplasm | 0.0018 | $min^{-1}$ | (Werner *et al.*,2005) |
| 43 | pd_c_2an | IκBαNFκB=>NFκB | Prot.deg | Cytoplasm | 0.00006 | $min^{-1}$ | (O'Dea *et al.*, 2007) |

| | | | | | | |
|---|---|---|---|---|---|---|
| 44 | pd_c_2bi | IKKIκBβ=>IKK | Prot.deg | Cytoplasm | 0.0006 $min^{-1}$ | (Werner *et al.*,2005) |
| 45 | pd_c_2bn | IκBβNFκB=>NFκB | Prot.deg | Cytoplasm | 0.00006 $min^{-1}$ | (O'Dea *et al.*, 2007) |
| 46 | pd_c_2ei | IKKIκBε=>IKK | Prot.deg | Cytoplasm | 0.0012 $min^{-1}$ | (Werner *et al.*,2005) |
| 47 | pd_c_2en | IκBεNFκB=>NFκB | Prot.deg | Cytoplasm | 0.00006 $min^{-1}$ | (O'Dea *et al.*, 2007) |
| 48 | pd_c_3ain | IKKIκBαNFκB=>IKK+NFκB | Prot.deg | Cytoplasm | 0.36 $min^{-1}$ | (Hoffmann *et al.*, 2002a) |
| 49 | pd_c_3bin | IKKIκBβNFκB=>IKK+NFκB | Prot.deg | Cytoplasm | 0.12 $min^{-1}$ | (Hoffmann *et al.*, 2002a) |
| 50 | pd_c_3ein | IKKIκBεNFκB=>IKK+NFκB | Prot.deg | Cytoplasm | 0.18 $min^{-1}$ | (Hoffmann *et al.*, 2002a) |
| 51 | pd_c_a | IκBα=> | Prot. deg. | Cytoplasm | 0.12 $min^{-1}$ | (O'Dea *et al.*, 2007) |
| 52 | pd_c_b | IκBβ=> | Prot. deg. | Cytoplasm | 0.18 $min^{-1}$ | (O'Dea *et al.*, 2007) |
| 53 | pd_c_e | IκBε=> | Prot. deg. | Cytoplasm | 0.18 $min^{-1}$ | (O'Dea *et al.*, 2007) |
| 54 | pd_n_2an | IκBαNFκBn=>NFκBn | Prot.deg | Nucleus | 0.0000 $min^{-1}$ | (O'Dea *et al.*, 2007) |
| 55 | pd_n_2bn | IκBβNFκBn=>NFκBn | Prot.deg | Nucleus | 0.00006 $min^{-1}$ | (O'Dea *et al.*, 2007) |
| 56 | pd_n_2en | IκBεNFκBn=>NFκBn | Prot.deg | Nucleus | 0.00006 $min^{-1}$ | (O'Dea *et al.*, 2007) |
| 57 | pd_n_a | IκBαn=> | Prot.deg | Nucleus | 0.12 $min^{-1}$ | (O'Dea *et al.*, 2007) |
| 58 | pd_n_b | IκBβn=> | Prot.deg | Nucleus | 0.18 $min^{-1}$ | (O'Dea *et al.*, 2007) |

| | | | | | | |
|---|---|---|---|---|---|---|
| 59 | pd_n_e | IκBεn=> | Prot.deg | Nucleus | 0.18 $min^{-1}$ | (O'Dea *et al.*, 2007) |
| 60 | ps_c_a | =>IκBα | Prot.synth. | Cytoplasm | 0.2448 $min^{-1}$ | (Hoffmann *et al.*, 2002a) |
| 61 | ps_c_b | =>IκBβ | Prot.synth. | Cytoplasm | 0.2448 $min^{-1}$ | (Hoffmann *et al.*, 2002a) |
| 62 | ps_c_e | =>IκBε | Prot.synth. | Cytoplasm | 0.2448 $min^{-1}$ | (Hoffmann *et al.*, 2002a) |
| 63 | rd_a | IκBαt=> | RNA deg. | Cytoplasm | 0.0168 $min^{-1}$ | (Werner *et al.*, 2005) (Kearns *et al.*, 2005) |
| 64 | rd_b | IκBβt=> | RNA deg. | Cytoplasm | 0.0168 $min^{-1}$ | (Werner *et al.*, 2005) (Kearns *et al.*, 2005) |
| 65 | rd_e | IκBεt=> | RNA deg. | Cytoplasm | 0.0168 $min^{-1}$ | (Werner *et al.*, 2005) (Kearns *et al.*, 2005) |
| 66 | rs_a | =>IκBαt (constitutive) | RNA synth. | Nuc->Cyt | 0.000185 $\mu M^{-1}min^{-1}$ | fit |
| 67 | rs_an | =>IκBαt (inducedbyNF-κB) | RNA synth. | Nuc->Cyt | 7.92 $\mu M^{-2}min^{-1}$ | (Werner *et al.*, 2005) (Kearns *et al.*, 2005) |
| 68 | rs_b | =>IκBβt(constitutive) | RNA synth. | Nuc->Cyt | 4.27E-05 $\mu M^{-1}min^{-1}$ | (Werner *et al.*, 2005) |
| 69 | rs_e | =>IκBεt(constitutive) | RNA synth. | Nuc->Cyt | 3.05E-05 $\mu M^{-1}min^{-1}$ | (Werner *et al.*, 2005) |
| 70 | rs_en | =>IκBεt(inducedbyNF-κB) | RNA synth. | Nuc->Cyt | 0.8 $\mu M^{-1}min^{-1}$ | (Werner *et al.*, 2005) |
| 71 | in_2an | IκBαNFκB=>IκBαNFκBn | Import | Cyt->Nuc | 0.276 $min^{-1}$ | (Werner *et al.*, 2008) |
| 72 | in_2bn | IκBβNFκB=>IκBβNFκBn | Import | Cyt->Nuc | 0.0276 $min^{-1}$ | (Werner *et al.*, 2008) |
| 73 | in_2en | IκBεNFκB=>IκBεNFκBn | Import | Cyt->Nuc | 0.138 $min^{-1}$ | (Werner *et al.*, 2008) |

| | | | | | | | | |
|---|---|---|---|---|---|---|---|---|
| 74 | h_an_a | Hill coefficient IκBα | | Association | Nucleus | 3 | | (Werner *et al.*, 2005) |
| 75 | h_an_b | Hill coefficient IκBβ | | Association | Nucleus | 3 | | (Werner *et al.*, 2005) |
| 76 | h_an_e | Hill coefficient IκBε | | Association | Nucleus | 3 | | (Werner *et al.*, 2005) |
| 77 | h_an_r | Hill coefficient RANTES | | Association | Nucleus | 3 | | |
| 78 | d_n_r | RANTESt=> | RNA deg. | | Nucleus | * | $min^{-1}$ | fitted |
| 79 | rsr_rn | =>RANTESt | (inducedbyNF-κB) | Association | Nucleus | * | $\mu M^{-2}min^{-1}$ | fitted |
| 80 | h_an_8 | Hill coefficient IL8 | | | Nucleus | 3 | | |
| 81 | d_n_8 | IL8t=> | | RNA deg. | Nucleus | * | $min^{-1}$ | fitted |
| 82 | rsr_8n | =>IL8t | (inducedbyNF-κB) | Association | Nucleus | * | $\mu M^{-2}min^{-1}$ | fitted |
| 83 | h_an_TNFα | Hill coefficient TNFαt | | | Nucleus | 3 | | |
| 84 | d_n_TNFα | TNFαt=> | | RNA deg. | Nucleus | * | $min^{-1}$ | fitted |
| 85 | rsr_TNFαn | =>TNFαt | (inducedbyNF-κB) | Association | Nucleus | * | $\mu M^{-2}min^{-1}$ | fitted |

### A.1.3 Initial values

Table A- 3 Initial values

| Component | initial value (μM) |
|---|---|
| IκBα | 0.013175886 |
| IκBαIKK | 0.006456278 |
| IκBαIKKNFκB | 0.054404075 |
| IκBαn | 0.007622051 |
| IκBαNFκB | 0.01402656 |
| IκBαNFκBn | 0.004892218 |
| IκBαt | 0.01100023 |
| IκBβ | 0.003285322 |
| IκBβIKK | 0.000308727 |
| IκBβIKKNFκB | 0.004993256 |
| IκBβn | 0.000137258 |
| IκBβNFκB | 0.006709498 |
| IκBβNFκBn | 0.000454998 |
| IκBβt | 0.002542857 |
| IκBε | 0.001988273 |
| IκBεIKK | 0.000281141 |
| IκBεIKKNFκB | 0.006115701 |
| IκBεn | 0.000415491 |
| IκBεNFκB | 0.005667757 |
| IκBεNFκBn | 0.001912401 |

| | |
|---|---|
| IκBεt | 0.001814309 |
| IKK | 0.027440822 |
| NFκB | 3.62916E-05 |
| NFκBn | 0.000787244 |
| RANTESt | 0.00000001 |
| IL8t | 0.00000001 |
| TNFαt | 0.00000001 |

### A.1.4 Input function ikkm

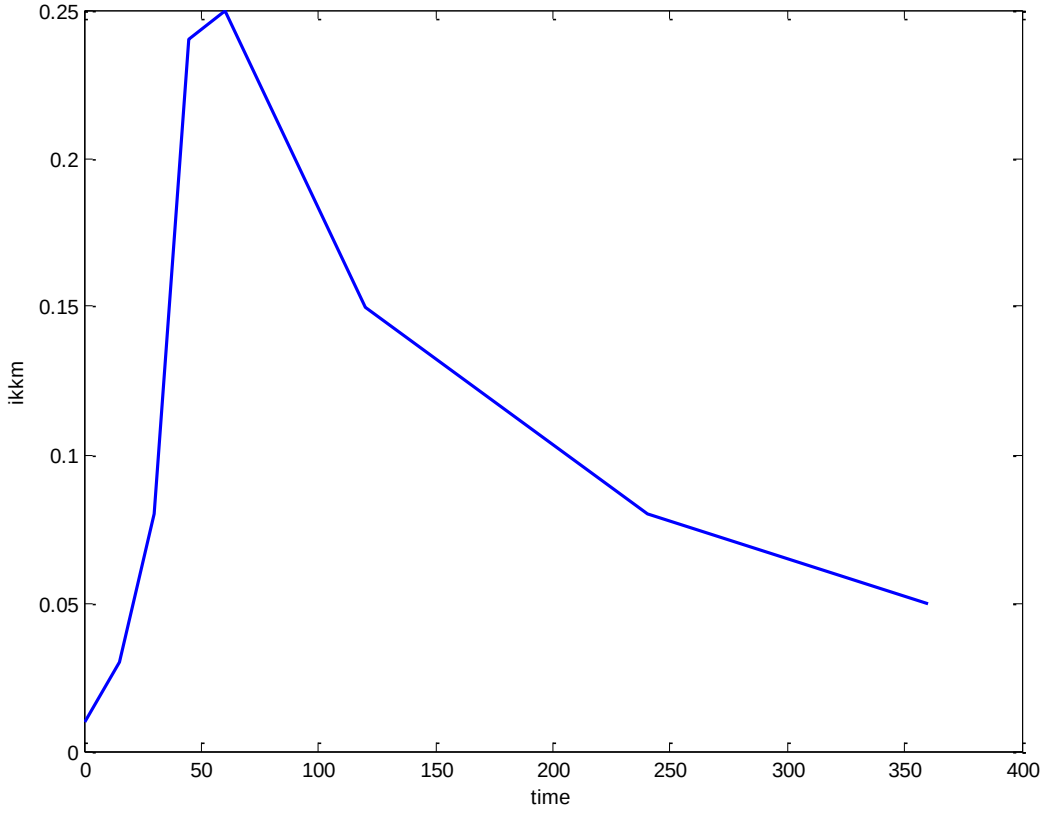


Figure A- 1The input function ikkm for the model simulating the *E. coli* challenge.

# Appendix B

## B.1 SBtoolbox model implementation

********** MODEL NAME

NFkB_werner_2_c_e_4_6

********** MODEL NOTES

********** MODEL STATES

d/dt(IκBa) = +flux_ps_c_a -flux_a_c_an +flux_d_c_an -flux_a_c_ai +flux_d_c_ai -flux_in_a +flux_ex_a -flux_pd_c_a

d/dt(IκBaIKK) = +flux_a_c_ai -flux_d_c_ai -flux_a_c_2ain +flux_d_c_2ain -flux_pd_c_2ai

d/dt(IκBaIKKNFkB) = +flux_a_c_2ani -flux_d_c_2ani +flux_a_c_2ain -flux_d_c_2ain -flux_pd_c_3ain

d/dt(IκBan) = -flux_a_n_an +flux_d_n_an +flux_in_a -flux_ex_a -flux_pd_n_a

d/dt(IκBaNFkB) = +flux_a_c_an -flux_d_c_an -flux_a_c_2ani +flux_d_c_2ani -flux_in_2an +flux_ex_2an -flux_pd_c_2an

d/dt(IκBaNFkBn) = +flux_a_n_an -flux_d_n_an +flux_in_2an -flux_ex_2an -flux_pd_n_2an

d/dt(IκBat) = +flux_rsu_a +flux_rsr_an -flux_rd_a

d/dt(IκBb) = +flux_ps_c_b -flux_a_c_bn +flux_d_c_bn -flux_a_c_bi +flux_d_c_bi -flux_in_b +flux_ex_b -flux_pd_c_b

d/dt(IκBbIKK) = +flux_a_c_bi -flux_d_c_bi -flux_a_c_2bin +flux_d_c_2bin -flux_pd_c_2bi

d/dt(IκBbIKKNFkB) = +flux_a_c_2bni -flux_d_c_2bni +flux_a_c_2bin -flux_d_c_2bin -flux_pd_c_3bin

d/dt(IκBbn) = -flux_a_n_bn +flux_d_n_bn +flux_in_b -flux_ex_b -flux_pd_n_b

d/dt(IκBbNFkB) = +flux_a_c_bn -flux_d_c_bn -flux_a_c_2bni +flux_d_c_2bni -flux_in_2bn +flux_ex_2bn -flux_pd_c_2bn

d/dt(IκBbNFkBn) = +flux_a_n_bn -flux_d_n_bn +flux_in_2bn -flux_ex_2bn -flux_pd_n_2bn

d/dt(IκBbt) = +flux_rsu_b +flux_rsr_bn -flux_rd_b

d/dt(IκBe) = +flux_ps_c_e -flux_a_c_en +flux_d_c_en -flux_a_c_ei +flux_d_c_ei -flux_in_e +flux_ex_e -flux_pd_c_e

d/dt(IκBeIKK) = +flux_a_c_ei -flux_d_c_ei -flux_a_c_2ein +flux_d_c_2ein -flux_pd_c_2ei

d/dt(IκBeIKKNFkB) = +flux_a_c_2eni -flux_d_c_2eni +flux_a_c_2ein -flux_d_c_2ein -flux_pd_c_3ein

d/dt(IκBen) = -flux_a_n_en +flux_d_n_en +flux_in_e -flux_ex_e -flux_pd_n_e

d/dt(IκBeNFkB) = +flux_a_c_en -flux_d_c_en -flux_a_c_2eni +flux_d_c_2eni -flux_in_2en +flux_ex_2en -flux_pd_c_2en

d/dt(IκBeNFkBn) = +flux_a_n_en -flux_d_n_en +flux_in_2en -flux_ex_2en -flux_pd_n_2en

d/dt(IκBet) = +flux_rsu_e +flux_rsr_en -flux_rd_e

d/dt(IKK) = -flux_a_c_ai -flux_a_c_bi -flux_a_c_ei +flux_d_c_ai +flux_d_c_bi +flux_d_c_ei -flux_a_c_2ani -flux_a_c_2bni -flux_a_c_2eni +flux_d_c_2ani +flux_d_c_2bni +flux_d_c_2eni +flux_pd_c_2ai +flux_pd_c_2bi +flux_pd_c_2ei +flux_pd_c_3ain +flux_pd_c_3bin +flux_pd_c_3ein

d/dt(NFkB) = -flux_a_c_an -flux_a_c_bn -flux_a_c_en +flux_d_c_an +flux_d_c_bn +flux_d_c_en -flux_a_c_2ain -flux_a_c_2bin -flux_a_c_2ein +flux_d_c_2ain +flux_d_c_2bin +flux_d_c_2ein -flux_in_n +flux_ex_n +flux_pd_c_2an +flux_pd_c_2bn +flux_pd_c_2en +flux_pd_c_3ain +flux_pd_c_3bin +flux_pd_c_3ein

d/dt(NFkBn) = -flux_a_n_an -flux_a_n_bn -flux_a_n_en +flux_d_n_an +flux_d_n_bn +flux_d_n_en +flux_in_n -flux_ex_n +flux_pd_n_2an +flux_pd_n_2bn +flux_pd_n_2en

d/dt(RANTESt) = +flux_rsu_r -flux_d_n_r +flux_rsr_rn

d/dt(IL8t) = +flux_rsu_8 -flux_d_n_8 +flux_rsr_8n

d/dt(TNFat) = +flux_rsu_TNFa -flux_d_n_TNFa +flux_rsr_TNFan

IκBa(0) =0.013175886

IκBaIKK(0) =0.006456278

IκBaIKKNFkB(0)=0.054404075

IκBan(0) =0.007622051

IκBaNFkB(0) =0.01402656

IκBaNFkBn(0)=0.004892218

IκBat(0) =0.01100023

IκBb(0) =0.003285322

IκBbIKK(0) =0.000308727

IκBbIKKNFkB(0)=0.004993256

IκBbn(0) =0.000137258

IκBbNFkB(0) =0.006709498

IκBbNFkBn(0)=0.000454998

IκBbt(0) =0.002542857

IκBe(0) =0.001988273

IκBeIKK(0) =0.000281141

IκBeIKKNFkB(0)=0.006115701

IκBen(0) =0.000415491

IκBeNFkB(0) =0.005667757

IκBeNFkBn(0)=0.001912401

IκBet(0) =0.001814309

IKK(0) =0.027440822

NFkB(0) =0.0000362916

NFkBn(0) =0.000787244

RANTESt(0) =0.00000001

IL8t(0) =0.00000001

TNFat(0) =0.00000001

********** MODEL PARAMETERS

| | | |
|---|---|---|
| d_n_r | = | 0.00039365 |
| rsr_rn | = | 5.28555 |
| rsu_r | = | 0 |
| delayd_nfkbn_r | = | 0 |
| d_n_8 | = | 0.00175918 |
| rsr_8n | = | 5.28555 |
| rsu_8 | = | 0 |
| delayd_nfkbn_8 | = | 0 |
| d_n_TNFa | = | 0.02060201 |
| rsr_TNFan | = | 1.67 |
| rsu_TNFa | = | 0 |
| delayd_nfkbn_TNFa | = | 0 |
| h_an_r | = | 3 |
| h_an_8 | = | 3 |

| | | |
|---|---|---|
| h_an_TNFa | = | 3 |
| ikkmyd88_in | = | 0 |
| ikkmyd88 | = | 0.01 |
| rsu_a | = | 0.0001848 |
| rsu_b | = | 0.00004272 |
| rsu_e | = | 0.00003048 |
| rsr_an | = | 7.92 |
| rsr_bn | = | 0 |
| rsr_en | = | 0.8 |
| delayd_nfkbn_a | = | 0 |
| delayd_nfkbn_b | = | 45 |
| delayd_nfkbn_e | = | 45 |
| h_an_a | = | 3 |
| h_an_b | = | 3 |
| h_an_e | = | 3 |
| rd_a | = | 0.0168 |
| rd_b | = | 0.0168 |
| rd_e | = | 0.0168 |
| ps_c_a | = | 0.2448 |
| ps_c_b | = | 0.2448 |
| ps_c_e | = | 0.2448 |
| a_c_an | = | 30 |
| a_c_bn | = | 30 |
| a_c_en | = | 30 |
| a_n_an | = | 30 |

| | | |
|---|---|---|
| a_n_bn | = | 30 |
| a_n_en | = | 30 |
| d_c_an | = | 0.00006 |
| d_c_bn | = | 0.00006 |
| d_c_en | = | 0.00006 |
| d_n_an | = | 0.00006 |
| d_n_bn | = | 0.00006 |
| d_n_en | = | 0.00006 |
| a_c_ai | = | 1.35 |
| a_c_bi | = | 0.36 |
| a_c_ei | = | 0.54 |
| d_c_ai | = | 0.075 |
| d_c_bi | = | 0.105 |
| d_c_ei | = | 0.105 |
| a_c_2ani | = | 11.1 |
| a_c_2bni | = | 2.88 |
| a_c_2eni | = | 4.2 |
| d_c_2ani | = | 0.075 |
| d_c_2bni | = | 0.105 |
| d_c_2eni | = | 0.105 |
| a_c_2ain | = | 30 |
| a_c_2bin | = | 30 |
| a_c_2ein | = | 30 |
| d_c_2ain | = | 0.00006 |
| d_c_2bin | = | 0.00006 |

| | | |
|---|---|---|
| d_c_2ein | = | 0.00006 |
| in_a | = | 0.09 |
| in_b | = | 0.009 |
| in_e | = | 0.045 |
| ex_a | = | 0.012 |
| ex_b | = | 0.012 |
| ex_e | = | 0.012 |
| in_2an | = | 0.276 |
| in_2bn | = | 0.0276 |
| in_2en | = | 0.138 |
| ex_2an | = | 0.828 |
| ex_2bn | = | 0.414 |
| ex_2en | = | 0.414 |
| in_n | = | 5.4 |
| ex_n | = | 0.0048 |
| pd_c_a | = | 0.12 |
| pd_c_b | = | 0.18 |
| pd_c_e | = | 0.18 |
| pd_n_a | = | 0.12 |
| pd_n_b | = | 0.18 |
| pd_n_e | = | 0.18 |
| pd_c_2an | = | 0.00006 |
| pd_c_2bn | = | 0.00006 |
| pd_c_2en | = | 0.00006 |
| pd_n_2an | = | 0.00006 |

pd_n_2bn = 0.00006

pd_n_2en = 0.00006

pd_c_2ai = 0.0018

pd_c_2bi = 0.0006

pd_c_2ei = 0.0012

pd_c_3ain = 0.36

pd_c_3bin = 0.12

pd_c_3ein = 0.18

********** MODEL VARIABLES

nfkbn_delay_e = delaySB(NFkBn,delayd_nfkbn_e)

nfkbn_delay_a = NFkBn

nfkbn_delay_b = nfkbn_delay_e

nfkbn_delay_r = NFkBn

nfkbn_delay_8 = NFkBn

nfkbn_delay_TNFa = NFkBn

********** MODEL REACTIONS

flux_ikkm = ikkmyd88_in + ikkmyd88

flux_rsu_a = rsu_a

flux_rsu_b = rsu_b

flux_rsu_e = rsu_e

flux_rsr_an = rsr_an*(nfkbn_delay_a^h_an_a)

flux_rsr_bn = rsr_bn*(nfkbn_delay_b^h_an_b)

flux_rsr_en = rsr_en*(nfkbn_delay_e^h_an_e)

flux_rd_a = rd_a*IκBat

flux_rd_b = rd_b*IκBbt

flux_rd_e = rd_e*IκBet

flux_ps_c_a = ps_c_a*IκBat

flux_ps_c_b = ps_c_b*IκBbt

flux_ps_c_e = ps_c_e*IκBet

flux_a_c_an = a_c_an*IκBa*NFkB

flux_a_c_bn = a_c_bn*IκBb*NFkB

flux_a_c_en = a_c_en*IκBe*NFkB

flux_a_n_an = a_n_an*IκBan*NFkBn

flux_a_n_bn = a_n_bn*IκBbn*NFkBn

flux_a_n_en = a_n_en*IκBen*NFkBn

flux_d_c_an = d_c_an*IκBaNFkB

flux_d_c_bn = d_c_bn*IκBbNFkB

flux_d_c_en = d_c_en*IκBeNFkB

flux_d_n_an = d_n_an*IκBaNFkBn

flux_d_n_bn = d_n_bn*IκBbNFkBn

flux_d_n_en = d_n_en*IκBeNFkBn

flux_a_c_ai = a_c_ai*IκBa*IKK

flux_a_c_bi = a_c_bi*IκBb*IKK

flux_a_c_ei = a_c_ei*IκBe*IKK

flux_d_c_ai = d_c_ai*IκBaIKK

flux_d_c_bi = d_c_bi*IκBbIKK

flux_d_c_ei = d_c_ei*IκBeIKK

flux_a_c_2ani = a_c_2ani*IκBaNFkB*IKK

flux_a_c_2bni = a_c_2bni*IκBbNFkB*IKK

flux_a_c_2eni = a_c_2eni*IκBeNFkB*IKK

flux_d_c_2ani = d_c_2ani*IκBaIKKNFkB

flux_d_c_2bni = d_c_2bni*IκBbIKKNFkB

flux_d_c_2eni = d_c_2eni*IκBeIKKNFkB

flux_a_c_2ain = a_c_2ain*IκBaIKK*NFkB

flux_a_c_2bin = a_c_2bin*IκBbIKK*NFkB

flux_a_c_2ein = a_c_2ein*IκBeIKK*NFkB

flux_d_c_2ain = d_c_2ain*IκBaIKKNFkB

flux_d_c_2bin = d_c_2bin*IκBbIKKNFkB

flux_d_c_2ein = d_c_2ein*IκBeIKKNFkB

flux_in_a = in_a*IκBa

flux_in_b = in_b*IκBb

flux_in_e = in_e*IκBe

flux_ex_a = ex_a*IκBan

flux_ex_b = ex_b*IκBbn

flux_ex_e = ex_e*IκBen

flux_in_2an = in_2an*IκBaNFkB

flux_in_2bn = in_2bn*IκBbNFkB

flux_in_2en = in_2en*IκBeNFkB

flux_ex_2an = ex_2an*IκBaNFkBn

flux_ex_2bn = ex_2bn*IκBbNFkBn

flux_ex_2en = ex_2en*IκBeNFkBn

flux_in_n = in_n*NFkB

flux_ex_n = ex_n*NFkBn

flux_pd_c_a = pd_c_a*IκBa

flux_pd_c_b = pd_c_b*IκBb

flux_pd_c_e = pd_c_e*IκBe

flux_pd_n_a = pd_n_a*IκBan

flux_pd_n_b = pd_n_b*IκBbn

flux_pd_n_e = pd_n_e*IκBen

flux_pd_c_2an = pd_c_2an*IκBaNFkB

flux_pd_c_2bn = pd_c_2bn*IκBbNFkB

flux_pd_c_2en = pd_c_2en*IκBeNFkB

flux_pd_n_2an = pd_n_2an*IκBaNFkBn

flux_pd_n_2bn = pd_n_2bn*IκBbNFkBn

flux_pd_n_2en = pd_n_2en*IκBeNFkBn

flux_pd_c_2ai = pd_c_2ai*IκBaIKK*flux_ikkm

flux_pd_c_2bi = pd_c_2bi*IκBbIKK*flux_ikkm

flux_pd_c_2ei = pd_c_2ei*IκBeIKK*flux_ikkm

flux_pd_c_3ain = pd_c_3ain*IκBaIKKNFkB*flux_ikkm

flux_pd_c_3bin = pd_c_3bin*IκBbIKKNFkB*flux_ikkm

flux_pd_c_3ein = pd_c_3ein*IκBeIKKNFkB*flux_ikkm

flux_d_n_r = d_n_r*RANTESt

flux_rsr_rn = rsr_rn*(nfkbn_delay_r^h_an_r)

flux_rsu_r = rsu_r

flux_d_n_8 = d_n_8*IL8t

flux_rsr_8n = rsr_8n*(nfkbn_delay_r^h_an_8)

flux_rsu_8 = rsu_8

flux_d_n_TNFa = d_n_TNFa*TNFat

flux_rsr_TNFan = rsr_TNFan*(nfkbn_delay_r^h_an_TNFa)

flux_rsu_TNFa = rsu_TNFa

********** MODEL FUNCTIONS

********** MODEL EVENTS

********** MODEL MATLAB FUNCTIONS

## B.2 Experimental file

```
********** EXPERIMENT NAME
ecoli
********** EXPERIMENT NOTES

********** EXPERIMENT INITIAL PARAMETER AND STATE SETTINGS
% The expression in this limiter will be evaluated when merging the
% experiment with the model.

********** EXPERIMENT PARAMETER CHANGES
% In this section parameter changes can be defined that are evaluated
during
% the merged models evaluation
ikkmyd88 =
interpcsSB([0,15,30,45,60,120,240,360],[0.01,0.03,0.08,0.24,0.25,0.15,0.08,
0.05],time)
********** EXPERIMENT STATE CHANGES
% State changes in the experiment description
```

## B.3 Matlab implementation

%% Matlab m file to run the model for 360 minutes

% define the model and experimental file

```
model_e_e = SBmodel('model.txt');
exp_e = SBexperiment('ecoli.exp');

% merge the model with the experimental conditions

model_e = SBmergemodexp(model_e_e,exp_e);

% define the experimental simulation time

time = [0:360];

% simulate the model

Simulation_output = SBPDsimulate(model_e,time);
```